A watercolor illustration depicting the effects of acute graft-versus-host disease (GVHD) on the gut. The central focus is a large, irregularly shaped area of teal color, representing the gut epithelium, which is surrounded by a layer of yellow and white. Above this area, several large, teardrop-shaped orange and black shapes are shown, suggesting the shedding of epithelial cells. To the right, a long, thin, teal-colored structure extends horizontally, with several circular cells containing teal nuclei and yellow outlines, representing the remaining epithelial cells. Below the main teal area, numerous small, scattered cells are depicted, some with teal nuclei and yellow outlines, and others with black outlines, representing the fragmented and shed epithelial cells. The overall style is artistic and illustrative, using soft watercolor textures and a palette of teal, orange, yellow, and black on a white background.

Epithelial injury in acute  
graft-versus-host disease  
of the gut

Suze A. Jansen



# Epithelial injury in acute graft-versus-host disease of the gut

Suze A. Jansen

## Colofon

Epithelial injury in acute graft-versus-host disease of the gut  
Doctoral thesis, Utrecht University, The Netherlands


ISBN: 978-94-6419-949-9

Author: Suze A. Jansen

Illustrations and cover design: Anneloes Gerdien – [www.anneloesgerdien.nl](http://www.anneloesgerdien.nl)

Lay-out: Ilse Modder – [www.ilsemodder.nl](http://www.ilsemodder.nl)

Printed by: Gildeprint – [www.gildeprint.nl](http://www.gildeprint.nl)

Flipbook: 

The research in this thesis was financially supported by an Alexandre Suerman stipend of the UMC Utrecht, the WKZ fund, and two NIH R01 grants.

© All rights reserved. No part of this thesis may be reproduced, stored in a retrieval system or transmitted in any form or by any means without prior permission in writing of the copyright owner.

# **Epithelial injury in acute graft-versus-host disease of the gut**

**Epitheelschade in acute graft-versus-host ziekte van de darm**  
(met een samenvatting in het Nederlands)

## **Proefschrift**

ter verkrijging van de graad van doctor aan de  
Universiteit Utrecht  
op gezag van de  
rector magnificus, prof.dr. H.R.B.M. Kummeling,  
ingevolge het besluit van het college voor promoties  
in het openbaar te verdedigen op

donderdag 30 november 2023 des ochtends te 10.15 uur

door

**Suze Anne Jansen**

geboren op 8 december 1990  
te Rotterdam

**Promotor:**

Prof. dr. E.E.S. Nieuwenhuis

**Copromotor:**

Dr. C.A. Lindemans

**Beoordelingscommissie:**

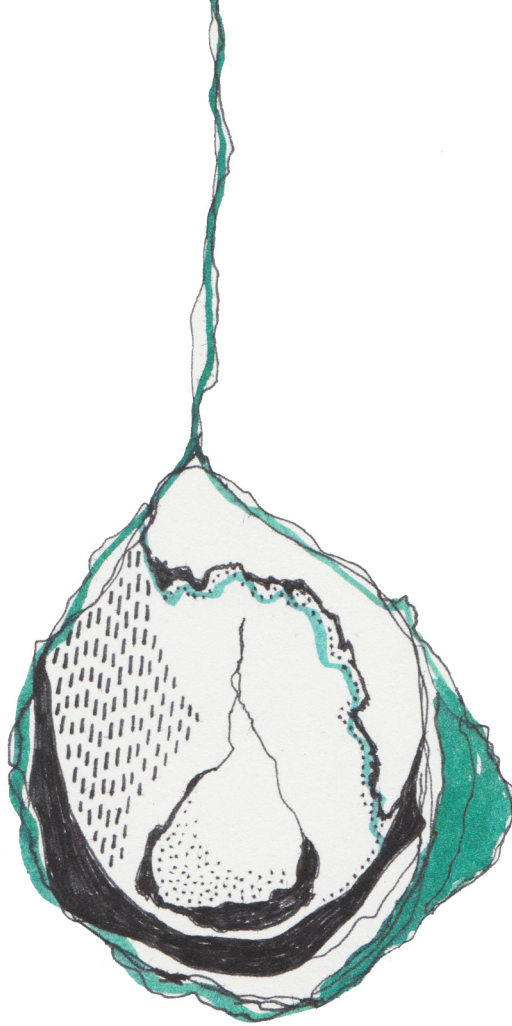
Prof. dr. J.M. Beekman

Prof. dr. M.D. Hazenberg

Dr. H.L. Leavis

Prof. dr. M.M. Maurice

Prof. dr. F. van Wijk (voorzitter)



De belangrijkste voorwaarde voor geluk is dat je wilt zijn wat je bent

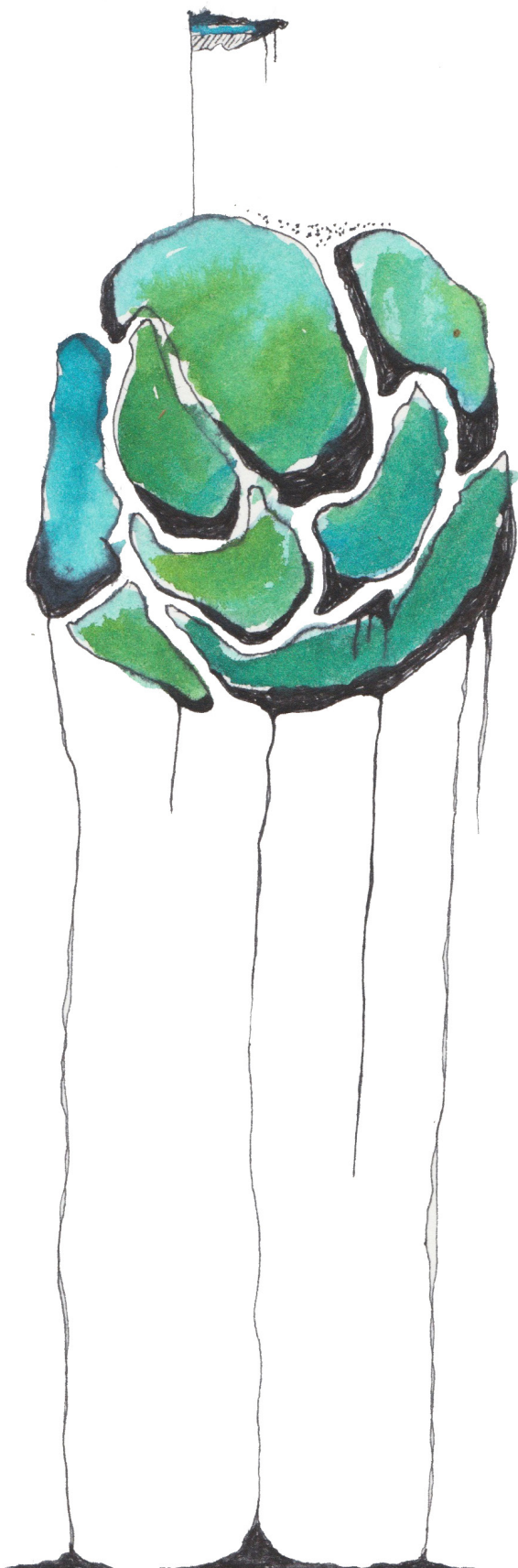
*Erasmus*





# Contents

Chapter 1	General introduction	11
Chapter 2	Clinical features, treatment and outcome of pediatric steroid refractory acute Graft-versus-Host disease: a multicenter study	27
Chapter 3	Broad virus detection and variant discovery in fecal samples of hematopoietic transplant recipients using targeted sequence capture metagenomics	53
Chapter 4	Chemotherapy-induced intestinal injury promotes Galectin-9-driven modulation of T cell function	71
Chapter 5	T cell-derived interferon- $\gamma$ programs stem cell death in immune-mediated intestinal damage	99
Chapter 6	Corticosteroids impair epithelial regeneration in immune-mediated intestinal damage	153
Chapter 7	Challenges and opportunities targeting mechanisms of epithelial injury and recovery in acute intestinal Graft-versus-Host disease	181
Chapter 8	Discussion	213
Appendices	Nederlandse samenvatting	240
	Dankwoord	242
	Curriculum vitae	246
	List of publications	247



# 1

General introduction

## The concept/principle of allogeneic hematopoietic stem cell transplantation

In multiple hematologic malignancies, non-malignant immunological disorders or metabolic enzyme deficiencies, only a transplantation of donor – or allogeneic – hematopoietic stem cells (allo-HSCT) can provide a cure (Fig. 1)<sup>1</sup>. In allo-HSCT, patients receive a 'graft' of hematopoietic stem cells from a donor that eventually replaces all lineages of blood cells, including those of the immune system. Different sources of stem cells are available for allo-HSCT, including freshly harvested bone marrow (BM), peripheral blood (PBSC) after recruitment of stem cells from the BM, and blood derived from the umbilical cord (CB) stored after birth.

Several requirements must be met in order for the transplantation to be successful. Before the transplantation can take place, the recipient of the transplant needs to undergo a conditioning regimen consisting of treatment with irradiation, chemotherapy and/or immune-cell eliminating antibodies. The conditioning aims to eliminate the host's own hematopoietic system to make space for the graft and to reduce the chances of the recipient's immune system rejecting the graft. In a malignant setting the regimen additionally eradicates any remaining cancer cells, and as such reduces the likelihood of relapse of the malignancy after transplant<sup>2</sup>. There are different types of conditioning, and the choice depends for instance on the transplantation indication or comorbidities of the patient. In the malignant setting myeloablative (MA) conditioning aims to completely eradicate a patient's own BM, while in some non-malignant diseases, or in patients that are older or are extra sensitive to DNA damage, a non-myeloablative (NMA) or reduced intensity (RIC) regimen is sufficient and preferred to reduce side-effects in other organs<sup>3-5</sup>.

Matching of the graft and recipient is based on the typing of multiple major histocompatibility complex (MHC) – in humans termed HLA – genes on the DNA<sup>1</sup>. The HLA complex is responsible for presenting peptides to T cells and as such functions as an alarm system for materials that are foreign to the body such as pathogens, but also cancer cells<sup>6</sup>. There are 2 types of HLA genes. Type I (e.g., HLA-A, B and C) is expressed on all cells except red blood cells and interacts with the T cell receptor (TCR) of CD8+ cytotoxic T cells. Type II HLA (e.g., HLA-DQ, DR, DP) is primarily expressed on professional antigen presenting cells (APCs) such as dendritic cells (DCs) and activates CD4+ T helper cells. HLA matching will limit the chance that donor immune cells will recognize the recipient's tissues as foreign and launch an inflammatory attack, a condition called acute graft-versus-host disease (aGVHD)<sup>7,8</sup>. The HLA complex has evolutionary evolved in such a way that each individual is unique in the combination of HLA gene composition. A good match may therefore be challenging to find. Ideally, grafts are obtained from identical siblings or matched related donors (MRD), but these are often not available. In those cases, a matched unrelated donor (MUD) or, in



the least preferable scenario, a mismatched unrelated bone marrow or cord blood donor (MMUD) will be selected from a donor registry<sup>1</sup>.

After the transplantation, the recipient experiences a period with low blood cell counts (aplasia) in most lineages, including all immune cells, platelets and sometimes red blood cells. Often multiple transfusions are required. After 14-28 days the first immune cells, neutrophils, differentiated from the transplanted stem cells, can be detected in blood, which marks engraftment<sup>1</sup>. In the most common type of allo-HSCT, T cells remain unmanipulated and are directly co-transplanted with the graft<sup>9</sup>. Since it may take up to 6 months for T cells to reconstitute from the donor marrow, these co-infused T cells are essential to bridge the period in which the recipient has a non-functioning immune system while still being exposed to infectious insults. In addition, in malignant settings, the T cells can eliminate any remaining cancer cells in a phenomenon known as the graft-versus-tumor or -leukemia (GVL) effect<sup>2</sup>. Also, the T cells may help to reduce rejection of the graft by eliminating any remaining recipient immune cells. However, these T cells may also cause aGVHD.

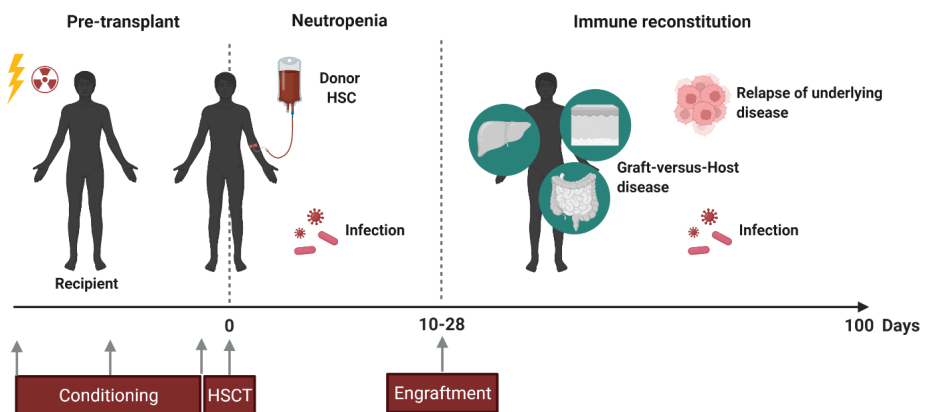


**Figure 1. Allo-HSCT timeline.** Before transplantation the recipient undergoes a conditioning regimen consisting of irradiation and/or chemotherapy to eradicate the recipients immune system and make space for the graft. At the time of allo-HSCT the recipient is infused with donor hematopoietic stem cells, often together with donor T cells. For the first 2-4 weeks after the transplant, the neutropenic phase, the recipient has low blood cell counts and is particularly vulnerable for specific infections such as Coagulase-Negative Staphylococci (in combination with the presence of central intravenous lines), Viridans Group Streptococci, facultative gram negatives, respiratory and enteral viruses, Candida and Aspergillus<sup>10</sup>. When the first immune cells start to come forth from the graft, neutrophil engraftment takes place usually within one month of HSCT, after which the lymphoid immune system also slowly starts to reconstitute over the course of many months. In that time the recipient remains vulnerable for infections (encapsulated bacteria, HSV, CMV, VZV, ADV, EBV, Candida, late Aspergillus and Pneumocytis jirovecii)<sup>10</sup>, but also Graft-versus-Host disease (GvHD) may develop when alloreactive T cells become activated. In case of a malignant HSCT indication the reconstituting immune system is also responsible for developing and maintaining a graft-versus-tumor effect, or else the underlying disease might relapse.

## Devastating Graft-versus-Host disease, of the gut in particular

The development of aGVHD poses a significant health threat for patients undergoing allo-HSCT. Approximately 50% of allo-HSCT recipients develop aGVHD, of which 14% a more severe phenotype as defined by grade III-IV of the Glucksberg criteria grading system (Table 1)<sup>11,12</sup>. Skin, gut and liver are the most commonly involved organs, but essentially all tissues of the body can be affected. Due to the high risk of developing aGVHD, all patients receive immunosuppressive prophylactic treatment consisting of calcineurin inhibitors (Cyclosporin A, CsA) with low dose corticosteroids (CS) in CB transplants, or with Mycophenolate Mofetil (MMF) or methotrexate (MTX) in BM transplants<sup>13</sup>. Nevertheless, aGVHD mortality is significant despite treatment. Especially gastro-intestinal aGVHD (GI-GVHD) is a severe complication of allo-HSCT, accounting for most GVHD-related deaths<sup>14</sup>. Patients develop severe secretory diarrhea, often multiple liters per day, mostly due to a failure of fluid resorption in the small intestine. In addition, the ability of the gut to absorb essential nutrients is hampered, leading to weight loss and risk of malnutrition. Furthermore, the combination of an impaired immune system and the disruption of the protective barrier that the gut epithelium constitutes, makes patients very vulnerable for infectious insults<sup>14</sup>. Because of the high morbidity and mortality, GI-GVHD is the focus of this thesis.

The pathophysiology of GI-GVHD has not been completely elucidated but is generally believed to comprise a complex interplay of preconditioning epithelial damage, donor and host immune cells and intestinal microbiota<sup>11</sup>. The first step in the development of GI-GVHD is tissue damage caused by the conditioning regimen<sup>15,16</sup>. In addition to inducing a local inflammatory response with the release of damage-associated molecular patterns (DAMPs)<sup>11</sup>, the tissue injury may lead to an intestinal barrier breach<sup>17-19</sup>, allowing intestinal pathogens and pathogen-associated molecular patterns (PAMPs) to enter, adding to the inflammatory milieu. Gut domination of certain strains of pathogenic bacteria has been directly linked to bacterial sepsis cases in transplant recipients<sup>20</sup>. Many transplant centers have therefore adopted total gut decontamination as part of the HSCT-treatment protocol<sup>21</sup>. Total gut decontamination is also associated with less GVHD<sup>22,23</sup>. However, more recent studies have shown that the implication of microbiota in the HSCT-setting is much more intricate and complex, contributing to both pathology and homeostasis, and that microbial diversity and persistence/presence of certain commensals is key<sup>24-26</sup>.

The released DAMPs and translocated PAMPs act as danger signals that activate the innate immune system through binding pattern recognition receptors (PRRs)<sup>27</sup>. This induces the release of pro-inflammatory cytokines such as TNF $\alpha$ , IL-1 $\beta$  and IL-6, and T-cell stimulating cytokines like IL-12. It enhances the expression of adhesion and costimulatory molecules and increases HLA-expression and allo-antigen presentation by APCs. As such, PAMPs



and DAMPS can fuel the development of donor T cell alloreactive (allo) responses<sup>27–29</sup>. In HLA-matched allo-HSCT, both host and donor APCs may activate donor allo T cells by presenting host-derived, ‘non-self’ minor histocompatibility antigens (mHAs) in the HLA<sup>30</sup>. In a HLA-mismatched setting the donor TCR in addition recognizes a mismatched host HLA loaded with host-derived ‘self’-peptides in a process known as molecular mimicry<sup>31</sup>. Both CD4 and CD8 T cells are involved in aGVHD allo-responses.

The tissue damage that results from the allo-responses is considerable. Upon endoscopic examination mucosal swelling and redness can be observed, as well as erosions, superficial or deep ulcerations or even complete mucosal denudation<sup>14</sup>. On a histological level, the characteristic feature of GI-GVHD pathology is apoptosis and loss of epithelial crypts, the region that harbors the stem cells of the intestinal epithelium<sup>32,33</sup>. As such, the golden standard of GI-GVHD diagnosis is the observation of these findings in patient GI biopsies, in combination with the clinical symptoms<sup>1</sup>.

**Table 1. Clinical grading of acute GVHD<sup>12</sup>**

Clinical stage of acute GVHD per organ				
Stage	Target organ			
	Skin (active erythema only)	Liver (serum total bilirubin)	Upper gastro-intestinal	Lower gastro-intestinal (stool output)
0	No active (erythematous) rash	<2 mg/dL (<34.21 μmol/L)	No or intermittent nausea, vomiting or anorexia	Adult: <500 mL per day Child: <10 mL/kg per day
1	Maculopapular rash, <25% BSA	2–3 mg/dL (34.21–51.31 μmol/L)	Persistent nausea, vomiting or anorexia	Adult: 500–999 mL per day Child: 10–19.9 mL/kg per day
2	Maculopapular rash, 25–50% BSA	3.1–6 mg/dL (53.02–102.62 μmol/L)	–	Adult: 1,000–1,500 mL per day Child: 20–30 mL/kg per day
3	Maculopapular rash, >50% BSA	6.1–15 mg/dL (104.33–256.56 μmol/L)	–	Adult: >1,500 mL per day Child: >30 mL/kg per day
4	Generalized erythroderma (>50% BSA), plus bullous formation and desquamation (>5% BSA)	>15 mg/dL (>256.56 μmol/L)	–	Severe abdominal pain with or without ileus or grossly bloody stool (regardless of volume)
Overall clinical grade of acute GVHD				
Grade	Criteria			
0	No stage 1–4 of any organ involvement			
I	Stage 1–2 skin involvement, without liver, upper gastrointestinal or lower gastrointestinal involvement			
II	Stage 3 skin involvement and/or stage 1 liver involvement and/or stage 1 upper gastrointestinal involvement and/or stage 1 lower gastrointestinal involvement			
III	Stage 2–3 liver involvement and/or stage 2–3 lower gastrointestinal involvement with stage 0–3 skin involvement and/or stage 0–1 upper gastrointestinal involvement			
IV	Stage 4 skin, liver or lower gastrointestinal involvement, with stage 0–1 upper gastrointestinal involvement			

## Treatment challenges in patients with acute GVHD

Treatment of aGVHD is primarily aimed at debilitating the overactive immune system and allo T cells with a variety of immunosuppressive medications or cell therapy. Due to the competing goals in the treatment of aGVHD on the one hand and maintaining GVL effect and reducing graft rejection and infection risk on the other hand, clinicians often find themselves key performers in a lethal balancing act. First-line therapy consists of high-dose (2 mg/kg bodyweight) CS, but up to 50% of aGVHD patients do not respond (sufficiently) and develop a condition known as steroid-refractory (SR-) aGVHD<sup>34,35</sup>. Additional lines of treatment are currently experimental and primarily target the immune system, with all the anticipated complications of infection, graft failure and relapse of underlying disease, as well as medication specific toxicities (Table 2). To date, there is only one proven effective second-line therapy for SR-aGVHD in adult patients, ruxolitinib<sup>36</sup>, and for children thus far no proven effective treatments are available<sup>37</sup>.

In **Chapter 2** we set the stage for the clinical challenges that are faced with GVHD, by presenting the group of 81 pediatric patients that developed SR-aGvHD in the Netherlands between 2010 and 2020. We describe their clinical course and outcome, the types of additional treatments that were given and identify risk factors for continued GVHD and mortality. In addition, we map the complications these patients experience and the causes of death. We demonstrate the high morbidity and mortality associated with SR-aGVHD at the current time, and as such show that new therapies for GI-GVHD are an absolute necessity. Further paralyzing the immune system does not seem to be an attractive approach.

**Table 2. Current options for second-line treatment of SR-aGVHD**

Generic	Mechanism of action	Side effects
<b>Lymphocyte-cytostatics</b>		
<b>Mycophenolate mofetil (MMF)<sup>38</sup></b>	Selective inhibition of inosine monophosphate dehydrogenase, involved in the de novo-synthesis of guanoside nucleotides	Infections, low blood cell counts, secondary malignancies, bone marrow failure
<b>T cell inhibitors</b>		
<b>Anti-thymocyte globulin (ATG)<sup>39</sup></b>	Immunoglobulin directed against human T lymphocytes	Infections, low blood cell counts, secondary malignancies
<b>CD52 inhibitors</b>		
<b>Alemtuzumab<sup>40</sup></b>	Monoclonal antibody blocking membrane-bound CD52 expressed on lymphocytes	Infections, low blood cell counts,
<b>CD25 inhibitors</b>		
<b>Basiliximab<sup>41</sup></b>	Monoclonal antibody selectively antagonizing interleukin-2 receptor	Infections
<b>IL-6 inhibitors</b>		
<b>Tocilizumab<sup>42</sup></b>	Monoclonal antibody binding IL-6 receptors	Infections, low blood cell counts





Table 2. *Continued.*

Generic	Mechanism of action	Side effects
<b>TNF-<math>\alpha</math> inhibitors<sup>43</sup></b>		
<b>Infliximab</b>	Monoclonal antibody binding TNF- $\alpha$	Infections, low blood cell counts, secondary malignancies
<b>Etanercept</b>	Human TNF-receptor p75 Fc fusion-peptide, binding TNF- $\alpha$	Infections, secondary malignancies, low blood cell counts, bone marrow failure
<b>Protein kinase inhibitors</b>		
<b>Ruxolitinib<sup>44</sup></b>	Inhibition of JAK1/2	Bleeding, low blood cell counts, infections
<b>Integrin inhibitors</b>		
<b>Vedolizumab<sup>45</sup></b>	Monoclonal antibody blocking $\alpha 4\beta 7$ -integrin on gut-homing T cells	Infections
<b>Cell therapy</b>		
<b>Mesenchymal stromal cells (MSCs)<sup>46</sup></b>	Immunomodulation by suppressing the proliferative activity of allogenic T lymphocytes	Infections?

## Intestinal damage as a common theme throughout the course of HSCT, and as the focus of this thesis

As outlined above, there are many instances of intestinal epithelial damage in the course of aGVHD development and propagation, including conditioning-induced injury, intrusion of pathogens, the allo immune response and toxicity of given therapy. Several risk factors for aGVHD development and severity are directly linkable to the different aspects of damage<sup>16,47</sup>, including the type and intensity of the conditioning regimen<sup>47,48</sup>, mucositis<sup>49</sup>, colonization by certain pathogens<sup>25,26,50</sup> and the level of HLA mismatch<sup>8,51,52</sup>. Nonetheless, many mechanistic questions remain unanswered, leaving possible therapeutic opportunities for aGVHD unexploited. In this thesis we study several different aspects of epithelial injury in the context of GHVD in the clinical (**Chapter 3**) and preclinical (**Chapters 4, 5, 6**) setting and possibilities to overcome this:

- In **Chapter 3** we use a method that enriches for viral sequences to study the intestinal virome in HSCT patients suspected of gut aGVHD<sup>53</sup>. Identifying which specific viruses are present will help us to better understand how viral presence predisposes for the development of aGVHD.
- In **Chapter 4** we study how chemotherapy used in the conditioning regimen damages the intestinal epithelium and how this affects allo T cell migration and activation.
- In **Chapter 5** we show how allo T cells damage the GI-tract in aGVHD and how the gut can be protected from these insults<sup>54</sup>.
- In **Chapter 6** we delineate how CS aimed at inhibiting allo T cells actually further limit the healing of the intestine in aGVHD, calling for additional regenerative measures.

- Finally, in **Chapter 7**, damage to the GI-tract is reviewed as a pivotal factor in both development and propagation of aGVHD. We discuss how protection of the GI-tract and intestinal epithelial restorative, and regenerative approaches may be promising in the future treatment of GI-GVHD.

To be able to study the different aspects of damage, several well-established and in-house developed models of aGVHD in both mice and human are utilized in Chapters 4, 5 and 6. Below these models will be introduced.

## Mouse models to study mechanisms of damage in GVHD

Much of what we know about aGVHD pathophysiology has been discovered using mouse models of aGVHD<sup>11,55</sup>. Given the complexity of aGVHD pathophysiology, comprising numerous processes throughout the body, with multiple cell types involved over time, the mere studying of patient samples at specific time points does not suffice. In addition, due to the severity of the condition and the do-not-harm principle patient materials are not readily or abundantly available for research purposes. The fact that aGVHD is a therapy-induced, iatrogenic condition makes it very suitable for mimicking in an animal model, in a so-called *in vivo* setting. Despite the apparent observation that mice are in fact not humans, many aspects of aGVHD pathology between our species have been found to be comparable<sup>55</sup>. In addition, the possibility of using knockout and transgenic mice strains to dissect certain aspects of, in this case, damage mechanisms involved in aGVHD, make mouse systems indispensable as preclinical research tools<sup>56</sup>.

To be able to study aGVHD in mice, mice undergo a BM transplantation with a trajectory comparable to that of a human patient (Fig. 2)<sup>56</sup>. Before the transplantation mice are co-housed to align their microbiota constitutions. The microbiome can differ greatly between mouse strains, vendor origins and housing facilities<sup>57</sup>, which has been shown to have a large impact on experimental BMT outcomes. These observations were the starting point for the research conducted to understand the impact of the microbiome on outcomes in clinical HSCT recipients<sup>24</sup>. After receiving conditioning with total body irradiation (TBI) in two doses to reduce GI toxicity, the hosts receive a BM graft from a donor via tail vein injection. In MHC-mismatched (also called major mismatched) BMT, different strains of mice with different MHC are used as donors and recipients. In MHC-matched, minor mismatched BMT, more resembling human HSCT, mice are used that have largely the same genetic background with only minor HA disparities to induce aGVHD. In an experimental setting, it is essential to include a control condition in which aGVHD does not develop to be able to attribute any findings specifically to the presence of aGVHD. In the minor mismatch setting, the control BMT is performed by transplanting the recipient with BM only, without any T



cells. In a major mismatch BMT, transplanting BM only is not an option since the large MHC disparity would cause the graft to be rejected by the host. Instead, a so-called 'syngeneic' transplant is used as a control, where the recipient receives BM+T cells from a donor of its own strain. After the experimental transplant has taken place, the survival is monitored and the mice are scored over time for certain validated aGVHD symptoms, including quality of the skin and fur, stool consistency, activity, body weight and posture<sup>58</sup>. In the course of these mouse BMTs, multiple aspects can be manipulated to study a specific mechanism, either by genetic modification in certain tissues or cell lines of the donor or recipient, by administering blocking or stimulating antibodies, or testing compounds of interest. In Table 3 the specific aGVHD mouse models used in the thesis are listed.

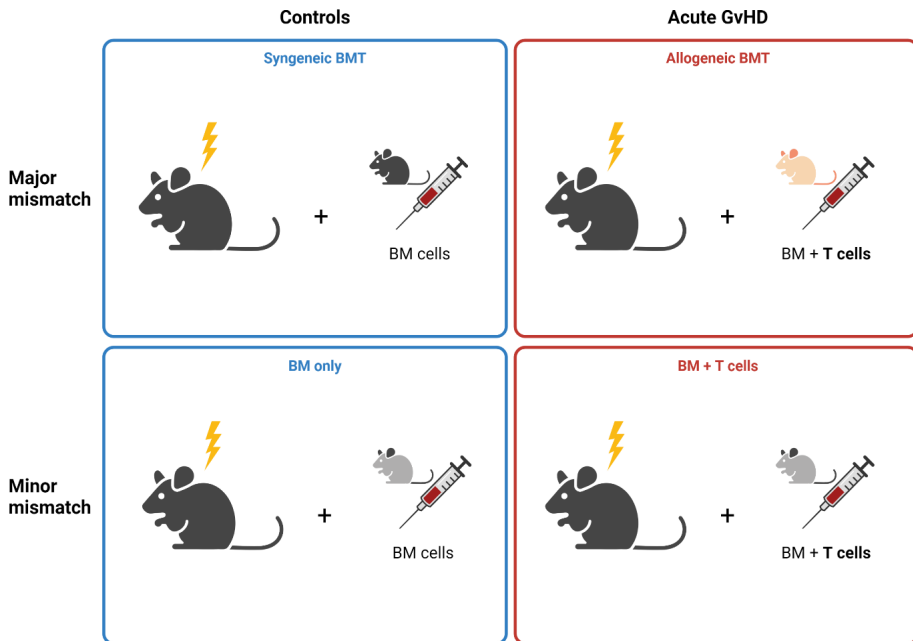


**Figure 2. aGVHD mouse model principles.** Mouse models of bone marrow transplantation (BMT) can be used to study the pathophysiology of Graft-versus-Host disease. In a major mismatch BMT, mice that are used as a recipient are from a different strain, and therefore disparate genetic background, than the donor ('allogeneic'). As a control, recipient mice receive a syngeneic BMT with BM from a donor from the same strain. In minor mismatch models the genetic background of the recipient and donor mice is the same. Instead, minor histogen antigens (mHAs) are disparate causing GvHD. To induce GvHD in this model system splenic T cells of the donor are co-transplanted with the BM-graft, while in the control setting only BM is transplanted.

**Table 3. aGVHD mouse models used in this thesis<sup>56</sup>**

Donor	Recipient	TBI dose (cGy, split)	aGVHD target	T cell dependence	Lethality
<b>Major MHC-mismatched models</b>					
<b>B10.Br (H-2<sup>k</sup>)</b>	C57BL/6 (B6) (H-2 <sup>b</sup> )	1100	MHC-I, II, mHAs	CD4 (+/- CD8)	Major
<b>B6 (H-2<sup>b</sup>)</b>	(B6 x DBA/2)F1 (H-2 <sup>b/d</sup> )	1300	MHC-I, II, mHAs	CD4 (+/- CD8)	Major
<b>B6 (H-2<sup>b</sup>)</b>	BALB/c (H-2 <sup>d</sup> )	900	MHC-I, II, mHAs	CD4 (+/- CD8)	Major
<b>Minor HA mismatched, MHC-matched models</b>					
<b>LP/J (H-2<sup>b</sup>)</b>	B6 (H-2 <sup>b</sup> )	1100	mHAs	CD4	Minor

## Intestinal epithelial organoids as a bridge between mouse and human studies

Despite the advantages of using mouse models to study GI-GVHD *in vivo*, ethical controversy increased efforts in the research community to reduce the part of animal studies over the last few decades. The discovery of the intestinal stem cell (ISC) in mice laid the foundation for the development of an *in vitro* intestinal epithelial culture system by the Clevers lab<sup>59</sup>. ISCs are harbored in a region of the epithelium known as the intestinal epithelial crypt. Crypts isolated from mice were found to be capable of forming self-organizing, 3-dimensional epithelial structures when embedded in a gel and supplemented with required growth factors (Fig. 3)<sup>60</sup>. These so-called ‘organoids’ harbored almost all cell types present in the murine intestinal epithelium, and importantly were expandable over long periods of time. A few years later, the same research group published a protocol with which organoids could be established and cultured from human GI biopsies<sup>61</sup>. This enabled the biobanking of organoids from both healthy individuals and patients, establishing a highly valuable source of material suitable for studies related to disease modelling, drug development and personalized medicine<sup>62</sup>.

In this thesis, we use both mouse and biobanked human intestinal organoids to model aspects of aGVHD pathology in a dish. For example, we culture organoids in the presence T cells in so-called ‘co-cultures’ to recapitulate allo-induced epithelial damage, as well as to study the effects of damaged epithelium on T cell responses. This allows us to unravel mechanisms of intestinal injury in aGVHD that are relevant to patients and study approaches to limit and restore this damage for future aGVHD treatment opportunities.

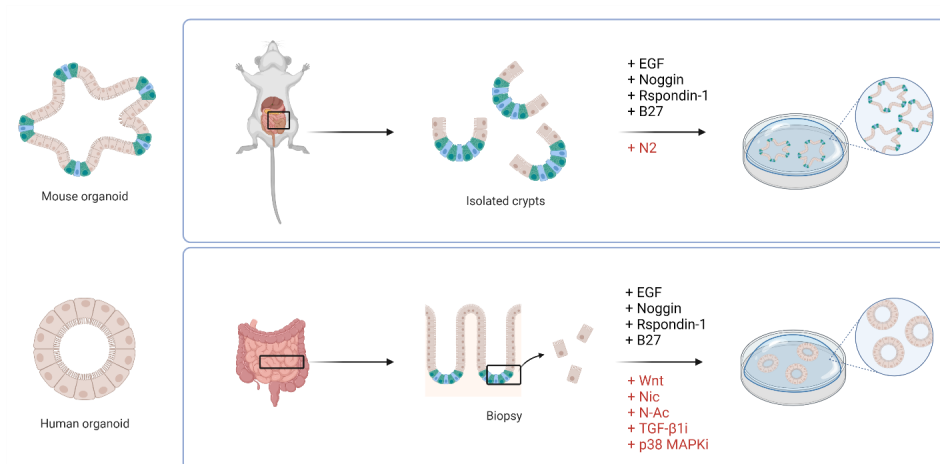


**Figure 3. Intestinal epithelial organoids.** The crypt region of the intestinal epithelium harbors the intestinal stem cells (ISC) (in light blue) from which all intestinal epithelial cell types develop as they move up out of the crypt and towards the gut-lumen protruding villus. In mice, the small intestinal epithelium is renewed every 5 days<sup>59</sup>. When crypts are isolated from either mouse intestines or human gut biopsies, they can form 3-dimensional structures in a plate with the right supply of growth and niche factors. Most growth factors have been identified by studying the stem cell and epithelial cell natural environment *in vivo* and are shared between mice and humans<sup>60,61</sup>. An essential difference between the mouse and human intestinal organoid system is the requirement of Wnt for the human culture<sup>61</sup>. Wnt is a stem cell factor, that is secreted by niche supporting Paneth cells (PC) (in azure) that lie interspersed between ISCs in the crypt<sup>63</sup>. PCs are present in mouse organoids and mouse organoids and supply the ISCs with Wnt, but in human organoids PCs are lost during culture and Wnt needs to be added to the medium for the cultures to survive. Due to the Wnt requirement, the constitution and therefore appearance of mouse and human organoids is quite different<sup>62</sup>. The local production of Wnt by PCs in mouse organoids creates a Wnt gradient causing the formation of crypt regions at the outward protruding organoid buds, and more differentiated cells towards the organoid lumen. Due to the overall presence of Wnt in human cultures, human organoids consist mostly of stem cell like cells that grow homogeneously in a ball-shape. By changing the constitution of growth factors in the medium differentiation of certain intestinal epithelial cell types can be induced in both human and mouse organoids. EGF, epithelial growth factor; Noggin, BMP antagonist; Rspodin-1, Lgr5 agonist and Wnt-signalling potentiator; B27, B27 supplement; N2, N2 supplement; Nic, nicotinamide; N-Ac, N-Acetylcysteine, TGF- $\beta$ 1i, transforming growth factor beta 1 inhibitor; p38 MAPKi, p38 mitogen activated protein kinase inhibitor.

## References

1. Forman SJ, Negrin RS, Antin JH, Appelbaum FR, eds. *Thomas' Hematopoietic Cell Transplantation*. 5th ed. John Wiley & Sons; 2015.
2. Appelbaum FR. Haematopoietic cell transplantation as immunotherapy. *Nature*. 2001;411(6835):385-389. doi:10.1038/35077251
3. Slavin S, Nagler A, Naparstek E, et al. Nonmyeloablative stem cell transplantation and cell therapy as an alternative to conventional bone marrow transplantation with lethal cytoreduction for the treatment of malignant and nonmalignant hematologic diseases. *Blood*. 1998;91(3):756-763.
4. Bacigalupo A, Ballen K, Rizzo D, et al. Defining the intensity of conditioning regimens: working definitions. *Biol Blood Marrow Transplant*. 2009;15(12):1628-1633. doi:10.1016/j.bbmt.2009.07.004
5. Benajiba L, Salvado C, Dalle JH, et al. HLA-matched related-donor HSCT in Fanconi anemia patients conditioned with cyclophosphamide and fludarabine. *Blood*. 2015;125(2):417-418. doi:10.1182/blood-2014-10-605113
6. Klein J, Sato A. The HLA system. First of two parts. *N Engl J Med*. 2000;343(10):702-709. doi:10.1056/NEJM200009073431006
7. Ferrara JLM, Levine JE, Reddy P, Holler E. Graft-versus-host disease. *Lancet*. 2009;373(9674):1550-1561. doi:10.1016/S0140-6736(09)60237-3
8. Loiseau P, Busson M, Balere ML, et al. HLA Association with hematopoietic stem cell transplantation outcome: the number of mismatches at HLA-A, -B, -C, -DRB1, or -DQB1 is strongly associated with overall survival. *Biol Blood Marrow Transplant*. 2007;13(8):965-974. doi:10.1016/j.bbmt.2007.04.010
9. Theilgaard-Mönch K, Raaschou-Jensen K, Palm H, et al. Flow cytometric assessment of lymphocyte subsets, lymphoid progenitors, and hematopoietic stem cells in allogeneic stem cell grafts. *Bone Marrow Transplant*. 2001;28(11):1073-1082. doi:10.1038/sj.bmt.1703270
10. Pereira MR, Pouch SM, Scully B. Infections in Allogeneic Stem Cell Transplantation. In: Safdar A, ed. *Principles and Practice of Transplant Infectious Diseases*. Springer New York; 2019:209-226. doi:10.1007/978-1-4939-9034-4\_11
11. Zeiser R, Blazar BR. Acute Graft-versus-Host Disease. *N Engl J Med*. 2018;378(6):586. doi:10.1056/NEJMc1716969
12. Przepiorka D, Weisdorf D, Martin P, et al. 1994 Consensus Conference on Acute GVHD Grading. *Bone Marrow Transplant*. 1995;15(6):825-828.
13. Carreras E, Dufour C, Mohty M, Kröger N, eds. *The EBMT Handbook. Hematopoietic Stem Cell Transplantation and Cellular Therapies*. Springer, Cham; 2019. doi:https://doi.org/10.1007/978-3-030-02278-5
14. Naymagon S, Naymagon L, Wong SY, et al. Acute graft-versus-host disease of the gut: considerations for the gastroenterologist. *Nat Rev Gastroenterol Hepatol*. 2017;14(12):711-726. doi:10.1038/nrgastro.2017.126
15. Hill GR, Crawford JM, Cooke KR, Brinson YS, Pan L, Ferrara JL. Total body irradiation and acute graft-versus-host disease: the role of gastrointestinal damage and inflammatory cytokines. *Blood*. 1997;90(8):3204-3213.
16. Flowers MED, Inamoto Y, Carpenter PA, et al. Comparative analysis of risk factors for acute graft-versus-host disease and for chronic graft-versus-host disease according to National Institutes of Health consensus criteria. *Blood*. 2011;117(11):3214-3219. doi:10.1182/blood-2010-08-302109
17. Fischer JC, Wintges A, Haas T, Poeck H. Assessment of mucosal integrity by quantifying neutrophil granulocyte influx in murine models of acute intestinal injury. *Cell Immunol*. 2017;316:70-76. doi:10.1016/j.cellimm.2017.04.003
18. Johansson JE, Brune M, Ekman T. The gut mucosa barrier is preserved during allogeneic, haemopoietic stem cell transplantation with reduced intensity conditioning. *Bone Marrow Transplant*. 2001;28(8):737-742. doi:10.1038/sj.bmt.1703230
19. Johansson JE, Ekman T. Gut toxicity during hemopoietic stem cell transplantation may predict acute graft-versus-host disease severity in patients. *Dig Dis Sci*. 2007;52(9):2340-2345. doi:10.1007/s10620-006-9404-x
20. Taur Y, Xavier JB, Lipuma L, et al. Intestinal domination and the risk of bacteremia in patients undergoing allogeneic hematopoietic stem cell transplantation. *Clin Infect Dis*. 2012;55(7):905-914. doi:10.1093/cid/cis580
21. Vossen JM, Guiot HFL, Lankester AC, et al. Complete suppression of the gut microbiome prevents acute graft-versus-host disease following allogeneic bone marrow transplantation. *PLoS One*. 2014;9(9):e105706. doi:10.1371/journal.pone.0105706
22. van Bekkum DW, Roodenburg J, Heidt PJ, van der Waaij D. Mitigation of secondary disease of allogeneic mouse radiation chimeras by modification of the intestinal microflora. *J Natl Cancer Inst*. 1974;52(2):401-404. doi:10.1093/jnci/52.2.401
23. Storb R, Prentice RL, Buckner CD, et al. Graft-versus-host disease and survival in patients with aplastic anemia treated by marrow grafts from HLA-identical siblings. Beneficial effect of a protective environment. *N Engl J Med*. 1983;308(6):302-307. doi:10.1056/NEJM198302103080602
24. Shono Y, van den Brink MRM. Gut microbiota injury in allogeneic haematopoietic stem cell transplantation. *Nat Rev Cancer*. 2018;18(5):283-295. doi:10.1038/nrc.2018.10
25. Peled JU, Gomes ALC, Devlin SM, et al. Microbiota as Predictor of Mortality in Allogeneic Hematopoietic-Cell Transplantation. *N Engl J Med*. 2020;382(9):822-834. doi:10.1056/NEJMoa1900623
26. Stein-Thoeringer CK, Nichols KB, Lazrak A, et al. Lactose drives Enterococcus expansion to promote graft-

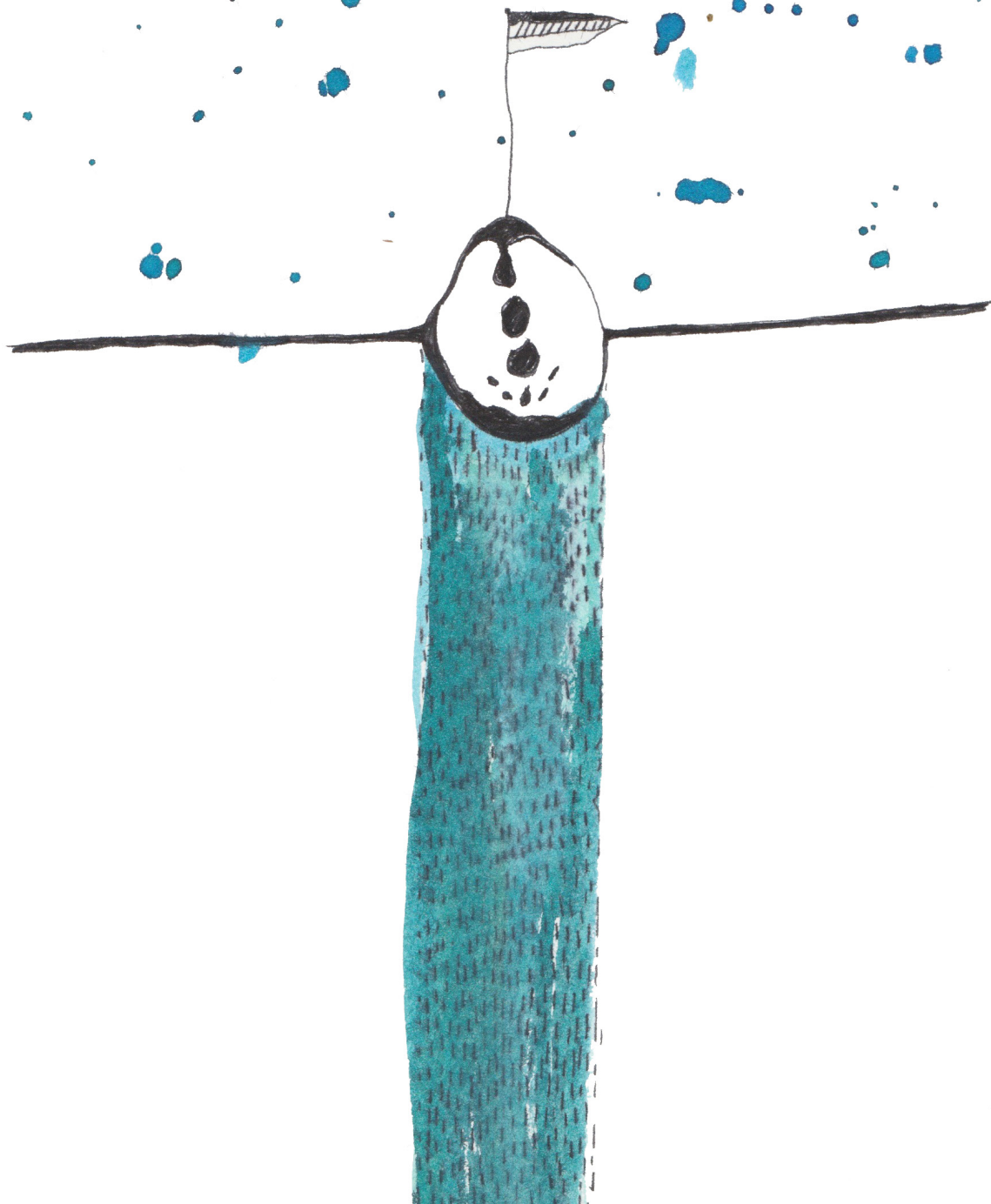


- versus-host disease. *Science*. 2019;366(6469):1143-1149. doi:10.1126/science.aax3760
27. Toubai T, Mathewson ND, Magenau J, Reddy P. Danger Signals and Graft-versus-host Disease: Current Understanding and Future Perspectives. *Front Immunol*. 2016;7:539. doi:10.3389/fimmu.2016.00539
  28. Jankovic D, Ganesan J, Bscheider M, et al. The Nlrp3 inflammasome regulates acute graft-versus-host disease. *J Exp Med*. 2013;210(10):1899-1910. doi:10.1084/jem.20130084
  29. Ferrara JL, Smith CM, Sheets J, Reddy P, Serody JS. Altered homeostatic regulation of innate and adaptive immunity in lower gastrointestinal tract GVHD pathogenesis. *J Clin Invest*. 2017;127(7):2441-2451. doi:10.1172/JCI90592
  30. Koyama M, Hill GR. The primacy of gastrointestinal tract antigen-presenting cells in lethal graft-versus-host disease. *Blood*. 2019;134(24):2139-2148. doi:10.1182/blood.2019000823
  31. Koyama M, Hill GR. Alloantigen presentation and graft-versus-host disease: fuel for the fire. *Blood*. 2016;127(24):2963-2970. doi:10.1182/blood-2016-02-697250
  32. Bombi JA, Nadal A, Carreras E, et al. Assessment of histopathologic changes in the colonic biopsy in acute graft-versus-host disease. *Am J Clin Pathol*. 1995;103(6):690-695. doi:10.1093/ajcp/103.6.690
  33. Epstein RJ, McDonald GB, Sale GE, Shulman HM, Thomas ED. The diagnostic accuracy of the rectal biopsy in acute graft-versus-host disease: a prospective study of thirteen patients. *Gastroenterology*. 1980;78(4):764-771.
  34. Martin PJ, Rizzo JD, Wingard JR, et al. First- and second-line systemic treatment of acute graft-versus-host disease: recommendations of the American Society of Blood and Marrow Transplantation. *Biol Blood Marrow Transplant*. 2012;18(8):1150-1163. doi:10.1016/j.bbmt.2012.04.005
  35. Penack O, Marchetti M, Ruutu T, et al. Prophylaxis and management of graft versus host disease after stem-cell transplantation for haematological malignancies: updated consensus recommendations of the European Society for Blood and Marrow Transplantation. *Lancet Haematol*. 2020;7(2):e157-e167. doi:10.1016/S2352-3026(19)30256-X
  36. Zeiser R, von Bubnoff N, Butler J, et al. Ruxolitinib for Glucocorticoid-Refractory Acute Graft-versus-Host Disease. *N Engl J Med*. 2020;382(19):1800-1810. doi:10.1056/NEJMoa1917635
  37. Lawitschka A, Lucchini G, Strahm B, et al. Pediatric acute graft-versus-host disease prophylaxis and treatment: surveyed real-life approach reveals dissimilarities compared to published recommendations. *Transpl Int*. 2020;33(7):762-772. doi:10.1111/tri.13601
  38. Furlong T, Martin P, Flowers MED, et al. Therapy with mycophenolate mofetil for refractory acute and chronic GVHD. *Bone Marrow Transplant*. 2009;44(11):739-748. doi:10.1038/bmt.2009.76
  39. MacMillan ML, Weisdorf DJ, Davies SM, et al. Early antithymocyte globulin therapy improves survival in patients with steroid-resistant acute graft-versus-host disease. *Biol Blood Marrow Transplant*. 2002;8(1):40-46. doi:10.1053/bbmt.2002.v8.pm11858189
  40. Gomez-Almaguer D, Ruiz-Arguelles GJ, del Carmen Tarin-Arzaga L, et al. Alemtuzumab for the treatment of steroid-refractory acute graft-versus-host disease. *Biol Blood Marrow Transplant*. 2008;14(1):10-15. doi:10.1016/j.bbmt.2007.08.052
  41. Massenkeil G, Rackwitz S, Genvresse I, Rosen O, Dörken B, Arnold R. Basiliximab is well tolerated and effective in the treatment of steroid-refractory acute graft-versus-host disease after allogeneic stem cell transplantation. *Bone Marrow Transplant*. 2002;30(12):899-903. doi:10.1038/sj.bmt.1703737
  42. Drobyski WR, Pasquini M, Kovatovic K, et al. Tocilizumab for the treatment of steroid refractory graft-versus-host disease. *Biol Blood Marrow Transplant*. 2011;17(12):1862-1868. doi:10.1016/j.bbmt.2011.07.001
  43. Couriel D, Saliba R, Hicks K, et al. Tumor necrosis factor-alpha blockade for the treatment of acute GVHD. *Blood*. 2004;104(3):649-654. doi:10.1182/blood-2003-12-4241
  44. Khandelwal P, Teusink-Cross A, Davies SM, et al. Ruxolitinib as Salvage Therapy in Steroid-Refractory Acute Graft-versus-Host Disease in Pediatric Hematopoietic Stem Cell Transplant Patients. *Biol Blood Marrow Transplant*. 2017;23(7):1122-1127. doi:10.1016/j.bbmt.2017.03.029
  45. Floisand Y, Lazarevic VL, Maertens J, et al. Safety and Effectiveness of Vedolizumab in Patients with Steroid-Refractory Gastrointestinal Acute Graft-versus-Host Disease: A Retrospective Record Review. *Biol Blood Marrow Transplant*. 2019;25(4):720-727. doi:10.1016/j.bbmt.2018.11.013
  46. Hashmi S, Ahmed M, Murad MH, et al. Survival after mesenchymal stromal cell therapy in steroid-refractory acute graft-versus-host disease: systematic review and meta-analysis. *Lancet Haematol*. 2016;3(1):e45-52. doi:10.1016/S2352-3026(15)00224-0
  47. Jagasia M, Arora M, Flowers MED, et al. Risk factors for acute GVHD and survival after hematopoietic cell transplantation. *Blood*. 2012;119(1):296-307. doi:10.1182/blood-2011-06-364265
  48. Nakasone H, Fukuda T, Kanda J, et al. Impact of conditioning intensity and TBI on acute GVHD after hematopoietic cell transplantation. *Bone Marrow Transplant*. 2015;50(4):559-565. doi:10.1038/bmt.2014.293
  49. Vokurka S, Steinerova K, Karas M, Koza V. Characteristics and risk factors of oral mucositis after allogeneic stem cell transplantation with FLU/MEL conditioning regimen in context with BU/CY2. *Bone Marrow Transplant*. 2009;44(9):601-605. doi:10.1038/bmt.2009.66
  50. Holler E, Butzhammer P, Schmid K, et al. Metagenomic analysis of the stool microbiome in patients receiving allogeneic stem cell transplantation: loss of diversity is associated with use of systemic antibiotics and more pronounced in gastrointestinal graft-versus-host disease. *Biol Blood Marrow Transplant*. 2014;20(5):640-645.

- doi:10.1016/j.bbmt.2014.01.030
51. Petersdorf EW, Longton GM, Anasetti C, et al. The significance of HLA-DRB1 matching on clinical outcome after HLA-A, B, DR identical unrelated donor marrow transplantation. *Blood*. 1995;86(4):1606-1613.
  52. Flomenberg N, Baxter-Lowe LA, Confer D, et al. Impact of HLA class I and class II high-resolution matching on outcomes of unrelated donor bone marrow transplantation: HLA-C mismatching is associated with a strong adverse effect on transplantation outcome. *Blood*. 2004;104(7):1923-1930. doi:10.1182/blood-2004-03-0803
  53. Jansen SA, Nijhuis W, Leavis HL, Riezebos-Brilman A, Lindemans CA, Schuurman R. Broad Virus Detection and Variant Discovery in Fecal Samples of Hematopoietic Transplant Recipients Using Targeted Sequence Capture Metagenomics. *Front Microbiol*. 2020;11:560179. doi:10.3389/fmicb.2020.560179
  54. Takashima S, Martin ML, Jansen SA, et al. T cell-derived interferon-gamma programs stem cell death in immune-mediated intestinal damage. *Sci Immunol*. 2019;4(42). doi:10.1126/sciimmunol.aay8556
  55. Zeiser R, Blazar BR. Preclinical models of acute and chronic graft-versus-host disease: how predictive are they for a successful clinical translation? *Blood*. 2016;127(25):3117-3126. doi:10.1182/blood-2016-02-699082
  56. Reddy P, Negrin R, Hill GR. Mouse models of bone marrow transplantation. *Biol Blood Marrow Transplant*. 2008;14(1 Suppl 1):129-135. doi:10.1016/j.bbmt.2007.10.021
  57. Beura LK, Hamilton SE, Bi K, et al. Normalizing the environment recapitulates adult human immune traits in laboratory mice. *Nature*. 2016;532(7600):512-516. doi:10.1038/nature17655
  58. Cooke KR, Kobzik L, Martin TR, et al. An experimental model of idiopathic pneumonia syndrome after bone marrow transplantation: I. The roles of minor H antigens and endotoxin. *Blood*. 1996;88(8):3230-3239.
  59. Barker N, van Es JH, Kuipers J, et al. Identification of stem cells in small intestine and colon by marker gene Lgr5. *Nature*. 2007;449(7165):1003-1007. doi:10.1038/nature06196
  60. Sato T, Vries RG, Snippert HJ, et al. Single Lgr5 stem cells build crypt-villus structures in vitro without a mesenchymal niche. *Nature*. 2009;459(7244):262-265. doi:10.1038/nature07935
  61. Sato T, Stange DE, Ferrante M, et al. Long-term expansion of epithelial organoids from human colon, adenoma, adenocarcinoma, and Barrett's epithelium. *Gastroenterology*. 2011;141(5):1762-1772. doi:10.1053/j.gastro.2011.07.050
  62. Sato T, Clevers H. Growing self-organizing mini-guts from a single intestinal stem cell: mechanism and applications. *Science*. 2013;340(6137):1190-1194. doi:10.1126/science.1234852
  63. Sato T, van Es JH, Snippert HJ, et al. Paneth cells constitute the niche for Lgr5 stem cells in intestinal crypts. *Nature*. 2011;469(7330):415-418. doi:10.1038/nature09637







# 2

## Clinical features, treatment and outcome of pediatric steroid refractory acute Graft-versus-Host disease: a multicenter study

Anne B. Verbeek\*, Suze A. Jansen\*, Erik G.J. von Asmuth,  
Arjan C. Lankester, Dorine Bresters, Marc Bierings, Alexander B. Mohseny,  
Caroline A. Lindemans, Emilie P. Budding.

Transplant Cell Ther. 2022 Sep;28(9):600.e1-600.e9.  
doi: 10.1016/j.jtct.2022.06.008. Epub 2022 Jun 16. PMID: 35717003.

# Abstract

## Background

Steroid refractory Acute Graft-versus-Host Disease (SR-aGvHD) is a severe complication in pediatric allogeneic hematopoietic stem cell transplantation (HSCT).

## Objective

We aimed to assess clinical course and outcomes of pediatric SR-aGvHD.

## Study Design

We performed a retrospective nationwide multicenter cohort study in the Netherlands. All patients aged 0-18 transplanted between 2010 and 2020 with SR-aGvHD were included. For each patient, weekly clinical aGvHD grade and stage, immunosuppressive treatment and clinical outcomes were collected. The primary study endpoint was clinical course of SR-aGvHD over time. As a secondary outcome, factors influencing overall survival and SR-aGvHD remission were identified using a multistate Cox model.

## Results

20% of transplanted children developed grade II-IV aGvHD, of which 51% (n=81) was SR-aGvHD. In these patients, second-line therapy was started at a median of 8 days after initial aGvHD-diagnosis. 49% of SR-aGvHD patients received three or more lines of therapy. One year after start of second-line therapy, 34 patients (42%) were alive and in remission of aGvHD, 14 patients (17%) had persistent GvHD and 33 patients (41%) had died. SR-aGvHD remission rate was lower in cord blood graft recipients than in bone marrow (BM) or peripheral blood stem cell (PBSC) recipients (HR 0.51, 0.27-0.94, p=0.031). Older age was associated with higher mortality (HR 2.62, 1.04-6.60, p=0.04, fourth quartile (aged 13.9-17.9) vs. first quartile (aged 0.175-3.01)). In BM/PBSC recipients older age was also associated with lower remission rates (HR 0.9, 0.83-0.96, p=0.004). Underlying diagnosis, donor matching or choice of second line therapy were not associated with outcome. Respiratory insufficiency due to pulmonary GvHD was a prominent cause of death (26% of deceased).

## Conclusions

Our study demonstrates that SR-aGvHD confers a high mortality risk in pediatric HSCT. Older age and use of CB grafts are associated with an unfavorable outcome. Multi-center studies investigating novel treatment strategies to prevent pediatric SR-aGvHD and inclusion of children in ongoing trials, together with timely initiation of second line interventions are pivotal to further reduce GvHD-related mortality.



## Introduction

Acute Graft-versus-Host Disease (aGvHD) is a major complication in pediatric patients after allogeneic hematopoietic stem cell transplantation (HSCT). More than half of the patients that develop aGvHD  $\geq$  grade II do not respond to first-line systemic corticosteroid treatment (steroid refractory SR))<sup>1-3</sup>, resulting in considerable morbidity and mortality<sup>4,5</sup>.

There is a broad choice of therapies for SR-aGvHD including MMF<sup>6,7</sup>, TNF- $\alpha$  inhibitors<sup>8-13</sup>, JAK/STAT inhibitors<sup>14-20</sup>,  $\alpha 4\beta 7$ -integrin inhibitors<sup>21-24</sup>, T cell inhibitors<sup>25-27</sup>, anti-CD52 antibodies<sup>28,29</sup>, CD25 inhibitors<sup>30-32</sup>, IL-6 inhibitors<sup>33-35</sup>, and mesenchymal stromal cells (MSCs)<sup>36</sup>. There are no prospective studies that evaluate which second-line treatment is most effective in children with aGvHD refractory to first-line high-dose corticosteroids. As a result, there is a lack of standardization in the management of pediatric SR-aGvHD, leading to a high variability in second-line treatment worldwide<sup>37</sup>. In order to establish more effective treatment strategies, it is important to meticulously evaluate current practices and outcomes over time.

In this retrospective multicenter cohort study, we evaluated the efficacy and safety of second-line treatment in children with grade II-IV SR-aGvHD following HSCT over the last 10 years in the Netherlands. In addition to endpoints such as aGvHD remission and survival, we report on aGvHD grade and staging in response to second-line therapy over time. This provides a detailed insight into the clinical course of SR-aGvHD in pediatric patients. Finally, we identified predictive factors for survival and SR-aGvHD remission using a multistate Cox model.

## Methods

We performed a retrospective nationwide cohort study in the two centers for pediatric HSCT in the Netherlands: the Willem-Alexander Children's Hospital/Leiden University Medical Center (LUMC) and the Princess Máxima Center for pediatric oncology (PMC)/Wilhelmina Children's Hospital, UMC Utrecht. All patients aged 0-18 years who suffered from grade II-IV SR-aGvHD between January 2010 and July 2020 were included in this study. There were no exclusion criteria.

SR disease was defined as progression of aGvHD within 3-5 days of first-line therapy initiation with  $\geq 2$  mg/kg/day of prednisone or failure to improve within 5-7 days after treatment initiation or incomplete response after more than 28 days of immunosuppressive treatment including steroids, according to the EBMT-NIH-CIBMTR Task Force position statement<sup>38</sup>. Data was collected by retrospective medical chart review. Onset of SR disease was determined by the treating physician's diagnosis and/or recorded disease progression

of each patient, as well as medication prescription data. Substitution of the initial GvHD prophylaxis for a similar agent (Cyclosporin A (CsA), sirolimus, tacrolimus, mycophenolate mofetil (MMF) or basiliximab) was not considered initiation of a new line of therapy. Only when one of these agents was added on top of already existing GvHD prophylaxis, it was considered a new line of therapy. Different therapeutic agents were categorized as combination therapy if they were started within 3 days of each other.

For each patient, weekly clinical aGvHD grade and stage were collected from start of aGvHD until the occurrence of persistent remission, onset of chronic GVHD or death. Both centers used the same institutional guidelines for aGvHD diagnosis and therapy. Grade and stage of aGvHD were copied from the medical chart if available, and otherwise retrospectively determined using the modified Glucksberg criteria (as used by the CIBMTR) based on percentage of affected skin reported at least weekly after physical examination by a supervising physician during grand rounds, stool volumes per m<sup>2</sup> body surface area recorded in daily digital nurse charts and/or bilirubin value available in digital lab records<sup>39</sup>. In case of missing data, the most recent known grade was imputed. Persistent remission was defined as grade 0 aGvHD (stage 0 in all organs) without relapse of aGvHD symptoms after tapering of immunosuppressive therapy<sup>38</sup>. Presence of chronic GvHD was determined based on the treating physician's diagnosis and medical chart review based on 2005 NIH consensus criteria<sup>40</sup>, and categorized as either quiescent or progressive<sup>38</sup>.

Matching of the stem cell donor (peripheral blood (PBSC), bone marrow (BM) or cord blood (CB)) was characterized with high-resolution (HR) HLA typing according to 10 alleles of five loci (HLA-A, B, C, DRB1, DQB1) where available. For CB transplantations without complete HR-typing (N=5), matching was based on serological typing for HLA-A and -B and HR-typing for HLA-DRB1 (6 alleles). Donor types included matched related (10/10 HLA matching), matched unrelated (10/10 or 6/6 HLA matching) and mismatched unrelated (less than 10/10 or 6/6 HLA matching).

Furthermore, data on all lines of immunosuppressive treatment, readmissions, Intensive Care Unit (ICU) admissions, viral reactivations, infections (excluding line associated coagulase-negative staphylococci infections), serious adverse events and complications during the first year since onset of SR disease were collected. GvHD prophylaxis regimens for BM and PBSC transplantations consisted generally of a calcineurin inhibitor (CsA/tacrolimus) with or without methotrexate or MMF. In the CB transplantation setting, a combination of a calcineurin inhibitor and prednisone 1 mg/kg was used, with the addition of MMF in case of an higher anticipated aGvHD risk. Serotherapy included treatment with either anti-thymocyte globulin or alemtuzumab. Infection prophylaxes were given per protocol and included HSV prophylaxis with valacyclovir until engraftment, VZV prophylaxis until 6-12 months post-transplant, gut decontamination antibiotics until engraftment and in case of

active gut aGvHD, oral yeast prophylaxis until engraftment and systemic anti-fungals for high-risk or aGvHD patients receiving more than 0,5 mg/kg steroids in combination with other lines of immune suppression. Viral reactivations were monitored by weekly viral load evaluation. Diagnosis of lower respiratory tract infections was either culture proven or presumed based on imaging. Bronchiolitis Obliterans Syndrome (BOS) was defined as diagnosed by typical HRCT changes, such as bronchial wall thickening, air trapping, or bronchiectasis, in the absence of signs of infection and, whenever pulmonary function testing could be done, abnormal pulmonary function test results (i.e. decrease in FEV1 of >20% or in FEV1/FVC of <70%)<sup>40,41</sup>. Medication related complications were defined as toxicity with direct treatment consequences, either by the ceasing or switching of the medication in question or the requirement of additional therapy.

Statistical analysis was performed in R version 4.0.3<sup>42</sup>. For all analyses, time was measured from onset of SR-aGvHD, i.e. start of second-line therapy. The primary study endpoint was clinical course of SR-aGvHD over time, represented by the proportions of patients with active aGvHD symptoms, patients with remission of aGvHD, patients with chronic GvHD and deceased patients during the first year since start of second-line therapy<sup>43</sup>.

As secondary study endpoints we aimed to investigate complication and infection rates and to identify factors influencing overall survival and SR-aGvHD remission using a multi-state Cox-regression model from the *mstate* package<sup>44-46</sup>. Three different states were included in this model: active GvHD, remission from aGvHD and death. Since predictive factors for death and aGvHD remission are the main interest of this study, chronic GvHD was not included as a separate state in our model. Patients that developed chronic GvHD while suffering from aGvHD remained in the 'GvHD state', while patients that developed chronic GvHD after they had achieved aGvHD remission remained in the 'remission state' for this analysis. Transition probabilities from one state to another were tested in a univariate analysis using the following covariates: age, gender, diagnosis, conditioning, stem cell source, donor type, time between aGvHD diagnosis and start of second-line therapy, type of second-line therapy and year of transplant, categorized as before or after 01-01-2015. Second-line therapy options were categorized as mesenchymal stromal cells (MSC), TNF-alpha inhibition (infliximab or etanercept), a combination of treatment modalities ("combination therapy") or other. The statistical methodology is explained in more detail in Supplementary Material 1. Informed consent for the use of patients' data for research purposes was collected from all included patients prior to HSCT. The Medical Research Ethics Committee Leiden The Hague Delft (MREC LDD) waived the need for additional specific informed consent in both centers for the analysis of the data used in the current study.

## Results

A total of 786 pediatric allogeneic HSCTs were performed in Leiden and Utrecht between 01-01-2010 and 01-07-2020. During this time, 158 patients (20%) suffered from grade II-IV aGvHD, which occurred after a median of 34.5 days. Of these 158 patients, 81 patients (51%) required second-line therapy due to absent or insufficient response to first-line treatment with corticosteroids. The current study focuses on these 81 SR-aGvHD patients, who all had a follow-up time until death or at least 1 year after start of second-line therapy. Patient, transplant and aGvHD characteristics are summarized in Table 1. Initial diagnosis of aGvHD occurred for 73 SR-aGvHD patients (90%) within the first 100 days after HSCT, whereas 8 SR-aGvHD patients (10%) developed aGvHD after more than 100 days (late onset), either in the context of immunosuppression tapering (N=5) or after a stem cell boost (N=3). The majority of patients had grade III as their maximal aGvHD grade (56%) and the gut was the most affected organ (77% at least stage 2 gut involvement). Weekly aGvHD grade and stage were available for 1162/1213 (96%) of evaluated weeks.

**Table 1. Patient, transplant and GvHD characteristics.**

Variable	Level	N=81
<b>Age at HSCT (median, IQR)</b>		8.9 (3.0 - 13.9)
<b>Sex (n, %)</b>	Male	47 (58%)
	Female	34 (42%)
<b>Diagnosis (n, %)</b>	Bone marrow failure	10 (12%)
	Hematologic malignancy	40 (49%)
	Hemoglobinopathy	4 (4.9%)
	Inborn errors of immunity	16 (20%)
	Inborn errors of metabolism	11 (14%)
<b>Donor (n, %)</b>	<b>BM/PBSC donors</b>	
	Matched related	13 (30%)
	Matched unrelated	19 (44%)
	Mismatched unrelated	11 (26%)
	<b>CB donors</b>	
	Matched related	0 (0%)
	Matched unrelated	2 (5.3%)
	Mismatched unrelated	36 (95%)
<b>Graft source (n, %)</b>	Bone marrow	36 (44%)
	Cord blood	36 (44%)
	Cord blood + bone marrow	1 (1.2%)
	Double cord blood	1 (1.2%)
	Peripheral blood	7 (8.6%)
<b>Conditioning (n, %)</b>	<b>Myeloablative chemotherapy</b>	64 (79%)
	Busulfan - Fludarabine based	43 (53%)
	Treosulfan - Fludarabine based	18 (22%)
	Other	3 (3.7%)
	<b>Myeloablative total body irradiation</b>	6 (7.4%)
	<b>Reduced intensity conditioning</b>	11 (14%)
	Busulfan - Fludarabine based	4 (4.9%)
	Other	7 (8.6%)



Table 1. Continued

Variable	Level	N=81
Serotherapy (n, %)	ATG (Genzyme)	56 (69%)
	Alemtuzumab	6 (7.4%)
	None	19 (23%)
Transplant number (n, %)	First transplant	72 (89%)
	Second transplant	8 (9.9%)
	Third transplant	1 (1.2%)
Stem cell boost (n%)	Yes (at d+67, d+91 and d+114 after HSCT)	3 (3.7%)
GvHD prophylaxis (n, %)	Calcineurin inhibitor (CsA/tacrolimus)	7 (8.6%)
	Calcineurin inhibitor + MMF/MTX	33 (41%)
	Calcineurin inhibitor + Prednisone	33 (41%)
	Calcineurin inhibitor + Prednisone + MMF	6 (7.4%)
	MMF + MTX/Prednisone	2 (2.5%)
<b>Days between HSCT and aGvHD grade <math>\geq</math> II (median, IQR)</b>		35 (24 - 55)
<b>Days between aGvHD grade <math>\geq</math> II and start second line therapy (median, IQR)</b>		8 (5 - 18)
aGvHD histologically confirmed (n, %)	Yes	74 (91%)
	No	7 (8.6%)
Maximum overall aGvHD grade (n, %)	II	13 (16%)
	III	45 (56%)
	IV	23 (28%)
Maximum skin aGvHD stage (n, %)	0-1	27 (33%)
	2-4	54 (67%)
Maximum gut aGvHD stage (n, %)	0-1	19 (23%)
	2-4	62 (77%)
Maximum liver aGvHD stage (n, %)	0-1	56 (69%)
	2-4	25 (31%)

In 34 patients (42%) second-line treatment was started within one week after aGvHD onset, in 36 patients (44%) after 8-28 days and in 11 patients (14%) after more than 28 days. MSC therapy was the most frequently used second-line therapy option (N=38, 47%), followed by infliximab (N=24, 30%). In 12 patients (15%) second-line therapy consisted of a combination of 2 or 3 of the following agents: infliximab, vedolizumab, basiliximab, MSC, etanercept, tacrolimus or ruxolitinib (Suppl. Table 1). 40 patients (49%) required an additional line of therapy (third or more) after second-line therapy (Suppl. Fig. 1).

One year after start of second-line therapy, 34 patients (42%) were alive and in remission of SR-aGvHD and 33 patients (41%) had died. 14 patients (17%) were still experiencing persistent GvHD symptoms 1 year after start of second-line therapy (Table 2, Fig. 1). Most patients achieved SR-aGvHD remission after more than 28 days since start of a line of therapy: 73,5% of the patients only receiving second-line therapy (25/35), 71% of the patients receiving a third line (5/7) and all patients receiving a fourth-line or more (5/5). Respiratory insufficiency (infectious and non-infectious) and multi-organ failure from GvHD and treatment related toxicity were the most frequent causes of death (35/38 total deaths) (Table 3). Non-infectious respiratory insufficiency due to BOS, Idiopathic Pneumonia Syndrome (IPS) or suspected

pulmonary GvHD contributed to 10/38 deaths (26%).

**Table 2. Main outcomes.**

Variable		N=81
<b>Death</b>	<b>Overall</b>	<b>38 (47%)</b>
	28 days	5 (6.2%)
	100 days	21 (26%)
	1 year	33 (41%)
	2 years	36 (44%)
<b>Remission of aGvHD (alive and in remission)</b>	<b>Overall (cumulative)</b>	<b>46 (57%)</b>
	28 days	9 (11%)
	100 days	25 (31%)
	1 year	34 (42%)
	2 years	38 (47%)
<b>Chronic GvHD (alive with cGvHD)</b>	<b>Overall (cumulative)</b>	<b>22 (27%)</b>
	Progressive	10 (12%)
	Quiescent	12 (15%)
	28 days	0 (0%)
	100 days	7 (8.6%)
	1 year	13 (16%)
	2 years	15 (19%)
<b>Relapse of underlying disease</b>		6 (7.4%)
<b>Retransplantation</b>		6 (7.4%)
<b>ICU admission within first year of start second line therapy</b>		38 (47%)
<b>Readmission within first year of start second line therapy</b>		42 (56%)

**Table 3. Causes of death.**

Cause of death	N=38
Multi organ failure (GvHD and treatment related toxicity)	14
Multi organ failure (GvHD and treatment related toxicity) and respiratory insufficiency (infectious)	1
Multi organ failure (GvHD and treatment related toxicity) and respiratory insufficiency (suspected pulmonary GvHD)	2
Sepsis	3
Relapse of underlying disease	2
Bronchiolitis Obliterans Syndrome with multiple infections	3
Respiratory insufficiency (infectious)	7
<i>Aspergillus infection</i>	4
<i>Other</i>	3
Respiratory insufficiency (non-infectious)	5
<i>Bronchiolitis Obliterans Syndrome</i>	2
<i>Idiopathic Pneumonia Syndrome</i>	2
<i>Suspected pulmonary GvHD</i>	1
Secondary malignancy (squamous cell carcinoma)	1



**Figure 1. Clinical course since start of second-line therapy and traditional Kaplan-Meier survival plot.** The proportions of patients with active GvHD symptoms, patients with remission of GvHD, patients with chronic GvHD and deceased patients during the first year since start of second-line therapy.

Using a multi-state model, we performed a covariate analysis for mortality and SR-aGvHD remission rates (Fig. 2, Table 4). In this covariate analysis, two patients who received a double CB graft and a composed graft (CB with haploidentical BM) were excluded. We found that older age was associated with higher mortality: children aged 13.9-17.9 (fourth quartile) had a significantly higher hazard of death compared to children aged 0.175-3.01 (first quartile) (HR 2.62, 1.04-6.60,  $p = 0.04$ ). CB graft recipients had a significantly lower chance to reach SR-aGvHD remission than BM or PBSC graft recipients (HR 0.51, 0.27-0.94,  $p = 0.031$ ) (Table 3). When modelling the interaction of graft source and age, the association between CB grafts and a lower chance of SR-aGvHD remission was even stronger (HR 0.18, 0.06-0.51,  $p = 0.001$ ). Older age was only associated with lower remission rates in children receiving BM/PBSC grafts (HR 0.9, 0.83-0.96,  $p = 0.004$ ). A graphical representation of the effects of graft source and age on clinical course is shown in Figure 3.

Over the years, preferred second-line treatment in our centers shifted from MSC monotherapy to a combination of multiple treatment modalities. There was no significant difference in outcome (survival or remission rates) between patients transplanted before or after 2015. None of the second-line treatments were significantly superior (Table 4).

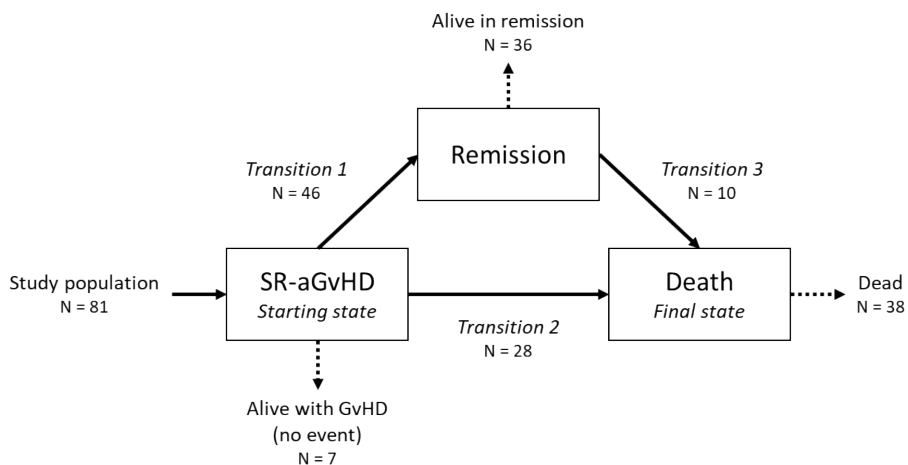


**Figure 2. Multi-state survival model with transitions and transition counts.**

Graphical representation of the multi-state survival model used for statistical analysis of covariates. The different states are indicated by boxes. All patients start in the GvHD state and remain in this state until a new event occurs (i.e. remission of GvHD or death). The arrows indicate possible transitions to other states. Death is the absorbing or final state which means no further transitions are possible when a patient has entered this state. The number of patients entering and leaving each state are depicted at the three different transitions. Dashed arrows indicate the number of patients in that stage at the end of their follow-up.



**Table 4. Multistate covariates.**

Multistate analysis with univariate testing of covariates						
Variable	Level	Outcome	HR	95% CI	p-value	
Age at transplant		Remission	0.97	0.92-1.02	0.2	
		Death	1.06	1.00-1.12	0.058	
Age (categorized in quartiles)	0.175-3.01 years (1 <sup>st</sup> quartile)	Remission	1.0			
		Death	1.0			
	3.01-8.9 years (2 <sup>nd</sup> quartile)	Remission	1.76	0.83-3.75	0.14	
		Death	1.07	0.37-3.05	>0.9	
	8.9-13.9 years (3 <sup>rd</sup> quartile)	Remission	0.69	0.29-1.63	0.4	
		Death	1.46	0.54-3.97	0.5	
	13.9-17.9 years (4 <sup>th</sup> quartile)	Remission	0.59	0.23-1.50	0.3	
		Death	2.62	1.04-6.60	<b>0.04</b>	
Gender	F	Remission	1.0			
		Death	1.0			
	M	Remission	0.64	0.36-1.16	0.14	
		Death	1.09	0.56-2.14	0.8	
Diagnosis	Bone marrow failure	Remission	1.0			
		Death	1.0			
	Hematologic malignancy	Remission	0.77	0.31-1.91	0.6	
		Death	0.68	0.27-1.71	0.4	
	Hemoglobinopathy	Remission	1.11	0.27-4.54	0.9	
		Death	0	0.00-Inf	>0.9	
	Inborn errors of immunity	Remission	0.69	0.24-1.95	0.5	
		Death	0.72	0.25-2.08	0.5	
	Inborn errors of metabolism	Remission	0.48	0.14-1.72	0.3	
		Death	0.7	0.21-2.29	0.6	
	Graft source	BM/PBSC	Remission	1.0		
			Death	1.0		
Cord blood		Remission	0.51	0.27-0.94	<b>0.031</b>	
		Death	1.35	0.70-2.62	0.4	
Donor	Matched related	Remission	1.0			
		Death	1.0			
	Matched unrelated	Remission	1.05	0.44-2.53	>0.9	
		Death	0.51	0.18-1.42	0.2	
	Mismatched unrelated	Remission	0.78	0.35-1.75	0.6	
		Death	0.8	0.35-1.79	0.6	
Time until start second line	<1 week	Remission	1.0			
		Death	1.0			
	8-28 days	Remission	1.14	0.61-2.12	0.7	
		Death	0.89	0.45-1.77	0.7	
	>28 days	Remission	0.6	0.22-1.62	0.3	
		Death	0.61	0.20-1.81	0.4	
Second line therapy	MSC	Remission	1.0			
		Death	1.0			
	TNF-alpha inhibitor	Remission	1.35	0.69-2.64	0.4	
		Death	0.6	0.26-1.38	0.2	
	Combination therapy	Remission	1.29	0.54-3.10	0.6	
		Death	1.28	0.53-3.06	0.6	
	Other	Remission	0.81	0.24-2.77	0.7	
		Death	0.92	0.27-3.14	0.9	

**Table 4.** *Continued*

<b>Multistate analysis with univariate testing of covariates</b>					
<b>Variable</b>	<b>Level</b>	<b>Outcome</b>	<b>HR</b>	<b>95% CI</b>	<b>p-value</b>
Conditioning	MAC (chemotherapy)	Remission	1.0		
		Death	1.0		
	MAC (TBI)	Remission	1.72	0.6-4.91	0.3
		Death	2.02	0.69-5.86	0.2
	RIC	Remission	1.45	0.61-3.47	0.4
		Death	2.06	0.89-4.78	0.091
Before or after 2015	Before	Remission	1.0		
		Death	1.0		
	After	Remission	1.01	0.55-1.85	>0.9
		Death	0.77	0.4-1.49	0.4
<b>Multistate analysis with interaction of age and graft source</b>					
<b>Variable</b>	<b>Level</b>	<b>Outcome</b>	<b>HR</b>	<b>95% CI</b>	<b>p-value</b>
Age in cord blood grafts		Remission	0.99	0.91-1.07	0.8
		Death	1.07	1.00-1.14	0.056
Age in BM/PBSC grafts		Remission	0.9	0.83-0.96	<b>0.004</b>
		Death	1.06	0.96-1.17	0.2
Graft source	BM/PBSC	Remission	1.0		
		Death	1.0		
	Cord blood	Remission	0.18	0.06-0.51	<b>0.001</b>
		Death	1.5	0.34-6.59	0.6

Infections within the first year since start of second-line therapy were frequent, occurring in 65/81 patients (80%), including bacterial (54% of patients), fungal (26% of patients) and viral infections (19% of patients) and viral reactivations (52% of patients) (Suppl. Table 2). The timing of infections and viral reactivations relative to the start of second-line therapy, and the GvHD activity at that time can be found in Suppl. Table 3. BOS (14/81), thrombotic microangiopathy (TMA) (13/81), cytopenia (12/81) and renal insufficiency (10/81) were the most common non-infectious complications. In total 38 patients (47%) were admitted to the ICU at least once within the first year since start of second-line therapy. 37 patients (46%) experienced medication toxicity and/or an Adverse Drug Reaction. In patients that were still alive after 1 year, the median duration of the hospital admission in which SR-aGvHD was diagnosed was 29 days. The disease burden in this population was high: of the 48 patients that were still alive 1 year after start of second-line therapy, 41 patients (85%) had experienced one or more of the following: ICU admission, readmission, chronic GvHD/BOS, relapse of underlying disease, retransplantation or secondary graft failure.

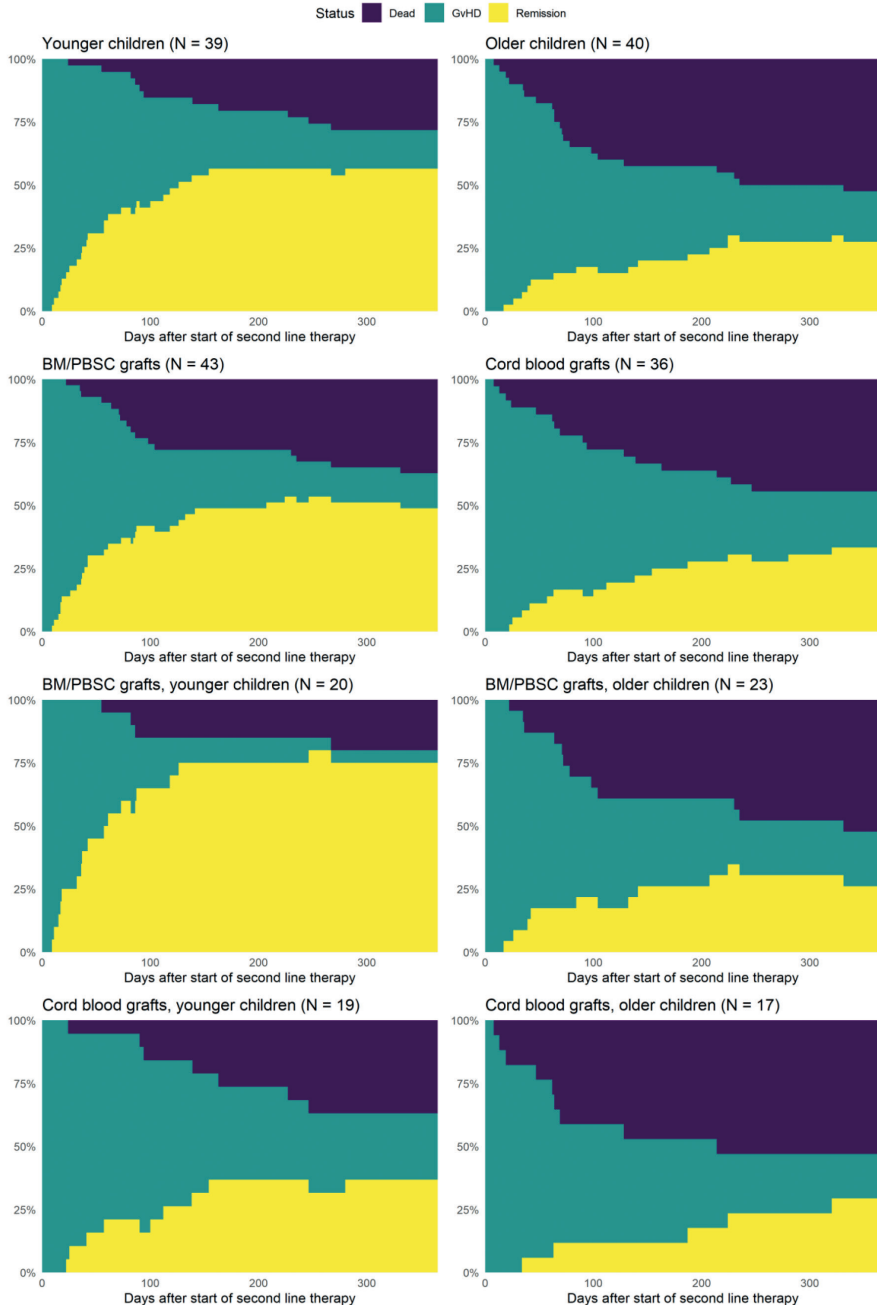


**Figure 3. Clinical course since start of second-line therapy in specified subgroups.**

The proportions of patients with active GvHD symptoms, patients with remission of GvHD, patients with chronic GvHD and deceased patients during the first year since start of second-line therapy, in younger children <8,8 years versus older children  $\geq$  8,8 years, BM/PBSC grafts and CB grafts, and combinations. Two patients who received a double CB graft and a composed graft were excluded.

## Discussion

SR-aGvHD in pediatric HSCT patients is a severe complication with a poor prognosis. Similar to other studies<sup>16,47,48</sup>, 47% of the 81 children with SR-aGvHD died in our study. There is a lack of evidence from prospective trials to help guide clinicians in determining which second-line treatment is most effective and safe in children with SR-aGvHD. Conducting clinical trials in this patient group is challenging. First of all, the number of patients with this condition is relatively low, hampering required statistical power to meet envisioned endpoints. Secondly, due to the severity of the disease and poor prognosis, multiple lines of treatment are often given concomitantly<sup>37</sup>, possibly leading to exclusion of the trial initially enrolled in based on formulated exclusion criteria.

Because of the lack of prospective trials, it is of vital importance to carefully review current practice. While, in general, survival rates are well reported, outcomes such as aGvHD remission are often only reported at day 28 after initiation of the investigative agent<sup>19,49–53</sup>, which was established as the best endpoint for treatment trials<sup>54</sup>. In this study we provide a detailed description of the clinical course of a relatively large group of pediatric SR-aGvHD patients during the course of one year. Persistent remission occurred in only 9 patients before day 28 since start of second-line therapy in our cohort (Table 2). Many patients experienced remission of their aGvHD after day 28 since start of the most recent line of therapy, which suggests that a 28-day period is too limited for the evaluation of a therapeutic effect in SR-aGvHD.

About half of the patients in our cohort with grade II-IV acute GvHD had steroid-refractory disease, similar to earlier reports<sup>1–3</sup>. Most patients with steroid-refractory disease are severely affected, with 84% in our study suffering from grade III-IV GvHD. Similar to other studies<sup>12,28,47,48,53</sup>, in our cohort patients with SR-aGvHD have a higher prevalence of liver involvement (36%) than patients with steroid-responsive aGvHD. In addition to the classical GvHD target organs being affected, many SR-aGvHD patients also suffer from other organ dysfunction, such as kidney, lung and endocrine dysfunction and cytopenia. This could either be due to these patients being generally ill, treatment toxicity, infection or direct targeting by alloreactivity. This underlines that pediatric SR-aGvHD is a multi-system disease with a high morbidity and mortality<sup>55</sup>, associated with substantial healthcare utilization and costs<sup>55,56</sup>.

In our cohort the TNF- $\alpha$  inhibitor infliximab and cell therapy with MSCs were most frequently prescribed, probably due to clinical studies in the two centers and the relatively favorable toxicity profiles<sup>8,12,36</sup>. The increased availability of new agents is having a clear impact on treatment choices in recent years. MSCs were the only prescribed second-line therapy in the first three years of our cohort, whereas multiple different agents were used in the last





few years. None of the specific second-line therapy options was associated with improved outcome, but this analysis is limited by the fact that therapy was highly individualized.

Complications and toxicities associated with immunosuppressive therapy in the aGvHD setting were highly prevalent in our SR-aGvHD cohort. Similar to other pediatric SR-aGvHD studies the majority of patients experienced infections and/or viral reactivations<sup>19,28,48–50,52,53</sup>. In about one-third of deceased patients, infections were considered causal. TMA was a common non-infectious complication in our cohort. Since aGvHD is a risk factor for the development of TMA in both children<sup>57,58</sup> and adults<sup>59</sup>, this finding was not surprising. The most frequently observed non-infectious complication in our cohort was the development of lung disease related to HSCT, such as BOS and IPS. In another pediatric SR-aGvHD cohort study BOS was also frequently observed<sup>16</sup>, but in most studies BOS and IPS are not separately reported from general chronic GvHD. In our cohort, 26% of the patient deaths were attributed to non-infectious, HSCT-related respiratory failure. Pulmonary involvement thus represents a significant clinical challenge in pediatric SR-aGvHD patients and more research is required to understand how to manage HSCT-related lung complications to improve outcome<sup>60</sup>.

To our knowledge only few studies identified risk factors for outcomes of SR-GvHD in children<sup>47</sup>. In our study, age and the use of CB grafts were associated with worse prognosis. Older age was associated with increased mortality, and with reduced SR-aGvHD remission rates in those transplanted with BM/PBSC grafts. In adults, older age has long been recognized as a risk factor for the development of GvHD<sup>61</sup>, worse outcomes in HSCT overall<sup>2,62</sup>, and higher mortality in adults with SR-aGvHD<sup>63</sup>. In children, the relationship between age and SR-aGvHD outcomes has not previously been reported. In addition, we found that CB grafts were associated with a lower chance of achieving remission of SR-aGvHD, irrespective of recipient age. CB grafts have generally been associated with a lower risk of GvHD in children<sup>64</sup>, leading to the acceptance of higher levels of HLA mismatching in this setting. In most cases, aGvHD after CB transplantation develops despite GvHD prophylaxis with prednisone 1 mg/kg. As such, it may be argued that aGvHD in the CB setting is already steroid-unresponsive to some extent. In adults, transplantation with a CB graft has been associated with the development of SR-GvHD<sup>65</sup>. However, it is still unknown why SR-aGvHD after transplantation with a CB graft is more refractory to additional immunosuppressive treatment than SR-aGvHD in a child that received a BM or PBSC graft. Because SR-aGvHD in the context of CB transplantation is associated with worse outcome, even more timely introduction of second-line treatment may be warranted in this setting. Other known predictive factors for GvHD severity, including degree of donor matching, malignancy as HSCT indication and MAC TBI conditioning<sup>2,66–68</sup> were not associated with worse outcomes in our SR-GvHD cohort.

There are several limitations to our study. Firstly, data was retrospectively collected, at risk of reporting bias due to missing information. Secondly, the studied group is heterogeneous, and received multiple lines of therapy concomitantly. That, together with a relatively small study size, complicates drawing more definitive conclusions.

In conclusion, the development of SR-aGvHD in children after allogeneic HSCT is still associated with both high morbidity and mortality. Older age of the recipient at transplant is a risk factor for death in the whole population, and in recipients of PBSC/BM grafts for lower remission rates of SR-aGvHD. In addition, we see reduced SR-aGvHD remission rates in children transplanted with a CB graft without a significant effect on survival. Choice of, and time to second-line therapy were not associated with differences in outcomes. The outcomes presented in this study emphasize the unmet need for multi-center studies investigating novel therapies for pediatric patients and inclusion of pediatric cohorts on ongoing trials for SR-aGvHD. The cohort described here can serve as a reference for future studies investigating novel treatments and treatment guidelines for SR-aGvHD in pediatric patients, which will hopefully improve the outcomes for these severely ill children.

### **Acknowledgements**

The authors would like to acknowledge all patients and their families as well as the clinical staff involved in the care of HSCT pediatric patients in Leiden and Utrecht.

### **Author contributions**

ABV and SAJ collected the data, performed analysis, interpreted data and drafted the manuscript. EGJA assisted with the statistical analysis. DB, MB and ABM assisted in the data collection. ACL provided expert advice. CAL and EPB supervised the research. All authors contributed to the manuscript.

### **Competing interests**

The authors have no competing interests.

## References

1. Van Lint MT, Uderzo C, Locasciulli A, et al. Early treatment of acute graft-versus-host disease with high- or low-dose 6-methylprednisolone: a multicenter randomized trial from the Italian Group for Bone Marrow Transplantation. *Blood*. 1998;92(7):2288-2293.
2. Martin PJ, Rizzo JD, Wingard JR, et al. First- and second-line systemic treatment of acute graft-versus-host disease: recommendations of the American Society of Blood and Marrow Transplantation. *Biol Blood Marrow Transplant*. 2012;18(8):1150-1163. doi:10.1016/j.bbmt.2012.04.005
3. Penack O, Marchetti M, Ruutu T, et al. Prophylaxis and management of graft versus host disease after stem-cell transplantation for haematological malignancies: updated consensus recommendations of the European Society for Blood and Marrow Transplantation. *Lancet Haematol*. 2020;7(2):e157-e167. doi:10.1016/S2352-3026(19)30256-X
4. Ferrara JLM, Levine JE, Reddy P, Holler E. Graft-versus-host disease. *Lancet*. 2009;373(9674):1550-1561. doi:10.1016/S0140-6736(09)60237-3
5. Deeg HJ. How I treat refractory acute GVHD. *Blood*. 2007;109(10):4119-4126. doi:10.1182/blood-2006-12-041889
6. Kim JG, Sohn SK, Kim DH, et al. Different efficacy of mycophenolate mofetil as salvage treatment for acute and chronic GVHD after allogeneic stem cell transplant. *European journal of haematology*. 2004;73(1):56-61. doi:10.1111/j.1600-0609.2004.00247.x
7. Furlong T, Martin P, Flowers MED, et al. Therapy with mycophenolate mofetil for refractory acute and chronic GVHD. *Bone Marrow Transplant*. 2009;44(11):739-748. doi:10.1038/bmt.2009.76
8. Sleight BS, Chan KW, Braun TM, Serrano A, Gilman AL. Infliximab for GVHD therapy in children. *Bone Marrow Transplant*. 2007;40(5):473-480. doi:10.1038/sj.bmt.1705761
9. Jacobsohn DA, Hallick J, Anders V, McMillan S, Morris L, Vogelsang GB. Infliximab for steroid-refractory acute GVHD: a case series. *Am J Hematol*. 2003;74(2):119-124. doi:10.1002/ajh.10392
10. Patriarca F, Sperotto A, Damiani D, et al. Infliximab treatment for steroid-refractory acute graft-versus-host disease. *Haematologica*. 2004;89(11):1352-1359.
11. Couriel D, Saliba R, Hicks K, et al. Tumor necrosis factor-alpha blockade for the treatment of acute GVHD. *Blood*. 2004;104(3):649-654. doi:10.1182/blood-2003-12-4241
12. Yang J, Cheuk DKL, Ha SY, et al. Infliximab for steroid refractory or dependent gastrointestinal acute graft-versus-host disease in children after allogeneic hematopoietic stem cell transplantation. *Pediatr Transplant*. 2012;16(7):771-778. doi:10.1111/j.1399-3046.2012.01756.x
13. Rao K, Rao A, Karlsson H, Jagani M, Veys P, Amrolia PJ. Improved survival and preserved antiviral responses after combination therapy with daclizumab and infliximab in steroid-refractory graft-versus-host disease. *Journal of pediatric hematology/oncology*. 2009;31(6):456-461. doi:10.1097/MPH.0b013e31819daf60
14. Spoerl S, Mathew NR, Bscheider M, et al. Activity of therapeutic JAK 1/2 blockade in graft-versus-host disease. *Blood*. 2014;123(24):3832-3842. doi:10.1182/blood-2013-12-543736
15. Zeiser R, Burchert A, Lengerke C, et al. Ruxolitinib in corticosteroid-refractory graft-versus-host disease after allogeneic stem cell transplantation: a multicenter survey. *Leukemia*. 2015;29(10):2062-2068. doi:10.1038/leu.2015.212
16. Khandelwal P, Teusink-Cross A, Davies SM, et al. Ruxolitinib as Salvage Therapy in Steroid-Refractory Acute Graft-versus-Host Disease in Pediatric Hematopoietic Stem Cell Transplant Patients. *Biol Blood Marrow Transplant*. 2017;23(7):1122-1127. doi:10.1016/j.bbmt.2017.03.029
17. González Vicent M, Molina B, González de Pablo J, Castillo A, Díaz MÁ. Ruxolitinib treatment for steroid refractory acute and chronic graft vs host disease in children: Clinical and immunological results. *American journal of hematology*. 2019;94(3):319-326. doi:10.1002/ajh.25376
18. Abedin S, McKenna E, Chhabra S, et al. Efficacy, Toxicity, and Infectious Complications in Ruxolitinib-Treated Patients with Corticosteroid-Refractory Graft-versus-Host Disease after Hematopoietic Cell Transplantation. *Biology of blood and marrow transplantation : journal of the American Society for Blood and Marrow Transplantation*. 2019;25(8):1689-1694. doi:10.1016/j.bbmt.2019.04.003
19. Laisne L, Neven B, Dalle JH, et al. Ruxolitinib in children with steroid-refractory acute graft-versus-host disease: A retrospective multicenter study of the pediatric group of SFGM-TC. *Pediatr Blood Cancer*. 2020;67(9):e28233. doi:10.1002/pbc.28233
20. Uygun V, Karasu G, Daloğlu H, et al. Ruxolitinib salvage therapy is effective for steroid-refractory graft-versus-host disease in children: A single-center experience. *Pediatric blood & cancer*. 2020;67(4):e28190. doi:10.1002/pbc.28190
21. Coltoff A, Lancman G, Kim S, Steinberg A. Vedolizumab for treatment of steroid-refractory lower gastrointestinal acute graft-versus-host disease. *Bone marrow transplantation*. 2018;53(7):900-904. doi:10.1038/s41409-018-0094-8
22. Danylesko I, Bukauskas A, Paulson M, et al. Anti-alpha4beta7 integrin monoclonal antibody (vedolizumab) for the treatment of steroid-resistant severe intestinal acute graft-versus-host disease. *Bone marrow transplantation*. 2019;54(7):987-993. doi:10.1038/s41409-018-0364-5



23. Floisand Y, Lazarevic VL, Maertens J, et al. Safety and Effectiveness of Vedolizumab in Patients with Steroid-Refractory Gastrointestinal Acute Graft-versus-Host Disease: A Retrospective Record Review. *Biol Blood Marrow Transplant.* 2019;25(4):720-727. doi:10.1016/j.bbmt.2018.11.013
24. Pai V, Abu-Arja R, Auletta JJ, Rangarajan HG. Successful treatment of steroid-refractory gastrointestinal acute graft-versus-host disease with adjuvant vedolizumab therapy in a pediatric allogeneic stem cell transplant recipient. *Pediatric blood & cancer.* 2020;67(8):e28298. doi:10.1002/pbc.28298
25. MacMillan ML, Weisdorf DJ, Davies SM, et al. Early antithymocyte globulin therapy improves survival in patients with steroid-resistant acute graft-versus-host disease. *Biol Blood Marrow Transplant.* 2002;8(1):40-46. doi:10.1053/bbmt.2002.v8.pm11858189
26. Macmillan ML, Couriel D, Weisdorf DJ, et al. A phase 2/3 multicenter randomized clinical trial of ABX-CBL versus ATG as secondary therapy for steroid-resistant acute graft-versus-host disease. *Blood.* 2007;109(6):2657-2662. doi:10.1182/blood-2006-08-013995
27. Dugan MJ, DeFor TE, Steinbuch M, Filipovich AH, Weisdorf DJ. ATG plus corticosteroid therapy for acute graft-versus-host disease: predictors of response and survival. *Annals of hematology.* 1997;75(1-2):41-46. doi:10.1007/s002770050310
28. Khandelwal P, Emoto C, Fukuda T, et al. A Prospective Study of Alemtuzumab as a Second-Line Agent for Steroid-Refractory Acute Graft-versus-Host Disease in Pediatric and Young Adult Allogeneic Hematopoietic Stem Cell Transplantation. *Biol Blood Marrow Transplant.* 2016;22(12):2220-2225. doi:10.1016/j.bbmt.2016.09.016
29. Gomez-Almaguer D, Ruiz-Arguelles GJ, del Carmen Tarin-Arzaga L, et al. Alemtuzumab for the treatment of steroid-refractory acute graft-versus-host disease. *Biol Blood Marrow Transplant.* 2008;14(1):10-15. doi:10.1016/j.bbmt.2007.08.052
30. Funke VAM, de Medeiros CR, Setubal DC, et al. Therapy for severe refractory acute graft-versus-host disease with basiliximab, a selective interleukin-2 receptor antagonist. *Bone marrow transplantation.* 2006;37(10):961-965. doi:10.1038/sj.bmt.1705306
31. Massenkeil G, Rackwitz S, Genvresse I, Rosen O, Dörken B, Arnold R. Basiliximab is well tolerated and effective in the treatment of steroid-refractory acute graft-versus-host disease after allogeneic stem cell transplantation. *Bone Marrow Transplant.* 2002;30(12):899-903. doi:10.1038/sj.bmt.1703737
32. Tan Y, Xiao H, Wu D, et al. Combining therapeutic antibodies using basiliximab and etanercept for severe steroid-refractory acute graft-versus-host disease: A multi-center prospective study. *Oncoimmunology.* 2017;6(3):e1277307. doi:10.1080/2162402X.2016.1277307
33. Drobyski WR, Pasquini M, Kovatovic K, et al. Tocilizumab for the treatment of steroid refractory graft-versus-host disease. *Biol Blood Marrow Transplant.* 2011;17(12):1862-1868. doi:10.1016/j.bbmt.2011.07.001
34. Ganetsky A, Frey N V, Hexner EO, et al. Tocilizumab for the treatment of severe steroid-refractory acute graft-versus-host disease of the lower gastrointestinal tract. *Bone marrow transplantation.* 2019;54(2):212-217. doi:10.1038/s41409-018-0236-z
35. Kolb M, Bhatia M, Madina GG, Satwani P. Effective use of tocilizumab for the treatment of steroid-refractory gastrointestinal acute graft versus host disease in a child with very high levels of serum interleukin-6. *Pediatric blood & cancer.* 2015;62(2):362-363. doi:10.1002/pbc.25231
36. Hashmi S, Ahmed M, Murad MH, et al. Survival after mesenchymal stromal cell therapy in steroid-refractory acute graft-versus-host disease: systematic review and meta-analysis. *The Lancet Haematology.* 2016;3(1):e45-52. doi:10.1016/S2352-3026(15)00224-0
37. Lawitschka A, Lucchini G, Strahm B, et al. Pediatric acute graft-versus-host disease prophylaxis and treatment: surveyed real-life approach reveals dissimilarities compared to published recommendations. *Transpl Int.* 2020;33(7):762-772. doi:10.1111/tri.13601
38. Schoemans HM, Lee SJ, Ferrara JL, et al. EBMT-NIH-CIBMTR Task Force position statement on standardized terminology & guidance for graft-versus-host disease assessment. *Bone marrow transplantation.* 2018;53(11):1401-1415. doi:10.1038/s41409-018-0204-7
39. Przepiorka D, Weisdorf D, Martin P, et al. 1994 Consensus Conference on Acute GVHD Grading. *Bone Marrow Transplant.* 1995;15(6):825-828.
40. Filipovich AH, Weisdorf D, Pavletic S, et al. National Institutes of Health consensus development project on criteria for clinical trials in chronic graft-versus-host disease: I. Diagnosis and staging working group report. *Biology of blood and marrow transplantation: journal of the American Society for Blood and Marrow Transplantation.* 2005;11(12):945-956. doi:10.1016/j.bbmt.2005.09.004
41. Afessa B, Peters SG. Chronic lung disease after hematopoietic stem cell transplantation. *Clinics in chest medicine.* 2005;26(4):571-586, vi. doi:10.1016/j.ccm.2005.06.012
42. R Core Team. R: A language and environment for statistical computing. Published online 2021.
43. Wickham H. ggplot2: Elegant Graphics for Data Analysis. Published online 2016.
44. de Wreede LC, Fiocco M, Putter H. The mstate package for estimation and prediction in non- and semi-parametric multi-state and competing risks models. *Computer methods and programs in biomedicine.* 2010;99(3):261-274. doi:10.1016/j.cmpb.2010.01.001
45. Putter H, Fiocco M, Geskus RB. Tutorial in biostatistics: competing risks and multi-state models. *Statistics in medicine.* 2007;26(11):2389-2430. doi:10.1002/sim.2712

46. de Wreede LC, Fiocco M, Putter H. mstate: An R Package for the Analysis of Competing Risks and Multi-State Models. *Journal of Statistical Software*. 2011;38(7 SE-Articles):1-30. doi:10.18637/jss.v038.i07
47. Berger M, Pessolano R, Carraro F, Saglio F, Vassallo E, Fagioli F. Steroid-refractory acute graft-versus-host disease graded III-IV in pediatric patients. A mono-institutional experience with a long-term follow-up. *Pediatr Transplant*. 2020;24(7):e13806. doi:10.1111/ptr.13806
48. Faraci M, Calevo MG, Giardino S, et al. Etanercept as Treatment of Steroid-Refractory Acute Graft-versus-Host Disease in Pediatric Patients. *Biol Blood Marrow Transplant*. 2019;25(4):743-748. doi:10.1016/j.bbmt.2018.11.017
49. Kurtzberg J, Abdel-Azim H, Carpenter P, et al. A Phase 3, Single-Arm, Prospective Study of Remestemcel-L, Ex Vivo Culture-Expanded Adult Human Mesenchymal Stromal Cells for the Treatment of Pediatric Patients Who Failed to Respond to Steroid Treatment for Acute Graft-versus-Host Disease. *Biol Blood Marrow Transplant*. 2020;26(5):845-854. doi:10.1016/j.bbmt.2020.01.018
50. Tang FF, Cheng YF, Xu LP, et al. Basiliximab as Treatment for Steroid-Refractory Acute Graft-versus-Host Disease in Pediatric Patients after Haploidentical Hematopoietic Stem Cell Transplantation. *Biol Blood Marrow Transplant*. 2020;26(2):351-357. doi:10.1016/j.bbmt.2019.10.031
51. Inagaki J, Fukano R, Kodama Y, Nishimura M, Shimokawa M, Okamura J. Safety and efficacy of low-dose methotrexate for pediatric patients with steroid-refractory acute graft-versus-host disease after hematopoietic stem cell transplantation. *Ann Hematol*. 2014;93(4):645-651. doi:10.1007/s00277-013-1923-x
52. Inagaki J, Kodama Y, Fukano R, Noguchi M, Okamura J. Mycophenolate mofetil for treatment of steroid-refractory acute graft-versus-host disease after pediatric hematopoietic stem cell transplantation. *Pediatr Transplant*. 2015;19(6):652-658. doi:10.1111/ptr.12545
53. Kurtzberg J, Prockop S, Teira P, et al. Allogeneic human mesenchymal stem cell therapy (remestemcel-L, Prochymal) as a rescue agent for severe refractory acute graft-versus-host disease in pediatric patients. *Biol Blood Marrow Transplant*. 2014;20(2):229-235. doi:10.1016/j.bbmt.2013.11.001
54. MacMillan ML, DeFor TE, Weisdorf DJ. The best endpoint for acute GVHD treatment trials. *Blood*. 2010;115(26):5412-5417. doi:10.1182/blood-2009-12-258442
55. Grabner M, Strati E, Sandman K, Forsythe A. Economic burden of acute steroid-refractory graft-versus-host disease in commercially insured pediatric patients. *Journal of managed care & specialty pharmacy*. 2021;27(5):607-614. doi:10.18553/jmcp.2021.27.5.607
56. Ricci A, Jin Z, Broglie L, et al. Healthcare utilization and financial impact of acute-graft-versus host disease among children undergoing allogeneic hematopoietic cell transplantation. *Bone marrow transplantation*. 2020;55(2):384-392. doi:10.1038/s41409-019-0688-9
57. Elfeky R, Lucchini G, Lum SH, et al. New insights into risk factors for transplant-associated thrombotic microangiopathy in pediatric HSCT. *Blood advances*. 2020;4(11):2418-2429. doi:10.1182/bloodadvances.2019001315
58. Schoettler M, Lehmann LE, Margossian S, et al. Risk factors for transplant-associated thrombotic microangiopathy and mortality in a pediatric cohort. *Blood advances*. 2020;4(11):2536-2547. doi:10.1182/bloodadvances.2019001242
59. Vasu S, Bostic MG, Zhao Q, et al. Acute GVHD, BK hemorrhagic cystitis and age are risk factors for transplant-associated thrombotic microangiopathy in adults. *Blood advances*. Published online December 2021. doi:10.1182/bloodadvances.2021004933
60. Wilhelmsson M, Vatanen A, Borgström B, et al. Adverse health events and late mortality after pediatric allogeneic hematopoietic SCT—two decades of longitudinal follow-up. *Bone Marrow Transplant*. 2015;50(6):850-857. doi:10.1038/bmt.2015.43
61. Qayed M, Wang T, Hemmer MT, et al. Influence of Age on Acute and Chronic GVHD in Children Undergoing HLA-Identical Sibling Bone Marrow Transplantation for Acute Leukemia: Implications for Prophylaxis. *Biology of blood and marrow transplantation : journal of the American Society for Blood and Marrow Transplantation*. 2018;24(3):521-528. doi:10.1016/j.bbmt.2017.11.004
62. Friend BD, Schiller GJ. Beyond steroids: A systematic review and proposed solutions to managing acute graft-versus-host disease in adolescents and young adults. *Blood reviews*. Published online September 2021:100886. doi:10.1016/j.blre.2021.100886
63. Rashidi A, DeFor TE, Holtan SG, Blazar BR, Weisdorf DJ, MacMillan ML. Outcomes and Predictors of Response in Steroid-Refractory Acute Graft-versus-Host Disease. *Biology of blood and marrow transplantation : journal of the American Society for Blood and Marrow Transplantation*. 2019;25(11):2297-2302. doi:10.1016/j.bbmt.2019.07.017
64. Rocha V, Wagner JEJ, Sobocinski KA, et al. Graft-versus-host disease in children who have received a cord-blood or bone marrow transplant from an HLA-identical sibling. Eurocord and International Bone Marrow Transplant Registry Working Committee on Alternative Donor and Stem Cell Sources. *The New England journal of medicine*. 2000;342(25):1846-1854. doi:10.1056/NEJM200006223422501
65. Pagliuca S, Prata PH, Xhaard A, et al. Long-term outcomes and risk factor analysis of steroid-refractory graft versus host disease after hematopoietic stem cell transplantation. *Bone marrow transplantation*. 2021;56(1):38-49. doi:10.1038/s41409-020-0977-3
66. Flowers MED, Inamoto Y, Carpenter PA, et al. Comparative analysis of risk factors for acute graft-versus-host disease and for chronic graft-versus-host disease according to National Institutes of Health consensus criteria. *Blood*. 2011;117(11):3214-3219. doi:10.1182/blood-2010-08-302109



67. Jacobsohn DA. Acute graft-versus-host disease in children. *Bone Marrow Transplant.* 2008;41(2):215-221. doi:10.1038/sj.bmt.1705885
68. Gatza E, Reddy P, Choi SW. Prevention and Treatment of Acute Graft-versus-Host Disease in Children, Adolescents, and Young Adults. *Biol Blood Marrow Transplant.* 2020;26(5):e101-e112. doi:10.1016/j.bbmt.2020.01.004

## Supplementary information

### Supplementary Material 1. Methodology multi-state survival analysis.

A multi-state model is a model for time-to-event data in which individuals can experience multiple states over time. All individuals start in a starting state (in this case SR-aGvHD) and may eventually transition to another state in case a specific event occurs (remission of aGvHD or death). Absorbing or final states are states from which no more transitions are possible (death). Between the starting and absorbing states, there can be one or more intermediate states (remission of aGvHD). Individuals may be censored before they transition to an absorbing state. The multi-state model used in our study, is an 'illness-death model', with one starting state, one intermediate state ('illness', in our case remission of aGvHD) and one final state ('death'). A schematic overview can be found in Figure 1. This model can be used to estimate transition possibilities between states in terms of hazards. Covariates of interest can be added to the model to estimate their effects on the different transition possibilities. To identify risk factors for death, we considered the hazards for death after SR-aGvHD and for death after remission of SR-aGvHD equal. This means that covariates were analyzed for their effect on transitions 2 and 3 combined. The multi-state model we used in this study is a 'Clock forward'-model, which means that time is measured relatively to when an individual first entered the starting state. For more information and statistical background on multi-state models, we refer to the papers about multi-state models and the mstate package by De Wreede et al. and Putter et al.<sup>44-46</sup>.

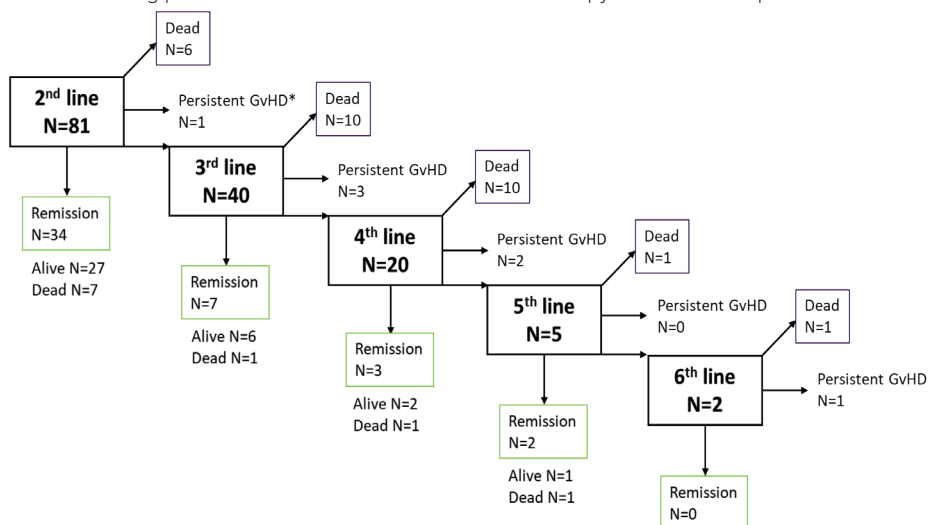
### Supplementary Table 1. All second line therapy outcomes.

The different second-line therapies that were given are listed, including outcomes of aGvHD remission and mortality for each line.

Medication	N	aGvHD remission	%	Mortality	%
MSC	38	19	50	20	52.6
Infliximab	24	16	66.7	7	29.2
Combination	12	7	58.3	7	58.3
Basiliximab	4	3	75	3	75
MMF	1	0	0	0	0
Etanercept	2	1	50	1	50

### Supplementary Figure 1. Flowchart with main outcomes for all lines of therapy.

Flowchart showing patient numbers in the different lines of therapy and the consequent outcomes.



\*Progressive cGvHD or ongoing aGvHD

### Supplementary Table 2. Complications, readmissions, ICU admissions and medication toxicity.

Table listing all complication, readmission, ICU admission and medication toxicity events, as well as the number of patients experiencing the events.

	Total events	Patients	Patients
Complications (since start of second line therapy)	N	n	%
Bronchiolitis Obliterans Syndrome	14	14	17.3%
Cytopenia	12	12	14.8%
Auto-immune	4	4	4.9%
Other	8	8	9.9%
Endocrine dysfunction	5	5	6.2%
Pancreatitis	2	2	2.5%
Liver failure leading to OLTx	1	1	1.2%
Renal insufficiency	12	10	12.3%
Dialysis required	4	3	3.7%
No dialysis required	8	8	9.9%
Secondary graft failure	3	3	3.7%
Secondary malignancy	3	3	3.7%
Short bowel/bowel resection	5	4	4.9%
Thrombotic microangiopathy	14	13	16.0%
Drug related	12	11	13.6%
Not drug related	2	2	2.5%
<b>Infections (within first year since start of second line therapy)</b>	<b>N=221</b>	<b>n=65</b>	<b>%</b>
Bacterial infection	88	44	54.3%
Blood	56	35	43.2%
Lower respiratory tract	12	11	13.6%
Other	20	18	22.2%
Fungal or yeast infection	31	21	25.9%
Blood	6	5	6.2%



Supplementary Table 2. *Continued*

	Total events	Patients	Patients
Lower respiratory tract	12	11	13.6%
Other	14	12	14.8%
Parasitic infection (Cryptosporidium)	<b>2</b>	<b>2</b>	<b>2.5%</b>
Viral infection	<b>18</b>	<b>15</b>	<b>18.5%</b>
Respiratory tract	10	9	11.1%
Gut	7	7	8.6%
Other	1	1	1.2%
Viral reactivations	<b>82</b>	<b>42</b>	<b>51.9%</b>
Adenovirus	26	22	27.2%
BK virus	13	12	14.8%
CMV	25	18	22.2%
EBV	8	4	4.9%
HHV6	2	2	2.5%
HSV1	3	3	3.7%
VZV	5	5	6.2%
<b>ICU admissions (within first year since start of second line therapy)</b>	<b>N=50</b>	<b>n=38</b>	<b>%</b>
Kidney insufficiency	<b>3</b>	<b>3</b>	<b>3.7%</b>
Pain relief	<b>4</b>	<b>3</b>	<b>3.7%</b>
Post-surgery	<b>4</b>	<b>4</b>	<b>4.9%</b>
Respiratory insufficiency	<b>19</b>	<b>18</b>	<b>22.2%</b>
Infectious	9	8	9.9%
Non-infectious	6	6	7.4%
Not specified	4	4	4.9%
Sepsis	<b>11</b>	<b>9</b>	<b>11.1%</b>
Other	<b>9</b>	<b>9</b>	<b>11.1%</b>
<b>Readmissions (within first year since start of second line therapy)</b>	<b>N=61</b>	<b>n=44</b>	<b>%</b>
Dehydration	<b>2</b>	<b>2</b>	<b>2.5%</b>
GvHD	<b>11</b>	<b>10</b>	<b>12.3%</b>
Infection	<b>21</b>	<b>17</b>	<b>21.0%</b>
Malaise	<b>13</b>	<b>10</b>	<b>12.3%</b>
Methylprednisolone pulse	<b>2</b>	<b>1</b>	<b>1.2%</b>
Nutrition problems	<b>2</b>	<b>2</b>	<b>2.5%</b>
Other	<b>10</b>	<b>10</b>	<b>12.3%</b>
<b>Medication related complications (since start of second line therapy)</b>	<b>N=61</b>	<b>n=37</b>	<b>%</b>
Adverse Drug Reaction - Toxicity	<b>58</b>	<b>34</b>	<b>43.2%</b>
Baricitinib	1	1	1.2%
Corticosteroids	23	18	23.5%
Cushing syndrome	1	1	1.2%
Diabetes - Hyperglycemia	13	13	16.0%
Osteonecrosis - Osteopenia	9	9	11.1%
CsA	10	9	11.1%
MMF	6	6	7.4%
Ruxolitinib	2	1	1.2%
Sirolimus	6	6	7.4%
Tacrolimus	10	10	12.3%
Allergic reaction	<b>3</b>	<b>3</b>	<b>3.7%</b>
Basiliximab	1	1	1.2%
Infliximab	1	1	1.2%
IVIg	1	1	1.2%



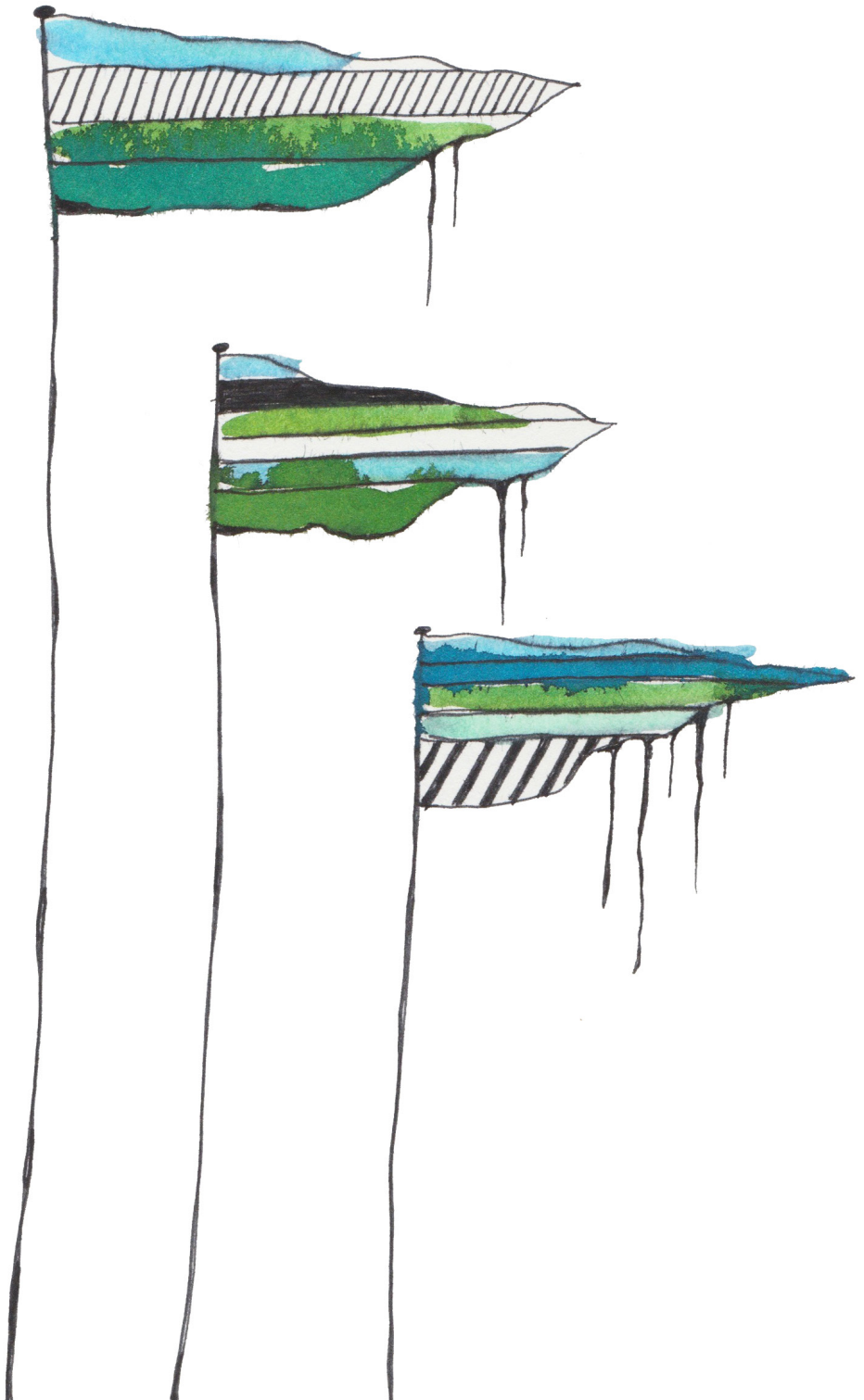
**Supplementary Table 3. Timing of infections since SR-aGvHD diagnosis and underlying acute GvHD activity**

Table listing the number of patients experiencing infections or viral reactivations, and the total number of infection and reactivation events, at different time points since SR-aGvHD diagnosis, as well as the aGvHD status at that time.

Type of infection	Within 7 days				8-28 days				29-365 days			
	Active aGvHD (N=81 at d7)		aGvHD in remission (N=0 at d7)		Active aGvHD (N=67 at d28)		aGvHD in remission (N=9 at d28)		Active aGvHD (N=14 at d365)		aGvHD in remission (N=34 at d365)	
	N	n	N	n	N	n	N	n	N	n	N	n
Bacterial infection	8	8	0	0	9	10	0	0	25	50	13	20
Fungal/yeast infection	2	2	0	0	1	1	0	0	12	16	7	12
Parasitic infection	0	0	0	0	0	0	0	0	1	1	1	1
Viral infection	0	0	0	0	1	1	0	0	6	6	9	11
Viral reactivation	10	10	0	0	15	20	0	0	23	43	6	9

N = number of patients, n = number of events





# 3

## Broad virus detection and variant discovery in fecal samples of hematopoietic transplant recipients using targeted sequence capture metagenomics

Suze A. Jansen, Wouter Nijhuis, Helen Leavis, Annelies Riezebos-Brilman, Caroline A. Lindemans<sup>§</sup>, Rob Schuurman<sup>§</sup>

## Abstract

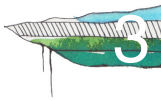
Pediatric allogeneic hematopoietic stem cell transplantation (HSCT) patients often suffer from gastro-intestinal (GI) disease caused by viruses, Graft-versus-Host Disease (GVHD) or a combination of the two. Currently, the GI eukaryotic virome of HSCT recipients remains relatively understudied, which complicates the understanding of its role in GVHD pathogenicity. As decisions regarding immunosuppressive therapy in the treatment of virus infection or GVHD respectively can be completely contradicting, it is crucial to better understand the prevalence and relevance of viruses in the GI tract in the HSCT setting. A real time PCR panel for a set of specific viruses widely used to diagnose the most common causes of GI viral gastroenteritis is possibly insufficient to grasp the full extent of viruses present. Therefore, we applied the targeted sequence capture method ViroCap to residual fecal samples of 11 pediatric allogeneic HSCT recipients with GI symptoms and a suspicion of GVHD, to enrich for nucleic acids of viruses that are known to infect vertebrate hosts. After enrichment, NGS was applied to broadly detect viral sequences. Using ViroCap, we were able to detect viruses such as norovirus and adenovirus (ADV), that had been previously detected using clinical diagnostic PCR on the same sample. In addition, multiple, some of which clinically relevant viruses were detected, including ADV, human rhinovirus (HRV) and BK polyomavirus (BKV). Interestingly, in samples in which specific PCR testing for regular viral GI pathogens did not result in a diagnosis, the ViroCap pipeline led to the detection of viral sequences of human herpesvirus (HHV)-7, BKV, HRV, KI polyomavirus and astrovirus. The latter was an only recently described variant and showed extensive sequence mismatches with the applied real time PCR primers and would therefore not have been detected if tested. Our results indicate that target enrichment of viral nucleic acids through ViroCap leads to sensitive and broad possibly clinically relevant virus detection, including the detection of newer variants in clinical HSCT recipient samples. As such, ViroCap could be a useful detection tool clinically, but also in studying the associations between viral presence and GVHD.

## Introduction

Immunodeficient patients, and in particular allogeneic stem cell transplant (HSCT) recipients, experience a high incidence of gastro-intestinal (GI) symptoms such as nausea and diarrhea. There are multiple causes that can underlie these complaints. Firstly, post-transplant patients are severely lymphopenic and therefore prone to a more severe course of viral infections, many of which circulate among healthy children<sup>1</sup>. Secondly, HSCT recipients are at risk of developing acute intestinal Graft-Versus-Host Disease (GVHD). This is an ultra-complex, life-threatening condition that can only be treated with additional immunosuppressive therapy. Despite matching for HLA, donor immune cells co-transplanted with the graft recognize the patient's tissues as foreign and launch an inflammatory response causing damage to multiple organs. Severe GI-GVHD (grade 3-4)<sup>2</sup> is associated with a high mortality risk, due to organ damage directly (wasting, malnutrition), or secondary to GVHD-therapy-related induced suppression of immune cells. The combination of enteric viral presence, a fragile and suppressed immune system and GI damage by recent chemotherapy and/or GVHD, provides a challenging treatment task for the clinician. Especially since decisions regarding immunosuppressive therapy in the treatment of virus infections or GVHD can be highly divergent. To complicate matters further, intestinal viral presence, even asymptomatic, has been shown to predispose for intestinal GVHD and compromise patients' outcome<sup>3</sup>. Given the above, the identification and characterization of viruses is important for dedicated treatment in HSCT recipients with both GI symptoms and a clinical suspicion of GVHD. Regular monitoring can be used to tailor immunosuppressive therapy or warrant antiviral treatment<sup>4</sup>. In addition, it could provide further insight into the association of viral presence and the development of GVHD.

Thus far, real-time polymerase chain reaction (real-time PCR) has been the gold standard for clinical diagnosis of viral infections<sup>5</sup>. Despite its unprecedented sensitivity, speed and cost-effectiveness, the technology is restricted to only detecting the specific primer-directed virus and limited in identifying and further characterizing virus variants which are genetically divergent from the original species. The unbiased approach of next generation sequencing (NGS) technology (reviewed in<sup>6,7</sup>) overcomes these limitations, albeit at the cost of speed and, more importantly, some detection sensitivity. The sequences reported by NGS in clinical samples are often dominated by those of human origin, which hinders the ability to detect viral nucleic acids in particular when present at low abundance<sup>8</sup>.

Several methods have been described to improve NGS sensitivity for the detection of virus in clinical samples. These methods include low speed centrifugation and filtration to remove cellular debris, ultra-centrifugation to collect virus particles, nuclease treatment to deplete unprotected (human) DNA and/or RNA and viral expansion in culture. As an alternative to DNA depletions, enrichment strategies have been proposed in which the viral nucleic acids



are specifically captured by hybridization with probe libraries. Capture techniques have gained popularity over the past decades in human genome diagnostics to search for rare mutations and disease causing variants<sup>9-12</sup>. More recently, targeted enrichment strategies were successfully implemented for the identification of virus in human samples<sup>13-18</sup>, including the ViroCap approach described by Wiley and colleagues<sup>19</sup>. This NGS hybridization-based capture technique consists of a large panel of probes spread across the genomes of 34 families of DNA and RNA viruses, including 337 species, that infect vertebrate hosts<sup>19</sup>. The probes were designed such that various regions of a species genome are covered and can therefore enrich for known viruses as well as for genetically similar new variants.

We applied ViroCap technology to broadly detect virus in stored stool samples of 11 clinical pediatric HSCT recipients with GI-symptoms that were suspected of GVHD.

## Materials and methods

### **Collection and storage of clinical samples**

According to standard clinical protocol, stool samples from clinical patients with gastrointestinal symptoms suspected of GI-GVHD after HSCT were collected in containers without additives for diagnostic viral PCR testing. Patients had received a related sibling bone marrow (BM) graft, a 10/10 HLA-matched BM, or an unrelated cord-blood (CB) transplantation. Residual fecal material was stored at -80°C within 1 hour after collection and retrospectively included for analysis with ViroCap under a protocol approved by the University Medical Center Utrecht Medical Research Ethics Committee. Informed consent was obtained for the use of clinical data of included HSCT recipients.

### **Nucleic acid extraction and reverse transcription**

Approximately 100 mg of fecal material was added to 1 ml of Stool Transport and Recovery (STAR) buffer (Roche Diagnostics), vortexed and subsequently centrifuged at 17,000 g for 1 minute. 500 µl of the supernatant was used for total RNA and DNA extraction with the MagnaPure 96 (Roche Diagnostics) automated nucleic acid isolation system and MagnaPure 96 DNA and Viral NA Large Volume Kit (Roche Diagnostics) according to the Viral NA Universal 4.0 Protocol. The purified nucleic acid elution volume was set to 50 µl. cDNA synthesis with TaqMan™ Reverse Transcription Reagents supplemented with random hexamers (Applied Biosystems, Foster City, CA, USA) was performed essentially according to manufacturer instructions with the following incubation steps: 10 min at 25 °C, 30 min at 48 °C, 5 min at 95 °C and subsequent hold at 4 °C. 20 µl of eluate was used per cDNA reaction. After cDNA synthesis, the sample was pooled with the original sample eluate for further processing. (c)DNA concentrations were measured using the Qubit 2.0 and the Qubit DS DNA HS Assay.



### **Enzymatic DNA fragmentation and library preparation**

Fragmentation of the DNA in the extraction eluates was achieved enzymatically using the KAPA Hyper Prep Kit (Roche) and a 20 min incubation time at room temperature (RT). Subsequently, library preparation was performed using the KAPA Dual-Indexed Adapters Kit and the SeqCap EZ HyperCap Workflow (Nimblegen). Adapter ligation was followed by two sequential bead clean up steps, using the AMPure XP reagent (Beckman Coulter, Indianapolis, IND, USA). Unique adapter barcodes were used to be able to identify the DNA sequences for each clinical sample. The (c)DNA libraries of up to a maximum of 10 samples plus a negative PBS control were pooled at equal concentrations. The 11 clinical samples described here were processed in 2 separate runs.



### **Sequence enrichment using the ViroCap probe library**

Viral sequence enrichment was achieved using the ViroCap massive sequence enrichment procedure and probe design described earlier<sup>19</sup>. In brief, to block nonspecific hybridization, 5 µl Cot DNA and 2 µl Hypercap Universal Blocking Oligos (Roche Diagnostics, Plaesanton, CA, USA) were added to the pooled sample libraries. After an Ampure bead cleanup the sample pools were eluted in 10.5 µl Hybridization Buffer (Roche Diagnostics, Plaesanton, CA, USA) and a single unit (4.5 µl) of biotinylated ViroCap probes was added (288 ng in the 1<sup>st</sup> run, 383 ng in the 2<sup>nd</sup> run) for hybridization. The hybridization reactions were incubated at 47 °C in a thermocycler with a heated lid set to 57 °C to prevent evaporation for a minimum of 48 hrs. Subsequently, the hybridized DNA was bound to previously washed Streptavidin-magnetic capture beads at 47 °C for 15 min. Following magnetic capture and multiple washing steps the DNA samples were amplified by LM-PCR and eluted from the capture beads using AMPure XP beads. The sample library pools were then treated with 0.2 N NaOH according to the MiSeq System Denature and Dilute Libraries Guide protocol (Illumina, San Diego, USA). Phix DNA (Illumina, San Diego, USA) was added to each sample pool at a final concentration of 1%. Sequencing was performed on a MiSeq system (Illumina, CA, USA), using the MiSeq reagent kit V3 for 2x300 cycles.

### **Metagenomic sequence data analysis and result confirmation**

The FASTQ files generated by the MiSeq system were analyzed using the Genome Detective Viral Metagenomics Data Analysis Pipeline, version 1.111 ([www.genomedetective.com](http://www.genomedetective.com), Belgium). Viral sequences identified and reported by Genome Detective were subsequently checked and confirmed by direct alignment of the FASTQ file with a reference sequence of the respective virus, using Geneious sequence analysis software, Version 9.1.6 ([www.geneious.com](http://www.geneious.com), USA). In addition, where possible, confirmation of the presence of the pathogen was performed by real time PCR.

## Results

### **Samples of clinical GVHD patients**

Stored, residual stool samples of 11 pediatric patients, five females and six males, that had undergone an allogeneic HSCT for a variety of malignant and non-malignant diseases were used for ViroCap analysis (Table 1). All patients suffered from GI-symptoms suspected of gut GVHD, enteric virus infection or a combination of both. Ten patients were diagnosed with GI-GVHD ranging from grade 1 to 4 according to consensus guidelines<sup>2</sup>, whereas the histological findings of the gut biopsy of 1/11 patients (patient 3) did not meet the requirements for a gut GVHD diagnosis. Nonetheless, patient 3 remained suspected of gut GVHD based on skin GVHD in combination with GI-symptoms.

All patients had received first line treatment with prednisone and continuation of calcineurin inhibitors as treatment of (intestinal) acute GVHD. Several patients required more extensive treatment with monoclonal antibodies such as basiliximab (anti- Interleukin (IL)-2 receptor, CD25) or infliximab (anti-TNF $\alpha$ ), cell therapy with Mesenchymal Stromal Cells (MSC) or even surgery. Only five patients are currently alive, reflecting the high risk profile of patients with acute GVHD. Two patients died due to relapse, two directly due to GVHD and two due to other – possibly GVHD-related – transplant mortality (sepsis a.o.).

### **Broad detection of virus in fecal samples of patients with a previous viral diagnosis**

We first aimed to determine whether ViroCap was able to confirm the presence of viruses that had been previously diagnosed by real time PCR in the same sample. Six patients (Sample ID 1-6) had a prior, real time PCR established viral diagnosis in the fecal (F) sample tested (Table 1, 2). In all but one patient (patient 6), the previous detection of adenovirus (ADV) and/or norovirus was confirmed using ViroCap target enrichment and the automated Genome Detective data analysis pipeline. Manual verification of the ViroCap by de novo alignment to an ADV reference virus genome using Geneious data analysis software did confirm the presence of ADV in all patients, including patient 6.

Additional pathogens were detected using ViroCap in five of six patients (Table 2A). The additional viruses detected included single cases of human rhinovirus (HRV), ADV and alphatorquevirus and two cases of BK polyomavirus (BKV). These results were confirmed upon subsequent real time PCR testing for BKV in patient 2 and 5 and for HRV in patient 5. ADV could not be confirmed in patient 4. No confirmatory testing was performed for the NGS reported alphatorquevirus detection in patient 6, because a PCR assay for this virus was not available in the laboratory.

**Table 1. Patient demographics**

Patient no.	Gender	Age at SCT (years)	SCT indication	Graft	Conditioning	Virus feces prior to GVHD	GVHD timing (days)	GVHD gut grade <sup>b</sup>	GVHD overall grade <sup>b</sup>	GVHD therapy	EFS	Survival
1	m	3	T-ALL	5/6 CB	ATG, Bu-Flu	yes	28	1	2	pred, CsA	relapse	deceased
2	f	13	PID	6/6 CB	RTX, ATG, Bu-Flu	yes	37	3	3	pred, CsA, tacrolimus, MMF, sirolimus, MSC 3x, monoclonals	TRM: MOF	deceased
3	m	1	PID	5/6 CB	ATG, Bu-Flu	yes	20	0	2	pred, CsA, MSC 2x, MMF, tacrolimus	no event	alive and well
4	m	15	MDS-AML	6/6 CB	ATG, Clo-Bu-Flu	yes	24	2	3	pred, CsA	relapse	deceased
5	f	9	AML relapse	6/6 CB	Clo-Bu-Flu	yes	35	2	3	pred, CsA, MMF	no event	alive and well
6	m	17	ALL	5/6 UCB	Clo-Bu-Flu	yes	45	3	3	pred, CsA, MMF, tacrolimus, sirolimus, monoclonals, MSC, etanercept, surgery	no event	alive and well
7	f	17	MDS-RAEB-T	10/10 BM	ATG, Bu-Flu	no	41	4	4	pred, CsA, MSC 3x	no event	alive
8	f	11	ALL relapse	10/10 sib BM	Bu-Flu	no	24	4	4	pred, CsA, MMF, MSC 4x	TRM: GVHD	deceased
9	f	16	Metabolic	4/6 CB	ATG, Bu-Flu	no	39	4	4	pred, CsA, MMF, monoclonals, MSC 5x	TRM: GVHD	deceased
10	m	2	PID	6/6 CB	ATG, Bu-flu	no	49	2	3	pred, CsA, tacrolimus, MMF	TRM: sepsis	deceased
11	m	1	PID	5/6 CB	ATG, Bu-Flu	no	89	3	3	pred, CsA, tacrolimus	no event	alive

<sup>a</sup> Abbreviations: EFS, Event free survival; T-ALL, T-cell Acute Lymphatic Leukemia; CB, Cord Blood; ATG, Anti-thymocyte globulin; Bu, Busulfan; Flu, Fludarabine; pred, prednisone; CsA, Cyclosporin A; PID, Primary immune deficiency; RTX, radiotherapy; MMF, mycophenolate mofetil; MSC, mesenchymal stromal cell infusions; TRM, tumor related mortality; MOF, multi-organ failure; MDS-AML, myelodysplastic syndrome-acute myeloid leukemia; Clo, clofarabine; UCB, unrelated cord blood; RAEB-T, refractory anemia with excess blasts in transformation; BM, bone marrow.

<sup>b</sup> Based on consensus <sup>2</sup>



Table 2A. Samples with previous diagnosis

Sample no.	Previous real time PCR result(s) same sample (Ct value)	Total number NGS reads	Genome Detective - automated pipeline (reads)	Coverage % (depth of coverage)	Geneious - manual verification (reads)	Real time PCR confirmation (Ct value)	Previous real time PCR result(s) other samples
1F	ADV (Ct 35)	1,261,170	ADV C (9,194) ADV A (430)	99.1 (38.3) 65.1 (3.5)	ADV C (9,424) ADV A (1,701)	NP	ADV pos
2F	ADV (Ct 32)	529,140	ADV C (24) BKV (348)	6.9 (1.7) 99.5 (10.8)	ADV C (201) ADV A (45)	BKV (Ct 26)	BKV pos ADV pos
3F	ADV (Ct 24)	1,632,432	Adeno-associated virus (34,000) ADV C (32,607)	96.3 (1164.9) 99.1 (136.1)	ADV A (212,743) ADV C (34,136)	NP	ADV neg
4F	noro (Ct 29)	1,570,098	noro (8,835)	97.9 (167.8)	noro (7,777)		
	noro (Ct 21)		noro (26,063)	95.3 (492.1)	noro (7,806) ADV A (15)	ADV neg	noro pos ADV neg
5F	ADV (Ct 20)	11,635,812	ADV A (8,139,232) BKV (171) HRV-A (39)	99.5 (40,229.4) 96.1 (7.7) 4.3 (1.1)	ADV A (96,108) HRV-C (18)	BKV (Ct 26) HRV (Ct 37)	ADV pos BKV pos (urine)
6F	ADV (Ct 41)	660,224	alphatorque virus (324)	96.1 (12.8)	ADV A (182)	NP	ADV neg

<sup>a</sup> Abbreviations: ADV, adenovirus; BKV, BK polyomavirus; Noro, norovirus; NP, not performed; HRV, human rhinovirus.

Table 2B. Samples without previous diagnosis

Sample no.	Previous real time PCR result(s) same sample (Ct value)	Total number NGS reads	Genome Detective - automated pipeline (reads)	Coverage % (depth of coverage)	Geneious - manual verification (reads)	Real time PCR confirmation (Ct value)	Previous real time PCR result(s) other samples
7F	ND	42,172	BKV (1,808)	4.3 (36.4)	BKV (2,037)	BKV neg	BKV pos
8F	ND	88,962	HRV-C (8)	9.5 (6.7)	HRV-C (631)	HRV (Ct 30)	-
9F	ND	106,936	-	-	-	-	-
10F	ND	603,938	HRV-B (918) Astrovirus VA3 (849) KI virus (301)	48.4 (52.9) 99.9 (25.7) 100 (21.4)	HRV-B (817) Astrovirus VA3 (6055) KI virus (534)	HRV (Ct 18) Astrovirus neg	-
11F	ND	1,856,410	alphatorque virus (2,055)	22.8 (272.3)	-	-	-

<sup>a</sup> Abbreviations: ND, no diagnosis; HHV, human herpes virus; BKV, BK polyomavirus; NA, not available; HRV, human rhinovirus; KI virus, KI polyomavirus.

### **Viruses identified in fecal samples without prior diagnosis by real time PCR**

Subsequently, fecal samples of 5 patients which had been tested negative for the presence of ADV, norovirus and rotavirus by real time PCR, direct enzyme immunoassays (EIA) or immune chromatographic testing (ICT) were tested using the ViroCap target enrichment (Table 2B). In addition to the aforementioned diagnostic tests, patient 9 had also been tested and found negative by real time PCR for astrovirus, enterovirus and parechovirus. In all but one patient, one or more viruses were detected in the fecal samples. In individual patients we detected single cases of BKV, KI polyomavirus (KI virus), human herpes virus 7 (HHV-7), astrovirus, and alphatorquevirus. HRV was detected in 2 individuals.



The number of reads were generally low and varied between 6 and 6000. In most cases the read counts were higher upon manual alignment using Geneious software in comparison to the automated Genome Detective pipeline. ViroCap detection of most of the viruses could be confirmed in available real time PCR assays. The HRV detections were confirmed at a Ct value of 18 for patient 10 and Ct 30 for patient 8, despite the low number of NGS reads reported by ViroCap for the HRV of patient 8. The detection of BKV by ViroCap in patient 7 could not be confirmed by real time PCR. However, this patient did have a high viral load of BKV in urine, close to moment of feces collection, as had been observed by routine real time PCR monitoring. No confirmatory real time PCR testing was performed for alphatorquevirus on sample 11F, KI virus on sample 10F and for HHV-7 on sample 7F.

### **ViroCap detects a recent astrovirus variant**

In patient 10F the abundant presence of astrovirus VA3 sequences was reported by Genome Detective. The inherent design of ViroCap enrichment probes containing multiple conserved regions of a virus genome allowed for the detection of this recently described new species of astrovirus VA3 (JX857868.1)<sup>20</sup>. The presence of astrovirus could not be confirmed using our diagnostic real time PCR assay. Detailed analysis of the reported NGS sequences revealed that the genome of this specific astrovirus clade VA3 contained extensive mutations in primer regions used in our diagnostic real time PCR assay explaining the failing PCR confirmation (Fig. 1).

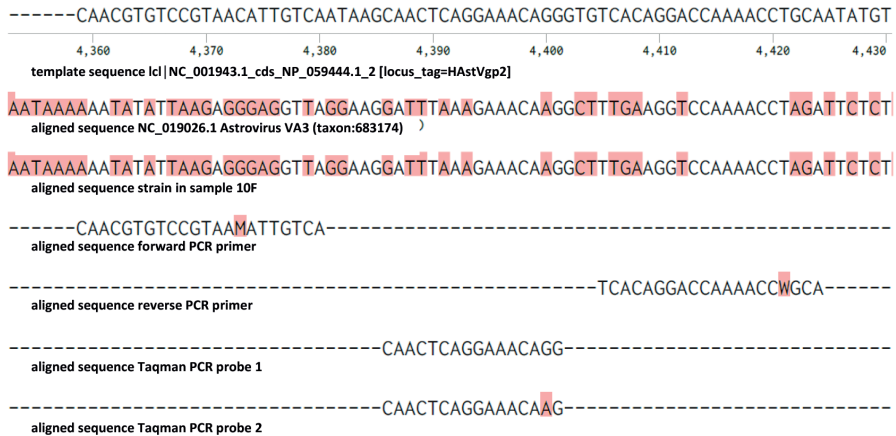


**Figure 1. Detailed presentation of the nucleotide sequences of the target region of the astrovirus and real time PCR used for routine application.** Top row: template sequence coding for human astrovirus capsid precursor protein (HAsrVgp2), aligned with Astrovirus VA3 sequence and the ViroCap detected astrovirus sequence in sample 10F. Mismatches with the template sequence are indicated in red. Forward PCR primer, reverse PCR primer and Taqman PCR probes applied in the diagnostic astrovirus PCR are indicated in the bottom lines of the figure.

## Discussion

The role of the intestinal microbiome in the development of GVHD has been a major field of study in the HSCT setting, but reports have mainly focused on the dynamics of bacteria<sup>21–24</sup>. Besides better known implications of some specific viruses post HSCT, such as ADV<sup>1,25–28</sup>, norovirus<sup>29</sup> and HHV<sup>30</sup>, to date only one study has explored the gut virome in HSCT using NGS<sup>31</sup>. Albeit the promise of unbiased virome mapping, virus discovery with NGS in clinical samples has been hindered by relatively lower sensitivity compared to real time PCR<sup>32</sup>. A study comparing the diagnostic efficiency of NGS versus gold standard real time PCR in 89 nasopharyngeal swabs reported a sensitivity of 78% and specificity of 80% for NGS<sup>33</sup>. More recently, a NGS sensitivity of 92% compared to real time PCR was found when testing a range of 52 clinical samples, including 8 of fecal origin<sup>34</sup>.

Target enrichment for sequences of viruses infecting vertebrate organisms, using biotinylated capture probes as a front-end procedure of NGS based metagenomic sequencing provides an opportunity for sensitive, broad detection of viruses<sup>19</sup>. In two sets of clinical samples (including 1 stool, 7 nasopharyngeal swabs and 1 plasma sample) applying ViroCap resulted in a median fold-increase of the viral reads percentage of 674 and 296, respectively. In the first set, the median breadth of coverage expanded from 2.1 to 83.2% and in the second set from 2.0% to 75.6%. Subsequently, the same authors tested ViroCap in a slightly larger set

of 26 clinical samples that were previously submitted to a diagnostic virology lab (including 2 stool samples and in addition whole blood, plasma, cerebrospinal fluid, nasopharyngeal swabs, tracheal aspirates and skin swabs) and found a consistent increase in the number and percentage of viral reads as well as breadth and depth of viral genome coverage<sup>35</sup>. Here we applied ViroCap capture-based enrichment to test virus presence in residual stored clinical stool samples of immunocompromised pediatric patients that had undergone a HSCT in an independent institute and were able to show its advantages even in a small cohort of patients.



ViroCap was capable of detecting all viruses that had previously been detected by pathogen-specific real time PCR assays, proving the robustness and sensitivity of the method. In ADV positive samples the number of NGS reads for ADV was higher at low PCR Ct values and vice versa, but this trend was not statistically significant (data not shown). In some cases we observed differences in the gross number of reads generated with the automated Genome Detective pipeline when comparing with manual alignment in Geneious software. This might be due to differences in the reference sequences used by both programs, an unbalanced representation of sequenced genome fragments or a combination of these factors.

ADV was the most prevalent detected pathogen in our modest patient cohort, in 5 out of 11 patients, which was similar to other reports on HSCT recipients<sup>36-38</sup> and immunocompromised patients<sup>39</sup> and non-human primates in general<sup>40</sup>. Systemic ADV reactivations are notoriously deadly in the pediatric HSCT setting<sup>1,27,28</sup>, for example the detected ADV C in 3 of our patients has been linked to multiple fatalities<sup>41</sup>. Exemplifying the broad detection potential of ViroCap, several other viruses for which the samples had not been previously tested, were detected. These included HHV-7 (n=1), BKV (n=3), ADV (n=1), HRV (n=3), alphatorquevirus (n=2), KI virus (n=1) and astrovirus (n=1). The implications of some of the aforementioned viral presence, and possible others, is debated and yet to be fully determined. Alphatorquevirus, for instance, is considered to be an apathogenic virus to humans and its DNA has been detected in various clinical samples, including stool, in up to 90% of tested healthy and diseased individuals<sup>42,43</sup>. Nonetheless, a relationship between alphatorquevirus peripheral blood titers and post HSCT complications has been suggested<sup>44</sup>. Others, like HHV-7, BKV, KI virus and HRV, have not yet been associated with GI symptoms or gut GVHD. In general, relatively mild viral infections in healthy individuals can be prolonged or more severe in immunocompromised children. If undetected they may spread among transplanted patients which could potentially lead to a clinical manifestation<sup>45-47</sup>. Interestingly, the mere presence of certain viruses in the gut both before HSCT<sup>3</sup> and before or within 1 week after HSCT<sup>31</sup> can be predictive of/predispose for the development of intestinal GVHD. Montfrans analyzed stool samples of 48 pediatric allo-HSCT patients using real time PCR before allo-HSCT and found that the presence of virus (ADV, norovirus, parechovirus or astrovirus combined) predisposed for the development of acute enteric GVHD, but not chronic GVHD<sup>3</sup>. All viral

positive patients remained positive for over 3 months post-HSCT. Similar associations were previously found in our institute between respiratory virus PCR positivity in nasopharyngeal aspirates or bronchoalveolar lavage samples early after transplant and the development of allo-immune lung disease<sup>48</sup>. It could however be hypothesized that if investigated with more sensitive and broad techniques such as ViroCap, not only a subgroup, but all HSCT recipients with GI-GVHD are colonized with specific viruses in the gut which may affect HSCT- and GVHD-related outcome.

Legoff and colleagues studied the peri-HSCT gut virome longitudinally using metagenomic NGS on 201 fecal samples collected from 44 HSCT patients<sup>31</sup>. The authors demonstrated a progressive increase in the overall proportion of vertebrate viruses in the gut of patients after transplantation, independent from the development of GVHD. However, acute intestinal GVHD patients did experience an increase in persistent DNA viruses, such as anneloviruses and herpesviruses. Additionally, picobirnaviruses (PBVs) were identified in 18 patients, either before or within a week after transplant and its detection pertained predictive of the occurrence of both overall and intestinal GVHD<sup>31</sup>. A hypothesis for the described associations is that virus causes mucosal damage, leading to the release of alarmins that activate remaining innate immune cells and increase antigen presentation by host antigen-presenting cells (APC), causing allo-activation and influx of donor T cells<sup>3</sup>. Perhaps some clues can be found in mouse studies, where it was postulated that viral presence modulates the occurrence of intestinal bacterial and viral infections in primary immune deficiency models. Latent murine herpes infection protected mice from *Listeria* bacteremia<sup>49</sup>. It was speculated that the chronic infection stimulated the innate immune system such that is compensated for early cytokine response deficiencies in immunodeficiency. More recently, Ingle et al. found that in primary immunodeficient mice astrovirus presence can protect against murine norovirus and rotavirus infections through upregulation of cell-intrinsic IFN- $\lambda$  in the intestinal epithelial barrier<sup>50</sup>. If these findings are transposed on an allogeneic HSCT setting, it can be postulated that specific viral presence leads to activation of the innate and thereby adaptive immune system, in this setting allo-reactive T cells, and provokes GVHD. In contrast, in recent GVHD mouse model studies, similar innate cytokine signaling pathways activated by viral sequence detection were linked to protection against GVHD. It was shown that activation of the RIG-I/MAVS and cGAS/STING pathways, both innate recognition pathways that induce IFN-I expression upon sensing of specific viral RNA and DNA sequences, attenuated intestinal GVHD injury<sup>51</sup>. Mechanistically, RIG-I activation before HSCT reduced the ability of specific recipient APCs to activate transplanted allogeneic T cells<sup>52</sup>. More research is warranted to elucidate the complex correlations between viral presence and the development of GVHD, in which ViroCap could play an important role.



Besides detecting a broader range of viruses than with specific respiratory tract or GI focused PCR panels, ViroCap has the ability to detect viral variants. ViroCap probes cover extensive proportions of the genomes of viral families, species or (sub)types, and as such genetic variants may be well detectable upon capturing the conserved regions of such virus. Nucleotide sequence identity as low as 58% demonstrated to be sufficient for the detection of novel variants<sup>19</sup>. In our study, we detected and characterized an astrovirus VA3 that had not been detected by our routine real time PCR assay. The genetic distance of this relatively recently identified astrovirus clade was high and could therefore not be detected in the applied diagnostic qPCR assay. Astrovirus VA3 has been identified rarely in human samples and was specifically reported in the stool samples of a child with diarrhea from India<sup>20</sup>. The current identification of this astrovirus clade in our patient cohort of severely immunocompromised symptomatic patients indicates that the potential clinical importance should be considered and further elucidated.



Despite aforementioned benefits, the ViroCap capture-bead technology also has limitations<sup>13,19</sup>. Firstly, the cost of the assay, in particular of the capture probes, is still considerable if only few samples are assayed. Pooling of samples subsequent to the library preparation can help to reduce the assay cost per sample as long as this does not affect the assay sensitivity. In our experiments, we did not observe a reduction in sensitivity upon pooling of up to 10 clinical samples, indicating that the amount of probes per reaction was not a limiting factor (data not shown). With this strategy, the cost per sample can be reduced to 300-400 Euros per sample, not yet comparable to multiple real time PCR. It is expected that the wider application of NGS and of probe capturing strategies will lead to a significant price reduction in the coming years. Furthermore, routine clinical application of ViroCap requires a significant reduction in the assay turnaround time (TAT). Currently, the TAT is in the order of 5 days, mainly caused by the 48-60 hours required for probe hybridization and 48 hours of sequencing on the MiSeq system. Commercial reagents reducing hybridization times to less than 4 hours have recently been introduced and can be considered an important factor for clinical application of the strategy. Finally, ViroCap will not be capable of efficiently enriching viral sequences of variants or sub-species that differ too much from the known species. Nonetheless, since the capture probes cover the full width of vertebrate viruses, the chance of missing a completely new and unidentified viral species of family is limited.

In summary, application of viral target enrichment strategies with limited virus detection bias, such as ViroCap, can lead to the detection of unexpected viruses and viral variants, as demonstrated in the modest number of allo-HSCT patients presented in this manuscript. As such, applying ViroCap to a larger cohort will be a feasible and important next step to elucidate associations of viruses with GI-symptoms and GVHD.

**Conflict of interest**

The authors have no conflict of interest to report.

**Author contributions**

S.A.J. performed the integration of NGS results and clinical information, and prepared the manuscript. W.N. performed experiments, H.L. and A.R.B. provided input to the project design and experiment interpretation. C.A.L. and R.S. initiated and designed the project, supervised the experiments, the interpretation and manuscript preparation. All authors contributed to the manuscript.

**Funding**

S.J. was supported by an Alexander Suerman Stipend awarded by the University Medical Center Utrecht. C.A.L. was supported by the Wilhelmina Children's Hospital Fund. Otherwise, this research received no specific grant from any funding agency in the public, commercial, or not-for-profit sectors.

**Data Availability Statement**

The generated sequencing data files for this study have been submitted to the NCBI BioProject database (<http://www.ncbi.nlm.nih.gov/bioproject>) under the BioProjectID PRJNA656436, and include accession numbers SAMN15784571 until SAMN15784581.

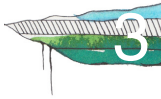
# References

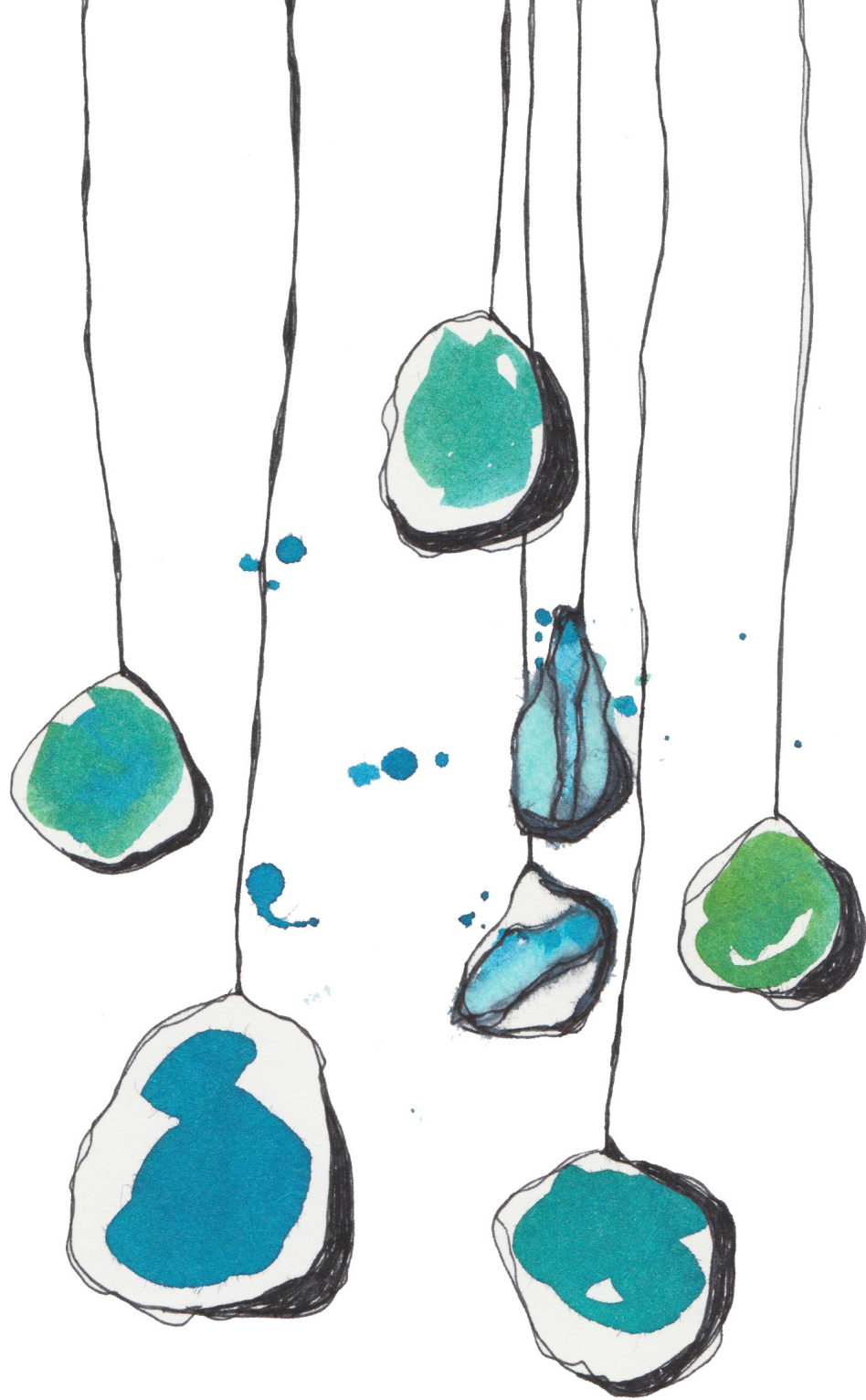
1. Pochon C, Voigt S. Respiratory Virus Infections in Hematopoietic Cell Transplant Recipients. *Front Microbiol.* 2018;9:3294. doi:10.3389/fmicb.2018.03294
2. Glucksberg H, Storb R, Fefer A, Buckner CD, Neiman PE, Clift RA, et al. Clinical manifestations of graft-versus-host disease in human recipients of marrow from HL-A-matched sibling donors. *Transplantation.* 1974;18(4):295-304. doi:10.1097/00007890-197410000-00001
3. van Montfrans J, Schulz L, Versluys B, de Wildt A, Wolfs T, Bierings M, et al. Viral PCR positivity in stool before allogeneic hematopoietic cell transplantation is strongly associated with acute intestinal graft-versus-host disease. *Biol Blood Marrow Transplant.* 2015;21(4):772-774. doi:10.1016/j.bbmt.2015.01.009
4. Feghoul L, Chevret S, Cuinet A, Dalle J-H, Ouachee M, Yacouben K, et al. Adenovirus infection and disease in paediatric haematopoietic stem cell transplant patients: clues for antiviral pre-emptive treatment. *Clin Microbiol Infect.* 2015;21(7):701-709. doi:10.1016/j.cmi.2015.03.011
5. Edwards MC, Gibbs RA. Multiplex PCR: advantages, development, and applications. *PCR Methods Appl.* 1994;3(4):S65-75. doi:10.1101/gr.3.4.s65
6. Shendure J, Ji H. Next-generation DNA sequencing. *Nat Biotechnol.* 2008;26(10):1135-1145. doi:10.1038/nbt1486
7. Barzon L, Lavezzo E, Militello V, Toppo S, Palu G. Applications of next-generation sequencing technologies to diagnostic virology. *Int J Mol Sci.* 2011;12(11):7861-7884. doi:10.3390/ijms12117861
8. Daly GM, Bexfield N, Heaney J, Stubbs S, Mayer AP, Palsler A, et al. A viral discovery methodology for clinical biopsy samples utilising massively parallel next generation sequencing. *PLoS One.* 2011;6(12):e28879. doi:10.1371/journal.pone.0028879
9. Hodges E, Xuan Z, Balija V, Kramer M, Molla MN, Smith SW, et al. Genome-wide in situ exon capture for selective resequencing. *Nat Genet.* 2007;39(12):1522-1527. doi:10.1038/ng.2007.42
10. Mamanova L, Coffey AJ, Scott CE, Kozarewa I, Turner EH, Kumar A, et al. Target-enrichment strategies for next-generation sequencing. *Nat Methods.* 2010;7(2):111-118. doi:10.1038/nmeth.1419
11. Fleming S, Harrison SJ, Blombery P, Joyce T, Stokes K, Seymour JF, et al. The choice of multiple myeloma induction therapy affects the frequency and severity of oral mucositis after melphalan-based autologous stem cell transplantation. *Clin Lymphoma Myeloma Leuk.* 2014;14(4):291-296. doi:10.1016/j.clml.2014.02.001
12. Choi M, Scholl UI, Ji W, Liu T, Tikhonova IR, Zumbo P, et al. Genetic diagnosis by whole exome capture and massively parallel DNA sequencing. *Proc Natl Acad Sci U S A.* 2009;106(45):19096-19101. doi:10.1073/pnas.0910672106
13. Gaudin M, Desnues C. Hybrid Capture-Based Next Generation Sequencing and Its Application to Human Infectious Diseases. *Front Microbiol.* 2018;9:2924. doi:10.3389/fmicb.2018.02924
14. O'Flaherty BM, Li Y, Tao Y, Paden CR, Queen K, Zhang J, et al. Comprehensive viral enrichment enables sensitive respiratory virus genomic identification and analysis by next generation sequencing. *Genome Res.* 2018;28(6):869-877. doi:10.1101/gr.226316.117
15. Paskey AC, Frey KG, Schroth G, Gross S, Hamilton T, Bishop-Lilly KA. Enrichment post-library preparation enhances the sensitivity of high-throughput sequencing-based detection and characterization of viruses from complex samples. *BMC Genomics.* 2019;20(1):155. doi:10.1186/s12864-019-5543-2
16. Metsky HC, Siddle KJ, Gladden-Young A, Qu J, Yang DK, Brehio P, et al. Capturing sequence diversity in metagenomes with comprehensive and scalable probe design. *Nat Biotechnol.* 2019;37(2):160-168. doi:10.1038/s41587-018-0006-x
17. Cummings MJ, Tokarz R, Bakamutumaho B, Kayiwa J, Byaruhanga T, Owor N, et al. Precision Surveillance for Viral Respiratory Pathogens: Virome Capture Sequencing for the Detection and Genomic Characterization of Severe Acute Respiratory Infection in Uganda. *Clin Infect Dis.* 2019;68(7):1118-1125. doi:10.1093/cid/ciy656
18. Brown JR, Roy S, Ruis C, Yara Romero E, Shah D, Williams R, et al. Norovirus Whole-Genome Sequencing by SureSelect Target Enrichment: a Robust and Sensitive Method. *J Clin Microbiol.* 2016;54(10):2530-2537. doi:10.1128/JCM.01052-16
19. Wylie TN, Wylie KM, Herter BN, Storch GA. Enhanced virome sequencing using targeted sequence capture. *Genome Res.* 2015;25(12):1910-1920. doi:10.1101/gr.191049.115
20. Finkbeiner SR, Holtz LR, Jiang Y, Rajendran P, Franz CJ, Zhao G, et al. Human stool contains a previously unrecognized diversity of novel astroviruses. *Viral J.* 2009;6:161. doi:10.1186/1743-422X-6-161
21. Takashima S, Hanash AM. The enteric virome in hematopoietic stem cell transplantation: ready for its close-up. *Nat Med.* 2017;23(9):1012-1013. doi:10.1038/nm.4403
22. Shono Y, van den Brink MRM. Gut microbiota injury in allogeneic haematopoietic stem cell transplantation. *Nat Rev Cancer.* 2018;18(5):283-295. doi:10.1038/nrc.2018.10
23. Peled JU, Gomes ALC, Devlin SM, Littmann ER, Taur Y, Sung AD, et al. Microbiota as Predictor of Mortality in Allogeneic Hematopoietic-Cell Transplantation. *N Engl J Med.* 2020;382(9):822-834. doi:10.1056/NEJMoa1900623
24. Shono Y, Docampo MD, Peled JU, Perobelli SM, Velardi E, Tsai JJ, et al. Increased GVHD-related mortality with broad-spectrum antibiotic use after allogeneic hematopoietic stem cell transplantation in human patients and



- mice. *Sci Transl Med*. 2016;8(339):339ra71. doi:10.1126/scitranslmed.aaf2311
25. Shields AF, Hackman RC, Fife KH, Corey L, Meyers JD. Adenovirus infections in patients undergoing bone-marrow transplantation. *N Engl J Med*. 1985;312(9):529-533. doi:10.1056/NEJM198502283120901
  26. Flomenberg P, Babbitt J, Drobyski WR, Ash RC, Carrigan DR, Sedmak G V, et al. Increasing incidence of adenovirus disease in bone marrow transplant recipients. *J Infect Dis*. 1994;169(4):775-781. doi:10.1093/infdis/169.4.775
  27. Lindemans CA, Leen AM, Boelens JJ. How I treat adenovirus in hematopoietic stem cell transplant recipients. *Blood*. 2010;116(25):5476-5485. doi:10.1182/blood-2010-04-259291
  28. Kosulin K, Geiger E, Vecsei A, Huber W-D, Rauch M, Brenner E, et al. Persistence and reactivation of human adenoviruses in the gastrointestinal tract. *Clin Microbiol Infect*. 2016;22(4):381.e1-381.e8. doi:10.1016/j.cmi.2015.12.013
  29. Roddie C, Paul JP V, Benjamin R, Gallimore CI, Xerry J, Gray JJ, et al. Allogeneic hematopoietic stem cell transplantation and norovirus gastroenteritis: a previously unrecognized cause of morbidity. *Clin Infect Dis*. 2009;49(7):1061-1068. doi:10.1086/605557
  30. Sehrawat S, Kumar D, Rouse BT. Herpesviruses: Harmonious Pathogens but Relevant Cofactors in Other Diseases? *Front Cell Infect Microbiol*. 2018;8:177. doi:10.3389/fcimb.2018.00177
  31. Legoff J, Resche-Rigon M, Bouquet J, Robin M, Naccache SN, Mercier-Delarue S, et al. The eukaryotic gut virome in hematopoietic stem cell transplantation: new clues in enteric graft-versus-host disease. *Nat Med*. 2017;23(9):1080-1085. doi:10.1038/nm.4380
  32. Sauvage V, Laperche S, Cheval J, Muth E, Dubois M, Boizeau L, et al. Viral metagenomics applied to blood donors and recipients at high risk for blood-borne infections. *Blood Transfus*. 2016;14(5):400-407. doi:10.2450/2016.0160-15
  33. Thorburn F, Bennett S, Modha S, Murdoch D, Gunson R, Murcia PR. The use of next generation sequencing in the diagnosis and typing of respiratory infections. *J Clin Virol*. 2015;69:96-100. doi:10.1016/j.jcv.2015.06.082
  34. Huang B, Jennison A, Whiley D, McMahon J, Hewitson G, Graham R, et al. Illumina sequencing of clinical samples for virus detection in a public health laboratory. *Sci Rep*. 2019;9(1):5409. doi:10.1038/s41598-019-41830-w
  35. Wylie KM, Wylie TN, Buller R, Herter B, Cannella MT, Storch GA. Detection of Viruses in Clinical Samples by Use of Metagenomic Sequencing and Targeted Sequence Capture. *J Clin Microbiol*. 2018;56(12). doi:10.1128/JCM.01123-18
  36. Yolken RH, Bishop CA, Townsend TR, Bolyard EA, Bartlett J, Santos GW, et al. Infectious gastroenteritis in bone-marrow-transplant recipients. *N Engl J Med*. 1982;306(17):1010-1012.
  37. Troussard X, Bauduer F, Gallet E, Freymuth F, Boutard P, Ballet JJ, et al. Virus recovery from stools of patients undergoing bone marrow transplantation. *Bone Marrow Transplant*. 1993;12(6):573-576.
  38. Chakrabarti S, Collingham KE, Stevens RH, Pillay D, Fegan CD, Milligan DW. Isolation of viruses from stools in stem cell transplant recipients: a prospective surveillance study. *Bone Marrow Transplant*. 2000;25(3):277-282. doi:10.1038/sj.bmt.1702164
  39. Monaco CL, Gootenberg DB, Zhao G, Handley SA, Ghebremichael MS, Lim ES, et al. Altered Virome and Bacterial Microbiome in Human Immunodeficiency Virus-Associated Acquired Immunodeficiency Syndrome. *Cell Host Microbe*. 2016;19(3):311-322. doi:10.1016/j.chom.2016.02.011
  40. Handley SA, Thackray LB, Zhao G, Presti R, Miller AD, Droit L, et al. Pathogenic simian immunodeficiency virus infection is associated with expansion of the enteric virome. *Cell*. 2012;151(2):253-266. doi:10.1016/j.cell.2012.09.024
  41. Mynarek M, Ganzenmueller T, Mueller-Heine A, Mielke C, Gonnermann A, Beier R, et al. Patient, Virus, and Treatment-Related Risk Factors in Pediatric Adenovirus Infection after Stem Cell Transplantation: Results of a Routine Monitoring Program. *Biol Blood Marrow Transplant*. 2014;20(2):250-256. doi:https://doi.org/10.1016/j.bbmt.2013.11.009
  42. Ssemadaali MA, Effertz K, Singh P, Kolyvushko O, Ramamoorthy S. Identification of heterologous Torque Teno Viruses in humans and swine. *Sci Rep*. 2016;6:26655. doi:10.1038/srep26655
  43. Matsubara H, Michitaka K, Horiike N, Yano M, Akbar SM, Torisu M, et al. Existence of TT virus DNA in extracellular body fluids from normal healthy Japanese subjects. *Intervirology*. 2000;43(1):16-19. doi:10.1159/000025018
  44. Gilles R, Herling M, Holtick U, Heger E, Awerkwiew S, Fish I, et al. Dynamics of Torque Teno virus viremia could predict risk of complications after allogeneic hematopoietic stem cell transplantation. *Med Microbiol Immunol*. 2017;206(5):355-362. doi:10.1007/s00430-017-0511-4
  45. Schwartz S, Vergoulidou M, Schreier E, Loddenkemper C, Reinwald M, Schmidt-Hieber M, et al. Norovirus gastroenteritis causes severe and lethal complications after chemotherapy and hematopoietic stem cell transplantation. *Blood*. 2011;117(22):5850-5856. doi:10.1182/blood-2010-12-325886
  46. Swartling L, Allard A, Torlen J, Ljungman P, Mattsson J, Sparrelid E. Prolonged outbreak of adenovirus A31 in allogeneic stem cell transplant recipients. *Transpl Infect Dis*. 2015;17(6):785-794. doi:10.1111/tid.12443
  47. van der Doef HPJ, Bathoorn E, van der Linden MPM, Wolfs TFW, Minderhoud ALC, Bierings MB, et al. Astrovirus outbreak at a pediatric hematology and hematopoietic stem cell transplant unit despite strict hygiene rules. *Bone Marrow Transplant*. 2016;51(5):747-750. doi:10.1038/bmt.2015.337
  48. Versluys AB, Rossen JWA, van Ewijk B, Schuurman R, Bierings MB, Boelens JJ. Strong association between respiratory viral infection early after hematopoietic stem cell transplantation and the development of life-

- threatening acute and chronic alloimmune lung syndromes. *Biol Blood Marrow Transplant*. 2010;16(6):782-791. doi:10.1016/j.bbmt.2009.12.534
49. MacDuff DA, Reese TA, Kimmey JM, Weiss LA, Song C, Zhang X, et al. Phenotypic complementation of genetic immunodeficiency by chronic herpesvirus infection. *Elife*. 2015;4. doi:10.7554/eLife.04494
  50. Ingle H, Lee S, Ai T, Orvedahl A, Rodgers R, Zhao G, et al. Viral complementation of immunodeficiency confers protection against enteric pathogens via interferon-lambda. *Nat Microbiol*. 2019;4(7):1120-1128. doi:10.1038/s41564-019-0416-7
  51. Fischer JC, Bscheider M, Eisenkolb G, Lin C-C, Wintges A, Otten V, et al. RIG-I/MAVS and STING signaling promote gut integrity during irradiation- and immune-mediated tissue injury. *Sci Transl Med*. 2017;9(386). doi:10.1126/scitranslmed.aag2513
  52. Fischer JC, Bscheider M, Gottert S, Thiele Orberg E, Combs SE, Bassermann F, et al. Type I interferon signaling before hematopoietic stem cell transplantation lowers donor T cell activation via reduced allogenicity of recipient cells. *Sci Rep*. 2019;9(1):14955. doi:10.1038/s41598-019-51431-2







# 4

## Chemotherapy-induced intestinal injury promotes Galectin-9-driven modulation of T cell function

Suze A. Jansen\*, Alessandro Cutilli\*, Coco de Koning, Marliek van Hoesel, Leire Saiz Sierra, Stefan Nierkens, Michal Mokry, Edward E.S. Nieuwenhuis, Alan M. Hanash·Enric Mocholi, Paul J. Coffers<sup>§</sup>, Caroline A. Lindemans<sup>§</sup>

Submitted

## Abstract

The intestine is vulnerable to chemotherapy-induced toxicity due to its high epithelial proliferative rate, making gut toxicity an off-target effect in several cancer treatments, including conditioning regimens for allogeneic hematopoietic cell transplantation (HSCT). In HSCT, intestinal damage is an important factor in the development of Graft-versus-Host Disease (GVHD), an immune complication in which donor immune cells attack the recipient's tissues. Here, we developed a novel human intestinal organoid-based 3D model system to study the direct effect of chemotherapy-induced intestinal epithelial damage on T cell behavior. Chemotherapy treatment using busulfan, fludarabine, and clofarabine led to damage responses in organoids resulting in increased T cell migration, activation, and proliferation in *ex-vivo* co-culture assays. We identified galectin-9 (Gal-9), a beta-galactoside-binding lectin released by damaged organoids, as a key molecule mediating T cell responses to damage. Increased levels of Gal-9 were also found in the plasma of HSCT patients who later developed acute GVHD, supporting the predictive value of the model system in the clinical setting. This study highlights the potential contribution of chemotherapy-induced epithelial damage to the pathogenesis of intestinal GVHD through direct effects on T cell activation and trafficking promoted by Gal-9.



## Introduction

The intestinal epithelium is comprised of a variety of secretory and absorptive intestinal epithelial cell (IEC) types that derive from the intestinal stem cells (ISC) at the bottom of intestinal epithelial crypts. As the IECs divide, they differentiate into their destined lineage along the crypt-villus axis<sup>1</sup>. The intestinal epithelium forms a physical barrier between the gut lumen and milieu interior, and as such provides the first layer of defense against harmful luminal components and pathogens<sup>2</sup>. Damage to the intestinal epithelium has been linked to immune activation with a T cell component in multiple disease settings, including inflammatory bowel disease (IBD), coeliac disease, and acute intestinal graft-versus-host disease (GVHD) after allogeneic hematopoietic stem cell transplantation (HSCT)<sup>2-9</sup>. How epithelial damage may directly influence T cell activation still needs to be completely elucidated.

Mechanisms of T cell activation after epithelial damage are thought to involve innate immune cell activation including neutrophils, monocytes and macrophages, leading to migration of T cells, and both local antigen presentation, as well as antigen presentation by professional antigen-presenting cells (APCs) in nearby lymphoid organs<sup>10</sup>. Chemotherapy used in the treatment of malignancies<sup>11,12</sup> and conditioning regimens prior to HSCT, damage IECs and disrupt the epithelial barrier<sup>13-15</sup>. After HSCT, the barrier breach may cause local inflammation and activation of T cells supporting the development of GVHD<sup>16,17</sup>. The type and intensity of the conditioning regimen and related regimen-related toxicity correlate with the development and severity of GVHD, and related outcomes in patients<sup>18-21</sup>.

It is currently unclear how conditioning-induced IEC damage directly affects T cell behavior, and as such could contribute to the development of GVHD. There is evidence that the intestinal epithelium and T cells closely interact under both homeostatic and pathogenic conditions, modulating T cell recruitment, differentiation, and function<sup>22-30</sup>. T cells exhibit dynamic behavior within the IEC compartment which adapts to intraluminal epithelial cell exposure to pathogens<sup>31,32</sup>. During both homeostatic and inflammatory conditions intestine-derived IL-18 modulates inflammation by suppressing Th17 cells and stimulating T regulatory (Treg) cell differentiation<sup>27,28</sup>. While Treg cell-derived IL-10 can support Lgr5<sup>+</sup> intestinal stem cell (ISC) self-renewal<sup>26</sup>. Gut-directed  $\alpha 4\beta 7$ -expressing T cells are preferentially recruited to intestinal crypts due to clustering of MAdCAM-1 expression on the endothelium of capillaries in the lower small intestinal crypt region making ISCs prone to damage<sup>30,33</sup>. Here, both CD4<sup>+</sup> and CD8<sup>+</sup> donor T cells cause non-specific intestinal epithelial crypt damage through the secretion of apoptosis-inducing interferon-gamma (IFN $\gamma$ ) in GVHD<sup>33</sup>. IECs have also been shown to play an essential role as APCs in murine GVHD<sup>24</sup> thereby having the potential to locally activate CD4<sup>+</sup> T cells. MHC-II expression by IECs is regulated through the presence of IFN $\gamma$  and was shown to be indispensable for the initiation of lethal acute GVHD in the GI tract<sup>24</sup>.



Until now most studies have focused on murine model systems. The identification of factors influencing these direct interactions between IECs and T cells is relevant in multiple settings, from the development of novel therapeutic strategies for the prevention or treatment of GVHD, to the identification of novel targets for cell- and immunotherapy. To this end it is important to develop *ex-vivo* human model systems to interrogate these interactions. Here, we have investigated the direct effects of intestinal epithelial damage caused by chemotherapy exposure on T cell behavior using a human intestinal organoid-based damage model. Intestinal organoids are 3D epithelial cultures that self-organize from isolated intestinal crypts when supplied with essential growth factors and have the potential to differentiate into all IEC types<sup>34,35</sup>. We and others have demonstrated organoids to be a relevant *ex-vivo* proxy for studying *in vivo* intestinal epithelial-immune cell interactions<sup>33,36–39</sup>. Here, we show that chemotherapy-induced epithelial injury increases T cell migration, proliferation and activation. In addition, utilizing this damage model we identify galectin-9 (Gal-9), a beta-galactoside-binding lectin released by the damaged epithelium, to play a role in IEC-mediated modulation of T cell behavior. Furthermore, Gal-9 was detectable in the plasma of clinical HSCT patients, and levels were increased in patients that eventually developed GVHD of the gut. Taken together, this study highlights the potential contribution of chemotherapy-induced epithelial damage to directly promoting T cell activation and trafficking. Furthermore, we have identified Gal-9 as a damage-associated molecule modulating T cell migration, proliferation, and IFN $\gamma$  production potentially contributing to the pathogenesis of immune disorders affecting the gut.

## Methods

### **T cell isolation and activation**

T cells were isolated from peripheral blood of healthy donors in the UMC Utrecht as approved by the METC (protocol 07/125) or from buffy coats (Sanquin, NL). After Ficoll-Paque (GE Healthcare) gradient separation, CD8<sup>+</sup> T cells were isolated from the peripheral blood mononuclear cells (PBMCs) in MACS buffer (2% heat-inactivated FBS, 2% 0,1M EDTA in PBSO) using the CD8<sup>+</sup> Dynabead isolation kit (Thermo Fisher) and BD IMag Cell Separation Magnet (BD Biosciences). CD4<sup>+</sup> T cells were isolated from the CD8-depleted PBMC fraction using the MagniSort human CD4<sup>+</sup> T cell enrichment kit (Thermo Fisher). T cell purity was checked by flow cytometry (routinely >80%). T cells were activated using plate-bound functional grade anti-human CD3 (1.6mg/ml in PBSO overnight at 4°C or 2h at 37°C, eBioscience) and soluble functional grade anti-human CD28 (1mg/ml, eBioscience) for 3 or 4 days as indicated at a concentration of 1 million cells/ml in T cell medium (TCM) (RPMI Medium 1640+GlutaMAX-I, Gibco, with 100U/ml pen-strep and 10% heat-inactivated FBS).

## Intestinal organoid cultures

Healthy human small intestinal epithelial organoids were established and cultured as previously described<sup>35</sup>. In short, organoids were generated from biopsies of individuals initially suspected of coeliac disease, but declared free of pathology, and stored in a biobank. All individuals provided written informed consent to participate in the study as approved by the medical ethical review board of the UMC Utrecht (METC) (protocol METC 10-402/K; TCBio 19-489). Organoids (>passage 7) were passaged via single cell dissociation using 1x TrypLE Express (Gibco) and resuspended in Advanced DMEM/F12 (Gibco), 100U/ml penicillin-streptomycin (Gibco), 10mM HEPES (Gibco) and Glutamax (Gibco) (GF- medium), and 50-66% Matrigel (Corning). After plating and Matrigel polymerization, human small intestinal organoid expansion medium (hSI-EM) was added consisting of GF-, Wnt-3a conditioned-medium (CM) (50%), R-spondin-1 CM (20%), Noggin CM (10%), murine EGF (50ng/ml, Peprotech), nicotinamide (10mM, Sigma), N-acetyl cysteine (1.25mM, Sigma), B27 (Gibco), TGF- $\beta$  inhibitor A83-01 (500nM, Tocris), p38 inhibitor SB202190 (10 $\mu$ M, Sigma), Rho-kinase/ROCK inhibitor Y-27632 (10 $\mu$ M, Abcam, for the first 2-3 days of culture), and Primocin (optional) (100 $\mu$ g/ml, Invitrogen). Medium was refreshed every 2-3 days. For indicated timepoints, treatment wells received different concentrations of Busulfan (Busilvex or TEVA), Fludarabinephosphate (Aerobindo), Clofarabine (Evoltra or Mylan) and rhIFN $\gamma$  (R&D systems).

## Migration transwell assay

Organoids were cultured in 24-well plates and treated for 48h with indicated conditions. After treatment, the medium was refreshed with hSI-EM without p38 inhibitor (no SB) for 24h. Simultaneously, isolated T cells were activated for 3 days or left resting in TCM. At the start of the assay, the T cells were stained with CTV and added to 3 $\mu$ m-pored transwell inserts (Greiner Bio-One) (400.000 T cells in 200 $\mu$ l) that were placed in the wells with organoids. After overnight incubation, inserts were removed and the contents of each well was dissociated with TrypLE and reconstituted in 300 $\mu$ l. The number of CTV<sup>+</sup> events per 150 $\mu$ L sample was counted using flow cytometry. For the Gal-9 blocking assays, 2 $\mu$ g/ml anti-Gal-9 mAb (BioLegend) was added to the lower compartment prior to start of the assay.

## T cell activation co-culture assay

For the evaluation of T cell activation and proliferation in the presence of chemotherapy treated organoids, organoids were cultured and treated with the indicated condition for 24h. Subsequently, organoids were mechanically disrupted. A portion of each condition was used to dissociate into single cells to infer the cell number and normalize between different conditions. T cells were isolated and stained with CTV. Co-cultures were set up in a 96-well plate, with 200,000 T cells and the equivalent of 1/6<sup>th</sup> of untreated organoids per well, in no SB medium with 10% BME. In activating conditions, wells had previously been coated with anti-CD3 and the medium was supplemented with anti-CD28. After 4



days of co-culture, the BME was disrupted in situ and the plate was cooled at 4°C for 30 min, before centrifugation at 500g 5 min at 4°C. When performing intracellular staining, GolgiStop (containing Monensin, BD Biosciences) was added to the medium 4h before staining. The pellets were dissociated to single cells with TrypLE, washed with PBSO and consequently stained for FC analysis as described above. For the Gal-9 blocking assays, 10µg/ml anti-Gal-9 mAb (BioLegend) was added to the co-culture from the start of the assay.

### **Immunofluorescent stainings**

For the  $\gamma$ H2AX-staining of organoids, treated organoids were harvested, washed in PBSO and fixated in formalin 4%/eosin 0.1% for 1h at room temperature and transferred to 70% ethanol. Consequently, the organoids were embedded in agarose (2.5%, Eurogentec, EP-0010-05), processed (Leica ASP 300 S) and embedded in paraffin (Surgipath Paraplast, Leica). The FFPE organoids were sectioned at 4µm, dried at 55 °C overnight and then deparaffinized in xylene and rehydrated in decreasing concentrations of alcohol (by using the leica autostainer). For antigen retrieval, the slides were incubated in sodium citrate buffer (10mM, pH 6, Merck) and washed with PBS/Tween20 (PBST). The slides were blocked with normal goat serum (10% in PBST) for 30 min and incubated with rabbit anti-phosphohistone H2A.X (Ser139) (20E3) (1:200, Cell Signaling, 9718) overnight at 4°C. The slides were washed with PBST and then incubated with goat anti-rabbit Alexa 647 (1:200, Thermo Fisher, a21244) for 1h at RT. After additional washing, the slides were mounted with fluoroshield with DAPI mounting medium (F6057, Sigma Aldrich).

### **Imaging of organoids**

Bright field (co-culture) images were acquired using an EVOS FL Cell Imaging System (Thermo Fisher Scientific). Fluorescence images were generated with a Leica (Wetzlar, Germany) SP8X laser-scanning confocal microscope.

### **Quantification of $\gamma$ H2AX-staining**

For the quantification of  $\gamma$ H2AX-staining in organoids, images acquired by the confocal microscope were processed in Fiji (ImageJ 1.53q) using a script<sup>40</sup>. In short, the channels of the RGB images were split, nuclei defined based on DAPI staining and maxima in the  $\gamma$ H2AX channel measured and quantified per nucleus. The number of foci per nucleus has then been analyzed.

### **CaspaseGlo assay**

Organoids were cultured in 96-well plates and treated with indicated conditions for 48h. Subsequently, the Matrigel was dissolved with GF- and the samples were transferred to a white opaque 96-well plate. Caspase-Glo 3/7 Reagent (Promega) was prepared as per protocol and added to the organoids in a 1:1 ratio to GF- up to a total volume of 100µl. The assay was incubated for 40 min and luminescence was measured with a TriStar2 Multimode

plate reader LB942 (Berthold Technologies).

### **Flow Cytometry**

T cells were stained with live/dead marker Zombie NIR (Biolegend) or Fixable Viability Dye eFluor 780 (Affymetrix eBioscience) and directly conjugated antibodies anti-CD3-PE and anti-CD4- or anti-CD8-FITC (BioLegend) either in FACS buffer (PBSO, 2mM EDTA, 0.5% BSA, Sigma) or MACS buffer (PBSO, 2mM EDTA, 2% FBS). For assessing T cell activation, anti-CD25-APC (BioLegend), anti-CD69-BV605 (BioLegend) were added to the staining. Intracellular IFN $\gamma$ -staining was performed using the Intracellular Fixation & Permeabilization Buffer Set (eBioscience Thermo Fisher) with anti-IFN $\gamma$ -PECy7 (BD Biosciences). For analysis of proliferation T cells were stained before start of the assay with CellTraceViolet (CTV) (Invitrogen, 5  $\mu$ M in PBSO) according to manufacturer's protocol. A Dead Cell Apoptosis Kit with Annexin V-FITC and propidium iodide was used according manufacturer for Annexin V FACS staining. FC data were acquired with a BD LSRFortessa Cell Analyzer (BD Biosciences) using FACSDiva (BD Biosciences) software and a CytoFLEX Flow Cytometer (Beckman Coulter) with CytExpert software. The data were analyzed with FlowJo (Treestar, 10.6.2) or CytExpert software (2.4).

### **CellTraceViolet proliferation assay**

For evaluation of the effect of chemotherapy treatment on organoid proliferation, organoids were dissociated into single cells and stained with CTV before plating. After 5 days of culture, organoids were harvested, processed into single cells, stained with Zombie NIR, and analyzed by FC.

### **Mitochondrial damage assay**

For the quantification of mitochondrial damage in chemotherapy treated organoids, organoids were incubated with MitoTracker Green FM (100nM, ThermoFisher) and Tetramethylrhodamine methyl ester perchlorate (TMRM) (150nM, ThermoFisher) for 45 min at 37 °C after treatment. After incubation organoids were dissociated into single cells, stained with Zombie NIR and analyzed by FC.

### **Luminex**

Biobanked plasma samples from HSCT patients at specific time points related to their HSCT date were used for luminex analysis. The data were collected after patients provided written informed consent (HSCT Biobank, local IRB approval 05-143 and 11-063k) in accordance with the Helsinki Declaration. Plasma had been stored at -80°C until analysis. With Luminex multiplex immunoassay technology, a total of 60 plasma proteins were measured; Gal-9, IL1RA, IL2, IL3, IL4, IL5, IL6, IL7, IL10, IL15, IL17, IL18, IL22, TNF $\alpha$ , IFN $\alpha$ , IFN $\gamma$ , APRIL, OSM, LAG3, Follistatin, I309, MIP1a, MIP1b, IL8, MIG, IP10, BLC, OPG, OPN, G-CSF, M-CSF, GM-CSF, SCF, HGF, EGF, AR, VEGF, CD40L, sPD1, FASL, IL1R1, IL1R2, ST2, TNFR1, TNFR2, sIL2R $\alpha$ ,



sCD27, IL7R $\alpha$ , sSCFR, Elastase, S100A8, Ang1, Ang2, LAP, TPO, sICAM, sVCAM, MMP3, Gal-3, C5a. The multiplex immunoassay was performed according to the protocol from the MultiPlex Core Facility of the UMCU<sup>41</sup>.

### **RNA sequencing**

For RNA sequencing of treated organoids, mRNA was isolated using Poly(A) Beads (NEXTflex). Sequencing libraries were prepared using the Rapid Directional RNA-Seq Kit (NEXTflex) and sequenced on a NextSeq500 (Illumina) to produce 75 base long reads (Utrecht DNA Sequencing Facility). Sequencing reads were mapped against the reference genome (hg19 assembly, NCBI37) using BWA41 package (mem -t 7 -c 100 -M -R)<sup>42</sup>. RNA sequencing was analyzed using DESeq2<sup>43</sup> in the R2: Genomics Analysis and Visualization Platform (<http://r2.amc.nl><http://r2.amc.nl>). A principle component analysis (PCA) was performed, and a list of differentially expressed genes (padj<0.1) was generated. Gene Ontology (GO) term analysis was done using either upregulated (logFoldChange>0) or downregulated (logFoldChange<0) DE genes as compared to control per condition using 2X2 contingency table analysis chi-square with continuity correction (padj<0.1). Gene Set Enrichment Analysis Pre-ranked analysis was performed with the GSEA software probing for enrichment of genes belonging to Hallmark datasets in the GSEA software<sup>44</sup>. A Venn Diagram was constructed using the webtool provided on (<https://bioinformatics.psb.ugent.be/webtools/Venn/>) and remade using Biorender.

### **Olink proximity extension proteomic analyses**

Organoids were cultured in 24-well plates and treated for 48h with indicated conditions. After treatment, the medium was refreshed with hSI-EM without p38 inhibitor (no SB) for 24h. Consequently, the CM was harvested and centrifuged 1000 g for 5 min. The supernatant was transferred to fresh Eppendorf tubes and stored at -80 °C until analysis. The Olink Target 96 Immuno-Oncology panel (v.3112) from Olink (Uppsala, Sweden) was used to quantify 92 immuno-oncology related proteins in each sample (IL-8, TNFRSF9, TIE2, MCP-3, CD40-L, IL-1 alpha, CD244, EGF, ANGPT1, IL-7, PGF, IL-6, ADGRG1, MCP-1, CRTAM, CXCL11, MCP-4, TRAIL, FGF2, CXCL9, CD8A, CAIX, MUC-16, ADA, CD4, NOS3, IL-2, Gal-9, VEGFR-2, CD40, IL-18, GZMH, KIR3DL1, LAP TGF-beta-1, CXCL1, TNFSF14, IL-33, TWEAK, PDGF subunit B, PDCD1, FASLG, CD28, CCL19, MCP-2, CCL4, IL-15, Gal-1, PD-L1, CD27, CXCL5, IL-5, HGF, GZMA, HO-1, CXCL1, CXCL10, CD70, IL-10, TNFRSF12A, CCL23, CD5, CCL3, MMP7, ARG1, NCR1, DCN, TNFRSF21, TNFRSF4, MIC-A/B, CCL17, ANGPT2, PTN, CXCL12, IFN-gamma, LAMP3, CASP-8, ICOSLG, MMP12, CXCL13, PD-L2, VEGFA, IL-4, LAG3, IL12RB1, IL-13, CCL20, TNF, KLRD1, GZMB, CD83, IL-12, CSF-1) Multiplex proximity extension assay panels were used to quantify each protein, as previously described<sup>45</sup>. The raw quantification cycle values were normalized and converted into normalized protein expression (NPX) units. The NPX values were expressed on a log<sub>2</sub> scale in which one unit higher in NPX values represents a doubling of the measured protein concentration. Quality control of the measured samples

was performed by using the standard quality control protocol of OLINK.

### Statistical analysis

Data are presented as mean  $\pm$  S.E.M. To take into account intra-individual and intra-experimental variation experiments were performed at least twice with several wells per condition, and sample material coming from at least two different human donors. Statistical significance was determined at  $P \leq 0.05$  using 2-way analysis of variance (ANOVA) with Tukey's multiple comparison test, 1-way ANOVA with Šidák's multiple comparison test, row-matched (RM) 1-way ANOVA with Dunnett's multiple comparison test, a Mann-Whitney  $U$  test, or a Student  $t$  test where appropriate. Significance is indicated as  $P \leq 0.05$  (\*),  $P \leq 0.01$  (\*\*), or  $P \leq 0.001$  (\*\*\*) or  $P < 0.0001$  (\*\*\*\*).

### Illustrations

All illustrations were made with BioRender.com.



## Results

### Modeling chemotherapy-induced damage in human small intestinal epithelial organoids

To study the direct effects of chemotherapy-induced epithelial damage on T cell behavior, we developed a novel damage model by exposing human intestinal epithelial organoids to three chemotherapeutics that are frequently used in HSCT conditioning regimens: busulfan (Bu), fludarabine (Flu) and clofarabine (Clo)<sup>46–53</sup>. Busulfan is an alkylating agent that crosslinks DNA strands, inhibiting DNA replication<sup>54</sup>, while fludarabine and clofarabine are both nucleoside analogs (NA), which are incorporated into the DNA during normal synthesis and thereby stall replication<sup>55</sup>. We evaluated chemotherapy concentrations that are used within the range of preclinical studies conducted in leukemia cell lines that eventually formed the basis for their clinical application<sup>47,56</sup>. Four-day chemotherapeutic exposure resulted in visible morphological changes, with smaller organoid size, a condense/folded phenotype and shedding of dead cells and cell debris both inward into the organoid lumen and outward into the organoid surroundings (Figure 1a). Sites of stalled DNA replication and DNA damage can be identified by nuclear foci of phosphorylated ( $\gamma$ ) histone (H)2AX complexes<sup>57</sup>. Indeed, exposure to all three chemotherapeutics caused a significant increase in  $\gamma$ H2AX complexes per nucleus in treated organoids (Figure 1b, Suppl. Fig. 1a). In treated organoids the induced replicative stress correlated with a reduction in proliferation compared to untreated organoids (Figure 1c). A dose-dependent decrease in mitochondrial membrane potential was also observed (Figure 1d) indicative of increased oxidative stress and apoptosis. Indeed, chemo-exposure induced apoptosis, as measured by a dose-dependent increase of caspase 3/7 activity (Figure 1e) and an increased percentage of Annexin-V positive cells (Figure 1f). Functionally, the number of organoids generated from

single cells was reduced, showing that chemo-treatment impaired their ability to regenerate (Figure 1g). Taken together, the tissue-damaging effects of chemotherapeutic-exposure on human intestinal epithelia can be modeled *ex-vivo* using organoids.

### **Chemotherapy treatment modulates intestinal transcriptional programs**

To evaluate transcriptional responses to chemotherapeutic exposure, bulk RNA sequencing (RNA-seq) of three independent organoid donors was performed. Treatment of organoids with Bu, Flu or Clo for 24 hours resulted in relatively subtle transcriptional changes with 66, 106 and 118 differentially expressed genes (DEGs) respectively (Figure 2a, Suppl. Table 1). A concise list of the top 50 DEGs identified for each individual treatment is shown in Figure 2b. While there are considerable differences between chemotherapeutics, all share certain similarities, in particular the two nucleoside analogs Flu and Clo, reflecting their common mechanism of action (Figure 2c, Suppl. Figure 1b). Flu and Clo treated organoids share the following DEGs: BACE1, BAX, CSNK2B, DDB2, GADD45A, GDF15, H1FO, IGFBP6, KIAA1430, KIAA1432, KIF3C, LAPTM4B, MDM2, PARP2, PKMYT1, RRM2B, TP53INP1, TRAPPC13, TXNIP, TYMS, UBR7, ZFH3. Bu, Flu and Clo-treated organoids share the following DEGs: C4ORF36, DENND2D, FAM126B, FOXO3B, PIPOX, SLC40A1. Gene Ontology (GO) term analysis of upregulated genes indicated a similar over-representation of upregulated gene sets in the nucleoside analog Flu- and Clo-treated organoids, including (mitotic) cell cycle processes, metabolic processes, and programmed cell death (Figure 2d; a complete list of GO gene sets is provided in Suppl. Table 1). Reflecting their mechanism of action, over-representation of genes related to DNA damage and repair as well as the p53 pathway was predominant in Flu- and Clo-treated organoids. Differences between the chemotherapy types, nucleoside analog or alkylating agent, were also observed by Gene Set Enrichment Analysis (GSEA) of chemo-treated organoids (Figure 2e). For example, a negative association between Bu-treatment and the p53 pathway was observed, in contrast to Flu- and Clo-treatment. However, a transcriptional change associated with inflammatory response was observed for all treatments. In summary, chemotherapeutics can evoke distinct transcriptional responses in the intestinal epithelium with nucleoside analogs Flu and Clo being more similar when compared with the alkylating agent Bu.



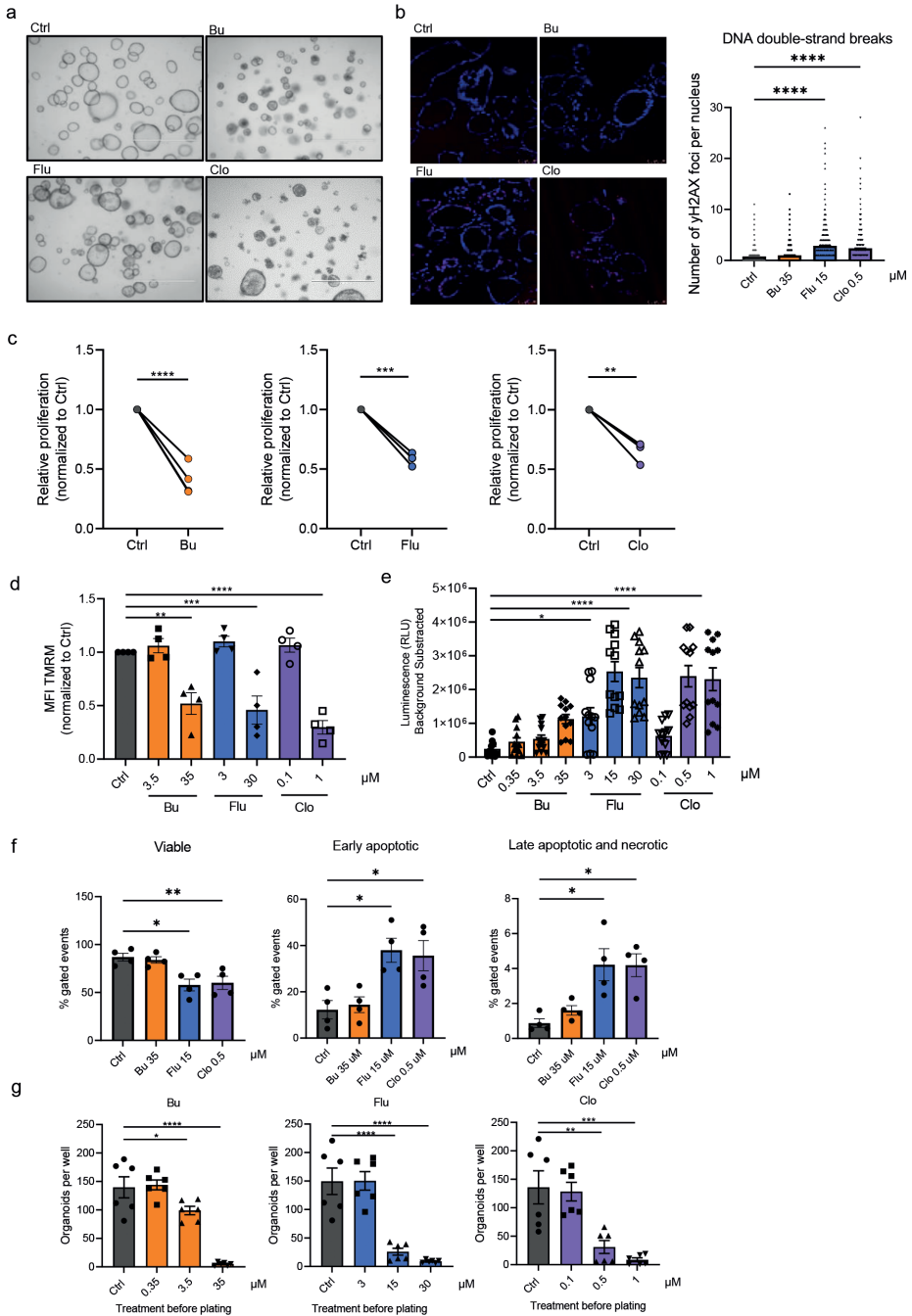


**Figure 1. Modeling chemotherapy-induced damage in human small intestinal epithelial organoids.** (a) Representative EVOS images of organoids treated for 96h with Busulfan (35 $\mu$ M), Fludarabine (15 $\mu$ M) or Clofarabine (1 $\mu$ M), scale bar = 1000 $\mu$ m. (b) Representative confocal images of organoids stained with DAPI (blue) and  $\gamma$ H2AX-complexes (red/AF647) 24h after chemo-treatment, at 40X, scale bar = 50 $\mu$ m



(left panel), quantification of  $\gamma$ H2AX foci per nucleus (right panel) (n=2 donors, >700 nuclei analyzed per condition), mean with SEM, ANOVA. **(c)** Relative proliferation of chemotherapy-treated organoids, quantified as CellTrace Violet MFI ratio by FACS after 72h of busulfan 35  $\mu$ M treatment (n=4 donors), fludarabine 7.5 $\mu$ M (n=2 donors), clofarabine 0.25 $\mu$ M (n=2 donors), Paired t test **(d)** Normalized MFI of TMRM staining for functional mitochondria after 48h of indicated chemo treatment damage, measured by FACS, n=2 donors, mean with SEM, ANOVA. **(e)** Levels of cleaved caspase 3/7 as measured by CaspaseGlo assay after 48h of indicated chemotherapy treatment, n=4 donors, mean with SEM, ANOVA. **(f)** Annexin-V and PI staining for early apoptotic (Annexin-V<sup>+</sup>) and late apoptotic or necrotic cells (Annexin-V<sup>+</sup>PI<sup>+</sup>) after 48h of indicated chemo treatment damage (right panels), measured by FACS. Representative FACS, n=2 donors, mean with SEM, ANOVA. **(g)** Reconstitution of single organoid cells into organoids after treatment with indicated chemo for 48h, n=2 donors, mean with SEM, ANOVA.

### **Chemotherapy-damaged organoids directly promote T cell activation**

To evaluate whether chemotherapy-damaged organoids can directly influence T cell responses, we first evaluated migration (Suppl. Figure 2a). Intermediate chemotherapeutic concentrations were chosen to model epithelial damage. In order to quantify T cell migration, we made use of a transwell system with 3 $\mu$ m-pored inserts. Organoids were treated with chemotherapeutics for 48 hours and subsequently cultured in drug-free medium for an additional 24 hours. Either unstimulated or polyclonally pre-activated CTV-stained human peripheral blood CD4<sup>+</sup> and CD8<sup>+</sup> T cells were subsequently added to the transwell insert (Suppl. Figure 2b). After 24 hours, the number of T cells that had migrated to the lower compartment was evaluated. Both unstimulated and pre-activated CD4<sup>+</sup> and CD8<sup>+</sup> T cells demonstrated significantly increased migration towards chemotherapy-treated organoids (Figure 3a).

Subsequently, the effect of chemotherapy-damaged epithelium on the polyclonal activation of T cells was evaluated (Suppl. Figure 2c). CD4<sup>+</sup> and CD8<sup>+</sup> T cells were isolated, stained with CTV, and activated by incubation with plate-bound anti-CD3 and soluble anti-CD28, in the presence of untreated or chemotherapy-treated organoids (representative images of organoids after treatment and before washing are shown in Suppl. Figure 2d). This co-culture system allows measurement of the effects of epithelial damage on T cell activation, as T cells received activation stimuli in the presence of damaged organoids. Proliferation and activation markers were assessed by flow cytometry after four days of co-culture. Co-culture with chemotherapy-treated epithelial organoids led to both increased IFN $\gamma$ -production (Figure 3b) and proliferation (Figure 3c). However, membrane expression levels of activation markers CD25 and CD69 (Figure 3d-e) were not significantly changed between conditions, with the exception of CD4<sup>+</sup> T cells co-cultured with Clo-treated organoids which expressed higher CD25. In conclusion, Bu-, Flu- and Clo-damaged intestinal epithelium promote T cell migration, and potentiated T cell activation, supporting T cell expansion and IFN $\gamma$  production.

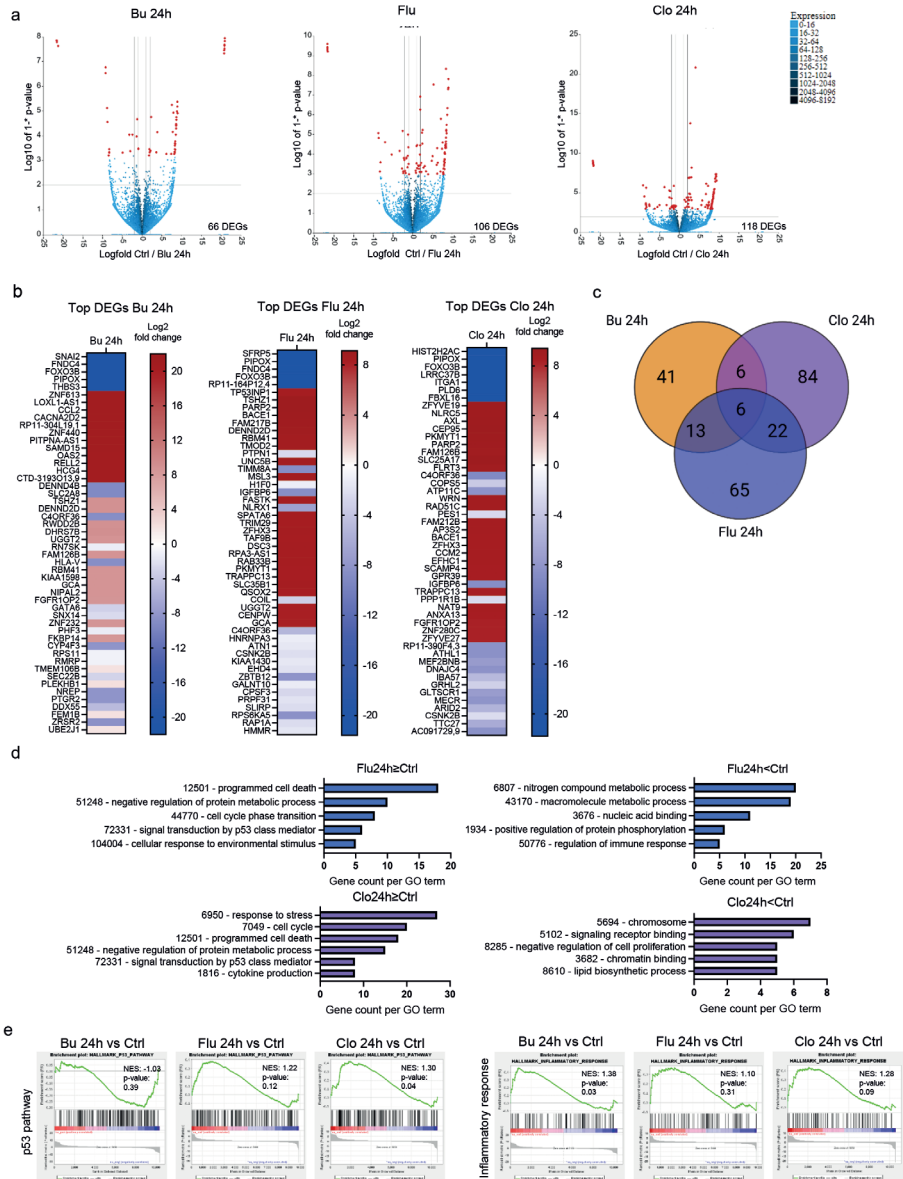


**Figure 2. Chemotherapy conditioning specifically reprograms the intestinal epithelial transcriptome.** (a-e) Human intestinal epithelial organoids (n=3 donors) were treated with busulfan (3.5 $\mu$ M), fludarabine (15 $\mu$ M), clofarabine (0.5 $\mu$ M) for 24h. RNA was isolated and subjected to bulk RNA-sequencing, after which bioinformatics analyses was performed. (a) Volcano plots indicating differentially expressed ( $\text{padj} < 0.1$ ) genes of 24h Bu- (left), Flu- (middle) and Clo- (right) treated organoids versus control in red. (b) Heatmaps of top most differentially expressed genes in 24h Bu- (left), Flu- (middle) and Clo- (right) treated organoids versus control (DESeq2,  $\text{padj} < 0.1$ ). (c) Venn-diagram showing numbers of overlapping and distinct DE genes between different chemotherapeutics (DESeq2,  $\text{padj} < 0.1$ ). (d) Gene Ontology (GO) term analysis of Biological Processes in genes upregulated (LFC>0) or downregulated (LFC<0) by 24h Bu- (top), Flu- (middle) and Clo- (bottom) treatment of organoids ( $\text{padj} < 0.1$ ). (e) Gene Set Enrichment Analysis (GSEA) on all genes in each indicated treatment-condition.

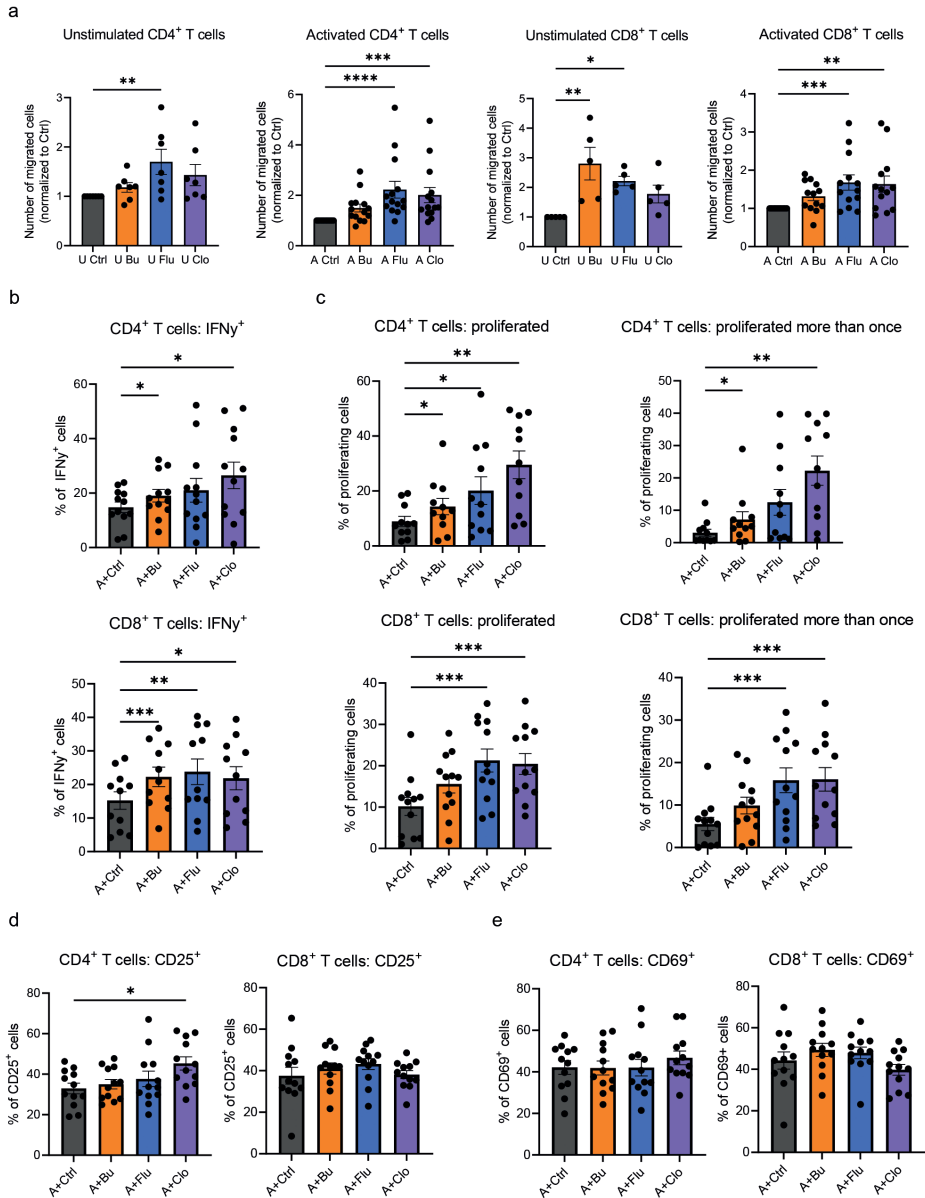


**Figure 3. Chemotherapy-induced damage promotes T cells migration and activation.** (a) Normalized number of unstimulated and pre-activated CD4<sup>+</sup> and CD8<sup>+</sup> T cells that have migrated overnight from a 3  $\mu$ m-pore sized insert (upper compartment) to the lower compartment containing organoids that were treated with busulfan (35 $\mu$ M), fludarabine (15 $\mu$ M), clofarabine (0.5 $\mu$ M) for 48h, and then refreshed for 24h, counted by FACS.  $n \geq 5$  T cell donors with 1 organoid donor, each data point indicates a T cell donor, mean with SEM, ANOVA. (b-e) (Membrane) activation marker expression and proliferation of CD4<sup>+</sup> and CD8<sup>+</sup> T cells as measured by CTV-dilution after 4-day co-culture with organoids that were previously treated with busulfan (35 $\mu$ M), fludarabine (15 $\mu$ M), clofarabine (0.5 $\mu$ M) for 24h before the start of the assay. Organoids were washed and disrupted mechanically before replating in co-culture with T cells.  $n \geq 11$  T cell donors with 1 organoid donor, each data point indicates a T cell donor, mean with SEM, ANOVA.

### Intestinal organoid-derived galectin-9 modulates T cell migration and activation

To gain mechanistic insight as to how epithelial damage can increase the migration and proliferation of T cells, we utilized the Olink proteomics platform. Here, we evaluated conditioned medium (CM) from both chemotherapy-damaged and untreated intestinal organoids<sup>45</sup>. 44 proteins were above level of detection (LOD), including chemokines such as C-X-C motif chemokine ligand 9 (CXCL9), CXCL10 and CXCL11; cytokines such as IFN $\gamma$  and IL-8; immune checkpoint molecules such as Programmed death-ligand 1 (PD-L1), and growth factors including EGF among others (Figure 4a). In the conditioned media from chemotherapy-damaged organoids the levels of galectin-9 (Gal-9), a beta-galactoside-binding lectin, were increased in CM predominantly from Flu- and Clo-treated organoids (Figure 4b). To determine whether Gal-9 may play a role in mediating the effects of chemotherapy-damaged organoids on T cell responses, an anti-Gal-9 blocking monoclonal antibody was utilized. Anti-Gal-9 added to the lower compartment significantly inhibited CD8<sup>+</sup> T cell migration and showed a trend towards decreased migration of CD4<sup>+</sup> T cells (Figure 4c). Furthermore, the presence of anti-Gal-9 abrogated both increased proliferation (Figure 4d) and IFN $\gamma$  levels (Figure 4e) observed in the presence of Bu-, Flu- and Clo-treated organoids. In contrast, T cells preserved the ability to express activation markers CD69 and, to a certain extent, CD25 (Suppl. Figure 3a). These data suggest that Gal-9 released by chemo-damaged epithelium can play an important role in T cell migration towards chemotherapy-damaged epithelium, consequently potentiating T cell activation supporting both expansion and IFN $\gamma$  production.

To evaluate whether Gal-9 levels following conditioning are also increased in a clinical setting, we measured Gal-9 levels in stored plasma samples of 17 pediatric transplant patients aged 12-18 at multiple early time points after HSCT. All patients received a conditioning regimen with Bu and Flu, and, in addition, some patients Clo, before undergoing transplantation with a cord blood graft. Seven patients developed acute GVHD grade II-IV with gastrointestinal involvement. Median time to GVHD was 24 days (range 15-45) and all patients had a follow-up of more than 100 days. Gal-9 levels were measurable in the plasma of all patients (Figure 4f) and were increased at the day of, or early after, transplant in patients that later on developed grade II-IV acute GVHD. Furthermore, Gal-9 levels remained elevated at several time points after HSCT in grade 2-4 GVHD patients. While correlative, this observation suggests that our model system can have predictive value in identifying novel intestinal damage biomarkers. Taken together, our data suggests that Gal-9 may be a biomarker for the development of GVHD in HSCT patients. Our functional data further support a pathogenic role for Gal-9, perhaps by increasing migration and activation of T cells at the site of the conditioning-damaged intestinal epithelium.



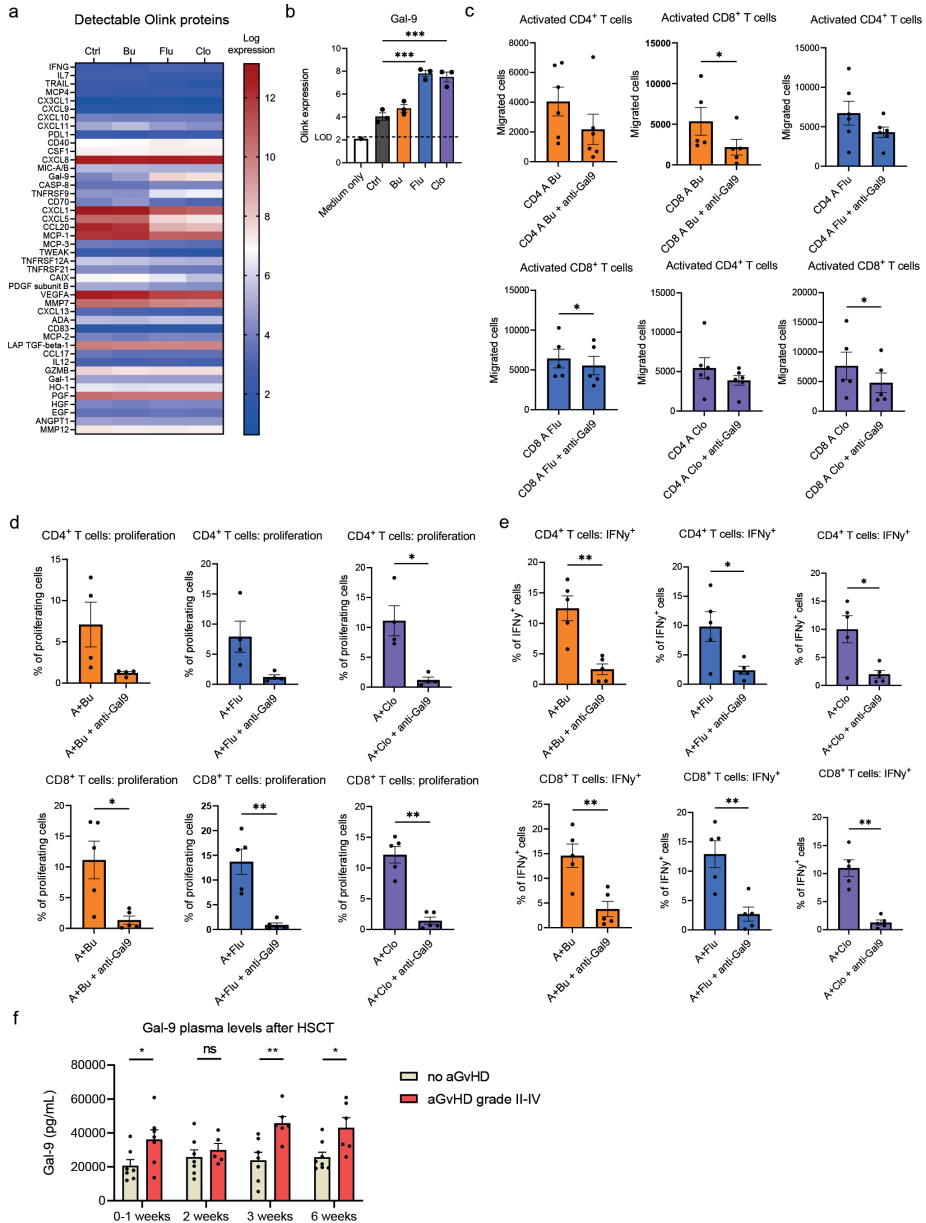


**Figure 4. Galactin-9 is released by chemo-damaged organoids and contributes to T cell migration, activation and proliferation.** (a-b) Analysis of proteins present in conditioned media of organoids treated with chemotherapeutics as in the ex-vivo T cell migration assay (Olink Proteomics) (n=3 donors). Each data point indicates the levels of Gal-9 in the CM from each organoid condition (log scale), mean with SEM, ANOVA. (c) Migration of activated CD4<sup>+</sup> and CD8<sup>+</sup> T cells towards treated organoids in the presence of anti-gGal-9 blocking mAb. n $\geq$ 5 T cell donors with 1 organoid donor, each data point indicates a T cell donor, mean with SEM, paired t-test. (d-e) CD4<sup>+</sup> and CD8<sup>+</sup> T cell activation after co-culture with treated organoids in the presence of anti-Gal-9 mAb. n $\geq$ 4 T cell donors with 1 organoid donor, each data point indicates a T cell donor, mean with SEM, paired t-test. (f) Galactin-9 levels in plasma of HSCT patients with and without acute grade II-IV (gut) GVHD as measured by Luminex. n $\geq$ 5 patients per condition

## Discussion

Immune activation after intestinal epithelial cell injury is a well-known phenomenon, but how such damage can directly affect T cell function remains unclear. Here we have developed a novel *ex-vivo* intestinal organoid model to mimic chemotherapy-induced damage which can occur during cancer treatment or conditioning preceding HSCT. This *ex-vivo* human model has allowed us to study the direct effect of epithelial damage on T cell homeostasis, without possible confounding or species-specific interactions that may occur in an *in vivo mouse* setting. In addition to developing our understanding of the biology of T cell responses during sterile inflammation, the model has the potential to serve as a platform for the discovery of new targets and testing of therapeutics in multiple intestinal disease settings including the field of HSCT and GVHD, as well as in the tailored development of autologous immunotherapy and CAR T cell therapy for solid tumors in sequence with chemo or radiotherapy<sup>58-61</sup>.

This is the first study comparing epithelial damage response to different clinically relevant chemotherapeutics. We observed that exposure of intestinal epithelial organoids to chemotherapeutics resulted in chemotherapy-distinct transcriptional responses. Their main chemotherapeutic mechanism of action is chain termination when incorporated in place of natural purine nucleosides, with stalling of the cells in S-phase resulting in induction of apoptosis. Clofarabine affects cells with lower proliferation rates as well. Busulfan on the other hand is an alkylating agent that crosslinks guanine bases in the DNA, therefore, making it impossible for DNA strands to unfold, thereby also resulting in apoptosis. Although we cannot completely exclude the contribution of the chemotherapeutic concentrations utilized, we observed a similar gene expression pattern and related T cell responses between Flu and Clo, the purine nucleoside analogs we included in our study. While it is currently not possible to reduce chemotherapy regimens, it is important to understand the differential consequences of exposure to each individual chemotherapeutic, and a further argument for pursuing the development of antibody-based conditioning for the future<sup>62</sup>.

We found that epithelial damage caused by chemotherapy increases the migration of both resting and polyclonally pre-activated T cells toward the site of injury. The migration assay studies the cells in two compartments, suggesting a soluble molecule gradient to be responsible for this. Interestingly, in our setting, migration occurred in the absence of endothelium, or any previously known intestinal-epithelial-derived chemokine. In particular, we did not observe an increase in the concentration of the chemokines CXCL9, CXCL10 and CXCL11. However, we observed decreased T cell migration when blocking Gal-9 during the migration assays, suggesting a possible new role for Gal-9 in modulating T cell trafficking to the damaged epithelium.



Besides the capacity of chemotherapy-induced epithelial damage to increase T cell migration, we also demonstrate a direct influence on the proliferation and activation of T cells. Besides peripheral and local hematopoietic APC-mediated activation, we have shown for the first time that damaged epithelium can directly additionally stimulate tissue-recruited activated T cells, which likely further propagates intestinal damage through local IFN $\gamma$  production. While the precise mechanism by which this occurs remains to be fully elucidated, we have identified Gal-9 as novel driver. Gal-9 is a beta-galactoside-binding lectin with immunomodulatory properties widely expressed by a variety of tissues<sup>63-65</sup>. The carbohydrate domains of Gal-9 can bind  $\beta$ -galactosides, such as lactose, found on O-glycans and N-glycans of glycosylated proteins or lipids<sup>66</sup>. Gal-9 expression can be nuclear as well as cytoplasmic, or extracellular where it is membrane-bound or in the extracellular matrix. It has many different receptors, among which TIM-3, DR3, 4-1BB, CD44, PD1 and Protein Disulfide Isomerase are expressed on T cells<sup>67-72</sup>. Interestingly, the expression of soluble TNFRSF9 (CD137 or 4-1BB), one of the receptors for Gal-9, was also significantly upregulated in chemo-treated organoids (Supp. Figure 3b). The reported effects of Gal-9 on T cells *in vitro*, *in vivo*, and deduced from human biomarker studies are pleiotropic and range from immunosuppressive to pro-inflammatory. The complexity of reported effects may be related to the Gal-9 doses utilized, species differences, as well as the cellular or tissue context. Gal-9 at low doses has been shown to increase T cell expansion and activation *ex-vivo*, inducing a Th1 phenotype with IFN $\gamma$  production<sup>73</sup>. This Th1-type response by Gal-9 has been linked to a pathway mimicking antigen-specific activation of the TCR resulting in cytosolic calcium mobilization<sup>74-76</sup>. However, which receptor mediates these effects remains unknown. The binding of Gal-9 to TIM3 on conventional T cells has been reported to induce apoptosis<sup>67</sup>, which we have not observed in our studies. However, Gal-9 TIM-3-induced apoptosis has only been observed under supraphysiological concentrations of Gal-9, and the relevance of this for human T cells is unclear. These effects are also likely to be immune context-dependent since CD4<sup>+</sup> T cells from rheumatoid arthritis patients also do not undergo apoptosis when exposed to increasing concentrations of Gal-9, compared to cells from healthy controls<sup>77</sup>.

Damage to the gastrointestinal tract plays a major role in the morbidity and mortality associated with GVHD. Currently, it remains difficult to predict the onset of intestinal GVHD due to a lack of early biomarkers. Our data show increased plasma levels of Gal-9 even early after conditioning which persist in patients that develop GVHD after HSCT. Others have shown increased serum Gal-9 later, at onset of GVHD, suggesting it to be a biomarker of the disease, which may or may not be directly related to its pathophysiology. Higher levels of Gal-9 measured from 4 weeks post HSCT, were associated with a higher incidence of GVHD, a higher transplant related mortality and a lower overall survival<sup>78</sup>. Gal-9 levels have also been associated with intestinal inflammation and correlate with disease severity in inflammatory bowel disease<sup>79</sup>. In contrast to our own data, a recent study has shown that large doses of Gal-9 administered intraperitoneally reduced acute GVHD in a murine



model<sup>80</sup>. However, in this study Gal-9 was administered only after the initial onset of GVHD and of note there was no improvement in overall survival. Despite the differences frequently observed between species, and especially for Gal-9, another murine study showed that perturbation of TIM3/Gal-9 interaction increased GVHD lethality, but reduced it when Treg cells were concomitantly depleted from the graft, resulting in improved survival<sup>81</sup>. Gal-9 has also recently received attention in the context of cancer immunotherapy<sup>82,83</sup> where anti-Gal-9 blocking antibodies are being developed as checkpoint inhibitors to induce the anti-tumor immune response. Ongoing clinical trials (NCT0466668) will provide important information regarding the safety and effectiveness of Gal-9 blockade, potentially helping the translation of Gal-9 targeting intervention for GVHD patients<sup>84</sup>. However, given the pleiotropic and diverse effects reported, strict control of Gal-9 perturbation must be in place in respect to timing, location and cell types involved.

In conclusion, we have modeled chemotherapy-induced damage to the human intestinal epithelium and studied its effects on T cell homeostasis. T cells demonstrate increased migration to chemotherapy-treated organoids, proliferated more and expressed higher levels of IFN $\gamma$ . We propose that damaged-organoid-derived Gal-9 may be a novel damage-associated molecule responsible for these effects, and we suggest that Gal-9 may be a possible biomarker for GVHD development in HSCT patients. In addition, treatment aimed at blocking/potentiating Gal-9 may be a new damage-dampening, preventive therapy in the context of immune-mediated diseases in which there is damage in the gut, such as GI-GVHD.

### **Acknowledgments**

We would like to thank all members of the Lindemans and Coffey groups for helpful discussions. Elsbeth van Liere, Bart Westendorp, Thomas Brand and Jet Segeren for help with the  $\gamma$ H2AX stainings and analysis. Sabine Middendorp for generation of organoid lines. Maaïke de Vries for help in acquiring  $\gamma$ H2AX confocal images. We thank the Hubrecht Institute FACS facility, the Olink facility at the UMC Utrecht, Noortje van den Dungen of the Epigenetics facility of the UMC Utrecht, USEQ, and Richard Volckmann from R2- support. We would also like to thank Nienke Vriesekoop for discussions on immune cell migration.

### **Author Contributions**

SAJ and AC designed, performed, and analyzed experiments, and wrote the manuscript. MH, LSS, CK and SN performed experiments. MM assisted with RNA sequencing analysis. EM assisted with experimental design. PJC and CAL supervised the research, helped in experimental design, and wrote the manuscript. EES and AMH provided expert advice. All authors contributed to the manuscript.

### **Conflict of Interest Disclosures**

The authors declare no conflicts of interest.



## References

1. Barker N, van Es JH, Kuipers J, Kujala P, van den Born M, Cozijnsen M, Haegebarth A, Korving J, Begthel H, Peters PJ, Clevers H. Identification of stem cells in small intestine and colon by marker gene Lgr5. *Nature*. 2007 Oct;449(7165):1003–7.
2. Odenwald MA, Turner JR. The intestinal epithelial barrier: a therapeutic target? *Nat Rev Gastroenterol Hepatol*. 2017 Jan;14(1):9–21.
3. Odenwald MA, Turner JR. Intestinal permeability defects: is it time to treat? *Clin Gastroenterol Hepatol*. 2013 Sep;11(9):1075–83.
4. Turpin W, Lee SH, Raygoza Garay JA, Madsen KL, Meddings JB, Bedrani L, Power N, Espin-Garcia O, Xu W, Smith MI, Griffiths AM, Moayyedi P, Turner D, Seidman EG, Steinhart AH, Marshall JK, Jacobson K, Mack D, Huynh H, Bernstein CN, Paterson AD, Croitoru K. Increased Intestinal Permeability Is Associated With Later Development of Crohn's Disease. *Gastroenterology*. 2020 Dec;159(6):2092–2100.e5.
5. Torres J, Petralia F, Sato T, Wang P, Telesco SE, Choung RS, Strauss R, Li XJ, Laird RM, Gutierrez RL, Porter CK, Plevy S, Princen F, Murray JA, Riddle MS, Colombel JF. Serum Biomarkers Identify Patients Who Will Develop Inflammatory Bowel Diseases Up to 5 Years Before Diagnosis. *Gastroenterology*. 2020 Jul;159(1):96–104.
6. Abadie V, Kim SM, Lejeune T, Palanski BA, Ernest JD, Tastet O, Voisine J, Discepolo V, Marietta E V, Hawash MBF, Ciszewski C, Bouziat R, Panigrahi K, Horwath I, Zurenski MA, Lawrence I, Dumaine A, Yotova V, Grenier JC, Murray JA, Khosla C, Barreiro LB, Jabri B. IL-15, gluten and HLA-DQ8 drive tissue destruction in coeliac disease. *Nature*. 2020 Feb;578(7796):600–4.
7. Dotsenko V, Oittinen M, Taavela J, Popp A, Peräaho M, Staff S, Sarin J, Leon F, Isola J, Mäki M, Viiri K. Genome-Wide Transcriptomic Analysis of Intestinal Mucosa in Celiac Disease Patients on a Gluten-Free Diet and Postgluten Challenge. *Cell Mol Gastroenterol Hepatol*. 2021;11(1):13–32.
8. Nalle SC, Zuo L, Ong MLDM, Singh G, Worthylake AM, Choi W, Manresa MC, Southworth AP, Edelblum KL, Baker GJ, Joseph NE, Savage PA, Turner JR. Graft-versus-host disease propagation depends on increased intestinal epithelial tight junction permeability. *J Clin Invest*. 2019 Feb;129(2):902–14.
9. Jansen SA, Nieuwenhuis EES, Hanash AM, Lindemans CA. Challenges and opportunities targeting mechanisms of epithelial injury and recovery in acute intestinal graft-versus-host disease. *Mucosal Immunol*. 2022 Apr;15(4):605–19.
10. van Wijk F, Cheroutre H. Mucosal T cells in gut homeostasis and inflammation. *Expert Rev Clin Immunol*. 2010 Jul;6(4):559–66.
11. Boussios S, Pentheroudakis G, Katsanos K, Pavlidis N. Systemic treatment-induced gastrointestinal toxicity: incidence, clinical presentation and management. Vol. 25, *Annals of gastroenterology*. 2012. p. 106–18.
12. Elting LS, Cooksley C, Chambers M, Cantor SB, Manzullo E, Rubenstein EB. The burdens of cancer therapy. Clinical and economic outcomes of chemotherapy-induced mucositis. *Cancer*. 2003 Oct;98(7):1531–9.
13. Fischer JC, Wintges A, Haas T, Poeck H. Assessment of mucosal integrity by quantifying neutrophil granulocyte influx in murine models of acute intestinal injury. *Cell Immunol*. 2017 Jun;316:70–6.
14. Johansson JE, Brune M, Ekman T. The gut mucosa barrier is preserved during allogeneic, haemopoietic stem cell transplantation with reduced intensity conditioning. *Bone Marrow Transplant*. 2001 Oct;28(8):737–42.
15. Johansson JE, Ekman T. Gut toxicity during hemopoietic stem cell transplantation may predict acute graft-versus-host disease severity in patients. *Dig Dis Sci*. 2007 Sep;52(9):2340–5.
16. Ferrara JLM, Levine JE, Reddy P, Holler E. Graft-versus-host disease. *Lancet*. 2009 May;373(9674):1550–61.
17. Zeiser R, Blazar BR. Acute Graft-versus-Host Disease. Vol. 378, *The New England journal of medicine*. United States; 2018. p. 586.
18. Jagasia M, Arora M, Flowers MED, Chao NJ, McCarthy PL, Cutler CS, Urbano-Ispizua A, Pavletic SZ, Haagenson MD, Zhang MJ, Antin JH, Bolwell BJ, Bredeson C, Cahn JY, Cairo M, Gale RP, Gupta V, Lee SJ, Litzow M, Weisdorf DJ, Horowitz MM, Hahn T. Risk factors for acute GVHD and survival after hematopoietic cell transplantation. *Blood*. 2012 Jan;119(1):296–307.
19. Nakasone H, Fukuda T, Kanda J, Mori T, Yano S, Kobayashi T, Miyamura K, Eto T, Kanamori H, Iwato K, Uchida N, Mori S, Nagamura-Inoue T, Ichinohe T, Atsuta Y, Teshima T, Murata M. Impact of conditioning intensity and TBI on acute GVHD after hematopoietic cell transplantation. *Bone Marrow Transplant*. 2015 Apr;50(4):559–65.
20. Flowers MED, Inamoto Y, Carpenter PA, Lee SJ, Kiem HP, Petersdorf EW, Pereira SE, Nash RA, Mielcarek M, Fero ML, Warren EH, Sanders JE, Storb RF, Appelbaum FR, Storer BE, Martin PJ. Comparative analysis of risk factors for acute graft-versus-host disease and for chronic graft-versus-host disease according to National Institutes of Health consensus criteria. *Blood*. 2011 Mar;117(11):3214–9.
21. Liu D, Yan C, Xu L, Wang Y, Han W, Zhang X, Liu K, Huang X. Diarrhea during the conditioning regimen is correlated with the occurrence of severe acute graft-versus-host disease through systemic release of inflammatory cytokines. *Biol Blood Marrow Transplant*. 2010 Nov;16(11):1567–75.
22. Koyama M, Kuns RD, Olver SD, Raffelt NC, Wilson YA, Don ALJ, Lineburg KE, Cheong M, Robb RJ, Markey KA, Varelias A, Malissen B, Hammerling GJ, Clouston AD, Engwerda CR, Bhat P, MacDonald KPA, Hill GR. Recipient nonhematopoietic antigen-presenting cells are sufficient to induce lethal acute graft-versus-host disease. *Nat*

- Med. 2011 Nov;18(1):135–42.
23. Koyama M, Hill GR. The primacy of gastrointestinal tract antigen-presenting cells in lethal graft-versus-host disease. *Blood*. 2019 Dec;134(24):2139–48.
  24. Koyama M, Mukhopadhyay P, Schuster IS, Henden AS, Hulsdunker J, Varelias A, Vetizou M, Kuns RD, Robb RJ, Zhang P, Blazar BR, Thomas R, Begun J, Waddell N, Trinchieri G, Zeiser R, Clouston AD, Degli-Esposti MA, Hill GR. MHC Class II Antigen Presentation by the Intestinal Epithelium Initiates Graft-versus-Host Disease and Is Influenced by the Microbiota. *Immunity*. 2019 Nov;51(5):885–898.e7.
  25. Yu Y, Jin QR, Mi Y, Liu JQ, Liu ZQ, Wang S, Liu ZG, Yang PC, Zheng PY. Intestinal Epithelial Cell-Derived CD83 Contributes to Regulatory T-Cell Generation and Inhibition of Food Allergy. *J Innate Immun*. 2021;13(5):295–305.
  26. Biton M, Haber AL, Rogel N, Burgin G, Beyaz S, Schnell A, Ashenberg O, Su CW, Smillie C, Shekhar K, Chen Z, Wu C, Ordovas-Montanes J, Alvarez D, Herbst RH, Zhang M, Tirosh I, Dionne D, Nguyen LT, Xifaras ME, Shalek AK, von Andrian UH, Graham DB, Rozenblatt-Rosen O, Shi HN, Kuchroo V, Yilmaz OH, Regev A, Xavier RJ. T Helper Cell Cytokines Modulate Intestinal Stem Cell Renewal and Differentiation. *Cell*. 2018 Nov;175(5):1307–1320.e22.
  27. Harrison OJ, Srinivasan N, Pott J, Schiering C, Krausgruber T, Ilott NE, Maloy KJ. Epithelial-derived IL-18 regulates Th17 cell differentiation and Foxp3<sup>+</sup> Treg cell function in the intestine. *Mucosal Immunol*. 2015 Nov;8(6):1226–36.
  28. Schiering C, Krausgruber T, Chomka A, Fröhlich A, Adelmann K, Wohlfert EA, Pott J, Griseri T, Bollrath J, Hegazy AN, Harrison OJ, Owens BMJ, Löhning M, Belkaid Y, Fallon PG, Powrie F. The alarmin IL-33 promotes regulatory T-cell function in the intestine. *Nature*. 2014 Sep;513(7519):564–8.
  29. Watanabe M, Ueno Y, Yajima T, Iwao Y, Tsuchiya M, Ishikawa H, Aiso S, Hibi T, Ishii H. Interleukin 7 is produced by human intestinal epithelial cells and regulates the proliferation of intestinal mucosal lymphocytes. *J Clin Invest*. 1995 Jun;95(6):2945–53.
  30. Fu YY, Egorova A, Sobieski C, Kuttiyara J, Calafiore M, Takashima S, Clevers H, Hanash AM. T Cell Recruitment to the Intestinal Stem Cell Compartment Drives Immune-Mediated Intestinal Damage after Allogeneic Transplantation. *Immunity*. 2019 Jul;51(1):90–103.e3.
  31. Sujino T, London M, Hoytema van Konijnenburg DP, Rendon T, Buch T, Silva HM, Lafaille JJ, Reis BS, Mucida D. Tissue adaptation of regulatory and intraepithelial CD4<sup>+</sup> T cells controls gut inflammation. *Science*. 2016 Jun 24;352(6293):1581–6.
  32. Hoytema van Konijnenburg DP, Reis BS, Pedicord VA, Farache J, Victora GD, Mucida D. Intestinal Epithelial and Intraepithelial T Cell Crosstalk Mediates a Dynamic Response to Infection. *Cell*. 2017 Nov 2;171(4):783–794.e13.
  33. Takashima S, Martin ML, Jansen SA, Fu Y, Bos J, Chandra D, O'Connor MH, Mertelsmann AM, Vinci P, Kuttiyara J, Devlin SM, Middendorp S, Calafiore M, Egorova A, Kleppe M, Lo Y, Shroyer NF, Cheng EH, Levine RL, Liu C, Kolesnick R, Lindemans CA, Hanash AM. T cell-derived interferon-gamma programs stem cell death in immune-mediated intestinal damage. *Sci Immunol*. 2019 Dec;4(42).
  34. Sato T, Vries RG, Snippert HJ, van de Wetering M, Barker N, Stange DE, van Es JH, Abo A, Kujala P, Peters PJ, Clevers H. Single Lgr5 stem cells build crypt-villus structures in vitro without a mesenchymal niche. *Nature*. 2009 May;459(7244):262–5.
  35. Sato T, Stange DE, Ferrante M, Vries RGJ, Van Es JH, Van den Brink S, Van Houdt WJ, Pronk A, Van Gorp J, Siersema PD, Clevers H. Long-term expansion of epithelial organoids from human colon, adenoma, adenocarcinoma, and Barrett's epithelium. *Gastroenterology*. 2011 Nov;141(5):1762–72.
  36. Lindemans CA, Calafiore M, Mertelsmann AM, O'Connor MH, Dudakov JA, Jenq RR, Velardi E, Young LF, Smith OM, Lawrence G, Ivanov JA, Fu YY, Takashima S, Hua G, Martin ML, O'Rourke KP, Lo YH, Mokry M, Romera-Hernandez M, Cupedo T, Dow L, Nieuwenhuis EE, Shroyer NF, Liu C, Kolesnick R, van den Brink MRM, Hanash AM. Interleukin-22 promotes intestinal-stem-cell-mediated epithelial regeneration. *Nature*. 2015 Dec;528(7583):560–4.
  37. Bar-Ephraim YE, Kretzschmar K, Clevers H. Organoids in immunological research. *Nat Rev Immunol*. 2020 May;20(5):279–93.
  38. Kelsen JR, Dawany N, Conrad MA, Karakasheva TA, Maurer K, Wei JM, Uman S, Dent MH, Behera R, Bryant LM, Ma X, Moreira L, Chatterji P, Shraim R, Merz A, Mizuno R, Simon LA, Muir AB, Giraudo C, Behrens EM, Whelan KA, Devoto M, Russo PA, Andres SF, Sullivan KE, Hamilton KE. Colonoids From Patients With Pediatric Inflammatory Bowel Disease Exhibit Decreased Growth Associated With Inflammation Severity and Durable Upregulation of Antigen Presentation Genes. *Inflamm Bowel Dis*. 2021 Jan;27(2):256–67.
  39. Rana N, Privitera G, Kondolf HC, Bulek K, Lechuga S, De Salvo C, Corridoni D, Antanaviciute A, Maywald RL, Hurtado AM, Zhao J, Huang EH, Li X, Chan ER, Simmons A, Bamias G, Abbott DW, Heaney JD, Ivanov AI, Pizarro TT. GSDMB is increased in IBD and regulates epithelial restitution/repair independent of pyroptosis. *Cell*. 2022 Jan;185(2):283–298.e17.
  40. Segeren HA, van Liere EA, Riemers FM, de Bruin A, Westendorp B. Oncogenic RAS sensitizes cells to drug-induced replication stress via transcriptional silencing of P53. *Oncogene*. 2022 May;41(19):2719–33.
  41. de Jager W, Prakken BJ, Bijlsma JWW, Kuis W, Rijkers GT. Improved multiplex immunoassay performance in human plasma and synovial fluid following removal of interfering heterophilic antibodies. *J Immunol Methods*. 2005 May;300(1–2):124–35.

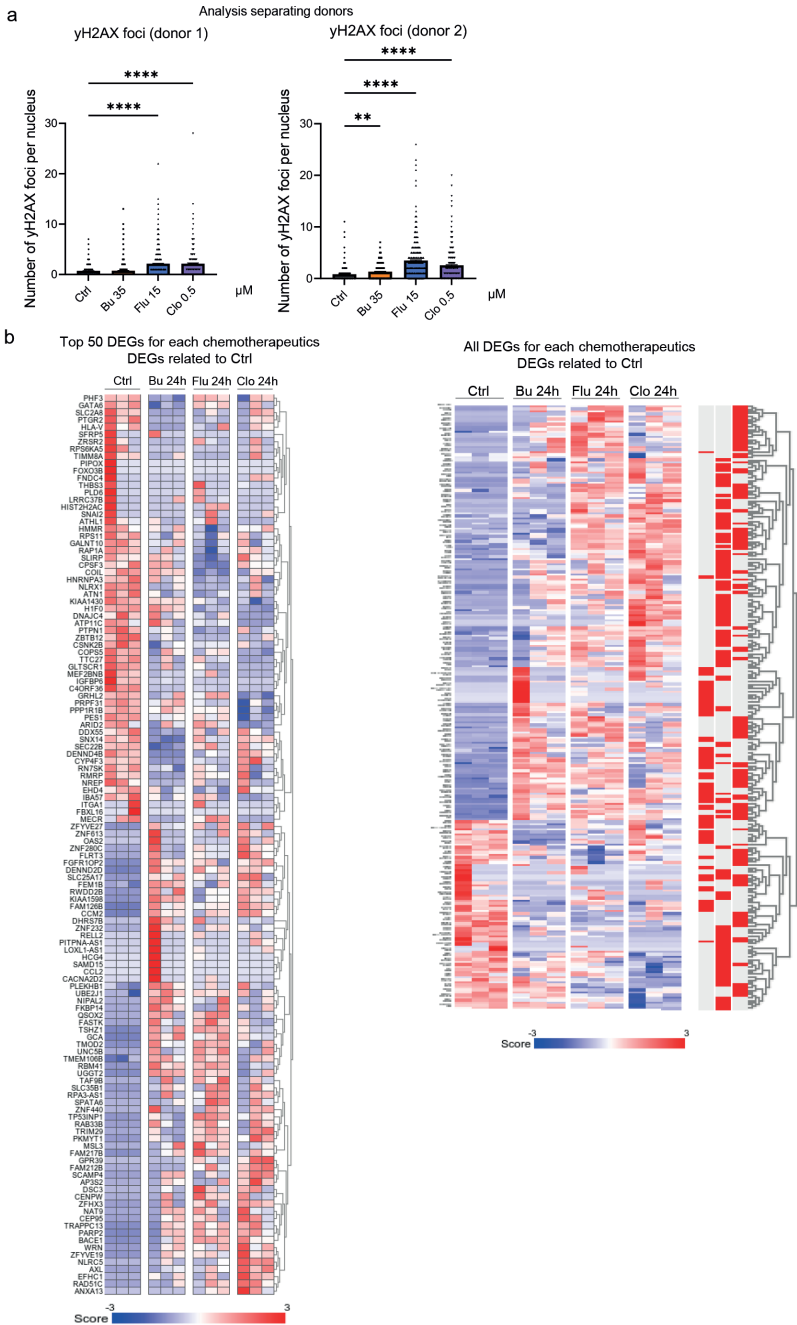


42. Li H, Durbin R. Fast and accurate short read alignment with Burrows-Wheeler transform. *Bioinformatics*. 2009 Jul 15;25(14):1754–60.
43. Love MI, Huber W, Anders S. Moderated estimation of fold change and dispersion for RNA-seq data with DESeq2. *Genome Biol*. 2014;15(12):550.
44. Subramanian A, Tamayo P, Mootha VK, Mukherjee S, Ebert BL, Gillette MA, Paulovich A, Pomeroy SL, Golub TR, Lander ES, Mesirov JP. Gene set enrichment analysis: a knowledge-based approach for interpreting genome-wide expression profiles. *Proc Natl Acad Sci U S A*. 2005 Oct 25;102(43):15545–50.
45. Assarsson E, Lundberg M, Holmquist G, Björkstén J, Thorsen SB, Ekman D, Eriksson A, Renzel Dickens E, Ohlsson S, Edfeldt G, Andersson AC, Lindstedt P, Stenvang J, Gullberg M, Fredriksson S. Homogenous 96-plex PEA immunoassay exhibiting high sensitivity, specificity, and excellent scalability. *PLoS One*. 2014;9(4):e95192.
46. Kebriaei P, Bassett R, Lyons G, Valdez B, Ledesma C, Rondon G, Oran B, Ciurea S, Alousi A, Popat U, Patel K, Ahmed S, Olson A, Bashir Q, Shah N, Jones R, Marin D, Rezvani K, Nieto Y, Khouri I, Qazilbash M, Hosing C, Shpall E, Champlin RE, Andersson BS. Clofarabine Plus Busulfan is an Effective Conditioning Regimen for Allogeneic Hematopoietic Stem Cell Transplantation in Patients with Acute Lymphoblastic Leukemia: Long-Term Study Results. *Biol Blood Marrow Transplant*. 2017 Feb;23(2):285–92.
47. Alatrash G, Thall PF, Valdez BC, Fox PS, Ning J, Garber HR, Janbey S, Worth LL, Popat U, Hosing C, Alousi AM, Kebriaei P, Shpall EJ, Jones RB, de Lima M, Rondon G, Chen J, Champlin RE, Andersson BS. Long-Term Outcomes after Treatment with Clofarabine ± Fludarabine with Once-Daily Intravenous Busulfan as Pretransplant Conditioning Therapy for Advanced Myeloid Leukemia and Myelodysplastic Syndrome. *Biol Blood Marrow Transplant*. 2016 Oct;22(10):1792–800.
48. Kebriaei P, Basset R, Ledesma C, Ciurea S, Parmar S, Shpall EJ, Hosing C, Khouri I, Qazilbash M, Popat U, Alousi A, Nieto Y, Jones RB, de Lima M, Champlin RE, Andersson BS. Clofarabine combined with busulfan provides excellent disease control in adult patients with acute lymphoblastic leukemia undergoing allogeneic hematopoietic stem cell transplantation. *Biol Blood Marrow Transplant*. 2012 Dec;18(12):1819–26.
49. Valdez BC, Li Y, Murray D, Champlin RE, Andersson BS. The synergistic cytotoxicity of clofarabine, fludarabine and busulfan in AML cells involves ATM pathway activation and chromatin remodeling. *Biochem Pharmacol*. 2011 Jan;81(2):222–32.
50. Ben Hassine K, Powys M, Svec P, Pozdechova M, Versluys B, Ansari M, Shaw PJ. Total Body Irradiation Forever? Optimising Chemotherapeutic Options for Irradiation-Free Conditioning for Paediatric Acute Lymphoblastic Leukaemia. *Front Pediatr*. 2021;9:775485.
51. Bartelink IH, van Reij EML, Gerhardt CE, van Maarseveen EM, de Wildt A, Versluys B, Lindemans CA, Bierings MB, Boelens JJ. Fludarabine and exposure-targeted busulfan compares favorably with busulfan/cyclophosphamide-based regimens in pediatric hematopoietic cell transplantation: maintaining efficacy with less toxicity. *Biol Blood Marrow Transplant*. 2014 Mar;20(3):345–53.
52. Versluys AB, Boelens JJ, Pronk C, Lankester A, Bordon V, Buechner J, Iffersen M, Jackmann N, Sundin M, Vettenranta K, Abrahamsson J, Mellgren K. Hematopoietic cell transplant in pediatric acute myeloid leukemia after similar upfront therapy; a comparison of conditioning regimens. *Bone Marrow Transplant*. 2021 Jun;56(6):1426–32.
53. Versluijs AB, de Koning CCH, Lankester AC, Nierkens S, Kollen WJ, Bresters D, Lindemans CA, Boelens JJ, Bierings M. Clofarabine-fludarabine-busulfan in HCT for pediatric leukemia: an effective, low toxicity, TBI-free conditioning regimen. *Blood Adv*. 2022 Mar;6(6):1719–30.
54. Iwamoto T, Hiraku Y, Oikawa S, Mizutani H, Kojima M, Kawanishi S. DNA intrastrand cross-link at the 5'-GA-3' sequence formed by busulfan and its role in the cytotoxic effect. *Cancer Sci*. 2004 May;95(5):454–8.
55. Ewald B, Sampath D, Plunkett W. Nucleoside analogs: molecular mechanisms signaling cell death. *Oncogene*. 2008 Oct;27(50):6522–37.
56. Andersson BS, Valdez BC, de Lima M, Wang X, Thall PF, Worth LL, Popat U, Madden T, Hosing C, Alousi A, Rondon G, Kebriaei P, Shpall EJ, Jones RB, Champlin RE. Clofarabine ± fludarabine with once daily i.v. busulfan as pretransplant conditioning therapy for advanced myeloid leukemia and MDS. *Biol Blood Marrow Transplant*. 2011 Jun;17(6):893–900.
57. Mah LJ, El-Osta A, Karagiannis TC. gammaH2AX: a sensitive molecular marker of DNA damage and repair. *Leukemia*. 2010 Apr;24(4):679–86.
58. Schnalzger TE, de Groot MH, Zhang C, Mosa MH, Michels BE, Röder J, Darvishi T, Wels WS, Farin HF. 3D model for CAR-mediated cytotoxicity using patient-derived colorectal cancer organoids. *EMBO J*. 2019 Jun;38(12).
59. Jacob F, Ming GL, Song H. Generation and biobanking of patient-derived glioblastoma organoids and their application in CAR T cell testing. *Nat Protoc*. 2020 Dec;15(12):4000–33.
60. Larson RC, Kann MC, Bailey SR, Haradhvala NJ, Llopis PM, Bouffard AA, Scarfó I, Leick MB, Grauwet K, Berger TR, Stewart K, Anekal PV, Jan M, Joung J, Schmidts A, Ouspenskaia T, Law T, Regev A, Getz G, Maus M V. CAR T cell killing requires the IFN $\gamma$ R pathway in solid but not liquid tumours. *Nature*. 2022 Apr;
61. Dijkstra KK, Cattaneo CM, Weeber F, Chalabi M, van de Haar J, Fanchi LF, Slagter M, van der Velden DL, Kaing S, Kelderman S, van Rooij N, van Leerdam ME, Depla A, Smit EF, Hartemink KJ, de Groot R, Wolkers MC, Sachs N, Snaebjornsson P, Monkhorst K, Haanen J, Clevers H, Schumacher TN, Voest EE. Generation of Tumor-Reactive T Cells by Co-culture of Peripheral Blood Lymphocytes and Tumor Organoids. *Cell*. 2018 Sep;174(6):1586-1598.

- e12.
62. Griffin JM, Healy FM, Dahal LN, Floisand Y, Woolley JF. Worked to the bone: antibody-based conditioning as the future of transplant biology. *J Hematol Oncol*. 2022 May 19;15(1):65.
  63. Wada J, Kanwar YS. Identification and characterization of galectin-9, a novel beta-galactoside-binding mammalian lectin. *J Biol Chem*. 1997 Feb;272(9):6078–86.
  64. Türeci O, Schmitt H, Fadle N, Pfreundschuh M, Sahin U. Molecular definition of a novel human galectin which is immunogenic in patients with Hodgkin's disease. *J Biol Chem*. 1997 Mar;272(10):6416–22.
  65. Spitzenberger F, Graessler J, Schroeder HE. Molecular and functional characterization of galectin 9 mRNA isoforms in porcine and human cells and tissues. *Biochimie*. 2001 Sep;83(9):851–62.
  66. Brewer CF, Miceli MC, Baum LG. Clusters, bundles, arrays and lattices: novel mechanisms for lectin–saccharide-mediated cellular interactions. *Curr Opin Struct Biol*. 2002 Oct 1;12(5):616–23.
  67. Zhu C, Anderson AC, Schubart A, Xiong H, Imitola J, Khoury SJ, Zheng XX, Strom TB, Kuchroo VK. The Tim-3 ligand galectin-9 negatively regulates T helper type 1 immunity. *Nat Immunol*. 2005 Dec;6(12):1245–52.
  68. Madireddi S, Eun SY, Mehta AK, Birta A, Zajonc DM, Niki T, Hirashima M, Podack ER, Schreiber TH, Croft M. Regulatory T Cell-Mediated Suppression of Inflammation Induced by DR3 Signaling Is Dependent on Galectin-9. *J Immunol*. 2017 Oct;199(8):2721–8.
  69. Madireddi S, Eun SY, Lee SW, Nemčovičová I, Mehta AK, Zajonc DM, Nishi N, Niki T, Hirashima M, Croft M. Galectin-9 controls the therapeutic activity of 4-1BB-targeting antibodies. *J Exp Med*. 2014 Jun;211(7):1433–48.
  70. Wu C, Thalhamer T, Franca RF, Xiao S, Wang C, Hotta C, Zhu C, Hirashima M, Anderson AC, Kuchroo VK. Galectin-9-CD44 interaction enhances stability and function of adaptive regulatory T cells. *Immunity*. 2014 Aug;41(2):270–82.
  71. Bi S, Hong PW, Lee B, Baum LG. Galectin-9 binding to cell surface protein disulfide isomerase regulates the redox environment to enhance T-cell migration and HIV entry. *Proc Natl Acad Sci U S A*. 2011 Jun;108(26):10650–5.
  72. Yang R, Sun L, Li CF, Wang YH, Yao J, Li H, Yan M, Chang WC, Hsu JM, Cha JH, Hsu JL, Chou CW, Sun X, Deng Y, Chou CK, Yu D, Hung MC. Galectin-9 interacts with PD-1 and TIM-3 to regulate T cell death and is a target for cancer immunotherapy. *Nat Commun*. 2021 Feb 5;12(1):832.
  73. Gooden MJM, Wiersma VR, Sampsonius DF, Gerssen J, van Ginkel RJ, Nijman HW, Hirashima M, Niki T, Eggleton P, Helfrich W, Bremer E. Galectin-9 activates and expands human T-helper 1 cells. *PLoS One*. 2013;8(5):e65616.
  74. Kashio Y, Nakamura K, Abedin MJ, Seki M, Nishi N, Yoshida N, Nakamura T, Hirashima M. Galectin-9 induces apoptosis through the calcium-calpain-caspase-1 pathway. *J Immunol*. 2003 Apr 1;170(7):3631–6.
  75. Lu LH, Nakagawa R, Kashio Y, Ito A, Shoji H, Nishi N, Hirashima M, Yamauchi A, Nakamura T. Characterization of galectin-9-induced death of Jurkat T cells. *J Biochem*. 2007 Feb;141(2):157–72.
  76. Lhuillier C, Barjon C, Niki T, Gelin A, Praz F, Morales O, Souquere S, Hirashima M, Wei M, Dellis O, Busson P. Impact of Exogenous Galectin-9 on Human T Cells: CONTRIBUTION OF THE T CELL RECEPTOR COMPLEX TO ANTIGEN-INDEPENDENT ACTIVATION BUT NOT TO APOPTOSIS INDUCTION. *J Biol Chem*. 2015 Jul;290(27):16797–811.
  77. Lee J, Park EJ, Noh JW, Hwang JW, Bae EK, Ahn JK, Koh EM, Cha HS. Underexpression of TIM-3 and blunted galectin-9-induced apoptosis of CD4+ T cells in rheumatoid arthritis. *Inflammation*. 2012 Apr;35(2):633–7.
  78. Yin J, Li L, Wang C, Zhang Y. Increased Galectin-9 expression, a prognostic biomarker of aGVHD, regulates the immune response through the Galectin-9 induced MDSC pathway after allogeneic hematopoietic stem cell transplantation. *Int Immunopharmacol*. 2020 Nov;88:106929.
  79. Chen HY, Wu YF, Chou FC, Wu YH, Yeh LT, Lin KI, Liu FT, Sytwu HK. Intracellular Galectin-9 Enhances Proximal TCR Signaling and Potentiates Autoimmune Diseases. *J Immunol*. 2020 Mar 1;204(5):1158–72.
  80. Sakai K, Kawata E, Ashihara E, Nakagawa Y, Yamauchi A, Yao H, Nagao R, Tanaka R, Yokota A, Takeuchi M, Hirai H, Kimura S, Hirashima M, Yoshimura N, Maekawa T. Galectin-9 ameliorates acute GVH disease through the induction of T-cell apoptosis. *Eur J Immunol*. 2011 Jan;41(1):67–75.
  81. Veenstra RG, Taylor PA, Zhou Q, Panoskaltis-Mortari A, Hirashima M, Flynn R, Liu D, Anderson AC, Strom TB, Kuchroo VK, Blazar BR. Contrasting acute graft-versus-host disease effects of Tim-3/galectin-9 pathway blockade dependent upon the presence of donor regulatory T cells. *Blood*. 2012 Jul;120(3):682–90.
  82. Kandel S, Adhikary P, Li G, Cheng K. The TIM3/Gal9 signaling pathway: An emerging target for cancer immunotherapy. *Cancer Lett*. 2021 Jul;510:67–78.
  83. Yang R, Sun L, Li CF, Wang YH, Yao J, Li H, Yan M, Chang WC, Hsu JM, Cha JH, Hsu JL, Chou CW, Sun X, Deng Y, Chou CK, Yu D, Hung MC. Galectin-9 interacts with PD-1 and TIM-3 to regulate T cell death and is a target for cancer immunotherapy. *Nat Commun*. 2021 Feb;12(1):832.
  84. Yang R, Sun L, Li CF, Wang YH, Xia W, Liu B, Chu YY, Bover L, Vien L, Hung MC. Development and characterization of anti-galectin-9 antibodies that protect T cells from galectin-9-induced cell death. *J Biol Chem*. 2022 Mar;298(4):101821.

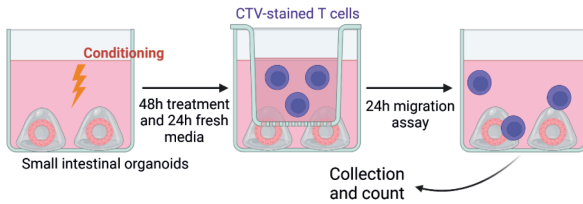


# Supplementary figures

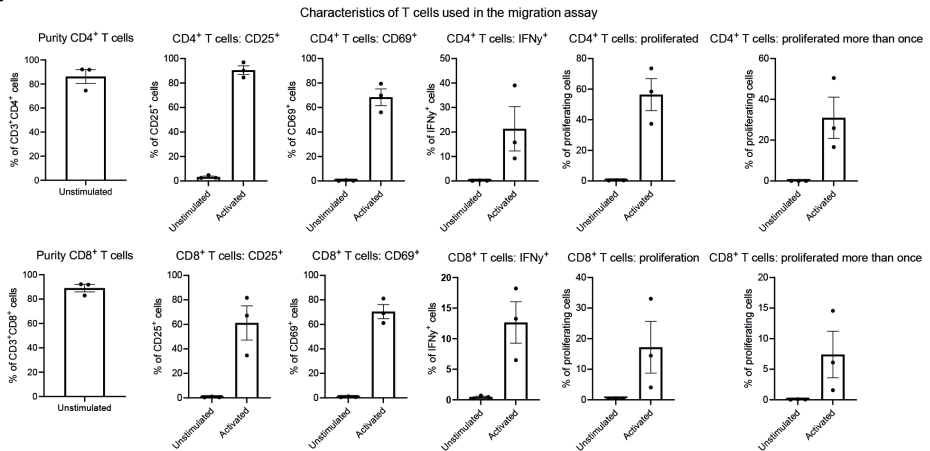


**Supplementary figure 1. (a)** Quantification of yH2AX foci per nucleus per donor. **(b)** Heatmaps of a combined list made from the top 50 DEGs of 24 hour Bu-, Flu- and Clo- treated organoids versus control showed in Figure 2b (left) or all DEGs (right).

**a** *Ex-vivo* modeling: T cell migration towards chemotherapy-damaged organoids

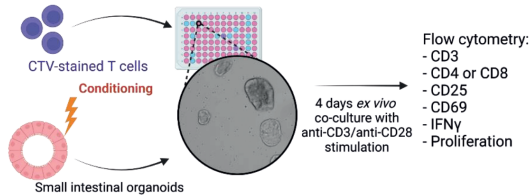


**b**

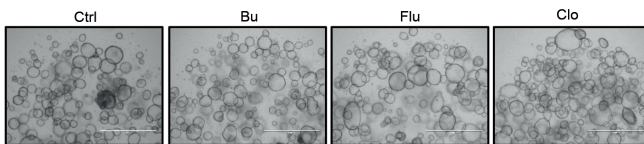


**c**

*Ex-vivo* modeling: T cell activation in co-culture with chemotherapy-damaged organoids

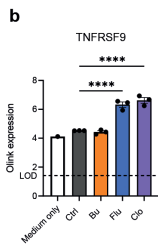
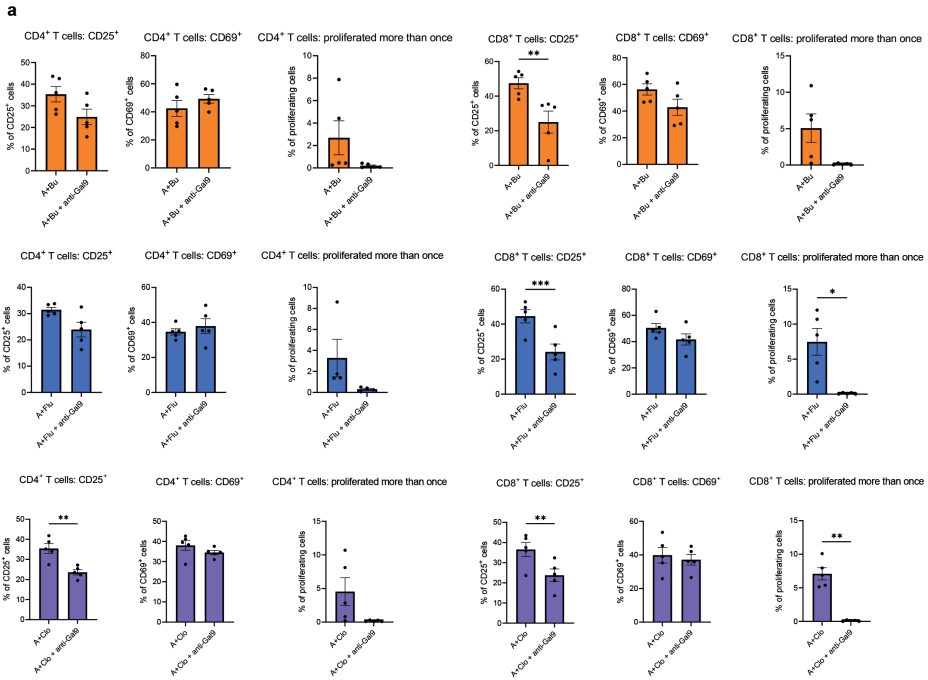


**d**



**Supplementary figure 2.** (a) Schematic overview of the migration assay. (b) Purity, activation markers and proliferation of CD4<sup>+</sup> and CD8<sup>+</sup> T cells polyclonally activated for 3 days before start of the migration assay (c) Schematic overview of the co-culture system to evaluate T cell activation by polyclonal stimulation in presence of organoids. (d) Representative EVOS images of organoids treated for 24h with Busulfan (35mM), Fludarabine (15mM), Clofarabine (0.5mM). Images are taken before the start of the co-culture assay, scale bar = 1000  $\mu$ m.





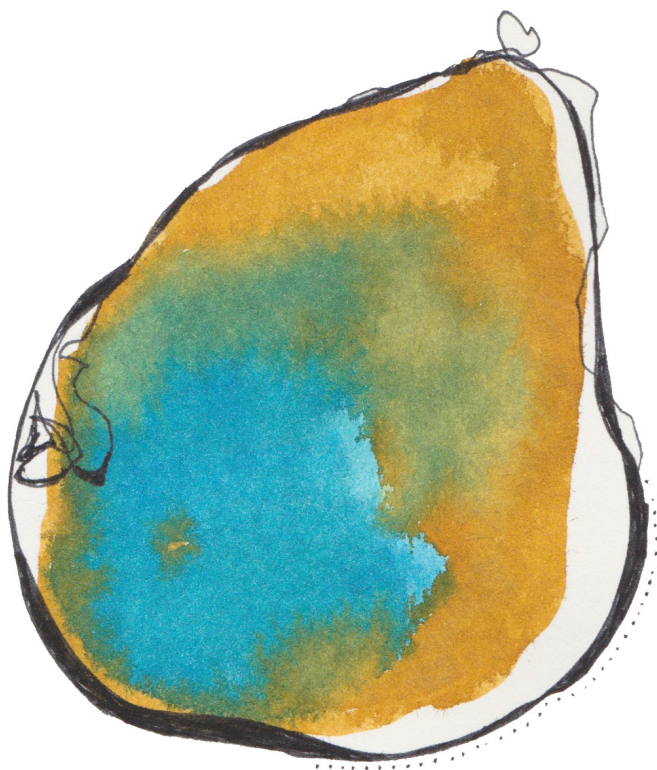
**Supplementary figure 3. (a)** CD4<sup>+</sup> and CD8<sup>+</sup> T cell activation after co-culture with treated organoids in the presence of anti-Gal-9 mAb. N≥5 T cell donors with 1 organoid donor, each data point indicates a T cell donor, mean with SEM, paired t-test. **(b)** Soluble-TNFRSF9 levels detected by Olink proteomics. Each data point indicates the levels of the detected protein in the CM from each organoid condition (log scale), mean with SEM, ANOVA.



**Supplementary table 1. RNAseq analysis of chemotherapy-damaged organoids.**

Supplementary table 1 combines Supplementary table 2-9 found at:  
<https://www.biorxiv.org/content/10.1101/2023.04.30.538862v1.full>





# T cell-derived interferon- $\gamma$ programs stem cell death in immune-mediated intestinal damage

Shuichiro Takashima\*, Maria L. Martin\*, Suze A. Jansen\*, Ya-Yuan Fu, Joris Bos, Daniel Chandra, Margaret H. O'Connor, Anna M. Mertelsmann, Paola Vinci, Jason Kuttiyara, Sean M. Devlin, Sabine Middendorp, Marco Calafiore, Anastasia Egorova, Maria Kleppe, Yuan-Hung Lo, Noah F. Shroyer, Emily H. Cheng, Ross L. Levine, Chen Liu, Richard Kolesnick<sup>§</sup>, Caroline A. Lindemans<sup>§</sup>, Alan M. Hanash<sup>§</sup>

## Abstract

Despite the importance of intestinal stem cells (ISCs) for epithelial maintenance and the significance of epithelial injury in immune-mediated intestinal diseases, there is limited understanding of how immune-mediated damage impacts ISCs and their niche. We found that stem cell compartment injury is a shared feature of both alloreactive and autoreactive intestinal immunopathology, reducing ISCs and impairing their recovery in T-cell-mediated injury models. While imaging revealed few T cells near the stem cell compartment in healthy mice, donor T cells infiltrating the intestinal mucosa after allogeneic bone marrow transplantation (BMT) primarily localized to the crypt region lamina propria. Further modeling with *ex vivo* epithelial cultures indicated ISC depletion and impaired human as well as murine organoid survival upon co-culture with activated T cells, and screening of effector pathways identified Interferon- $\gamma$  as a principal mediator of ISC compartment damage. Interferon- $\gamma$  induced JAK1- and STAT1-dependent toxicity, initiating a pro-apoptotic gene expression program and stem cell death. BMT with Interferon- $\gamma$ -deficient donor T cells, with recipients lacking the Interferon- $\gamma$  receptor (IFN $\gamma$ R) specifically in the intestinal epithelium, and with pharmacologic inhibition of JAK signaling all resulted in protection of the stem cell compartment. Additionally, epithelial cultures with Paneth cell-deficient organoids, IFN $\gamma$ R-deficient Paneth cells, IFN $\gamma$ R-deficient ISCs, and purified stem cell colonies all indicated direct targeting of the ISCs that was not dependent on injury to the Paneth cell niche. Dysregulated T cell activation and Interferon- $\gamma$  production are thus potent mediators of ISC injury, and blockade of JAK/STAT signaling within target tissue stem cells can prevent this T-cell-mediated pathology.

## Introduction

Epithelial stem cells are critical for physiologic self-renewal as well as regeneration after injury<sup>1</sup>. Toxic insults to the gastrointestinal (GI) tract frequently result in acceleration of epithelial turnover, and tissue pathology can develop if regeneration does not adequately respond to the insult and replace the injured tissue. The trans-membrane protein leucine-rich repeat-containing G protein-coupled receptor 5 (Lgr5) marks crypt base columnar intestinal stem cells (ISCs) capable of regenerating all the cells of the epithelium in the small intestine (SI) and large intestine (LI)<sup>2</sup>. Paneth cells, which are progeny of ISCs, provide an epithelial niche for Lgr5+ ISCs in SI by producing growth factors including Wnt3 and epidermal growth factor (EGF)<sup>3,4</sup>.

Despite the critical importance of the stem cell compartment for epithelial maintenance and regeneration after injury<sup>5,6</sup>, numerous associations of immune dysregulation and tissue damage<sup>7-16</sup>, and increasing evidence for immunologic effects on tissue regeneration<sup>17-19</sup>, there is little understanding of the interactions between the immune system and tissue stem cells and of the effects of immune-mediated damage on the stem cell compartment. Within the GI tract, a frequent site of tissue damage after allogeneic hematopoietic transplantation, injury to crypts containing the ISC compartment is a characteristic finding of graft vs. host disease (GVHD) post- transplant<sup>20,21</sup>. GVHD is an immune-mediated complication of bone marrow transplantation (BMT) in which donor T cells attack recipient tissues, and it has been reported that both ISCs and their Paneth cell niche are reduced in mice with GVHD<sup>18,22-25</sup>. However, the mechanisms leading to their loss, the relationship between these cell populations during tissue injury, and the relevance of these findings to tissue damage beyond the transplant setting are all poorly understood.

Expression of cytotoxic molecules and production of cytokines are principal effector functions of T cells, and both functions, have been studied considerably in GVHD models<sup>26-39</sup>. Although T cells can mediate potent tissue damage in the GI tract, the impacts of these effector pathways on the ISC compartment are not well defined. Inflammatory cytokines such as IFN $\gamma$  and TNF $\alpha$  have been associated with damage to the Paneth cell niche<sup>40-42</sup>, and IFN $\gamma$  contributes to reduced epithelial proliferation in mice with colitis<sup>43</sup>. Given that group 3 innate lymphoid cells and IL-22 can signal to ISCs to protect them and promote epithelial regeneration, it is possible that there are also direct interactions between ISCs and inflammatory cytokines during pathologic immune responses that compromise the ISC compartment. We thus sought to examine the specific cellular interactions and molecular mechanisms underlying ISC loss in immune-mediated GI damage. Using a combination of phenotypic and functional characterizations of the ISC compartment after alloreactive and autoreactive intestinal injury *in vivo*, coupled with *ex vivo* modeling of T cell interactions with ISCs and their Paneth cell niche in organoid cultures, we found that ISCs can be directly targeted by T-cell- derived cytotoxic cytokine signaling.



## Results

### **Alloreactive and autoreactive immune responses impair the intestinal stem cell compartment**

We first evaluated ISC kinetics in immune-mediated GI damage using a clinically relevant major histocompatibility complex (MHC)-matched allogeneic BMT model. Three days after transplantation and the pre-transplant conditioning (total body irradiation), BMT recipients receiving marrow alone (no GVHD) or marrow and T cells (for induction of GVHD) both demonstrated a reduction in SI Lgr5+ ISCs compared to normal mice that had not undergone BMT or pre-transplant conditioning (Fig. 1, A and B, top panels). One week later, on day 10 post-BMT, Lgr5+ ISC numbers had recovered in recipients transplanted without T cells, but ISC numbers remained reduced in GVHD recipients transplanted with donor T cells, demonstrating failure of ISC recovery in immune-mediated GI damage occurring after BMT (Fig. 1, A and B, bottom panels). In contrast, lysozyme+ Paneth cell numbers remained intact early after transplant, but were reduced by day 10 post-BMT in mice transplanted with donor T cells (Fig. 1C and fig. S1A), indicating that the ISCs were reduced prior to Paneth cells in mice with GVHD. Similar to the MHC-matched model, testing an independent haploidentical MHCmismatched transplant model demonstrated rapid Lgr5+ ISC reduction followed by substantial recovery in mice without GVHD, but persistent severe diminution of Lgr5+ ISCs in T cell recipients (Fig. 1D). Paneth cells also were reduced in this model of GVHD, but again this occurred only following the reduction in ISCs (Fig. 1E and fig. S2).

To determine if T-cell-dependent stem cell loss was specific to alloreactive immune-mediated GI damage and BMT, we examined the ISC compartment in mice with systemic autoimmunity by crossing *Foxp3*-diphtheria toxin receptor (DTR) mice<sup>44</sup> with Lgr5-LacZ reporters. Mutations in the *FOXP3* gene in humans result in IPEX (Immune dysregulation, polyendocrinopathy, enteropathy, X-linked) syndrome, which is frequently associated with intestinal autoimmunity<sup>45</sup>, and ablation of *Foxp3*+ regulatory T cells (Tregs) in mice leads to rapid systemic and intestinal autoimmunity<sup>46</sup>. Induction of systemic autoimmunity by DT-mediated Treg depletion quickly resulted in fewer Lgr5+ ISCs, while Paneth cell numbers were maintained (Fig. 1, F and G). Reduction of ISCs was thus a shared feature of alloreactive and autoreactive immune-mediated GI damage, and it was not subsequent to epithelial niche damage in the form of Paneth cell deficiency.

We next evaluated the effects of immune-mediated damage on the ISC compartment functionally, assessing *ex vivo* organoid-forming capacity after *in vivo* challenge. Intestinal crypts are functional units containing epithelial stem, progenitor, and niche cells, and isolated crypts can generate intestinal organoids *ex vivo*, recapitulating the *in vivo* intestinal organization with crypt-villus structures and central lumens<sup>47</sup>. Consistent with the quantification of Lgr5+ ISCs (Fig. 1, A and B), SI crypts isolated early post-transplant

demonstrated significant impairment in organoid-forming capacity compared to normal mice that had not received a transplant or pre-transplant conditioning (Fig. 1H). The functional ability to generate organoids rapidly recovered in mice without GVHD, but organoid formation from crypts of mice transplanted with allogeneic donor T cells remained impaired ten days after BMT (Fig. 1I). Likewise, Treg depletion in *Foxp3-DTR* mice treated *in vivo* with DT significantly impaired *ex vivo* organoid formation from isolated crypts in comparison to cultures from control mice treated with DT (Fig. 1J). Furthermore, we also examined the *in vivo* function of ISCs after BMT using genetic marking of the stem cells and their progeny. In addition to *Lgr5*, *Olfm4* also marks crypt base ISCs in mouse SI, and *Olfm4*-driven Cre expression has been shown to be more robust than that of *Lgr5*<sup>48</sup>. We thus performed allogeneic BMT into *Olfm4-CreERT2xRosa26* reporter mice, treating the BMT recipients with Tamoxifen prior to transplantation to activate Cre-driven lineage tracing (fig. S3). In comparison to unirradiated normal controls, transplanted mice demonstrated reduced lineage tracing from *Olfm4*<sup>+</sup> cells after allogeneic BMT even without donor T cells, suggesting ISC damage due to the pre-transplant conditioning. Moreover, allogeneic BMT with T cells led to significant further reduction in tracing, providing additional functional validation for the loss of ISCs in GVHD (fig. S3). In total, both alloreactive and autoreactive *in vivo* immune responses resulted in loss of ISCs and functional impairment of the stem cell compartment.

### **Allogeneic T cells preferentially invade crypt region lamina propria after BMT**

In order to examine the intramucosal localization of T cells mediating epithelial injury and ISC reduction after BMT, we next performed 3-D confocal microscopy of intact whole-mount intestinal tissue. This approach has recently identified preferential infiltration of crypt region mucosa after allogeneic BMT<sup>49</sup>, but such localization has not been distinguished between the intraepithelial and lamina propria components of the mucosa, and it has not been defined in homeostasis either. Staining for CD3, nuclei, and cellular membranes followed by imaging of full-thickness ileum allowed for accurate determination of mucosal architecture as well as precise localization and quantification of T cells in the epithelial and lamina propria regions of SI crypt and villus compartments. Normal control (unirradiated and untransplanted) B6 mice demonstrated similar T cell densities in crypt and in villus regions of ileal lamina propria at steady state (Fig. 2, A and B). In contrast, intraepithelial T cells were much more abundant in villus epithelium than in crypt epithelium at steady state in B6 ileum (Fig. 2, A and B).



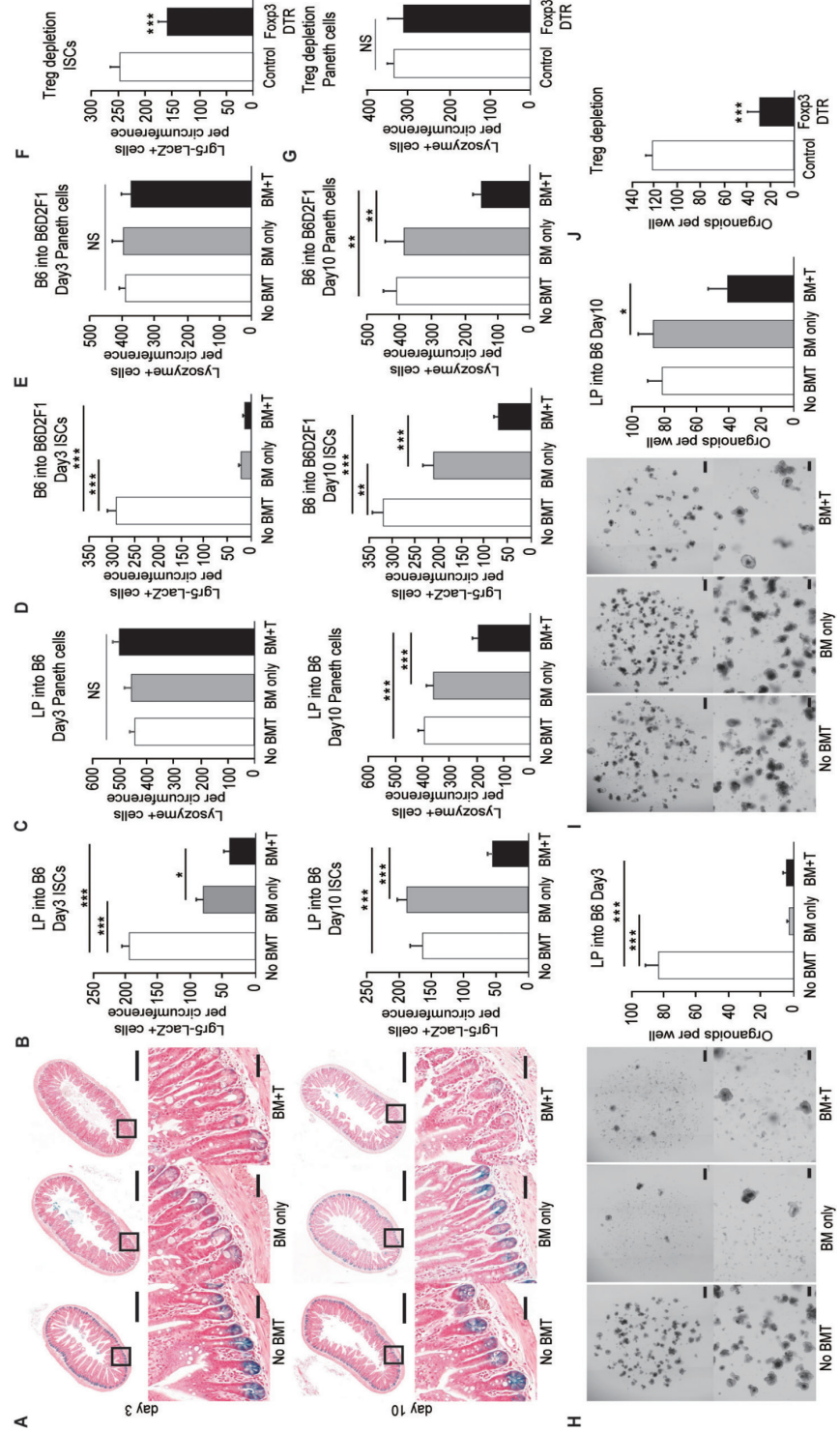




**Fig. 1. Alloreactive and autoreactive immune responses injure the intestinal stem cell compartment.** (A to C) LP-into-Lgr5-LacZ-B6 MHC-matched BMT. "No BMT" group represents controls that did not undergo transplantation or pre-transplant conditioning. (A) Representative images of SI (ileum) Lgr5-LacZ staining on day 3 and day 10 post-BMT. Scale bars = 500µm (Full circumference panels) or 50µm (High powered panels). (B) SI ISC frequency and (C) SI lysozyme+ Paneth cell frequency on day 3 and day 10 post-BMT; Analysis of n = 12 (No BMT), n = 19 (TCD BM only), or n = 23 (BM plus T) independent sections for day 3 ISC analysis; n = 8 (No BMT), n = 17 (TCD BM only), or n = 25 (BM plus T) independent sections for day 10 ISC analysis; n = 5 (No BMT), n = 11 (TCD BM only), or n = 13 (BM plus T) independent sections for day 3 Paneth cell analysis; n = 6 (No BMT), n = 15 (TCD BM only), or n = 15 (BM plus T) independent sections for day 10 Paneth cell analysis; from 2-5 mice per group. (D and E) B6-into-Lgr5-LacZ-BDF1 MHC-mismatched BMT, SI ISC frequency (D) and SI lysozyme+ Paneth cell frequency (E) on day 3 and day 10 post-BMT; Analysis of n = 8 (No BMT), n = 8 (TCD BM only), or n = 15 (BM plus T) independent sections for day 3 ISC analysis; n = 5 (No BMT), n = 6 (TCD BM only), or n = 15 (BM plus T) independent sections for day 10 ISC analysis; n = 8 (No BMT), n = 8 (TCD BM only), or n = 13 (BM plus T) independent sections for day 3 Paneth cell analysis; n = 9 (No BMT), n = 8 (TCD BM only), or n = 6 (BM plus T) independent sections for day 10 Paneth cell analysis; from 3-8 mice per group. (F and G) Foxp3-WT and Foxp3-DTR mice treated with DT. SI ISC frequency (F) and SI lysozyme+ Paneth cell frequency (G) 5 days after DT treatment; analysis of 19-20 independent sections from 3 mice per group. (H and I) Representative images and numbers of day 5 SI organoids from recipients day 3 (H) and day 10 (I) after LP-into-B6 BMT. Organoid culture from 150 crypts. Scale bars = 500µm (Upper) or 200µm (Lower). Analysis of n = 3 mice per group. (J) Day 5 SI organoid numbers from 150 crypts harvested 9 days after DT treatment; n = 4 mice per group. Data are mean and s.e.m.; comparisons performed with t-tests (two groups) or one-way ANOVA (multiple groups); \*P < 0.05, \*\*P < 0.01, \*\*\*P < 0.001. Data are representative of two (H and I) or three (F, G and J) independent experiments, or combined from two experiments (A to E)

We next evaluated the location of donor T cells in recipient intestinal mucosa after allogeneic BMT, using B6-GFP mice as the source of donor T cells. Four days after BMT, the early infiltration of GFP<sup>+</sup> donor T cells in recipient ileum was primarily located in the lamina propria of the crypt region, and few donor T cells could be identified in the villi (Fig. 2, C and D). Three days later, donor T cell invasion of the intestinal mucosa was much more substantial, and again most donor T cells were located in the crypt region lamina propria (Fig. 2, E and F). In contrast to intraepithelial T cells in B6 ileum at steady state, intraepithelial donor T cells one week after BMT were significantly more frequent in the crypts than in the villi (Fig. 2, E and F). These results indicated that allogeneic donor T cells mediating GVHD primarily infiltrated the lamina propria of the crypt region, in proximity to the ISC compartment, and most donor T cells invading the intestinal epithelium after BMT were present in the crypt region as well.

### **Activated T cells produce IFN $\gamma$ that targets the intestinal epithelium, reduces ISCs, and eliminates organoids *ex vivo***

Investigation of T-cell-derived molecules mediating tissue injury can be complicated by redundancies in effector pathways and by the complex systemic nature of immunologic pathophysiology, with numerous potential targets exhibiting divergent responses to similar molecules<sup>26-39,50,51</sup>. Conflicting experimental results may be due at least in part to the lack of models for studying specific interactions between immune effectors and primary cells as well as challenges in deciphering immune responses against specific cellular subsets within a tissue. As such, we sought to establish a model for studying interactions between T cells and the ISC compartment by culturing intestinal organoids with allogeneic T cells *ex vivo*. While co-culture with naive allogeneic T cells had no effect on regeneration from dissociated mouse organoid cells, allo-activated T cells significantly reduced allogeneic SI and LI organoid numbers in a concentration-dependent fashion (Fig. 3A and fig. S4A). Co-culture with polyclonally-activated allogeneic T cells also impaired organoid formation, and both CD4<sup>+</sup> and CD8<sup>+</sup> T cells were able to mediate organoid suppression (fig. S4, B and C). In addition to murine co-cultures, human T cells suppressed the growth of genetically disparate human duodenal organoids as well (Fig. 3B).

As organoid formation and survival were impaired by activated allogeneic T cells but not by naive allogeneic T cells (Fig. 3A), we hypothesized that antigenic disparity was important for T cell activation but was not required for target suppression once the T cells were already activated. Indeed, syngeneic co-cultures with allo-activated T cells or with polyclonally-stimulated T cells both impaired the viability of syngeneic mouse organoids (Fig. 3C and fig. S4D). Furthermore, upon co-culturing T cells and organoids from the same donors, activated human CD4<sup>+</sup> and CD8<sup>+</sup> T cells suppressed the growth of autologous human colon organoids (Fig. 3D). These findings indicated that T cell activation can impair the viability of intestinal epithelium *ex vivo*, even in the absence of genetic disparity with the epithelial targets.

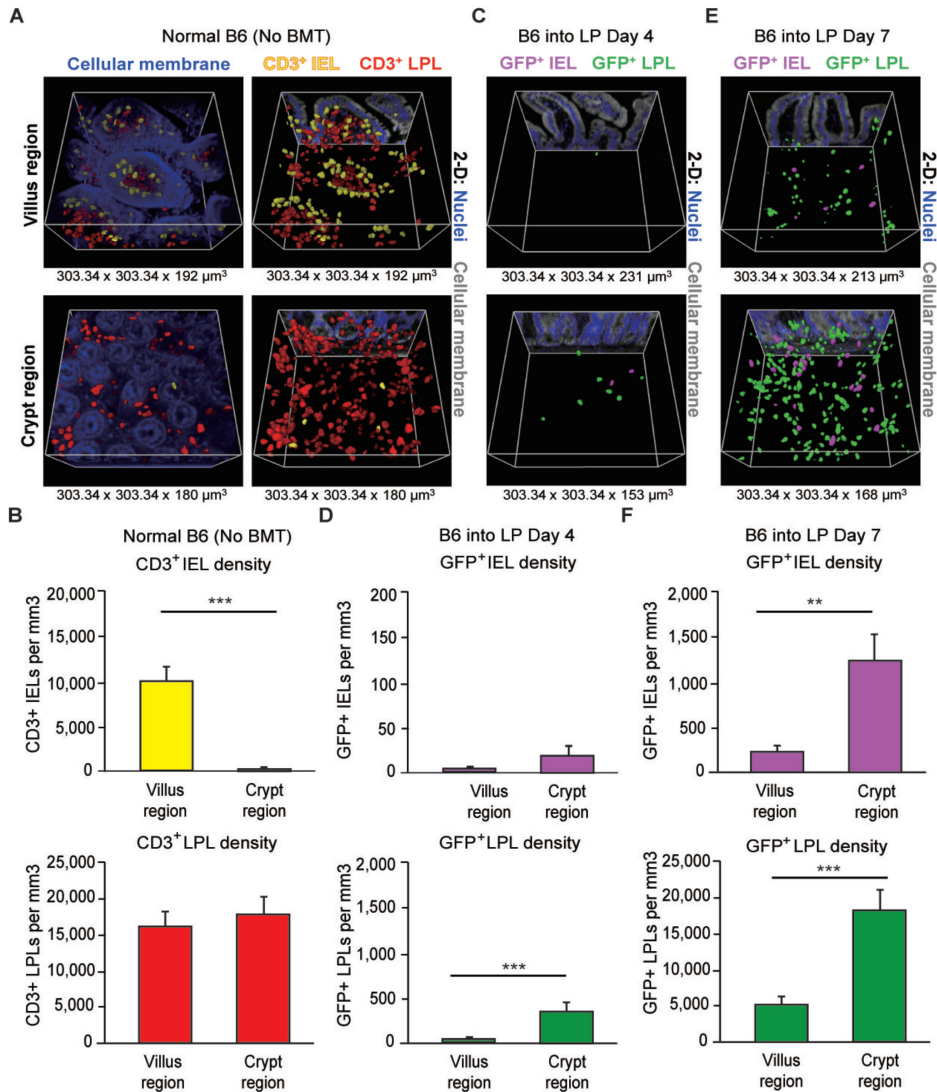


**Fig. 2. Donor T cells infiltrate the epithelial layer and lamina propria in the crypt region after bone marrow transplantation.** 3-D whole-mount immunofluorescent confocal imaging of mouse ileum. **(A and B)** T cells in normal (untransplanted and unirradiated) B6 mice were identified by anti-CD3 immunofluorescence. **(A)** Left panels: Representative 3-D projection images of full-thickness SI tissue divided into villus and crypt regions, with cellular membrane staining (DiI lipophilic dye; blue) indicating the tissue architecture utilized for distinguishing IELs and LPLs within the ileum; yellow, CD3<sup>+</sup> IELs; red, CD3<sup>+</sup> LPLs. Right panels: 3-D projections of CD3<sup>+</sup> IELs and CD3<sup>+</sup> LPLs in the villus and crypt regions, with cellular membrane staining removed and tissue orientation (and thus T cell localization within the 3-D tissues) indicated by 2-D slices shown on the posterior projection walls. **(B)** Quantification of CD3<sup>+</sup> IEL and CD3<sup>+</sup> LPL densities in normal B6 (n = 3 independent 3-D views). **(C to F)** B6-into-LP allogeneic BMT was performed using wild-type B6 marrow and purified GFP<sup>+</sup> B6 T cells, with donor T cells in the epithelium shown in purple and donor T cells in the lamina propria shown in green. **(C)** Representative 3-D projections and **(D)** quantifications of donor T cells in the villus and crypt regions four days post-BMT (n = 24 independent 3-D views combined from 2 transplants). **(E)** Representative 3-D projections

and (F) quantifications of donor T cells in the villus and crypt regions seven days post-BMT (n = 12 independent 3-D views). Tissue orientation and T cell localization are again indicated by 2-D slices shown on the posterior walls of the 3-D projections. Graphs indicate mean and s.e.m.; comparisons performed with t-tests; \*\*P < 0.01, \*\*\*P < 0.001. Data are representative of two independent experiments unless otherwise mentioned.

In order to define the T cell effector pathways mediating organoid toxicity, we performed cocultures under several conditions with either genetically-deficient T cells or with neutralizing antibodies. Inhibition of perforin, FasL, TRAIL, IL-1 $\beta$ , IL-6, IL-17A, IL-22, and TNF $\alpha$  had no effect on organoid numbers (fig. S5, A to F). In contrast, T cell co-culture with anti-Interferon- $\gamma$  (IFN $\gamma$ ) neutralizing antibodies restored murine SI organoid growth (Fig. 3E), and IFN $\gamma$  blockade with neutralizing antibodies also protected human duodenal organoids from human allogeneic T cells (Fig. 3F). It was possible that addition of anti-IFN $\gamma$  neutralizing antibodies to co-cultures protected organoids by preventing paracrine/autocrine IFN $\gamma$  activity among the T cells or by suppressing IFN $\gamma$  signaling within the organoids. However, *lfngr*<sup>-/-</sup> T cells demonstrated intact organoid suppression (fig. S5, G and H), while *lfngr*<sup>-/-</sup> organoids were significantly resistant to activated allogeneic or syngeneic T cells (Fig. 3G and fig. S5I), indicating that IFN $\gamma$  targeted the epithelium during co-culture with activated T cells.

In the absence of T cells, IFN $\gamma$  alone was sufficient for mediating organoid toxicity. Addition of recombinant murine (rm) IFN $\gamma$  to organoid cultures without co-cultured T cells demonstrated concentration-dependent suppression of organoid numbers (Fig. 3H). Tracking T cell kinetics in co-cultures using GFP<sup>+</sup> T cells, we found that T cell frequencies decreased by day 4 of the culture (Fig. 3I and fig. S4E), suggesting that T-cell-mediated organoid suppression was initiated within the first few days of the culture. Consistent with this, IFN $\gamma$  was detected in the culture media on day three of co-culture, and the concentration of IFN $\gamma$  decreased by day five of culture (Fig. 3J). Moreover, flow cytometry analysis showed a significant reduction of Lgr5-GFP<sup>high</sup> ISCs in organoids after 16 hours of incubation with IFN $\gamma$ , and this ISC depletion progressed substantially by 72 hours after exposure to IFN $\gamma$  (Fig. 3K).

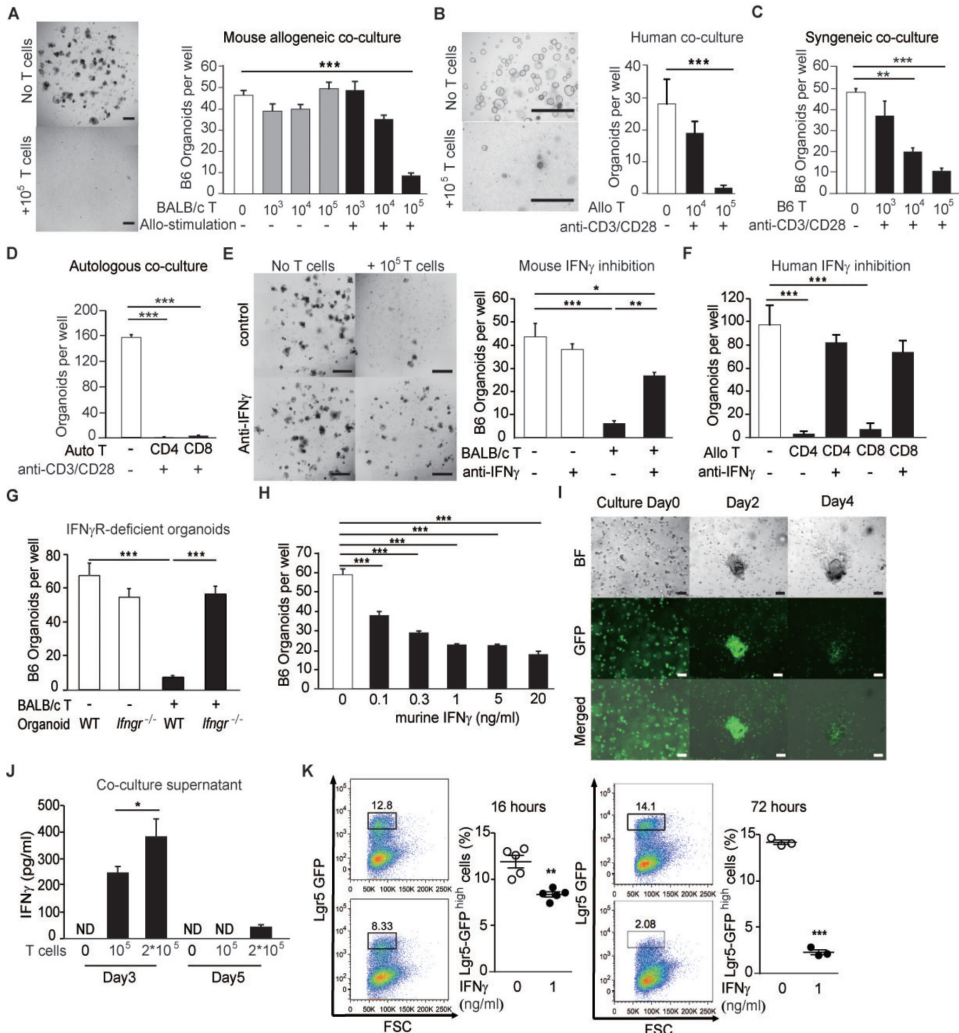


**Fig. 3. T-cell-derived IFN $\gamma$  targets intestinal epithelium leading to reduction of Lgr5<sup>+</sup> stem cells.** (A) Representative images and number of SI organoids after co-culture of B6 organoid cells with activated or naive allogeneic BALB/c T cells (day 7 of culture, n = 3-6 wells per group). Prior to organoid culture, T cells were activated by stimulation with allogeneic B6 dendritic cells. Scale bars = 500 $\mu$ m. (B) Representative images and number of human SI organoids cultured with human allogeneic CD8<sup>+</sup> T cells (culture day 7, n = 7-13 wells per group). Scale bars = 1000 $\mu$ m. (C) Numbers of B6 SI organoids after culture with anti-CD3/CD28-activated B6 syngeneic T cells (culture day 7, n = 3 wells per group). (D) Human LI organoids after culture with autologous human CD4<sup>+</sup> and CD8<sup>+</sup> T cells (culture day 7, n = 3 wells per group). (E) Representative images and numbers of B6 SI organoids after culture with anti-CD3/CD28-activated BALB/c T cells and anti-IFN $\gamma$  neutralizing antibodies (culture day 7, n = 4 wells/group); scale bars = 500 $\mu$ m. (F) Human SI organoids after culture with human allogeneic T cells and anti-IFN $\gamma$  (culture day 7, n = 9 wells/group). (G) WT or *Ifngr*<sup>-/-</sup> B6 SI organoids cultured with BALB/c T cells (culture day 7, n = 4 wells/group). (H) B6 SI organoids after culture with rmlFN $\gamma$  (culture day 7, n = 3 wells/group). (I) Representative images after coculture of BDF1 organoid cells with GFP<sup>+</sup> allogeneic B6 T cells. Shown are bright field (upper), fluorescent (middle), or overlap (lower) images; scale bars = 50 $\mu$ m. (J) IFN $\gamma$  ELISA on supernatants from culture of B6 SI organoids with BALB/c T cells (n = 4-8 wells/group. ND; not detected). (K) FACS analysis of Lgr5-GFP<sup>high</sup> ISCs in organoids cultured with rmlFN $\gamma$  for 16 or 72 hours;

n = 3 or 5 wells/group. Data are mean and s.e.m.; comparisons performed with t-tests (two groups) or one-way ANOVA (multiple groups); \*P < 0.05, \*\*P < 0.01, \*\*\*P < 0.001. Data are representative of two (A, C, H and K), three (D), four (G and I) or five (E) independent experiments, or combined from two (J) or three (B, F) independent experiments.

### **IFN $\gamma$ programs stem cell death, and Inhibition of JAK/STAT signaling protects ISCs from IFN $\gamma$**

We next investigated the signaling pathways involved in IFN $\gamma$ -mediated organoid and ISC suppression. Ruxolitinib is an immunosuppressive JAK 1/2 inhibitor capable of preventing T cell function, suppressing production of inflammatory cytokines by CD4+ T cells and promoting increased frequencies of Foxp3+ regulatory T cells in the setting of transplant<sup>52</sup>. Recent work has established ruxolitinib as a therapeutic option in GVHD, particularly for steroid refractory disease, and it has received FDA approval for this indication<sup>53-55</sup>. However, the potentially distinct effects of ruxolitinib on the T cells mediating tissue damage in GVHD and on the target tissues themselves have yet to be delineated. Modeling immune-mediated damage *ex vivo*, we found that culture with ruxolitinib significantly protected mouse intestinal organoids from allogeneic T cells (Fig. 4A). Culture with ruxolitinib also protected mouse (Fig. 4B) and human (Fig. 4C) intestinal organoids from IFN $\gamma$  in the absence of allogeneic T cells. Furthermore, ISC frequencies were significantly preserved in organoids cultured with IFN $\gamma$  in the presence of ruxolitinib (Fig. 4D).

Protection of organoids from IFN $\gamma$  in the absence of T cells suggested that ruxolitinib was acting on the organoids themselves, mediating IFN $\gamma$  resistance by suppressing epithelial JAK signaling. We next tested specific signaling molecules within the epithelium potentially involved in IFN $\gamma$ -mediated toxicity. Using organoids from *Jak1*-floxed x *Rosa-cre-ert2* mice, we found that passaged organoid cells pretreated with 4-OHT to delete *Jak1* were resistant to allogeneic T cells and to IFN $\gamma$  (Fig. 4E and fig. S6). Furthermore, ruxolitinib prevented phosphorylation of Stat1 by IFN $\gamma$  in SI crypts (Fig. 4F), and *Stat1*<sup>-/-</sup> organoids were resistant to IFN $\gamma$  as well (Fig. 4G). We thus concluded that allogeneic T cells and IFN $\gamma$  targeted the intestinal epithelium via *Jak1*/STAT1 signaling, and inhibition of epithelial *Jak1* could protect intestinal tissue from immune-mediated damage.

In addition to the reduction of ISCs identified by flow cytometry (Fig. 3K), qPCR analysis of intestinal organoids showed that gene expression associated with ISCs (*Lgr5*, *Olfm4*) decreased quickly (within 24 hours) in mouse and human cultures after treatment with IFN $\gamma$  (fig. S7, A and B). Target genes of Wnt signaling (*Axin2*) and Notch signaling (*Hes1*) were also reduced (fig. S7C), and gene expression associated with Paneth cells (*Lyz1*, *Defa1*), enterocytes (*Alpi*), goblet cells (*Muc2*), enteroendocrine cells (*Chga*), and tuft cells (*Trpm5*) were all reduced as well (Fig. S7, D and E). Consistent with these *ex vivo* results, qPCR analysis of crypts from recipients of allogeneic BMT with T cells demonstrated reduced

gene expression associated with ISCs (*Lgr5*, *Olfm4*), Paneth cells (*Lyz1*, *Defa1*), goblet cells (*Muc2*), enteroendocrine cells (*Chga*), and tuft cells (*Trpm5*) in comparison with recipients of only T-cell-depleted bone marrow, while *Alpi* expression, which is associated with the enterocyte lineage, trended down even after BMT without T cells (fig. S7F). Overall, these gene expression patterns suggested that ISCs were not being lost due to increased differentiation of ISCs into their progeny.

Given the reduction of ISCs *in vivo* and *ex vivo*, and given that this reduction could not easily be explained by differentiation, we next evaluated the role of programmed cell death. Gene expression in mouse SI organoids cultured with IFN $\gamma$  demonstrated multiple transcriptional changes consistent with induction of apoptosis, as there was decreased expression of the antiapoptotic genes *Bcl2* and *Bcl2l1* (*Bcl-xL*) and increased expression of the pro-apoptotic gene *Bak* (Fig. 5A). Similar transcriptional changes were observed in human duodenal organoids treated with IFN $\gamma$  (Fig. 5B). No changes were observed in expression of the anti-apoptotic gene *Mcl1* or the pro-apoptotic gene *Bax* (fig. S8A). Moreover, Annexin V analysis showed increased Annexin+DAPI- and Annexin+DAPI+ *Lgr5*-GFP+ cells 16 hours after treatment with IFN $\gamma$ , consistent with increased early apoptotic and dead ISCs, even though there was already a statistically significant reduction in ISC frequency at that point (Fig. 5, C and D). Increased apoptosis was also identified in human intestinal organoids incubated with IFN $\gamma$ , as determined by increased caspase-3/7 activity and confirmed by increased detection of cleaved caspase-3 (Fig. 5, E and F). Additionally, culture with ruxolitinib inhibited the pro-apoptotic transcriptional changes observed in intestinal organoids treated with IFN $\gamma$  (Fig. 5G), thus specifically linking JAK signaling to the apoptotic phenotype. Therefore in total, *ex vivo* experiments indicated that T cells induced organoid toxicity via production of IFN $\gamma$ , which activated JAK1-dependent STAT1 activation within the epithelium, resulting in an apoptotic transcriptional program and elimination of ISCs.

### **T-cell-derived IFN $\gamma$ promotes stem cell apoptosis and intestinal pathology in immunemediated GI damage *in vivo***

We next sought to evaluate the role of IFN $\gamma$  in T-cell-mediated stem cell injury *in vivo*. Anti-IFN $\gamma$  antibody treatment after BMT significantly protected ISC numbers in *Lgr5*-LacZ reporter mice transplanted with allogeneic donor marrow and T cells for induction of GVHD, confirming the *in vivo* relevance of IFN $\gamma$  for the stem cell compartment (Fig. 6A). Additionally, anti-IFN $\gamma$  neutralizing antibodies increased ISC frequencies during autoimmunity occurring after Treg depletion in *Foxp3*-DTR mice (Fig. 6B). Furthermore, inhibition of JAK/STAT signaling *in vivo* by treating allogeneic BMT recipients with ruxolitinib significantly protected ISCs from donor T cells and GVHD (Fig. 6C and fig. S1B).



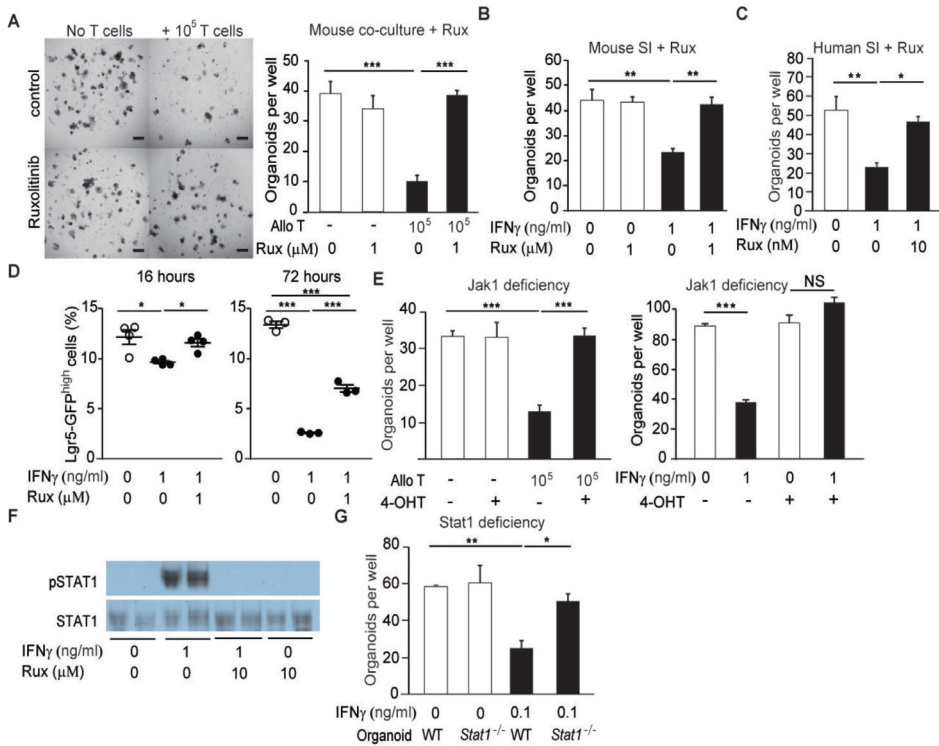


**Fig. 4. JAK/STAT inhibition protects intestinal stem cells from IFN<sub>γ</sub>.** (A) Representative images and numbers of B6 organoids after culture with BALB/c T cells and ruxolitinib (culture day 7, n = 4 wells/group); scale bars = 500μm. (B) Numbers of B6 SI organoid cells after culture with rmIFN<sub>γ</sub> and ruxolitinib (culture day 7, n = 4 wells/group). (C) Human SI organoids cultured with rhIFN<sub>γ</sub> (culture day 7, n = 3 wells/group) and ruxolitinib. (D) FACS analysis of Lgr5-GFP<sup>high</sup> ISCs in organoids cultured with rmIFN<sub>γ</sub> and ruxolitinib for 16 or 72 hours; n = 3 or 4 wells/group. (E) Jak1-deficient B6 SI organoids from *Rosa-cre-ert2-Jak1<sup>fl/fl</sup>* mice. Organoids were pretreated with control media or 4-OHT (1μM) to delete Jak1 and then cultured with BALB/c T cells or rmIFN<sub>γ</sub> (culture day 7, n = 4 wells/group). (F) Crypt pSTAT1 western blots after 30 minutes incubation with rmIFN<sub>γ</sub> +/- ruxolitinib. (G) WT or *Stat1*<sup>-/-</sup> B6 SI organoids cultured with rmIFN<sub>γ</sub> (culture day 7, n = 4 wells/group). Graphs indicate mean and s.e.m.; t-tests (two groups) or one-way ANOVA (multiple groups); \*P < 0.05, \*\*P < 0.01, \*\*\*P < 0.001. Data are representative of two (A, C to G) or three (B) independent experiments.



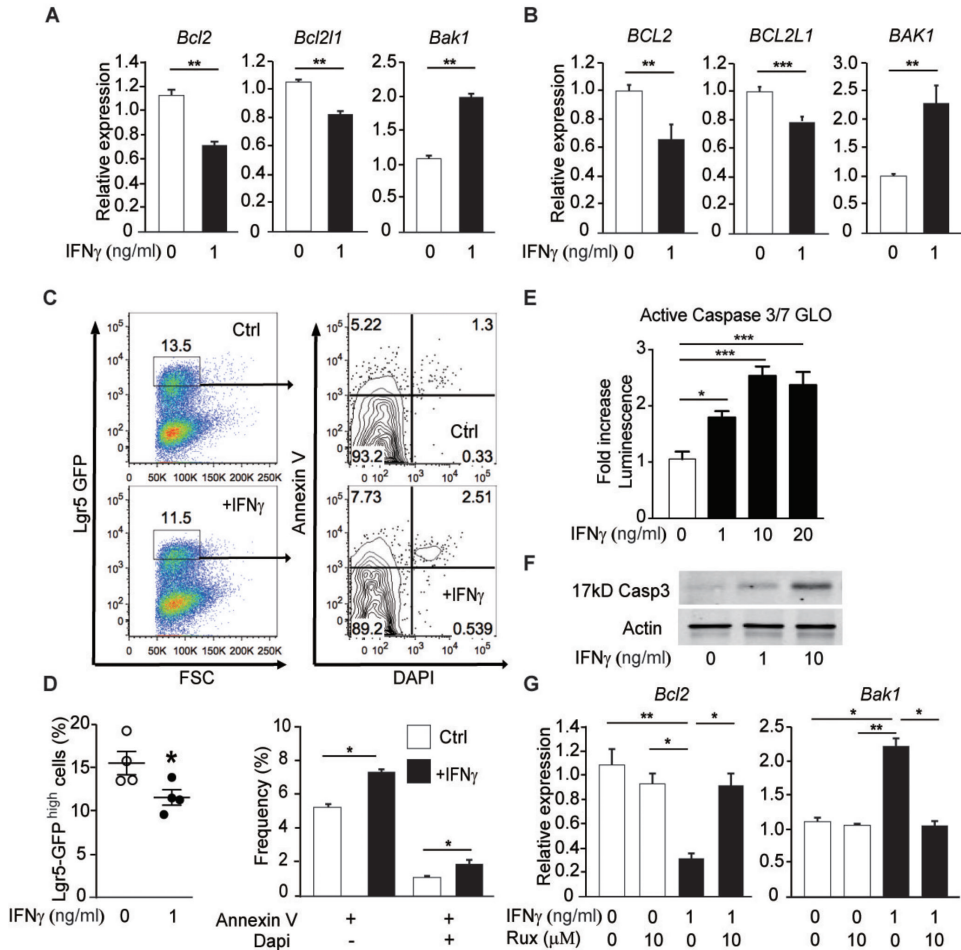


**Fig. 5. IFN $\gamma$  programs stem cell death.** (A) Apoptosis-related genes expression in mouse SI organoids cultured with rmIFN $\gamma$  for 6 hours; n = 6 wells/group; Mann–Whitney U analysis. (B) Apoptosis-related genes expression in human SI organoids cultured with rhIFN $\gamma$  for 24 hours; n = 9 or 10 wells/group, data are from 3 different SI donors; Mann–Whitney U analysis. (C and D) FACS plots (C) and quantifications (D) of Lgr5-GFP<sup>high</sup> cells and Annexin V analysis from SI organoids cultured with rmIFN $\gamma$  for 16 hours; n = 4 wells/group. (E) Relative caspase-3/7 activity as evaluated by Caspase-Glo assay; fold increase over baseline after treatment with rhIFN $\gamma$  for 24 hours (n = 6 wells/group). (F) Human organoid cleaved caspase-3 western blot after 48 hours incubation with rhIFN $\gamma$ . (G) Apoptosis-related genes expression in mouse SI organoids cultured with rmIFN $\gamma$  and ruxolitinib for 24 hours; n = 6 wells/group Kruskal–Wallis analysis. Graphs indicate mean and s.e.m.; comparisons performed with t-tests (two groups) or one-way ANOVA (multiple groups) unless otherwise stated; \*P < 0.05, \*\*P < 0.01, \*\*\*P < 0.001. Data are representative of two (A to D and F to G) or combined from two (E) independent experiments.

To identify *in vivo* sources of IFN $\gamma$  promoting ISC reduction, we first performed FACS-based phenotyping of IFN $\gamma$ + cells in recipient mucosa post-transplant. After mechanically dissociating the villi to enrich for crypt region mucosa, lamina propria lymphocytes (LPLs) were isolated and incubated with a golgi inhibitor to facilitate immunostaining and flow cytometric analysis for IFN $\gamma$ . Substantially more IFN $\gamma$ + cells were identified in recipient intestinal mucosa after allogeneic BMT than after syngeneic BMT, and the vast majority of these IFN $\gamma$ + cells identified after allogeneic BMT were indeed donor T cells (fig. S9, A and B). Further analysis indicated Tbet+ Th1 helper T cells with an activated phenotype (fig. S9, C and D).

Investigating the functional impacts of donor-derived IFN $\gamma$ , we performed allogeneic BMT using *Ifng*<sup>-/-</sup> T cells or *Ifng*<sup>-/-</sup> donor marrow. While transplantation with *Ifng*<sup>-/-</sup> donor marrow did not impact the reduction in ISC numbers in GVHD (Fig. 6D), allogeneic BMT with *Ifng*<sup>-/-</sup> donor T cells resulted in significantly greater ISC recovery (Fig. 6E), functionally confirming donor T cells to be the critical source of IFN $\gamma$  resulting in ISC reduction post-transplant. Furthermore, broader histopathologic analysis after allogeneic BMT with *Ifng*<sup>-/-</sup> donor T cells showed significant reduction in overall GVHD pathology, including reduced SI crypt loss and villus blunting (Fig. 6, F and G, and fig. S1C). We also observed increased epithelial proliferation along with the tissue injury occurring in GVHD, which was significantly reduced in BMT recipients transplanted with IFN $\gamma$ -deficient T cells (Fig. 6H).

Consistent with the IFN $\gamma$ -dependent pro-apoptotic gene expression pattern identified *ex vivo*, qPCR analysis post-BMT indicated increased expression of *Bcl2*, increased expression of *Bcl2l1*, and decreased expression of *Bak1* in recipients transplanted with *Ifng*<sup>-/-</sup> donor T cells (Fig. 6I). Additionally, anti-cleaved-caspase-3 and TUNNEL staining both indicated significantly reduced crypt apoptosis in mice transplanted with *Ifng*<sup>-/-</sup> donor T cells (Fig. 6, J to L). Furthermore, anticlaved-caspase-3 and anti- $\beta$ -gal double immunofluorescent staining demonstrated apoptotic Lgr5+ ISCs in GVHD, and the frequency of cleaved caspase-3+ ISCs was significantly reduced in mice transplanted with IFN $\gamma$ -deficient donor T cells (Fig. 6L and fig. S10). Finally, SI crypts isolated after *in vivo* BMT with *Ifng*<sup>-/-</sup> donor T cells demonstrated significantly greater organoid formation than crypts isolated from mice transplanted with wild-type (WT) T cells (Fig. 6M), indicating functional improvement in addition to the histologic amelioration described above. Overall, *in vivo* studies thus supported the *ex vivo* findings of ISC reduction induced by T-cell derived IFN $\gamma$  and JAK/STAT signaling.

### **IFN $\gamma$ directly targets intestinal stem cells and induces apoptosis**

Given the broad expression of the IFN $\gamma$  receptor on numerous cell types, T-cell-derived IFN $\gamma$  could have many targets *in vivo*, including the donor T cells themselves or other immune cells, leading to indirect effects on the epithelial stem cell compartment. To examine if T-cell-

derived IFN $\gamma$  was targeting the recipient epithelium directly *in vivo*, selective depletion of the IFN $\gamma$  receptor from recipient intestinal epithelium was investigated by performing allogeneic BMT into *Ifngr<sup>fl/fl</sup> x Villin-Cre (Ifngr $\Delta$ IEC)* mice. Given the lack of an ISC reporter in *Ifngr $\Delta$ IEC* mice, SI ISCs were quantified by immunohistochemistry for Olfm4. Elimination of the IFN $\gamma$  receptor from recipient intestinal epithelium significantly protected Olfm4+ ISCs from allogeneic T cells (Fig. 7A and fig. S1D). In addition to the stem cell protection, *Ifngr $\Delta$ IEC* recipients also demonstrated reduced overall GVHD pathology, greater crypt numbers, decreased villus blunting, and significantly less crypt apoptosis (Fig. 7, B to D).

These results indicated that IFN $\gamma$  could act directly on the intestinal epithelium to promote tissue pathology and ISC reduction in GVHD. However, it remained possible that effects on ISCs were secondary to targeting some other cell population in the intestinal epithelium rather than direct targeting of the stem cells with IFN $\gamma$ . Crypt base ISCs repopulate other intestinal epithelial cells including Paneth cells, which in turn produce several supportive factors such as Wnt3, EGF, and Notch ligands (4). While allogeneic T cells and IFN $\gamma$  eliminated intestinal organoids and depleted ISCs in our experiments, Paneth cell frequencies and Paneth-cell-associated gene expression were also reduced (Fig. 1, C and E, fig. S2B, and fig. S7, D and F). Additionally, IFN $\gamma$  has been reported to induce apoptosis and loss of Paneth cells<sup>40,41</sup>. ISC reduction and organoid elimination could thus have been due to direct ISC injury or indirect effects resulting from damage to the Paneth cell niche. We investigated IFN $\gamma$  receptor expression on intestinal epithelium by flow cytometry and confirmed expression of the IFN $\gamma$  receptor (IFN $\gamma$ R1, CD119) on both CD24+c-kit+CD44+ Paneth cells and Lgr5-GFP<sup>high</sup> ISCs (Fig. 7E and fig. S2A). Given that ISC-restricted cre-driven gene deletion is not possible *in vivo* because genetic manipulation of the stem cells is rapidly transmitted to their progeny with faster kinetics than GVHD pathophysiology and at times even faster kinetics than the genetic manipulation can manifest protein-level changes within the ISCs, we therefore examined *ex vivo* if T-cell-mediated injury was due to targeting of the ISCs or Paneth cells. Supplementation of organoid culture media with the Paneth-cell-derived factors Wnt3 and Jagged1 did not protect intestinal organoids from activated allogeneic T cells (Fig. 7F), suggesting that loss of Paneth cell niche support was not a critical component of T-cell-mediated elimination of intestinal organoids. Indeed, prevention of Paneth cell targeting by co-culturing T cells or IFN $\gamma$  with Paneth-cell-deficient *Atoh1 $\Delta$ IEC* organoids did not protect the organoids from T cells either (Fig. 7G).

To further determine if targeting of Paneth cells was critical for T-cell-mediated organoid elimination and ISC damage, we co-cultured purified ISCs and purified Paneth cells such that organoid formation from ISCs was dependent on support provided by the Paneth cells. Cultures with WT and *Ifngr*<sup>-/-</sup> Paneth cells were both sensitive to activated T cells, indicating that Paneth cell targeting with IFN $\gamma$  was dispensable for T-cell-mediated organoid elimination (Fig. 7H). Given that ISCs expressed IFN $\gamma$ R1 (Fig. 7E), we investigated if the receptor was



functional, treating sorted Lgr5<sup>high</sup> cells with IFN $\gamma$  for 1.5 hours. RNA sequencing confirmed a robust IFN $\gamma$  transcriptional signature in the stem cells, as several IFN $\gamma$ -related genes were upregulated shortly after exposure, indicating direct activity of IFN $\gamma$  in ISCs (Fig. 7I). We next tested direct T cell targeting of ISCs by performing T cell co-culture with purified ISCs in the presence of Wnt3.

Organoid growth from WT ISCs was significantly reduced by co-culture with allogeneic T cells, but *Ifngr*<sup>-</sup> ISCs demonstrated intact organoid-forming capacity and were thus resistant to T-cell mediated suppression (Fig. 7J).

To exclude the possibility that cultures of WT ISCs were sensitive to IFN $\gamma$  because of damage to their immediate progeny and to further evaluate the direct effects of IFN $\gamma$  on ISCs, we utilized a niche-independent high-purity ISC culture system composed nearly entirely of Lgr5<sup>+</sup> cells<sup>56</sup>. In this system, the combination of a GSK3 $\beta$  inhibitor and a histone deacetylase inhibitor enables culture of homogenous symmetrically dividing Lgr5<sup>+</sup> ISC colonies from purified ISCs. Despite the potent activation of the Wnt and Notch pathways in this culture system that maintained the high frequency of Lgr5<sup>+</sup> cells (fig. S8B), IFN $\gamma$  directly induced apoptosis within the ISC colonies as evidenced by staining for cleaved caspase-3 (Fig. 7K). Apoptotic ISCs identified within the cellular layer of the colonies peaked after eight hours (Fig. 7, K and L) and subsequently accumulated in the colony lumen (Fig. 7, K and M). Gene expression analyses revealed the same apoptotic program identified in organoids exposed to IFN $\gamma$ , with downregulation of *Bcl2* and upregulation of *Bak*, as well as downregulation of *Bcl2l1* without a significant change in expression of *Mcl1* or *Bax* (Fig. 7N and fig. S8C). IFN $\gamma$ -induced ISC apoptosis also led to substantial colony death confirmed by propidium iodine uptake (Fig. 7, O and P). Furthermore, addition of the pan-caspase inhibitor Q-VD-Oph to WT ISC colonies (Fig. 7, O and Q) or genetic depletion of *Bak* and *Bax* using ISC colonies derived from double-deficient (*Bak*<sup>-/-</sup>/*Bax*-floxed x *Rosa*-cre-ert2) mice (Fig. 7, P and Q) both maintained ISC colony viability despite exposure to IFN $\gamma$ . In conclusion, T-cell-derived IFN $\gamma$  directly targeted the intestinal epithelium *in vivo* resulting in ISC reduction and intestinal pathology, and IFN $\gamma$  induced *Bak*/*Bax*-dependent ISC apoptosis by directly acting on the stem cells themselves.

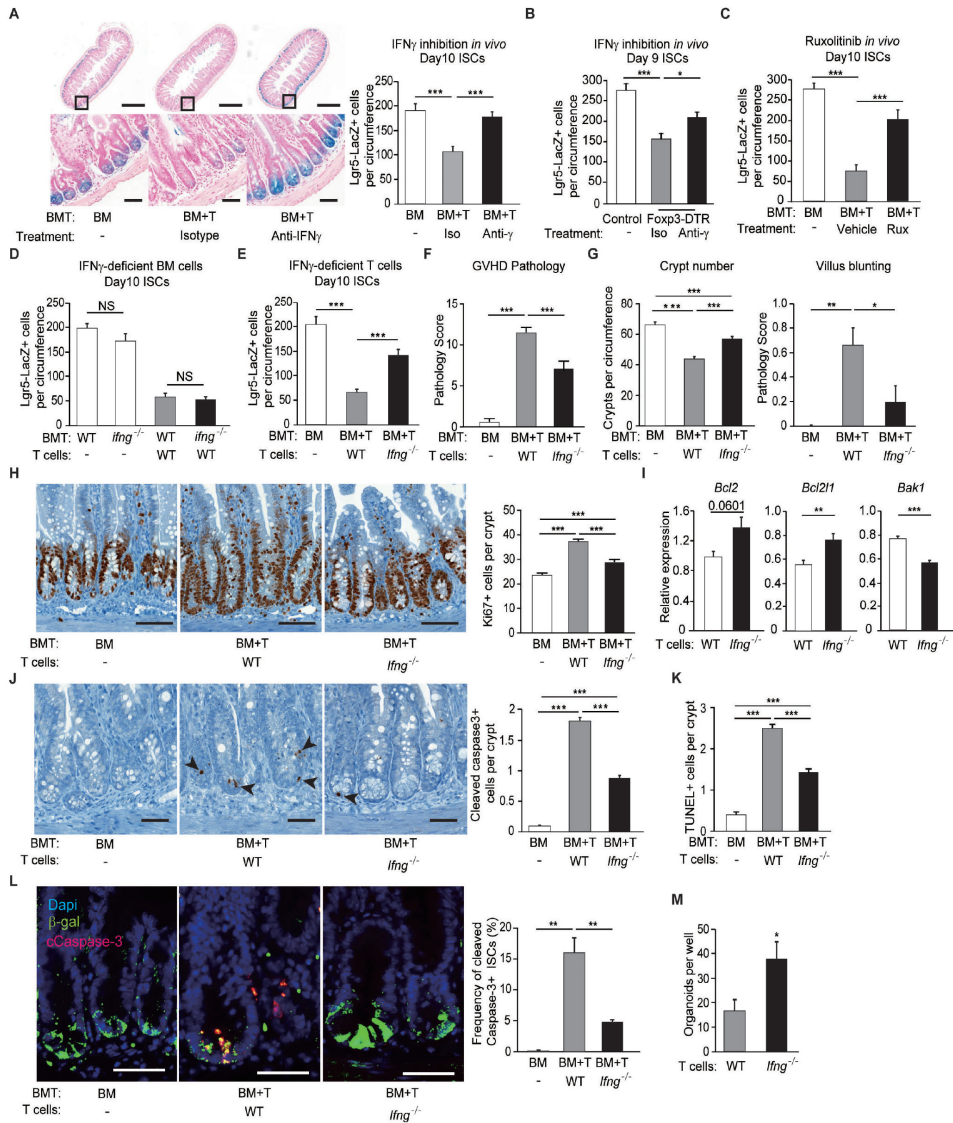


**Fig. 6. T-cell-derived-IFN $\gamma$  decreases ISCs *in vivo*.** (A) ISCs 10 days after LP-into-B6 BMT with isotype or anti-IFN $\gamma$  antibodies (0.5mg every three days starting the day of BMT). Representative images and frequency of SI Lgr5-LacZ<sup>+</sup> ISCs; analysis of n = 15 (TCD BM only), n = 27 (Isotype), or n = 19 (Anti-IFN $\gamma$ ) independent sections from 6-8 mice per group; scale bars = 500 $\mu$ m (upper images) or 50 $\mu$ m (lower images). (B) SI Lgr5<sup>+</sup> ISCs in Foxp3-DTR<sup>+</sup> or Foxp3-DTR<sup>-</sup> Lgr5-LacZ reporter mice 5 days after DT treatment along with Isotype or anti-IFN $\gamma$  antibodies (0.5mg every three days starting the day of DT treatment); analysis of n = 29 (Control), n = 31 (Isotype), or n = 29 (Anti-IFN $\gamma$ ) independent sections from 4-6 mice per group. (C) Frequency of SI Lgr5-LacZ<sup>+</sup> ISCs 10 days after LP-into-B6 BMT with vehicle or ruxolitinib (30mg/kg twice every day starting the day -1 of BMT); Analysis of n = 10 (TCD BM only), n = 8 (Vehicle), or n = 7 (Rux) independent sections from 3-4 mice per group. (D) Frequency of SI Lgr5-LacZ<sup>+</sup> ISCs 10 days after B6-into-BDF1 BMT with wild type or *Ifng*<sup>-/-</sup> marrow. Analysis of n = 5 (WT TCD BM only), n = 6 (*Ifng*<sup>-/-</sup> TCD BM only), n = 11 (WT BM plus WT T cells), or n = 13 (*Ifng*<sup>-/-</sup> BM plus WT T cells) independent sections from 2-4 mice per group. (E to M) B6-into-BDF1 BMT with wild type or *Ifng*<sup>-/-</sup> T cells. (E) Frequency of SI Lgr5-LacZ<sup>+</sup> ISCs; Analysis of n = 5 (TCD BM only), n = 11 (WT), or n = 9 (*Ifng*-

*-/-* independent sections. **(F)** Intestinal GVHD histopathology score 10 days after BMT; *n* = 6 (TCD BM only), *n* = 12 (WT), or *n* = 10 (*Ifng**-/-*) mice per group. **(G)** Crypt numbers and villus blunting histopathology scores 10 days after BMT; for crypt quantifications, *n* = 8 (TCD BM only), *n* = 21 (WT), or *n* = 16 (*Ifng**-/-*) independent sections from 3-7 mice per group; for villus blunting scores, *n* = 6 (TCD BM only), *n* = 12 (WT), or *n* = 10 (*Ifng**-/-*) mice per group. **(H)** Representative images and quantification of Ki67 IHC in the crypt area 10 days after BMT; analysis of *n* = 47 (TCD BM only), *n* = 59 (WT), or *n* = 77 (*Ifng**-/-*) crypts. Scale bars = 100 $\mu$ m. **(I)** Apoptosis-related genes expression in mouse SI crypts 10 days after BMT; *n* = 10 mice per group; Mann–Whitney U analysis. **(J)** Images and quantification of crypt cleaved caspase-3 IHC 10 days after BMT. Arrows indicate cleaved caspase-3+ apoptotic crypt cells; *n* = 489 (TCD BM only), *n* = 718 (WT), or *n* = 974 (*Ifng**-/-*) crypts per group; scale bars = 50 $\mu$ m. **(K)** Quantification of crypt TUNEL staining 10 days after BMT; *n* = 251 (TCD BM only), *n* = 346 (WT), or *n* = 491 (*Ifng**-/-*) crypts per group. **(L)** Double immunofluorescent staining of  $\beta$ -gal (green) and cleaved caspase-3 (red) from Lgr5-LacZ recipient mice 10 days after BMT. Shown are representative images and average frequencies of cleaved caspase-3+ apoptotic ISCs per mouse ileum as a percentage of the total Lgr5+ ISCs detected; scale bars = 50 $\mu$ m. **(M)** Day 5 SI organoid numbers per 100 crypts cultured 10 days after BMT; *n* = 7 (WT), or *n* = 5 (*Ifng**-/-*) mice per group. Graphs demonstrate mean and s.e.m.; comparisons performed with t-tests (two groups) or one-way ANOVA (multiple groups) unless otherwise stated; \**P*<0.05, \*\**P*<0.01, \*\*\**P*<0.001. Data are representative of two (C to E, H, and J to M) independent experiments, or combined from two (A, B, F, G and I) independent experiments.

**Fig. 7. IFN $\gamma$  directly targets intestinal stem cells and induces apoptosis [Figure at next page]. (A to D)** Allogeneic B10.Br-into-B6 (Allo) or syngeneic B6-into-B6 (Syn) BMT using *Ifngr**fl/fl**xVillin-Cre* (*Ifngr* $\Delta$ IEC) or Cre-negative *Ifngr**fl/fl* (*Ifngr*WT) littermate controls. **(A)** Representative images and frequency of SI (ileum) IHC for Olfm4+ ISCs 7 days after BMT; Analysis of *n* = 8 (Syn, *Ifngr*WT), *n* = 6 (Syn, *Ifngr* $\Delta$ IEC), *n* = 17 (*Ifngr*WT), or *n* = 17 (*Ifngr* $\Delta$ IEC) independent sections from 2-5 mice per group. Scale bars = 100 $\mu$ m. **(B)** Intestinal GVHD histopathology score 9 days after BMT; *n* = 3 (Syn), *n* = 4 (Allo, *Ifngr*WT), or *n* = 5 (Allo, *Ifngr* $\Delta$ IEC) mice per group. **(C)** Crypt number quantification and villus blunting histopathologic scoring 9 days after BMT; *n* = 9 (Syn), *n* = 14 (Allo, *Ifngr*WT), or *n* = 17 (Allo, *Ifngr* $\Delta$ IEC) independent sections from 3-5 mice per group for crypt count; *n* = 3 (Syn), *n* = 4 (Allo, *Ifngr*WT), or *n* = 5 (Allo, *Ifngr*WT) mice per group for villus blunting histologic scoring. **(D)** Quantification of crypt cleaved caspase-3 IHC 9 days after BMT; *n* = 489 (Syn), *n* = 718 (Allo, *Ifngr*WT), or *n* = 974 (Allo, *Ifngr* $\Delta$ IEC) crypts from 3-5 mice per group. **(E)** FACS analysis of CD119 (IFN $\gamma$ R1) expression on ISCs and Paneth cells. **(F)** Numbers of B6 SI organoids after culture with BALB/c T cells +/- Wnt3a and Jagged1 (1ng/ml); culture day 7, *n* = 3 wells/group. **(G)** Paneth-cell-deficient *Atoh1* $\Delta$ IEC SI organoids cultured in WNT3-supplemented ENR media +/- BALB/c T cells or IFN $\gamma$ ; culture day 7, *n* = 4 wells/group. **(H)** SI organoids from sort-purified SI Lgr5-GFP<sup>high</sup> ISCs and sort-purified Paneth cells cultured +/- BALB/c T cells; culture day 7, *n* = 3-6 wells/group. **(I)** RNAseq indicating IFN $\gamma$ -responsive gene expression in sorted Lgr5-GFP<sup>high</sup> ISCs incubated with IFN $\gamma$  for 1.5 hours. **(J)** Organoids from sorted WT or *Ifng**-/-* Lgr5-GFP<sup>high</sup> SI ISCs cultured +/- BALB/c T cells (culture day 6, *n* = 7-8 wells/group). **(K to Q)** ISC colonies cultured in WENR with HDAC and GSK3 $\beta$  inhibition +/- IFN $\gamma$ . **(K)** Representative confocal images of cleaved caspase-3 (cCaspase-3) immunofluorescence in ISC colonies cultured +/- IFN $\gamma$  (culture day 6, arrows indicate apoptotic ISCs in the cellular layer, and arrow heads indicate apoptotic ISCs in the colony lumen, scale bars = 50 $\mu$ m). **(L)** Frequency of epithelial-layer cleaved caspase-3+ ISCs; analysis of *n* = 65 (0 hour), *n* = 65 (2 hour), *n* = 64 (4 hour), *n* = 40 (8 hour), *n* = 72 (12 hour), and *n* = 57 (16 hour) colonies per group. **(M)** Cleaved caspase-3 staining intensity in the lumen area; analysis of *n* = 83 (0 hour), *n* = 104 (2 hour), *n* = 86 (4 hour), *n* = 76 (8 hour), *n* = 136 (12 hour), and *n* = 82 (16 hour) colonies per group. **(N)** qPCR analysis of apoptosis-related genes in mouse SI ISC colonies cultured with rIFN $\gamma$  for 24 hours; *n* = 6 wells/group; Mann–Whitney U analysis. **(O to Q)** Representative images and viability quantification of ISC colonies cultured with IFN $\gamma$ . Images show bright field microscopy (upper panels), Hoechst staining (middle panels), or propidium iodide (lower panels); scale bars = 200  $\mu$ m **(O)** Images of Lgr5-GFP+ SI ISC colonies cultured with rIFN $\gamma$  +/- caspase inhibitor Q-VD-OPh (culture day 7). **(P)** Images of SI ISC colonies initiated from sorted WT or Bak/Bax double knockout (DKO) SI ISCs cultured with IFN $\gamma$  (culture day 7). **(Q)** Quantification of ISC colony survival after cultured with rIFN $\gamma$  (*n* = 3 wells/group); t-tests at each concentration of IFN $\gamma$ . Graphs indicate mean and s.e.m.; comparisons performed with one-way ANOVA unless otherwise stated; \**P*<0.05, \*\**P*<0.01, \*\*\**P*<0.001. Data are representative of two (A to F, H, J to N, and P) or three (G, O and Q) independent experiments, or combined from three independent experiments (I).

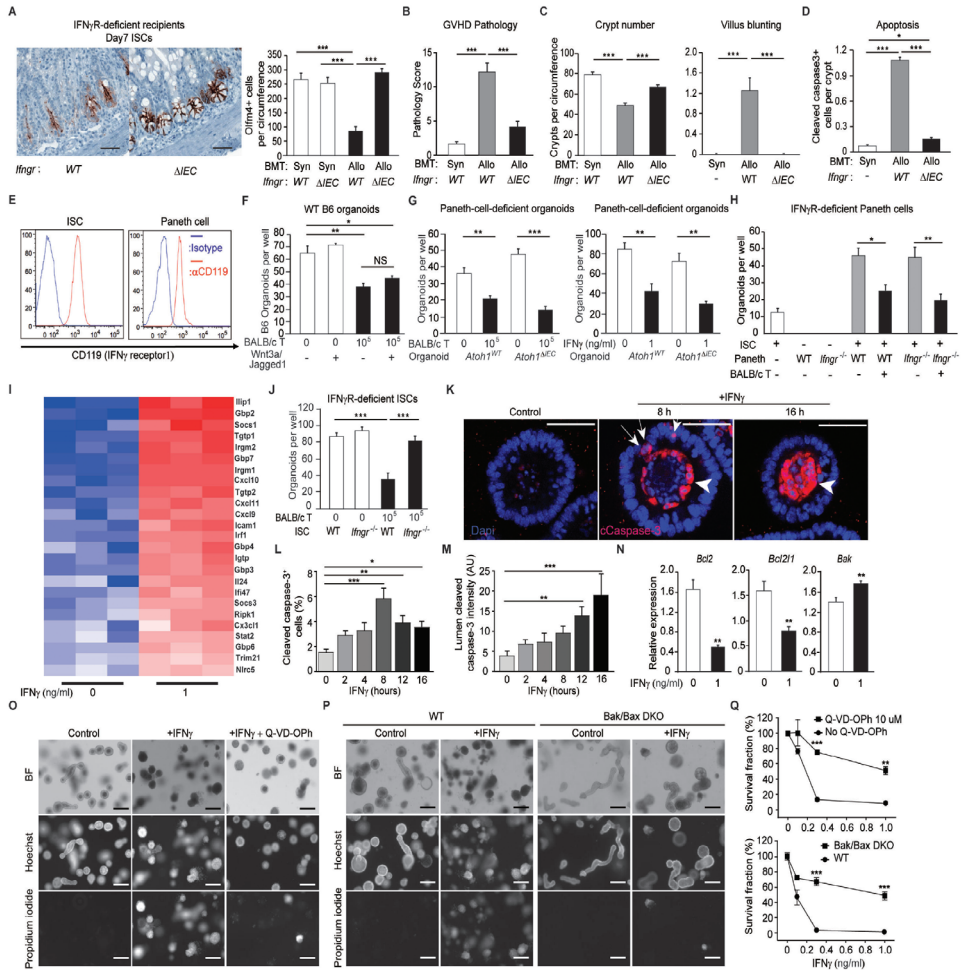


Fig. 7. IFN $\gamma$  directly targets intestinal stem cells and induces apoptosis [Legend at previous page].

## Discussion

T-cell-mediated tissue damage, particularly in the BMT setting, is the culmination of a systemic process involving cellular activation, migration, and effector function. Given this complexity and the involvement of numerous cell types in various tissues at specific time points, it is challenging to comprehensively and accurately elucidate the specific interactions occurring between T cells and individual subsets of intestinal epithelial cells. To overcome these limitations, we established an *ex vivo* co-culture system of intestinal organoids and T cells. Using this system to model Tcell-induced ISC damage, we identified a direct role for T-cell-derived IFN $\gamma$  and subsequent JAK/STAT signaling in ISC apoptosis occurring during immune-mediated GI damage. Consistent with this cytokine-mediated pathology, whole-mount 3-D microscopy after allogeneic BMT demonstrated that donor T cells invading the small intestine post-transplant primarily infiltrated the lamina propria of the crypt compartment. Donor T cells thus invaded the intestinal mucosa near the stem cells, but were mostly not located precisely within the targeted epithelium. Further analysis of these T cells confirmed that they were the principle source of IFN $\gamma$  in this area after BMT. Surprisingly though, there were remarkably few T cells present within the crypt epithelium at baseline, as most intraepithelial T cells were found within the villi. The lamina propria showed roughly similar T cell densities within the crypt and villus regions at baseline, so the preferential infiltration of the crypt region after allogeneic BMT represented a substantial redistribution of T cell localization within the mucosa of the ileum. Interestingly, a recent study showed that depletion of donor CD4+ T cells immediately after BMT resulted in increased serum IFN $\gamma$  and reduced intestinal GVHD pathology with fewer donor CD8+ T cells in the colon<sup>57</sup>, suggesting that IFN $\gamma$  from donor T cells in proximity to the crypt compartment, rather than the IFN $\gamma$  present in circulation, may be essential for its direct epithelial toxicity. While naive T cells had no impact on epithelial growth in *ex vivo* co-cultures, activated T cells induced substantial organoid toxicity and reduction of ISCs. This toxicity did not require genetic disparity between the T cells and their epithelial targets once the T cells were activated, as T cells activated by allogeneic DCs or anti-CD3/CD28 antibodies suppressed both allogeneic and syngeneic mouse intestinal organoid numbers. This was also true in human co-culture models, with human T cells eliminating allogeneic human organoids and even eliminating autologous organoids generated from the same donors as the T cells. This organoid toxicity was mediated by T-cell-derived IFN $\gamma$ , which also induced the ISC reduction observed *ex vivo* as well as *in vivo*. Antigen specificity of this pathologic immune response appeared to occur at the level of initial T cell activation, which led to substantial production of IFN $\gamma$ . These results are consistent with experiments indicating that inflammatory cytokines can mediate tissue damage induced by allogeneic T cells irrespective of antigen presentation by epithelial cells<sup>58</sup>, although antigen presentation by epithelial cells including ISCs may be critical for certain other immune responses<sup>59-61</sup>.



Effects of IFN $\gamma$  on the GI tract have been studied in various experimental models, and it has been reported to induce epithelial toxicity through both cell-autonomous and non-autonomous negative regulatory feedback loops<sup>43,62,63</sup>. IFN $\gamma$  has also been found to induce loss of Paneth cells in models of infection and autoimmunity<sup>40,41</sup>. Studies in transplant models have identified both pathologic and protective roles for IFN $\gamma$  in GVHD, as discussed below. However, there has been little exploration of the direct interactions between ISCs and IFN $\gamma$ . The exclusive use here of primary cells, containing the full diversity of lineages present in normal epithelial tissue (such as stem cells, niche cells, progenitors, and mature post-mitotic cells), for *in vivo* and *ex vivo* models of tissue damage has allowed for identification of ISCs as direct targets of T-cell mediated cytokine-dependent GI damage. Such a finding would not be possible using model systems such as transformed cell lines lacking a stem cell compartment. In studying the ISC compartment directly, we found that reduction of ISCs preceded any reduction of Paneth cells in multiple models of immune-mediated GI damage. The reduction of ISCs was validated using two distinct functional approaches: culturing organoids from crypts isolated after *in vivo* challenge and lineage tracing for stem cell-derived progeny. Both functional approaches were consistent with the kinetics indicated by ISC quantifications. Furthermore, these kinetics suggested that ISCs were the primary target, though a decrease in ISCs could also have been due to niche dysfunction, rather than loss of the niche. While Paneth cells are not the only component of the stem cell niche, which includes stromal and immunologic members as well<sup>18,19,24,64,65</sup>, and consideration should also be paid to progenitors and mature epithelial cells for a comprehensive understanding of intestinal immunopathology<sup>66-69</sup>, *ex vivo* modeling revealed that IFN $\gamma$ -receptor-deficient ISCs were resistant to T cells and IFN $\gamma$ , while niche-dependent cultures of ISCs with IFN $\gamma$ -receptor-deficient Paneth cells as well as cultures of niche independent stem cell colonies were not. These findings thus indicated that ISCs were indeed direct targets of T cells and IFN $\gamma$ .

Further investigation of the stem cell compartment indicated that IFN $\gamma$  could directly program ISC death, inducing transcriptional changes capable of shifting the cells toward induction of apoptosis. BCL-2 and BCL-XL are anti-apoptotic BCL-2 family members, and their downregulation, as described here in ISCs due to IFN $\gamma$ , can result in activation of pro-apoptotic effectors BAX and BAK<sup>70</sup>. Activated BAX and BAK can then form oligomers which permeabilize the mitochondrial outer membrane and release cytochrome c to activate caspases and further propagate the apoptotic cascade<sup>71</sup>. The downregulation of *Bcl2* and *Bcl2l1* and the upregulation of *Bak*, along with stable expression of *Bax* (i.e., without reciprocal decrease in *Bax* that could counterbalance the increase in *Bak*), clearly implicate initiation of apoptosis as a major direct effect of IFN $\gamma$  in ISCs. Furthermore, we observed increased caspase-3 activity and cleaved caspase-3 protein in human organoids treated with IFN $\gamma$ . *In vivo* IFN $\gamma$  signaling blockade with neutralizing antibodies, IFN $\gamma$  deletion from donor T cells, IFN $\gamma$  receptor deletion from the intestinal epithelium, and ruxolitinib all protected ISCs from T cells *in vivo*, although the specific mechanisms of ISC protection may



be distinct between GVHD and autoimmunity after Treg deletion. Nonetheless, these results suggest that IFN $\gamma$ -induced apoptosis is a central mechanism of ISC impairment caused by T cells, using a secreted cytokine to kill stem cells via activation of JAK/STAT signaling and subsequent gene expression driving the cell toward programmed death.

Due to its pleiotropic effects, IFN $\gamma$  has demonstrated strikingly distinct impacts depending on the BMT model. Deficiency of donor-derived IFN $\gamma$  resulted in increased GVHD mortality and limited GVL in a CD8+ T-cell-mediated experimental transplant model<sup>38</sup>. A subsequent study showed opposing effects of IFN $\gamma$  in distinct tissues, with IFN $\gamma$  playing a protective role in the lungs, but mediating GI toxicity in mice with GVHD<sup>28</sup>, and another study indicated that IFN $\gamma$  can reduce intestinal GVHD pathology after depletion of CD4+ T cells<sup>57</sup>. These studies illustrate the complex role played by IFN $\gamma$  in the transplant setting, and undesirable complications could thus result from targeting IFN $\gamma$  in clinical BMT. IFN $\gamma$  signaling is transduced by the JAK/STAT pathway, including JAK1/2 and STAT1<sup>72</sup>, which could represent another approach for interfering with IFN $\gamma$ -mediated GI damage and loss of ISCs. Indeed, we found that treatment with the JAK1/2 inhibitor ruxolitinib protected ISCs from T-cell-mediated damage *ex vivo* and *in vivo*. While inhibition of JAK signaling can suppress T cell activity<sup>52</sup>, we found that JAK inhibition also protected intestinal epithelium from T-cell mediated injury by suppressing the tissue's response to IFN $\gamma$ . This was consistent with our findings that deletion of the IFN $\gamma$  receptor on the intestinal epithelium protected the stem cells and the tissue overall from T-cell-mediated pathology. JAK inhibition has been investigated clinically in GVHD with promising results<sup>53-55</sup>, and it has recently been approved for GVHD treatment in the setting of steroid refractory disease. JAK inhibitors thus provide a promising approach for protecting the ISC compartment from pathologic immune responses. Additionally, these findings suggest that part of the clinical efficacy of JAK inhibition in GVHD, particularly in settings where other potent immunosuppressive agents such as corticosteroids have failed, could be due to suppression of pathologic cytokine signaling outside of the T cell compartment and perhaps within the GVHD target organs.

In summary, we found that damage to the ISC compartment was a shared feature of GVHD and autoimmunity, and T-cell-derived IFN $\gamma$  was a key mediator of ISC reduction in immune-mediated GI damage. Intestinal organoid cultures were used to assay epithelial function during immune-mediated damage *in vivo* and to interrogate specific interactions between T cells and epithelial targets *ex vivo*. T cell localization within the intestinal mucosa differed substantially between homeostasis and the setting of damage post-transplant, with donor T cells primarily localizing to the lamina propria of the crypt region where they were the dominant producers of IFN $\gamma$ . IFN $\gamma$  directly targeted ISCs, inducing a gene expression program resulting in stem cell apoptosis, and JAK inhibition protected ISCs from T cells by suppressing their response to IFN $\gamma$ . IFN $\gamma$  thus played a central role in the T-cell-mediated stem cell damage studied here, and pharmacologic JAK inhibition may provide clinically

efficacious immunosuppression in part by suppressing tissue responses to pathologic signals from the immune system.

## Materials and Methods

### Study design

The purpose of the study was to investigate mechanisms of T cell effects on ISCs during immune-mediated GI damage. We used two types of *in vivo* animal models: allogeneic BMT and Treg-depletion-induced autoimmunity. To perform detailed evaluation of direct interactions between T cells and ISCs, we established a method of co-culturing T cells with intestinal organoids. Analyses of experiments were performed with histologic staining, 3-D imaging, flow cytometry, qPCR, and western blotting. Statistical issues are described below. There were no pre-defined study end points. Experiments were generally performed a minimum of two times, and the number of independent experiments and statistical methods are described in the figure legends. For further details, please see the Supplementary Materials and Methods.

### Acknowledgments

We thank Hans Clevers, Johan van Es, and Alexander Rudensky for generous sharing of mice and advice, and we gratefully acknowledge the technical assistance of the MSKCC Research Animal Resource Center and Molecular Cytology Core Facility. We thank Jarrod A. Dudakov, Enrico Velardi, Marcel R.M. van den Brink, Matthias Schewe, Riccardo Fodde, Jorik M. van Rijn and Edward E.S. Nieuwenhuis for their valuable advice. We also thank the Integrated Genomics Operation Core, funded by the NCI Cancer Center Support Grant (CCSG, P30 CA08748), Cycle for Survival, and the Marie-Josée and Henry R. Kravis Center for Molecular Oncology.

### Funding

This research was supported by National Institutes of Health award numbers K08-HL115355 (A.M.H.), R01-HL125571 (A.M.H), R01-HL146338 (A.M.H), and P30-CA008748 (MSKCC Core Grant). Support was also received from the Susan and Peter Solomon Divisional Genomics Program, the Ludwig Center for Cancer Immunotherapy, the Parker Institute for Cancer Immunotherapy, and the Anna Fuller Fund (A.M.H.). A.M.H. was also supported by the Amy Strelzer Manasevit Research Program. S.T. was supported by a scholarship from the Mochida Memorial Foundation for Medical and Pharmaceutical Research and an American Society for Blood and Marrow Transplantation (ASBMT) New Investigator Award from Millenium, the Takeda Oncology Company. Y.F. was also supported by an ASBMT New Investigator Award, and P.V. was supported by an ASBMT New Investigator Award and the American Italian Cancer Foundation. C.A.L. was supported by the WKZ fund of the UMC Utrecht, and



S.A.J. was supported by the Jo Kolk Study Fund Foundation, Nijbakker-Morra Foundation, Dutch Digestive Foundation, K.F. Hein Foundation, Renswoude Foundation and Alexandre Suerman Stipend of the UMC Utrecht.

### **Author contributions**

S.T. designed, performed, and analyzed *in vivo* and *ex vivo* experiments and drafted the manuscript. M.L.M. designed, performed, and analyzed experiments including the mouse ISC colony assay. S.A.J. performed and analyzed *in vivo* experiments and human *ex vivo* experiments. J.B. performed and analyzed human *ex vivo* experiments. Y.F., J.K., D.C., M.H.O., A.M.M. and P.V. performed and analyzed *in vivo* experiments. S.M.D. assisted with statistical analyses. S.M. provided input and the human organoids and helped with various assays. M.C. provided input and helped with various assays and stem cell cultures. A.E. performed and monitored bone marrow transplants and maintained the mouse colonies. M.K. and R.L.L. assisted with Jak1 deficiency experiments. Y.H.L. and N.F.S. assisted with Paneth cell deficiency experiments. E.H.C. provided input and helped with apoptosis assays. C.L. analyzed intestinal histopathology. R.K., C.A.L., and A.M.H. supervised the research.

### **Competing interests**

The authors declare no competing financial interests. A.M.H. holds intellectual property related to Interleukin-22 and in the last three years has performed consulting for Ziopharm and Nexus Global Group.

## References

1. H. Gehart, H. Clevers, Repairing organs: lessons from intestine and liver. *Trends Genet* **31**, 344-351 (2015).
2. N. Barker, J. H. van Es, J. Kuipers, P. Kujala, M. van den Born, M. Cozijnsen, A. Haegebarth, J. Korving, H. Begthel, P. J. Peters, H. Clevers, Identification of stem cells in small intestine and colon by marker gene *Lgr5*. *Nature* **449**, 1003-1007 (2007).
3. H. Clevers, The intestinal crypt, a prototype stem cell compartment. *Cell* **154**, 274-284 (2013).
4. T. Sato, J. H. van Es, H. J. Snippert, D. E. Stange, R. G. Vries, M. van den Born, N. Barker, N. F. Shroyer, M. van de Wetering, H. Clevers, Paneth cells constitute the niche for *Lgr5* stem cells in intestinal crypts. *Nature* **469**, 415-418 (2011).
5. N. Barker, M. Huch, P. Kujala, M. van de Wetering, H. J. Snippert, J. H. van Es, T. Sato, D. E. Stange, H. Begthel, M. van den Born, E. Danenberg, S. van den Brink, J. Korving, A. Abo, P. J. Peters, N. Wright, R. Poulsom, H. Clevers, *Lgr5*(+ve) stem cells drive selfrenewal in the stomach and build long-lived gastric units in vitro. *Cell Stem Cell* **6**, 25-36 (2010).
6. C. Metcalfe, N. M. Kijavini, R. Ybarra, F. J. de Sauvage, *Lgr5*+ stem cells are indispensable for radiation-induced intestinal regeneration. *Cell Stem Cell* **14**, 149-159 (2014).
7. J. Legoff, M. Resche-Rigon, J. Bouquet, M. Robin, S. N. Naccache, S. Mercier-Delarue, S. Federman, E. Samayoa, C. Rousseau, P. Piron, N. Kapel, F. Simon, G. Socie, C. Y. Chiu, The eukaryotic gut virome in hematopoietic stem cell transplantation: new clues in enteric graft-versus-host disease. *Nat Med*, (2017).
8. A. Beilhack, S. Schulz, J. Baker, G. F. Beilhack, C. B. Wieland, E. I. Herman, E. M. Baker, Y. A. Cao, C. H. Contag, R. S. Negrin, In vivo analyses of early events in acute graft-versus-host disease reveal sequential infiltration of T-cell subsets. *Blood* **106**, 1113-1122 (2005).
9. D. R. Withers, M. R. Hepworth, X. Wang, E. C. Mackley, E. E. Halford, E. E. Dutton, C. L. Marriott, V. Brucklacher-Waldert, M. Veldhoen, J. Kelsen, R. N. Baldassano, G. F. Sonnenberg, Transient inhibition of ROR-gammat therapeutically limits intestinal inflammation by reducing TH17 cells and preserving group 3 innate lymphoid cells. *Nat Med* **22**, 319-323 (2016).
10. A. Saha, R. S. O'Connor, G. Thangavelu, S. B. Lovitch, D. B. Dandamudi, C. B. Wilson, B. G. Vincent, V. Tkachev, J. M. Pawlicki, S. N. Furlan, L. S. Kean, K. Aoyama, P. A. Taylor, A. Panoskaltis-Mortari, R. Foncea, P. Ranganathan, S. M. Devine, J. S. Burrill, L. Guo, C. Sacristan, N. W. Snyder, I. A. Blair, M. C. Milone, M. L. Dustin, J. L. Riley, D. A. Bernlohr, W. J. Murphy, B. T. Fife, D. H. Munn, J. S. Miller, J. S. Serody, G. J. Freeman, A. H. Sharpe, L. A. Turka, B. R. Blazar, Programmed death ligand-1 expression on donor T cells drives graft-versus-host disease lethality. *J Clin Invest* **126**, 2642-2660 (2016).
11. C. S. N. Klose, T. Mahlakoiv, J. B. Moeller, L. C. Rankin, A. L. Flamar, H. Kabata, L. A. Monticelli, S. Moriyama, G. G. Putzel, N. Rakhilin, X. Shen, E. Kostenis, G. M. Konig, T. Senda, D. Carpenter, D. L. Farber, D. Artis, The neuropeptide neuromedin U stimulates innate lymphoid cells and type 2 inflammation. *Nature* **549**, 282-286 (2017).
12. A. N. J. McKenzie, H. Spits, G. Eberl, Innate lymphoid cells in inflammation and immunity. *Immunity* **41**, 366-374 (2014).
13. S. L. Sanos, A. Diefenbach, Innate lymphoid cells: from border protection to the initiation of inflammatory diseases. *Immunol Cell Biol* **91**, 215-224 (2013).
14. N. R. West, A. N. Hegazy, B. M. J. Owens, S. J. Bullers, B. Linggi, S. Buonocore, M. Coccia, D. Gortz, S. This, K. Stockenhuber, J. Pott, M. Friedrich, G. Ryzhakov, F. Baribaud, C. Brodmerkel, C. Cieluch, N. Rahman, G. Muller-Newen, R. J. Owens, A. A. Kuhl, K. J. Maloy, S. E. Plevy, I. B. D. C. I. Oxford, S. Keshav, S. P. L. Travis, F. Powrie, Oncostatin M drives intestinal inflammation and predicts response to tumor necrosis factor-neutralizing therapy in patients with inflammatory bowel disease. *Nat Med* **23**, 579-589 (2017).
15. N. D. Mathewson, R. Jenq, A. V. Mathew, M. Koenigsnecht, A. Hanash, T. Toubai, K. Oravecz-Wilson, S. R. Wu, Y. Sun, C. Rossi, H. Fujiwara, J. Byun, Y. Shono, C. Lindemans, M. Calafiore, T. C. Schmidt, K. Honda, V. B. Young, S. Pennathur, M. van den Brink, P. Reddy, Gut microbiome-derived metabolites modulate intestinal epithelial cell damage and mitigate graft-versus-host disease. *Nat Immunol* **17**, 505-513 (2016).
16. G. E. Diehl, R. S. Longman, J. X. Zhang, B. Breart, C. Galan, A. Cuesta, S. R. Schwab, D. R. Littman, Microbiota restricts trafficking of bacteria to mesenteric lymph nodes by CX(3)CR(hi) cells. *Nature* **494**, 116-120 (2013).
17. K. Taniguchi, L. W. Wu, S. I. Grivnenikov, P. R. de Jong, I. Lian, F. X. Yu, K. Wang, S. B. Ho, B. S. Boland, J. T. Chang, W. J. Sandborn, G. Hardiman, E. Raz, Y. Maehara, A. Yoshimura, J. Zucman-Rossi, K. L. Guan, M. Karin, A gp130-Src-YAP module links inflammation to epithelial regeneration. *Nature* **519**, 57-62 (2015).
18. C. A. Lindemans, M. Calafiore, A. M. Mertelsmann, M. H. O'Connor, J. A. Dudakov, R. R. Jenq, E. Velardi, L. F. Young, O. M. Smith, G. Lawrence, J. A. Ivanov, Y. Y. Fu, S. Takashima, G. Hua, M. L. Martin, K. P. O'Rourke, Y. H. Lo, M. Mokry, M. Romera-Hernandez, T. Cupedo, L. E. Dow, E. E. Nieuwenhuis, N. F. Shroyer, C. Liu, R. Kolesnick, M. R. van den Brink, A. M. Hanash, Interleukin-22 promotes intestinal-stemcell-mediated epithelial regeneration. *Nature* **528**, 560-564 (2015).
19. P. Aparicio-Domingo, M. Romera-Hernandez, J. J. Karrich, F. Cornelissen, N. Papazian, D. J. Lindenbergh-Kortleve, J. A. Butler, L. Boon, M. C. Coles, J. N. Samsom, T. Cupedo, Type 3 innate lymphoid cells maintain



- intestinal epithelial stem cells after tissue damage. *J Exp Med* **212**, 1783-1791 (2015).
20. R. J. Epstein, G. B. McDonald, G. E. Sale, H. M. Shulman, E. D. Thomas, The diagnostic accuracy of the rectal biopsy in acute graft-versus-host disease: a prospective study of thirteen patients. *Gastroenterology* **78**, 764-771 (1980).
  21. G. E. Sale, H. M. Shulman, G. B. McDonald, E. D. Thomas, Gastrointestinal graft-versus-host disease in man. A clinicopathologic study of the rectal biopsy. *Am J Surg Pathol* **3**, 291-299 (1979).
  22. Y. Eriguchi, H. Uryu, K. Nakamura, S. Shimoji, S. Takashima, H. Iwasaki, T. Miyamoto, N. Shimono, D. Hashimoto, K. Akashi, T. Ayabe, T. Teshima, Reciprocal expression of enteric antimicrobial proteins in intestinal graft-versus-host disease. *Biol Blood Marrow Transplant* **19**, 1525-1529 (2013).
  23. R. R. Jenq, C. Ubeda, Y. Taur, C. C. Menezes, R. Khanin, J. A. Dudakov, C. Liu, M. L. West, N. V. Singer, M. J. Equinda, A. Gouborne, L. Lipuma, L. F. Young, O. M. Smith, A. Ghosh, A. M. Hanash, J. D. Goldberg, K. Aoyama, B. R. Blazar, E. G. Pamer, M. R. van den Brink, Regulation of intestinal inflammation by microbiota following allogeneic bone marrow transplantation. *J Exp Med* **209**, 903-911 (2012).
  24. A. M. Hanash, J. A. Dudakov, G. Hua, M. H. O'Connor, L. F. Young, N. V. Singer, M. L. West, R. R. Jenq, A. M. Holland, L. W. Kappel, A. Ghosh, J. J. Tsai, U. K. Rao, N. L. Yim, O. M. Smith, E. Velardi, E. B. Hawryluk, G. F. Murphy, C. Liu, L. A. Fouser, R. Kolesnick, B. R. Blazar, M. R. van den Brink, Interleukin-22 protects intestinal stem cells from immune-mediated tissue damage and regulates sensitivity to graft versus host disease. *Immunity* **37**, 339-350 (2012).
  25. S. Takashima, M. Kadowaki, K. Aoyama, M. Koyama, T. Oshima, K. Tomizuka, K. Akashi, T. Teshima, The Wnt agonist R-spondin1 regulates systemic graft-versus-host disease by protecting intestinal stem cells. *J Exp Med* **208**, 285-294 (2011).
  26. M. B. Baker, N. H. Altman, E. R. Podack, R. B. Levy, The role of cell-mediated cytotoxicity in acute GVHD after MHC-matched allogeneic bone marrow transplantation in mice. *J Exp Med* **183**, 2645-2656 (1996).
  27. M. Y. Braun, B. Lowin, L. French, H. Acha-Orbea, J. Tschopp, Cytotoxic T cells deficient in both functional fas ligand and perforin show residual cytolytic activity yet lose their capacity to induce lethal acute graft-versus-host disease. *J Exp Med* **183**, 657-661 (1996).
  28. A. C. Burman, T. Banovic, R. D. Kuns, A. D. Clouston, A. C. Stanley, E. S. Morris, V. Rowe, H. Bofinger, R. Skoczylas, N. Raffelt, O. Fahy, S. R. McColl, C. R. Engwerda, K. P. McDonald, G. R. Hill, IFN $\gamma$  differentially controls the development of idiopathic pneumonia syndrome and GVHD of the gastrointestinal tract. *Blood* **110**, 1064-1072 (2007).
  29. C. A. Ellison, J. M. Fischer, K. T. HayGlass, J. G. Gartner, Murine graft-versus-host disease in an F1-hybrid model using IFN- $\gamma$  gene knockout donors. *J Immunol* **161**, 631-640 (1998).
  30. T. A. Graubert, J. F. DiPersio, J. H. Russell, T. J. Ley, Perforin/granzyme-dependent and independent mechanisms are both important for the development of graft-versus-host disease after murine bone marrow transplantation. *J Clin Invest* **100**, 904-911 (1997).
  31. Z. Jiang, E. Podack, R. B. Levy, Major histocompatibility complex-mismatched allogeneic bone marrow transplantation using perforin and/or Fas ligand double-defective CD4(+) donor T cells: involvement of cytotoxic function by donor lymphocytes prior to graft-versus-host disease pathogenesis. *Blood* **98**, 390-397 (2001).
  32. W. J. Murphy, L. A. Welniak, D. D. Taub, R. H. Wiltrot, P. A. Taylor, D. A. Vallera, M. Kopf, H. Young, D. L. Longo, B. R. Blazar, Differential effects of the absence of interferon- $\gamma$  and IL-4 in acute graft-versus-host disease after allogeneic bone marrow transplantation in mice. *J Clin Invest* **102**, 1742-1748 (1998).
  33. I. K. Na, S. X. Lu, N. L. Yim, G. L. Goldberg, J. Tsai, U. Rao, O. M. Smith, C. G. King, D. Suh, D. Hirschhorn-Cymerman, L. Palomba, O. Penack, A. M. Holland, R. R. Jenq, A. Ghosh, H. Tran, T. Merghoub, C. Liu, G. D. Sempowski, M. Ventevogel, N. Beauchemin, M. R. van den Brink, The cytolytic molecules Fas ligand and TRAIL are required for murine thymic graft-versus-host disease. *J Clin Invest* **120**, 343-356 (2010).
  34. R. J. Robb, G. R. Hill, The interferon-dependent orchestration of innate and adaptive immunity after transplantation. *Blood* **119**, 5351-5358 (2012).
  35. C. Schmaltz, O. Alpdogan, B. J. Kappel, S. J. Muriglan, J. A. Rotolo, J. Ongchin, L. M. Willis, A. S. Greenberg, J. M. Eng, J. M. Crawford, G. F. Murphy, H. Yagita, H. Walczak, J. J. Peschon, M. R. van den Brink, T cells require TRAIL for optimal graft-versus-tumor activity. *Nat Med* **8**, 1433-1437 (2002).
  36. H. Wang, W. Asavarengchai, B. Y. Yeap, M. G. Wang, S. Wang, M. Sykes, Y. G. Yang, Paradoxical effects of IFN- $\gamma$  in graft-versus-host disease reflect promotion of lymphohematopoietic graft-versus-host reactions and inhibition of epithelial tissue injury. *Blood* **113**, 3612-3619 (2009).
  37. Y. G. Yang, B. R. Dey, J. J. Sergio, D. A. Pearson, M. Sykes, Donor-derived interferon gamma is required for inhibition of acute graft-versus-host disease by interleukin 12. *J Clin Invest* **102**, 2126-2135 (1998).
  38. Y. G. Yang, J. Qi, M. G. Wang, M. Sykes, Donor-derived interferon gamma separates graft-versus-leukemia effects and graft-versus-host disease induced by donor CD8 T cells. *Blood* **99**, 4207-4215 (2002).
  39. T. Yi, Y. Chen, L. Wang, G. Du, D. Huang, D. Zhao, H. Johnston, J. Young, I. Todorov, D. T. Umetsu, L. Chen, Y. Iwakura, F. Kandeel, S. Forman, D. Zeng, Reciprocal differentiation and tissue-specific pathogenesis of Th1, Th2, and Th17 cells in graft-versus-host disease. *Blood* **114**, 3101-3112 (2009).
  40. H. F. Farin, W. R. Karthaus, P. Kujala, M. Rakhshandehroo, G. Schwank, R. G. Vries, E. Kalkhoven, E. E. Nieuwenhuis, H. Clevers, Paneth cell extrusion and release of antimicrobial products is directly controlled by immune cell-

- derived IFN-gamma. *J Exp Med* **211**, 1393-1405 (2014).
41. M. Raetz, S. H. Hwang, C. L. Wilhelm, D. Kirkland, A. Benson, C. R. Sturge, J. Mirpuri, S. Vaishnav, B. Hou, A. L. Defranco, C. J. Gilpin, L. V. Hooper, F. Yarovinsky, Parasite-induced TH1 cells and intestinal dysbiosis cooperate in IFN-gamma-dependent elimination of Paneth cells. *Nat Immunol* **14**, 136-142 (2013).
  42. C. Gunther, E. Martini, N. Wittkopf, K. Amann, B. Weigmann, H. Neumann, M. J. Waldner, S. M. Hedrick, S. Tenzer, M. F. Neurath, C. Becker, Caspase-8 regulates TNF $\alpha$ -induced epithelial necroptosis and terminal ileitis. *Nature* **477**, 335-339 (2011).
  43. P. Nava, S. Koch, M. G. Laukoetter, W. Y. Lee, K. Kolegraff, C. T. Capaldo, N. Beeman, C. Addis, K. Gerner-Smidt, I. Neumaier, A. Skerra, L. Li, C. A. Parkos, A. Nusrat, Interferon-gamma regulates intestinal epithelial homeostasis through converging betacatenin signaling pathways. *Immunity* **32**, 392-402 (2010).
  44. J. M. Kim, J. P. Rasmussen, A. Y. Rudensky, Regulatory T cells prevent catastrophic autoimmunity throughout the lifespan of mice. *Nat Immunol* **8**, 191-197 (2007).
  45. C. L. Bennett, J. Christie, F. Ramsdell, M. E. Brunkow, P. J. Ferguson, L. Whitesell, T. E. Kelly, F. T. Saulsbury, P. F. Chance, H. D. Ochs, The immune dysregulation, polyendocrinopathy, enteropathy, X-linked syndrome (IPEX) is caused by mutations of FOXP3. *Nat Genet* **27**, 20-21 (2001).
  46. T. Chinen, P. Y. Volchkov, A. V. Chervonsky, A. Y. Rudensky, A critical role for regulatory T cell-mediated control of inflammation in the absence of commensal microbiota. *J Exp Med* **207**, 2323-2330 (2010).
  47. T. Sato, R. G. Vries, H. J. Snippert, M. van de Wetering, N. Barker, D. E. Stange, J. H. van Es, A. Abo, P. Kujala, P. J. Peters, H. Clevers, Single Lgr5 stem cells build cryptvillus structures in vitro without a mesenchymal niche. *Nature* **459**, 262-265 (2009).
  48. J. Schuijers, L. G. van der Flier, J. van Es, H. Clevers, Robust cre-mediated recombination in small intestinal stem cells utilizing the *olm4* locus. *Stem Cell Reports* **3**, 234-241 (2014).
  49. Y. Y. Fu, A. Egorova, C. Sobieski, J. Kuttiyara, M. Calafiore, S. Takashima, H. Clevers, A. M. Hanash, T Cell Recruitment to the Intestinal Stem Cell Compartment Drives Immune-Mediated Intestinal Damage after Allogeneic Transplantation. *Immunity* **51**, 90-103 e103 (2019).
  50. C. Abraham, P. S. Dulai, S. Vermeire, W. J. Sandborn, Lessons Learned From Trials Targeting Cytokine Pathways in Patients With Inflammatory Bowel Diseases. *Gastroenterology* **152**, 374-388 e374 (2017).
  51. R. R. Jenq, M. R. van den Brink, Allogeneic haematopoietic stem cell transplantation: individualized stem cell and immune therapy of cancer. *Nat Rev Cancer* **10**, 213-221 (2010).
  52. S. Spoerl, N. R. Mathew, M. Bscheider, A. Schmitt-Graeff, S. Chen, T. Mueller, M. Verbeek, J. Fischer, V. Otten, M. Schmickl, K. Maas-Bauer, J. Finke, C. Peschel, J. Duyster, H. Poeck, R. Zeiser, N. von Bubnoff, Activity of therapeutic JAK 1/2 blockade in graft-versus-host disease. *Blood* **123**, 3832-3842 (2014).
  53. S. Abedin, E. McKenna, S. Chhabra, M. Pasquini, N. N. Shah, J. Jerkins, A. Baim, L. Runaas, W. Longo, W. Drobyski, P. N. Hari, M. Hamadani, Efficacy, Toxicity, and Infectious Complications in Ruxolitinib-Treated Patients with Corticosteroid-Refractory Graft-versus-Host Disease after Hematopoietic Cell Transplantation. *Biol Blood Marrow Transplant*, (2019).
  54. N. von Bubnoff, G. Ihorst, O. Grishina, N. Rothling, H. Bertz, J. Duyster, J. Finke, R. Zeiser, Ruxolitinib in GvHD (RIG) study: a multicenter, randomized phase 2 trial to determine the response rate of Ruxolitinib and best available treatment (BAT) versus BAT in steroid-refractory acute graft-versus-host disease (aGvHD) (NCT02396628). *BMC Cancer* **18**, 1132 (2018).
  55. R. Zeiser, A. Burchert, C. Lengerke, M. Verbeek, K. Maas-Bauer, S. K. Metzelder, S. Spoerl, M. Ditschkowski, M. Ecsedi, K. Sockel, F. Ayuk, S. Ajib, F. S. de Fontbrune, I. K. Na, L. Penter, U. Holtick, D. Wolf, E. Schuler, E. Meyer, P. Apostolova, H. Bertz, R. Marks, M. Lubbert, R. Wasch, C. Scheid, F. Stolzel, R. Ordemann, G. Bug, G. Kobbe, R. Negrin, M. Brune, A. Spyridonidis, A. Schmitt-Graff, W. van der Velden, G. Huls, S. Mielke, G. U. Grigoleit, J. Kuball, R. Flynn, G. Ihorst, J. Du, B. R. Blazar, R. Arnold, N. Kroger, J. Passweg, J. Halter, G. Socie, D. Beelen, C. Peschel, A. Neubauer, J. Finke, J. Duyster, N. von Bubnoff, Ruxolitinib in corticosteroid-refractory graft-versus-host disease after allogeneic stem cell transplantation: a multicenter survey. *Leukemia* **29**, 2062-2068 (2015).
  56. X. Yin, H. F. Farin, J. H. van Es, H. Clevers, R. Langer, J. M. Karp, Niche-independent high-purity cultures of Lgr5+ intestinal stem cells and their progeny. *Nat Methods* **11**, 106-112 (2014).
  57. X. Ni, Q. Song, K. Cassidy, R. Deng, H. Jin, M. Zhang, H. Dong, S. Forman, P. J. Martin, Y. Z. Chen, J. Wang, D. Zeng, PD-L1 interacts with CD80 to regulate graft-versus-leukemia activity of donor CD8+ T cells. *J Clin Invest* **127**, 1960-1977 (2017).
  58. T. Teshima, R. Ordemann, P. Reddy, S. Gagin, C. Liu, K. R. Cooke, J. L. Ferrara, Acute graft-versus-host disease does not require alloantigen expression on host epithelium. *Nat Med* **8**, 575-581 (2002).
  59. M. Koyama, R. D. Kuns, S. D. Olver, N. C. Raffelt, Y. A. Wilson, A. L. Don, K. E. Lineburg, M. Cheong, R. J. Robb, K. A. Markey, A. Varelias, B. Malissen, G. J. Hammerling, A. D. Clouston, C. R. Engwerda, P. Bhat, K. P. MacDonald, G. R. Hill, Recipient nonhematopoietic antigen-presenting cells are sufficient to induce lethal acute graft-versus-host disease. *Nat Med* **18**, 135-142 (2011).
  60. J. Agudo, E. S. Park, S. A. Rose, E. Alibo, R. Sweeney, M. Dhainaut, K. S. Kobayashi, R. Sachidanandam, A. Baccarini, M. Merad, B. D. Brown, Quiescent Tissue Stem Cells Evade Immune Surveillance. *Immunity* **48**, 271-285 e275 (2018).
  61. M. Biton, A. L. Haber, N. Rogel, G. Burgin, S. Beyaz, A. Schnell, O. Ashenberg, C. W. Su, C. Smillie, K. Shekhar, Z.



- Chen, C. Wu, J. Ordovas-Montanes, D. Alvarez, R. H. Herbst, M. Zhang, I. Tirosh, D. Dionne, L. T. Nguyen, M. E. Xifaras, A. K. Shalek, U. H. von Andrian, D. B. Graham, O. Rozenblatt-Rosen, H. N. Shi, V. Kuchroo, O. H. Yilmaz, A. Regev, R. J. Xavier, T Helper Cell Cytokines Modulate Intestinal Stem Cell Renewal and Differentiation. *Cell* **175**, 1307-1320 e1322 (2018).
62. P. Nava, R. Kamekura, M. Quiros, O. Medina-Contreras, R. W. Hamilton, K. N. Kolegraff, S. Koch, A. Candelario, H. Romo-Parra, O. Laur, R. S. Hilgarth, T. L. Denning, C. A. Parkos, A. Nusrat, IFN $\gamma$ -induced suppression of beta-catenin signaling: evidence for roles of Akt and 14.3.3zeta. *Mol Biol Cell* **25**, 2894-2904 (2014).
  63. C. T. Capaldo, N. Beeman, R. S. Hilgarth, P. Nava, N. A. Louis, E. Naschberger, M. Sturzl, C. A. Parkos, A. Nusrat, IFN- $\gamma$  and TNF- $\alpha$ -induced GBP-1 inhibits epithelial cell proliferation through suppression of beta-catenin/TCF signaling. *Mucosal Immunol* **5**, 681-690 (2012).
  64. M. Shoshkes-Carmel, Y. J. Wang, K. J. Wangenstein, B. Toth, A. Kondo, E. E. Massasa, S. Itzkovitz, K. H. Kaestner, Subepithelial telocytes are an important source of Wnts that supports intestinal crypts. *Nature* **557**, 242-246 (2018).
  65. Z. Kabiri, G. Greicius, B. Madan, S. Biechele, Z. Zhong, H. Zaribafzadeh, Edison, J. Aliyev, Y. Wu, R. Bunte, B. O. Williams, J. Rossant, D. M. Virshup, Stroma provides an intestinal stem cell niche in the absence of epithelial Wnts. *Development* **141**, 2206-2215 (2014).
  66. U. Jadhav, M. Saxena, N. K. O'Neill, A. Saadatpour, G. C. Yuan, Z. Herbert, K. Murata, R. A. Shivdasani, Dynamic Reorganization of Chromatin Accessibility Signatures during Dedifferentiation of Secretory Precursors into Lgr5+ Intestinal Stem Cells. *Cell Stem Cell* **21**, 65-77 e65 (2017).
  67. P. W. Tetteh, O. Basak, H. F. Farin, K. Wiebrands, K. Kretzschmar, H. Begthel, M. van den Born, J. Korving, F. de Sauvage, J. H. van Es, A. van Oudenaarden, H. Clevers, Replacement of Lost Lgr5-Positive Stem Cells through Plasticity of Their Enterocyte-Lineage Daughters. *Cell Stem Cell* **18**, 203-213 (2016).
  68. S. J. Buczacki, H. I. Zecchini, A. M. Nicholson, R. Russell, L. Vermeulen, R. Kemp, D. J. Winton, Intestinal label-retaining cells are secretory precursors expressing Lgr5. *Nature* **495**, 65-69 (2013).
  69. J. H. van Es, T. Sato, M. van de Wetering, A. Lyubimova, A. N. Nee, A. Gregorieff, N. Sasaki, L. Zeinstra, M. van den Born, J. Korving, A. C. Martens, N. Barker, A. van Oudenaarden, H. Clevers, Dll1+ secretory progenitor cells revert to stem cells upon crypt damage. *Nat Cell Biol* **14**, 1099-1104 (2012).
  70. H. C. Chen, M. Kanai, A. Inoue-Yamauchi, H. C. Tu, Y. Huang, D. Ren, H. Kim, S. Takeda, D. E. Reyna, P. M. Chan, Y. T. Ganesan, C. P. Liao, E. Gavathiotis, J. J. Hsieh, E. H. Cheng, An interconnected hierarchical model of cell death regulation by the BCL-2 family. *Nat Cell Biol* **17**, 1270-1281 (2015).
  71. P. E. Czabotar, G. Lessene, A. Strasser, J. M. Adams, Control of apoptosis by the BCL-2 protein family: implications for physiology and therapy. *Nat Rev Mol Cell Biol* **15**, 49-63 (2014).
  72. L. C. Platanias, Mechanisms of type-I- and type-II-interferon-mediated signalling. *Nat Rev Immunol* **5**, 375-386 (2005).
  73. M. Kleppe, M. H. Spitzer, S. Li, C. E. Hill, L. Dong, E. Papalexi, S. De Groot, R. L. Bowman, M. Keller, P. Koppikar, F. T. Rapaport, J. Teruya-Feldstein, J. Gandara, C. E. Mason, G. P. Nolan, R. L. Levine, Jak1 Integrates Cytokine Sensing to Regulate Hematopoietic Stem Cell Function and Stress Hematopoiesis. *Cell Stem Cell* **21**, 489-501 e487 (2017).
  74. M. E. Rothenberg, Y. Nusse, T. Kalisky, J. J. Lee, P. Dalerba, F. Scheeren, N. Lobo, S. Kulkarni, S. Sim, D. Qian, P. A. Beachy, P. J. Pasricha, S. R. Quake, M. F. Clarke, Identification of a cKit(+) colonic crypt base secretory cell that supports Lgr5(+) stem cells in mice. *Gastroenterology* **142**, 1195-1205 e1196 (2012).
  75. N. F. Shroyer, M. A. Helmrath, V. Y. Wang, B. Antalffy, S. J. Henning, H. Y. Zoghbi, Intestine-specific ablation of mouse atonal homolog 1 (Math1) reveals a role in cellular homeostasis. *Gastroenterology* **132**, 2478-2488 (2007).
  76. O. Alpdogan, S. J. Muriglian, J. M. Eng, L. M. Willis, A. S. Greenberg, B. J. Kappel, M. R. van den Brink, IL-7 enhances peripheral T cell reconstitution after allogeneic hematopoietic stem cell transplantation. *J Clin Invest* **112**, 1095-1107 (2003).
  77. D. Yafilin, K. Xu, M. Turkekel, N. Fan, Y. Romin, S. Fijisawa, A. Barlas, K. Manova-Todorova, Machine-based method for multiplex in situ molecular characterization of tissues by immunofluorescence detection. *Sci Rep* **5**, 9534 (2015).
  78. Y. Y. Fu, C. W. Lin, G. Enikolopov, E. Sibley, A. S. Chiang, S. C. Tang, Microtome-free 3-dimensional confocal imaging method for visualization of mouse intestine with subcellular-level resolution. *Gastroenterology* **137**, 453-465 (2009).
  79. Y. Y. Fu, S. J. Peng, H. Y. Lin, P. J. Pasricha, S. C. Tang, 3-D imaging and illustration of mouse intestinal neurovascular complex. *Am J Physiol Gastrointest Liver Physiol* **304**, G1-11 (2013).
  80. A. Merlos-Suarez, F. M. Barriga, P. Jung, M. Iglesias, M. V. Cespedes, D. Rossell, M. Sevillano, X. Hernandez-Momblona, V. da Silva-Diz, P. Munoz, H. Clevers, E. Sancho, R. Mangues, E. Battle, The intestinal stem cell signature identifies colorectal cancer stem cells and predicts disease relapse. *Cell Stem Cell* **8**, 511-524 (2011).
  81. K. R. Cooke, L. Kobzik, T. R. Martin, J. Brewer, J. Delmonte, Jr., J. M. Crawford, J. L. Ferrara, An experimental model of idiopathic pneumonia syndrome after bone marrow transplantation: I. The roles of minor H antigens and endotoxin. *Blood* **88**, 3230-3239 (1996).
  82. M. Schewe, P. F. Franken, A. Sacchetti, M. Schmitt, R. Joosten, R. Bottcher, M. E. van Royen, L. Jeammot, C. Payre, P. M. Scott, N. R. Webb, M. Gelb, R. T. Cormier, G. Lambeau, R. Fodde, Secreted Phospholipases A2 Are Intestinal



- Stem Cell Niche Factors with Distinct Roles in Homeostasis, Inflammation, and Cancer. *Cell Stem Cell* **19**, 38-51 (2016).
83. A. Dobin, C. A. Davis, F. Schlesinger, J. Drenkow, C. Zaleski, S. Jha, P. Batut, M. Chaisson, T. R. Gingeras, STAR: ultrafast universal RNA-seq aligner. *Bioinformatics* **29**, 15-21 (2013).
  84. P. G. Engstrom, T. Steijger, B. Sipos, G. R. Grant, A. Kahles, G. Ratsch, N. Goldman, T. J. Hubbard, J. Harrow, R. Guigo, P. Bertone, R. Consortium, Systematic evaluation of spliced alignment programs for RNA-seq data. *Nat Methods* **10**, 1185-1191 (2013).



## Supplementary Materials

### Material and Methods

**Mice.** C57BL/6 (B6, H-2b), LP (H-2b), B10.Br (H-2k), B6D2F1 (BDF1, H-2b/d), C57BL/6-Tg (UBC-GFP)30Scha/J (B6-GFP), B6.129S7-*lfng*r1tm1Agt/J (*lfng*r<sup>-/-</sup>), C57BL/6-Prfltm1Sdz/J (*Prfl*<sup>-/-</sup>), B6.129S-Tnfrsf1atm1lmx Tnfrsf1btm1lmx/J (*Tnfr*<sup>-/-</sup>), and B6.129S7-*lfng*tm1Ts/J (*lfng*<sup>-/-</sup>) mice were purchased from Jackson Laboratories. 129S6/SvEv-Stat1tm1Rds (*Stat1*<sup>-/-</sup>) and 129S6/SvEvTac were purchased from Taconic. *Lgr5-lacZ* B6 (Lgr5-LacZ), B6 *lgr5-gfp-ires-CreERT2* (Lgr5-GFP) and *olfm4-gfp-ires-CreERT2* (Olfm4-CreERT2) mice were provided by Hans Clevers. BALB/c *Il22*<sup>-/-</sup> mice were provided by Genetech. *lfng*r<sup>-/-</sup>-Lgr5-GFP mice were created by mating *lfng*r<sup>-/-</sup> mice with Lgr5-GFP mice. Lgr5-LacZ BDF1 mice were created by mating female Lgr5-LacZ mice with male DBA/2 mice (Jackson Laboratories). *Rosa-cre-ert2-Jak1fl/fl* mice were created by mating *Jak1fl/fl* mice<sup>73</sup> with male *rosa-cre-ert2* mice (Jackson Laboratories). *Bak*<sup>-/-</sup> *Rosa-cre-ert2-Baxfl/fl* mice were created as described before<sup>70</sup>. *lfng*rΔIEC mice were created by mating *lfng*r<sup>fl/fl</sup> mice (C57BL/6N-*lfng*r1tm1.1Rds/J, Jackson Laboratories) with Villin-Cre mice (B6.Cg-Tg(Vil1-cre)997Gum/J, Jackson Laboratories). Lineage tracing mice for Olfm4 were created by mating B6.129S4-Gt(ROSA)26Sortm1Sor/J (R26R, Jackson Laboratories) mice with Olfm4-CreERT2 mice. All animal experiments were performed in accordance with the institutional protocol guideline of the Memorial Sloan Kettering Cancer Center (MSKCC) Institutional Animal Care and Use Committee. Mice were housed in microisolator cages, five per cage, in MSKCC pathogen-free facilities, and received standard chow and autoclaved sterile drinking water. To adjust for differences in weight and intestinal flora among other factors, identical mice were purchased from Jackson and then randomly distributed over different cages and groups by a non-biased technician who had no insight or information about the purpose or details of the experiment. The investigations assessing clinical outcome parameters were performed by non-biased technicians with no particular knowledge or information regarding the hypotheses of the experiments and no knowledge of the specifics of the individual groups.

**Crypt isolation and cell dissociation.** Isolation of intestinal crypts and the dissociation of cells for flow cytometry analysis were largely performed as previously described<sup>18</sup>. In brief, after euthanizing the mice with CO<sub>2</sub> and collecting small and/or large intestines, the organs were opened longitudinally and washed with PBS. To dissociate the crypts, small intestine was incubated at 4 °C in EDTA (10 mM) for 20 min. Large intestine was incubated in collagenase D (Sigma) for 30 min at 37 °C to isolate the crypts. To isolate single cells from small and large intestine crypts, the pellet was further incubated in 1× TrypLE express (Gibco, Life Technologies) supplemented with 2 kU/ml DNaseI (Roche).

**Organoid and ISC colony culture.** For mouse organoids, depending on the experiments, 100–200 crypts or 2000–3000 dissociated single organoid cells per well were suspended

in growthfactor- reduced Matrigel (Corning) mixed with DMEM/F12 medium (Gibco). After Matrigel polymerization, complete ENR medium containing advanced DMEM/F12 (Sigma), 2 mM Glutamax (Invitrogen), 10 mM HEPES (Sigma), 100 U/ml penicillin, 100 µg/ml streptomycin (Sigma), B27 supplement (Invitrogen), N2 supplement (Invitrogen), 50 ng/ml mouse EGF (Peprotech), 100 ng/ml mouse Noggin (Peprotech) and 10% human R-spondin-1-conditioned medium from R-spondin-1-transfected HEK 293T cells was added to small intestine crypt cultures. For mouse large intestine, crypts were cultured in 'WENR' medium containing 50% WNT3a-conditioned medium, and supplemented with SB202190 (10 µM, Sigma), ALK5 inhibitor A83-01 (500 nM, Tocris Bioscience) and nicotinamide (10 mM, Sigma). Media was replaced every 2–3 days. Along with medium changes, treatment wells received different concentrations of rmlFNy (R&D systems) and/or ruxolitinib (Selleckchem). ISC were isolated from Lgr5–GFP mice as above followed by several strainer steps and a 5-min incubation with TrypLE and 2 kU/ml DNase1 under minute-to-minute tapping to make a single-cell suspension. The Lgr5–GFP high cells were isolated by flow cytometry. Approximately 2,000-3,000 ISC were plated in 20 µl Matrigel and cultured in WENR media containing Rho-kinase/ROCK inhibitor Y-27632 (10 µM, Tocris Bioscience) and Jagged1 (1 µM, Anaspec). Starting from day 4, ISC were cultured without Wnt.

ISC colonies were cultured from sort-purified single Lgr5-GFP+ cells or from ISCs sort-purified based on cell surface phenotype<sup>74</sup> as per the method reported by Yin et al<sup>56</sup>. Approximately 3,000 ISCs were plated in 30 µl Matrigel and cultured in ENR-VC media with Valproic Acid (V, 1.5 mM, Sigma) and CHIR99021 (C, 3 µM Stemgent), containing Rhokinase/ROCK inhibitor Y-27632 (10 µM) and Jagged1 (1 µM) only for the first 48h. Under these culture conditions ISCs divide symmetrically without differentiating, growing into homogeneous stem cell colonies. ISC colonies were passaged once per week as single cells following a 3-min incubation with TrypLE containing 2 kU/ml DNase1, N-acetylcysteine, and Y-27632. Along with medium changes, treatment wells received different concentrations of rmlFNy and/or QVD-Oph (Millipore Sigma). To confirm ISC colony death, ISC colonies were stained with Hoechst 33342 (1 µg/ml, Sigma) and propidium iodine (1.5 µM, Life Technologies) one hour before taking images.

For co-culture of intestinal organoids with T cells, CD5+, CD4+, or CD8+ cells were isolated from splenocytes using magnetic Microbeads with the MACS system (Miltenyi Biotec) according to the manufacturer's instructions. Methods to generate DCs were previously described<sup>25</sup>. T cell purity was determined by flow cytometry, and was routinely approximately 90%. T cells were cultured at a concentration of  $1 \times 10^5$  T cells per well with  $1 \times 10^4$  irradiated DCs per well, or with 5 µg/ml plate-bound anti-CD3 monoclonal antibodies (mAbs) and 2 µg/ml anti-CD28 mAbs. After 3-5 days of culture, harvested T cells and passaged single cells were cultured in Matrigel with a 0.5-50:1 T cell: single cell ratio.



For Jak1-deficient organoid culture, intestinal crypts isolated from *Rosa-cre-ert2-Jak1fl/fl* mice were cultured with 4-OHT (1  $\mu$ M, Sigma) for 6 days to induce the deletion of JAK1. Organoids from these mice were dissociated as single cells and then incubated with rmlFNy or co-cultured with T cells. For Paneth-cell-deficient organoid cultures, frozen crypts from *Atoh1 $\Delta$ IEC* mice<sup>75</sup> depleted of Paneth cells were used to culture organoids. As previously described, *Atoh1 $\Delta$ IEC* mice (and littermate controls) were given an intraperitoneal injection of tamoxifen (1 mg per mouse, Sigma, dissolved in corn oil) for 5 consecutive days to achieve deletion of ATOH1 from intestinal epithelium. Animals were euthanized on day 7 after the first injection, and intestinal crypts were isolated and frozen in 10% dimethylsulfoxide (DMSO) and 90% FBS.

For Bak/Bax double knockout ISC colony culture, *Bak-1-Rosa-cre-ert2-Baxfl/fl* mice were treated with 4-OHT (50 mg/kg) every other day for a total of 5 doses. Single CD44<sup>high</sup>kit- cells were sorted from 4-OHT treated mice, and ISC colony culture was performed as described above.

Human healthy duodenal organoids were cultured from banked frozen organoids (> passage 7) that had been previously generated from biopsies obtained during duodenoscopy of healthy human controls. All healthy controls had been investigated for celiac disease, but turned out to have normal pathology. They had previously provided written informed consent to participate in this study according to a protocol reviewed and approved by the review board of the UMC Utrecht, the Netherlands (protocol STEM study, METC 10-402/K). Organoids were passaged via mechanical disruption or single cell dissociation using 1 $\times$  TrypLE express (Gibco, Life Technologies) or 0,25% Trypsin-EDTA (Sigma-Aldrich) and FBS (Biowest) in medium without growth factors (GF-) comprised of Advanced DMEM/F12 (GIBCO), 100 U/ml penicillinstreptomycin (GIBCO), 10 mM HEPES (GIBCO) and Glutamax (GIBCO). Single cells or disrupted organoids were resuspended in GF- containing 50-66% Matrigel (BD Biosciences) and plated on pre-warmed 24-, 48- or 96- well cell culture plates (Costar). After Matrigel polymerisation, organoid culture medium (hSI EM) was added consisting of GF- medium, Wnt conditioned medium (50% final concentration) R-spondin-conditioned medium (20% final concentration) and Noggin conditioned medium (10% final concentration), 50ng/ml murine EGF (Peprotech), 10mM nicotinamide (SIGMA), 1,25mM N-acetyl (Sigma), B27 (Gibco), 500nM TGF- $\beta$  inhibitor A83-01 (Tocris), 10uM P38 inhibitor SB202190 (Sigma), and 100ug/ml Primocin (optional) (Invitrogen). For single cells, 10 $\mu$ M ROCK inhibitor Y-27632 (Abcam) was added for the first 2-3 days of the culture. Medium was refreshed every 2-3 days. Along with medium changes, treatment wells received different concentrations of rhIFNy (R&D systems) and/or ruxolitinib (Jakavi, Novartis).

For human co-cultures: 1000-2000 single cells from with Trypsin or TrypLE dissociated organoids were cultured with activated human T cells in a ratio of 1:5 and 1:50 where

applicable. Single cells were added to T cells and plated together in 50% Matrigel on pre-warmed 24- or 48-wells cell culture plates. Media containing human Interleukin-2 (Proleukin; 12 IE/ml, Prometheus) and ROCK inhibitor Y-27632 was added to the co-cultures after Matrigel polymerization for the first 2-3 days of culture.

T cells were isolated from human blood which was collected from healthy donors in the UMC Utrecht as approved by the UMC Utrecht's Ethics Committee under protocol number 07/125. After Ficoll gradient separation, T cells were isolated from the peripheral blood mononuclear cells (PBMCs), using MACS kits with magnetic beads, BD IMag™ Cell Separation Magnet (BD Biosciences), and MACS buffer consisting of PBS supplemented with 2% heat-inactivated FBS and 2% 0,1M EDTA. CD8+ T cells were isolated from PBMCs using column-based CD8+ T cell isolation kits (Miltenyi) or CD8+ Dynabead isolation kits (ThermoFisher). CD4+ T cells were isolated from the PBMC fraction depleted of CD8+ T cells using the MagniSort human CD4 T cell enrichment kit (Thermo Fisher). Isolated T cells rested overnight in RPMI 1640 media with 1% GlutaMAX (GIBCO) supplemented with 100 U/ml penicillin-streptomycin (GIBCO) and 10% heat-inactivated FBS. Resting T cells were cultured in the presence of Proleukin (12 IE/ml). Rested T cells were activated with anti-CD3 and anti-CD28 antibody stimulation for four days at a concentration of 1 million cells per well. For this purpose, 24-well plates were coated with 0.8ug/ml anti-CD3 (BioLegend) overnight at 4 °C or two hours at 37 °C. After plate washing, harvested T cells were concentrated and 0.8ug/ml anti-CD28 (BioLegend) was added.

After seven days of mouse and human co-cultures, total organoid numbers per well were counted by light microscopy to evaluate growth efficiency. Neutralizing antibodies against cytokines and T cell effector molecules were purchased from eBioscience, and experiments were performed according to the manufacturer's instruction. See table S1 for full description of antibodies used. R-spondin-1-transfected HEK293T cells were provided by C. Kuo. WNT3a- transfected and Noggin-transfected HEK293T cells were provided by H. Clevers. Cell lines were tested for mycoplasma and confirmed to be negative.

**Imaging of organoids and colonies.** Random representative non-overlapping images of organoids and colonies were acquired from each well using a Zeiss Axio Observer Z1 inverted microscope or LSM880 (Carl Zeiss) using 20x/0.8NA objective. For size evaluation, the images were analyzed using ImageJ software.

**BMT.** BMT procedures were performed as previously described<sup>76</sup>. A minor or major histocompatibility antigen-mismatched BMT model (LP into B6, H-2b into H-2b; B6 into BDF1, H-2b into H-2b/d; B10.Br into B6, H-2k into H-2b) or syngeneic BMT model (B6-into-B6) was used. Female mice were typically used as recipients for transplantation at an age of 8–10 weeks. Recipient mice received 1100 (for B6 and LP) or 1300 cGy (for BDF1) in 2



doses split at 3-4 h intervals to reduce gastrointestinal toxicity. To obtain bone marrow cells from euthanized donor mice, the femurs and tibiae were collected aseptically and the bone marrow canals washed out with sterile media. Bone marrow cells were depleted of T cells by incubation with anti-Thy 1.2 and low-TOX-M rabbit complement (Cedarlane Laboratories). The TCD bone marrow was analyzed for purity by quantification of the remaining T cell contamination using flow cytometry. T cell contamination was usually about 0.2% of all leukocytes after a single round of complement depletion. Donor T cells were prepared as above. Recipients typically received  $5 \times 10^6$  TCD bone marrow cells with or without  $1-4 \times 10^6$  T cells per mouse via tail vein injection.

Rat anti-mouse IFN $\gamma$  (XMG1.2) and isotype control (HRPN) antibodies were purchased from BioXCell and reconstituted to a concentration of 2.5 mg/ml in PBS. Mice were treated every three days starting day 0 of BMT via i.p. injection with either 200  $\mu$ l PBS containing 500  $\mu$ g anti-mouse IFN $\gamma$  mAb or isotype.

Ruxolitinib dissolved in 2% dimethyl sulfoxide (DMSO), 30% PEG300, and water according to the manufacturer's instructions was administered by oral gavage at a daily dose of 30 mg/kg twice daily starting from day -1 after BMT. The control group received PEG/DMSO alone. For lineage tracing experiments, tamoxifen dissolved in sunflower oil was administered via i.p. injection, with two 4 mg doses administered per mouse on the day of BMT.

**Diphtheria toxin treatment.** *Foxp3DTR* mice were kindly provided by A. Rudensky<sup>44</sup>. Diphtheria toxin (DT) was purchased from Sigma-Aldrich and reconstituted in PBS. Mice were treated via i.p. injection with 0.5  $\mu$ g DT for five consecutive days. Five days after the last injection, mice were euthanized and organs were harvested for analysis.

**LacZ staining.** For evaluation of stem cell numbers, small intestines were collected from Lgr5-LacZ recipient mice or non-transplanted controls.  $\beta$ -galactosidase (LacZ) staining was performed as previously described<sup>2</sup>. Washed 2.5-cm-sized small intestine fragments were incubated with an ice-cold fixative, consisting of 1% formaldehyde, 0.02% Igepal and 0.2% glutaraldehyde. After removing the fixative, organs were stained for the presence of LacZ according to manufacturer's protocol (LacZ staining kit, Invivogen). The organs were then formalin-preserved, paraffin-embedded, sectioned, and counterstained with Nuclear Fast Red (Vector Labs).

**Immunohistochemical staining.** Immunohistochemistry detection of lysozyme was performed at the Molecular Cytology Core Facility of MSKCC using a Discovery XT processor (Ventana Medical Systems). Formalin-fixed tissue sections were deparaffinized with EZPrep buffer (Ventana Medical Systems), antigen retrieval was performed with CC1 buffer (Ventana Medical Systems) and sections were blocked for 30 min with Background Buster solution

(Innovex). Slides were incubated with anti-lysozyme (DAKO, 2 µg/ml), anti-Ki67 (Abcam, 1 µg/ml), anti-Olfm4 (Cell Signaling, 1 µg/ml), anti-Cleaved-Caspase-3 (Cell Signaling, 0.1 µg/ml) antibodies or isotype (4 µg/ml) for 6 h, followed by a 60-min incubation with biotinylated goat anti-rabbit IgG (Vector Laboratories) at 1:200 dilution. The detection was performed with a DAB detection kit (Ventana Medical Systems) according to the manufacturer's instructions. Slides were counterstained with haematoxylin (Ventana Medical Systems), and coverslips were added with Permount (Fisher Scientific). See table S1 for full description of antibodies used.

**Immunofluorescent staining.** For immunofluorescent staining, the slides were prepared as for IHC. After blocking with Background Buster solution (Innovex), the sections were followed by avidin-biotin blocking for 8 minutes (Ventana Medical Systems) Multiplex immunofluorescent stainings were performed as previously described<sup>77</sup>. First, sections were incubated with anti-β-gal (eBioscience, 1 µg/ml) for 5 hours, followed by 60 minutes incubation with biotinylated goat anti-rabbit IgG (Vector labs) at 1:200 dilution. The detection was performed with Streptavidin-HRP D (part of DABMap kit, Ventana Medical Systems), followed by incubation with Tyramide Alexa 488 (Invitrogen, B40953) prepared according to manufacturer instruction with predetermined dilutions. Second, sections were incubated with anti-Cleaved-Caspase-3 (Cell Signaling, 0.1 µg/ml) for 5 hours, followed by 60 minutes incubation with biotinylated goat anti-rabbit IgG (Vector labs) at 1:200 dilution. The detection was performed with Streptavidin-HRP D (part of DABMap kit, Ventana Medical Systems), followed by incubation with CF594 (Biotium, 92174) prepared according to manufacturer instruction with predetermined dilutions. After staining slides were counterstained with DAPI (Sigma Aldrich, 5 µg/ml) for 10 min and coverslipped with Mowiol.

**3-D immunostaining and imaging.** Immunofluorescent staining was performed as previously described<sup>78,79</sup>. Mouse small intestines were fixed by paraformaldehyde (4%) perfusion. The fixed tissues were immersed in 2% Triton-X 100 solution for permeabilization. Before the staining steps, tissues were blocked with the blocking solution. Small intestines were then incubated with CD3 primary antibody (R&D systems) at 1:100 dilution. An Alexa Fluor 647 conjugated goat-anti-rat secondary antibody (Invitrogen) at 1:250 dilution was then used to reveal the immunopositive structure. Afterward, tissues were incubated with DiD (4-chlorobenzene sulfonate salt; 2 µg/ml; Invitrogen) to label cellular membrane and DAPI (20 µg/ml, Invitrogen) to label the nuclei. Finally, the labeled specimens were immersed in the FocusClear solution (CelExplorer, Hsinchu, Taiwan) for optical clearing before being imaged via confocal microscopy (Zeiss LSM 880). Amira 6.0.1 image reconstruction software (FEI) was used for 3-D processing and projection of the confocal images.

**Whole mount staining of cleaved-Caspase-3.** Matrigel-embedded intestinal organoids, plated in 8-well chambered coverglass (Lab-Tek, #155411), were stained according to the



reported method with slight modifications<sup>80</sup>. Briefly, Matrigel-embedded organoids were washed twice with PBS for 5 min and then were fixed in 4% Paraformaldehyde (PFA) for 30 min at room temperature (RT). After washing with PBS 3 times for 5 min, organoids were permeabilized with PBS/0.1% TritonX100 (PBST) for 30 min at RT. Blocking was achieved by incubation with PBST/2%BSA/10%goat for 1h at RT. Staining with primary antibody anti-cleaved-caspase-3 (Cell Signaling) was done over-night at 4°C in PBS/2%BSA. After 5 washes with PBST for 5 min each, samples were incubated with secondary antibody for 1 hr at RT (Goat-anti-rabbit Alexa 594). Samples were washed twice with PBST and twice with PBS for 5 min each, stained with DAPI to visualize nuclei and mounted with VectaShield (Vector Laboratories, Burlingame,CA, USA) prior to analyses using inverted confocal microscope Zeiss-LSM880.

Images were analyzed using ImageJ/FIJI software in which colonies were segmented using DAPI channel. Lumen region was defined as enclosed area 15 µm away from the edge of the organoid. Area and morphology of lumen region were measured, as well as the total intensity of cleaved caspase-3 signal. The edge of the organoid was defined as within 15 µm from the outer edge. Area of the edge region as well as total intensity of cleaved caspase-3 in the region were measured. Total intensity of cleaved caspase-3 was normalized to the area of the region analyzed to calculate normalized density of cleaved caspase-3.

**GVHD histopathology analysis.** Mice were sacrificed for histopathological analysis 7 or 10 days after BMT using CO<sub>2</sub> asphyxiation. The small intestines were formalin-preserved, paraffinembedded, sectioned, and stained with haematoxylin and eosin. An expert in the field of GVHD histopathology performed blinded assessment of the sections for histologic evidence of GVHD pathology. A semiquantitative score consisting of 19 different parameters associated with GVHD was calculated<sup>81</sup>.

**Flow cytometry.** DAPI, APC conjugated anti-annexin V, and annexin V buffer (BD Phamingen) were used for annexin V staining. Paneth cells were identified based on bright CD24 staining and side scatter granularity in combination with CD44 and c-kit expression<sup>4,74,82</sup> (fig. S2A). For flow cytometry of small intestine organoid cells, organoids were dissociated using TrypLE (37°C). After vigorously pipetting through a p200 pipette causing mechanical disruption, the crypt suspension was washed with 10 ml of DMEM/F12 medium containing 10% FBS and 2 kU/ml DNase1 and passaged through a 40 µm cell strainer. All staining with live cells was performed in DMEM/F12 medium with 2% FBS.

Flow cytometry analyses were performed with an LSRII cytometer (BD Biosciences) using FACSDiva (BD Biosciences), and the data were analyzed with FlowJo software (Treestar).

**ELISA.** For measuring IFN $\gamma$  (BD Bioscience) levels, we performed ELISA according to the



manufacturer's instructions with sensitivities of 31.25 pg/ml.

**Caspase-Glo assay.** Disrupted human organoids were cultured in 96-well cell culture plates. After 2-3 days, organoids were treated with 0–20 ng/ml rhIFN $\gamma$  for 24 hours. After 24 hours, the Matrigel was dissolved with GF- and equilibrated to room temperature. Caspase-Glo 3/7 Reagents (Promega) were mixed and equilibrated to room temperature. Reagent was added to the organoids in a 1:1 ratio to GF- up to a total volume of 200ul. The reagents were mixed for 1 hour using a plate shaker, and luminescence was measured with a TriStar2 Multimode plate reader LB942 (Berthold Technologies).

**Western blotting.** Western blot analysis was carried out on total protein extracts. Free-floating crypts isolated from small intestine were treated in DMEM supplemented with Y-27632 (10 ng/ml, Tocris), IFN $\gamma$  (1 ng/ml, 30 min), and ruxolitinib (10 $\mu$ m, 30min). Vehicle (PBS) was added to control wells. Crypts were then lysed in RIPA buffer containing a cocktail of protease and phosphatase inhibitors (Sigma). After sonication, protein amounts were determined using the bicinchoninic acid assay Kit (Pierce). Loading 30  $\mu$ g per lane of lysate, proteins were separated using electrophoresis in a 10% polyacrylamide gel and transferred to nitrocellulose. Membranes were blocked for 1 h at room temperature with 1% Blot-Qualified BSA (Promega, W384A) and 1% non-fat milk (LabScientific, M0841) and then incubated overnight at 4 °C with the following primary antibodies: rabbit anti-phospho-STAT1 (7649P), rabbit anti-STAT1 (9172P) and rabbit from Cell Signaling. This was followed by incubation with the secondary antibody anti-rabbit HRP (7074P2) and visualization with the Pierce ECL Western Blotting Substrate (Thermo Scientific, 32106).

For human cultures, disrupted organoids were grown in a 24-well cell culture plate and harvested in cold GF- medium. After washing, organoids were resuspended in Laemmli buffer (10% SDS, 87% glycerol, 1M Tris pH 6.8, H<sub>2</sub>O). Samples were heated 5 minutes at 100°C. Total protein concentration was quantified using Pierce BCA (bicinchoninic acid) Protein Assay Kit (ThermoFisher) according to manufacturer's protocol. 20 ug protein samples were run in 12% or 15% acrylamide SDS PAGE gels (H<sub>2</sub>O, Acrylamide 30%, 1,5M Tris (pH 8,8) for running gel, 1M Tris (pH 6,8) for stacking gel, SDS 10%, APS 10%, TEMED) of 1,5mm with 10 or 15 slots for 90 minutes at 130V (constant Voltage). Proteins were transferred to PVDF membranes using Trans-Blot®Turbo Transfer System (Bio-Rad) according to protocol. Blocking was done with 5% ELK in TBST (Tris Buffered Saline Tween) (5M NaCl, 1M Tris pH 8, Tween 20, aqua dest.) overnight at 4°C or for one hour at room temperature. After blocking, the membrane was washed three times with TBST and rocked overnight at 4°C or for one hour at room temperature in a primary antibody solution containing Anti-active-caspase-3 antibody (Ab32042, Abcam) and  $\beta$ -Actin antibody (sc-47778, Santa Cruz) in 0.5% ELK in TBST. After primary antibody binding, the membrane was washed once with TBST and incubated with 1:10000 secondary antibody solution (IRDye® 800CW Donkey anti-



Mouse IgG, IRDye® 680RD Donkey anti-Rabbit IgG, LI-COR) in 0,5% ELK in TBST in a light protected tube for one hour at RT. The membrane was washed three times with TBST and once with PBS before visualising the bands through measuring fluorescence with Odyssey Imaging System technology (LI-COR). Images were processed using Adobe Photoshop CS6 Extended.

**RT-qPCR.** For qPCR, RNA was isolated from organoids after *ex vivo* culture or crypts isolated from BMT recipients. Extracted RNA was also stored at  $-80^{\circ}\text{C}$ . Reverse transcriptase PCR (RT-PCR) was performed with a QuantiTect Reverse Transcription Kit (QIAGEN) or a High-Capacity RNA-to-cDNA Kit (Applied Biosystems) for mouse, and iScript cDNA Synthesis Kit (BioRad) for human samples. qPCR was performed on a Step-One Plus or QuantStudio 7 Flex System (Applied Biosystems) using TaqMan Universal PCR Master Mix (Applied Biosystems). For mouse genes, specific primers were obtained from Applied Biosystems: *Gapdh*: Mm99999915\_g1; *Olfm4*: Mm01320260\_m1; *Axin2*: Mm00443610\_m1; *Lyz1*: Mm00657323\_m1; *Defa1*: Mm02524428\_g1; *Alpi*: Mm01285814\_g1; *Muc2*: Mm01276696\_m1; *Chga*: Mm00514341\_m1; *Trpm5*: Mm01129032\_m1; *Bcl2*: Mm00477631\_m1; and *Bak*: Mm00432045\_m1; *Bcl2l1*: Mm00437783\_m1; *Mcl1*: Mm01257351\_g1. Other primers were obtained from PrimerBank: *Gapdh* (ID 6679937a1), *Hes1* (ID 6680205a1), *Bax* (ID 6680770a1), *Ccnd1* (ID 6680868a1). For human genes, specific primers were obtained from integrated Dna Technologies after primer-design with the NCBI nucleotide and primer blast databases and having checked them for effectiveness: *LGR5*: Fw GAATCCCCTGCCAGTCTC and rv TCTTAAACGCTTCGGAAGTTA, *HPLBP3*: Fw CCCACGTCCAAGATGGAT and rv AAGGTCTTCTACCACGTAGTC, *BCL2*: Fw CCGCGACTCCTGATTCATT and rv AGTCTACTTCTCTGTGATGTTGT, *BAK1*: Fw CATCAACCGACGCTATGACTC and rv GTCAGGCCATGCTGGTAGAC, *BCL2L1* (specific sequences for *BCL-XL*): Fw ACCTAGAGCCTTGGATCCAGGA and rv GTGGATGGTCAGTGTCTGGTCA.

cDNAs were amplified for mouse primers with TaqMan or SYBR master mix (Applied Biosystems) in QuantStudio 7 Flex System (Applied Biosystems) and for human samples with a SYBR master mix (BioRad) in a CFX96™ Real-Time PCR Detection System (BioRad). Relative amounts of mRNA were calculated by the comparative  $\Delta\text{Ct}$  method with *Gapdh* as housekeeping gene for mouse samples and with *HPIBP3* for human samples.

**RNAseq.** Lgr5-GFP high cells sorted from Lgr5-GFP mice were incubated with IFN $\gamma$  in ENR for 1.5 hours. RNA was extracted using Trizol reagent followed manufacture protocol (Invitrogen). After RNA extraction, the quantity and quality of RNA was accessed by Agilent BioAnalyzer Pico chip, 2ng of total RNA underwent cDNA pre-Amplification using Clontech SMART-Seq v4 Ultra Low Input RNA Kit followed manufacture instruction with 12 cycles of PCR. Library preparation was followed by using KAPA Hyper prep kit according to instruction provided by KAPA Biosystems, cDNA input was normalized to 10 ng per sample

as library input, with 8 cycles of PCR. Samples were barcoded and run on a HiSeq 2500 in a Paired End 50 bp run, using the TruSeq SBS Kit v4 (Illumina). An average of 52.1 million reads was generated per sample. At the most the ribosomal reads represented 0.01% and the percent of mRNA bases was 66.1% on average.

The output data (FASTQ files) were mapped to the target genome using the rnaStar aligner<sup>83</sup> that maps reads genomically and resolves reads across splice junctions. We used the 2 pass mapping method outlined in<sup>84</sup> in which the reads were mapped twice. The first mapping pass used a list of known annotated junctions from Ensemble. Novel junctions found in the first pass were then added to the known junctions and a second mapping pass was done (on the second pass the RemoveNoncanonical flag is used). After mapping we posted process the output SAM files using the PICARD tools to: add read groups, AddOrReplaceReadGroups which in additional sorts the file and converts it to the compressed BAM format.

We then computed the expression count matrix from the mapped reads using HTSeq ([www.huber.embl.de/users/anders/HTSeq](http://www.huber.embl.de/users/anders/HTSeq)) and one of several possible gene model databases. The raw count matrix generated by HTSeq was then processed using the R/Bioconductor package DESeq ([www-huber.embl.de/users/anders/DESeq](http://www-huber.embl.de/users/anders/DESeq)), which is used to both normalize the full dataset and analyze differential expression between sample groups. A heatmap was generated using the heatmap.2 function from the gplots R package. The data plot was the mean centered normalized log<sub>2</sub> expression of the top 100 significant genes. For simple hierarchical clustering the correlation metric was used ( $D_{ij} = 1 - \text{cor}(X_i, X_j)$ ) with the Pearson correlation on the normalized log<sub>2</sub> expression values.

**Quantification and Statistical Analyses.** No statistical methods were used to predetermine sample size. To detect an effect size of >50% difference in means, with an assumed coefficient of variation of 30%, common in biological systems, we attempted to have at least five samples per group, particularly for *in vivo* studies. All experiments were repeated at least once, unless otherwise stated. No mice were excluded from experiments.

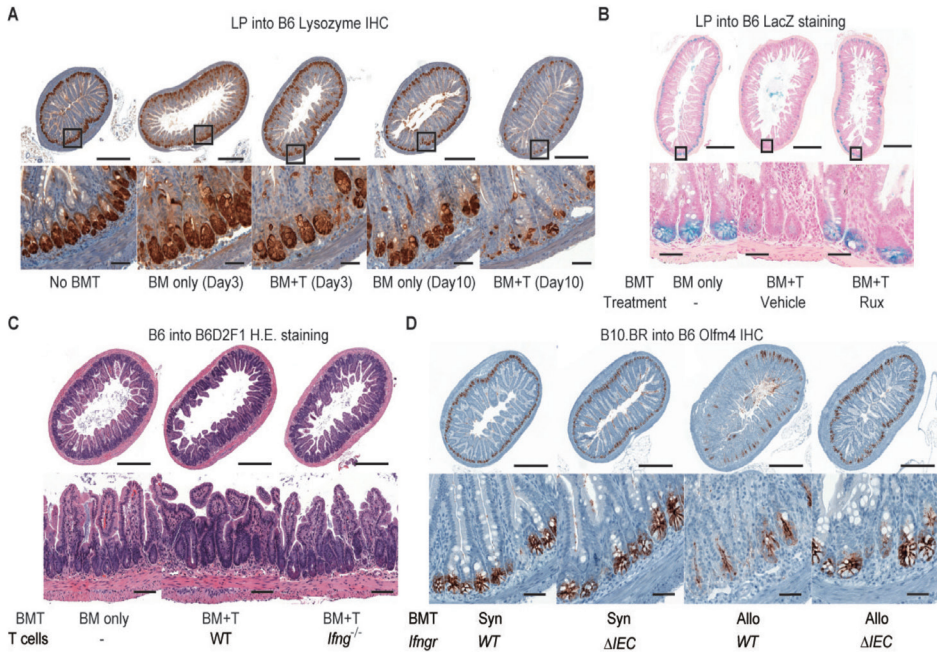
Graphs indicate the mean and standard error of the mean (S.E.M.) for the various groups. Statistics are based on 'n' biological replicates. All statistical tests performed were two-sided. For the comparisons of two groups, a t-test or non-parametric test was performed. RT-qPCR reactions and ordinal outcome variables were tested non-parametrically. All analyses of statistical significance were calculated and displayed compared with the reference control group unless otherwise stated.

Statistical analyses of organoid numbers were based on individual wells. To take into account intra-individual and intra-experimental variation as well, all *ex vivo* experiments

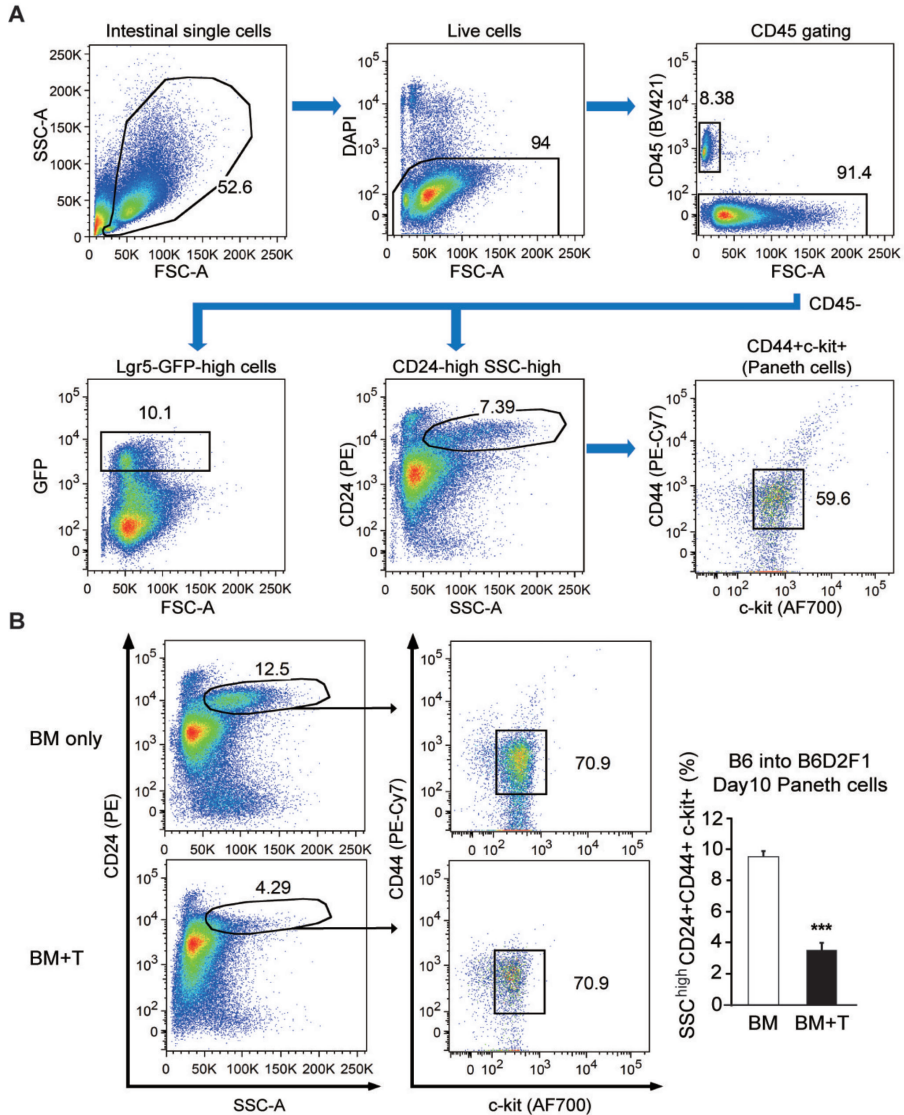


were performed at least twice with several wells per condition, and sample material coming from at least two different mice or three different human donors. Statistical analyses of stem cell numbers *in vivo* using Lgr5-LacZ mice or WT mice analyzed by Olfm4 IHC were performed on several independent sections from multiple mice. Statistics were calculated and display graphs were generated using Graphpad Prism.  $P < .05$  was considered statistically significant.

## Supplementary figures



**Fig. S1. Representative images post-BMT.** (A) Representative images of Paneth cells: SI (ileum) lysozyme staining on day 3 and day 10 after LP-into-B6 MHC-matched BMT. (B) Representative images of ruxolitinib treatment: SI (ileum) Lgr5-LacZ staining on day 10 after LP-into-B6 BMT using Lgr5-LacZ recipients treated with vehicle or ruxolitinib (30mg/kg twice every day starting the day -1 of BMT). (C) Representative images of GVHD histology related to donor T cell IFN $\gamma$ : SI (ileum) H & E staining on day 10 after B6-into-BDF1 BMT with WT or *Ifng*<sup>-/-</sup> donor T cells. Scale bars = 500 $\mu$ m (upper images) or 100 $\mu$ m (lower images). (D) Representative images of SI (ileum) Olfm4 IHC staining on day 7 post-BMT: B6 (Syn) or B10.Br (Allo) donor cells transplanted into *Ifngr* $\Delta$ IEC or Crenegative B6 littermates (*Ifngr*WT). Scale bars = 500 $\mu$ m (upper images) or 50 $\mu$ m (lower images), unless otherwise mentioned.



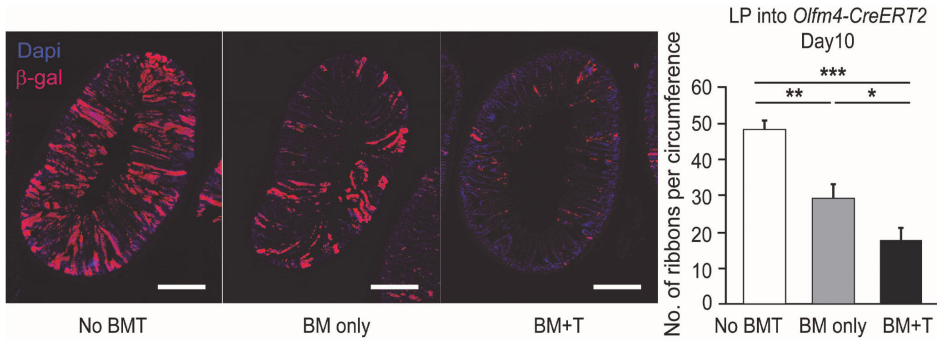


**Fig. S3. Allogeneic BMT decreases lineage tracing from intestinal stem cells.** LP-into-*Olfm4-CreERT2xRosa26-LacZ* BMT: Shown are representative images and quantification of lineage tracing ribbons 10 days after BMT; combined from two experiments. Scale bars = 500 $\mu$ m. Bar graph indicates mean and s.e.m.; comparisons performed with one-way ANOVA; \* $P < 0.05$ , \*\* $P < 0.01$ , \*\*\* $P < 0.001$ .

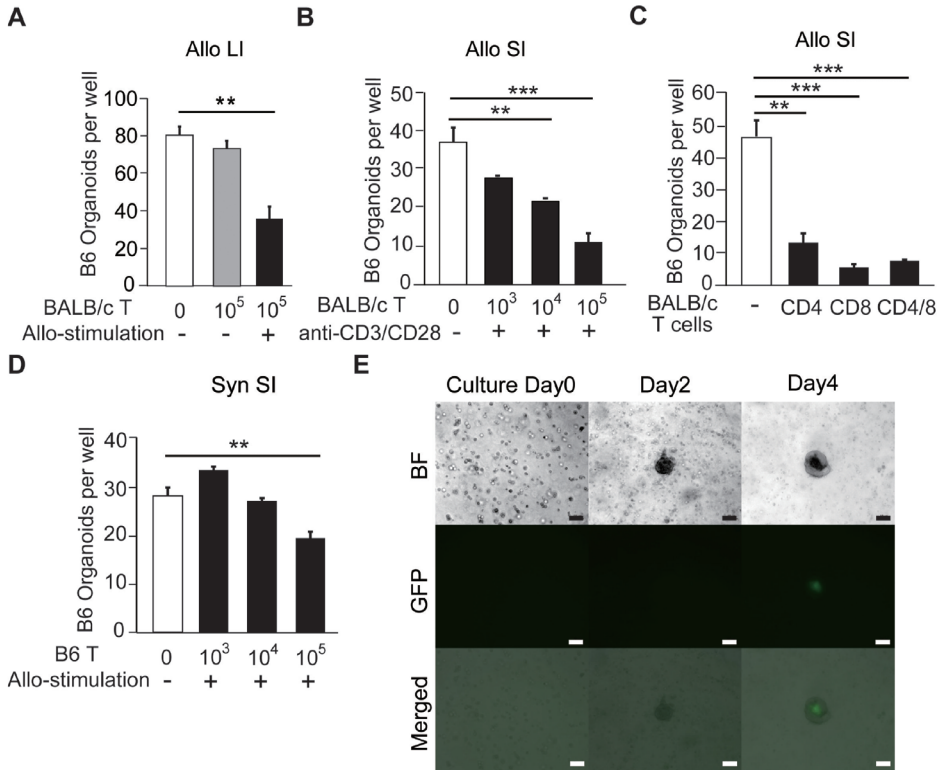


**Fig. S4. Co-culture of activated T cells and intestinal organoids.** (A to C) Co-culture of B6 organoid cells with activated allogeneic BALB/c T cells. Prior to organoid culture, T cells were activated by stimulation with allogeneic B6 dendritic cells (A) or anti-CD3/CD28 antibodies (B and C). Shown are numbers of LI (A) and SI (B and C) organoids after co-culture with T cells (day 7 of culture,  $n = 3-6$  wells per group). (D) Co-culture of B6 organoid cells with activated syngeneic B6 T cells. T cells were activated by stimulation with BALB/c dendritic cells. Shown are numbers of SI organoids (culture day 7,  $n = 3$  wells per group). (E) Representative negative control images of WT (GFP-negative) allogeneic B6 T cells co-cultured with BDF1 organoid cells. Shown are bright field (upper), fluorescent (middle), and overlap (lower) images; scale bars =  $50\mu\text{m}$ . Bar graphs indicate mean and s.e.m.; comparisons performed with one-way ANOVA; \*\* $P < 0.01$ , \*\*\* $P < 0.001$ . Data are representative of two (A and B), three (C and D) or four (E) independent experiments.



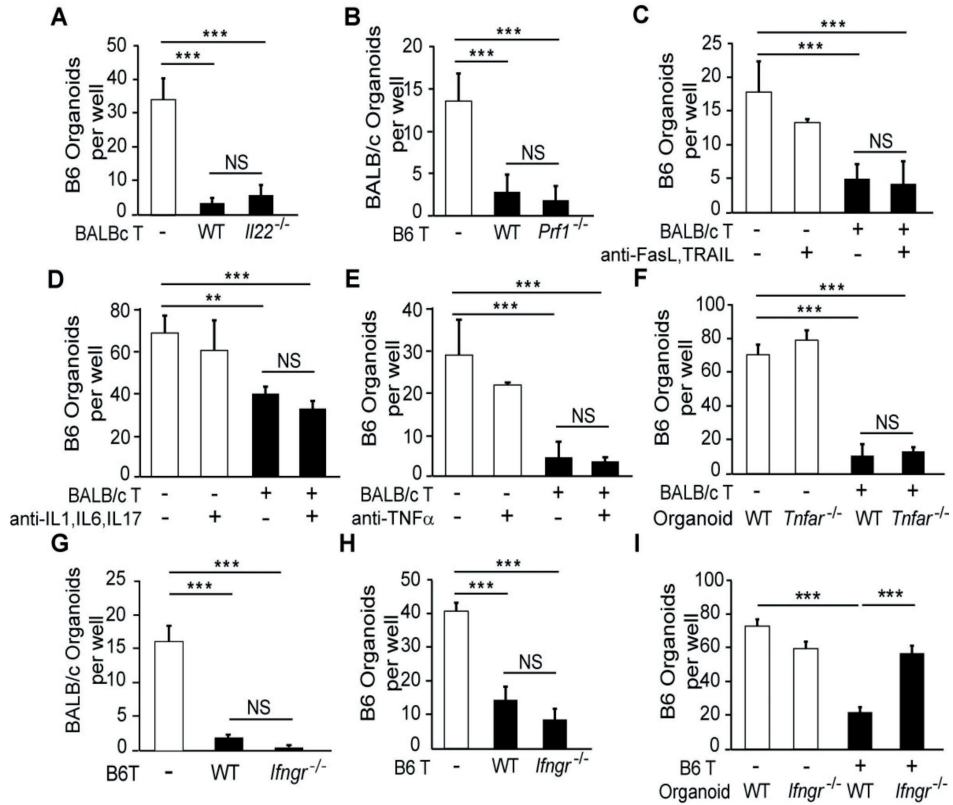


**Fig. S5. Investigation of T cell effector pathways responsible for T-cell-mediated intestinal organoid toxicity.** (A) Numbers of B6 SI organoids after culture with WT or *Il22*<sup>-/-</sup> BALB/c T cells (culture day 7, n = 3 or 6 wells/group). (B) Numbers of BALB/c SI organoids after culture with WT or *Perfl*<sup>-/-</sup> B6 T cells (culture day 7, n = 5 wells/group). (C to E) Numbers of B6 SI organoids after culture with BALB/c T cells and neutralizing antibodies (culture day 7, n = 4 wells/group); anti-FasL and TRAIL (C), anti-IL-1 $\beta$ , IL-6 and IL-17A (D), and anti-TNF $\alpha$  (E). (F) WT or *Tnfr*<sup>-/-</sup> B6 SI organoids cultured with BALB/c T cells (culture day 7, n = 4 wells/group). (G) BALB/c SI organoids after culture with WT or *lfng*<sup>-/-</sup> B6 T cells (culture day 7, n = 4 wells/group). (H) B6 SI organoids after syngeneic culture with WT or *lfng*<sup>-/-</sup> B6 T cells (culture day 7, n = 4 wells/group). (I) WT or *lfng*<sup>-/-</sup> B6 SI organoids cultured with syngeneic B6 T cells (culture day 7, n = 4 wells/group). Graphs indicate mean and s.e.m.; comparisons performed with one-way ANOVA; \*\*P < 0.01, \*\*\*P < 0.001. Data are representative of two (C to F, H), three (B, G, and I) or four (A) independent experiments.



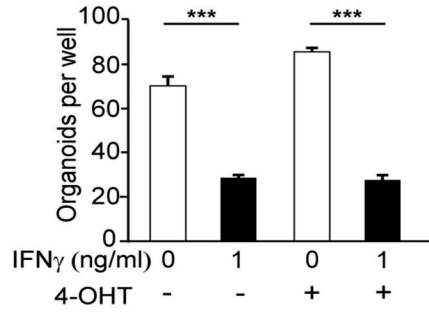


**Fig. S6. Tamoxifen treatment does not impair efficiency of organoid growth.** WT B6 SI organoids cultured +/- rmIFN $\gamma$  (culture day 7, n = 4 wells/group) after pretreatment with control media or 4-OHT (1 $\mu$ M). Data indicate mean and s.e.m.; comparisons performed with one-way ANOVA; \*\*\*P < 0.001. Data are representative of two independent experiments.

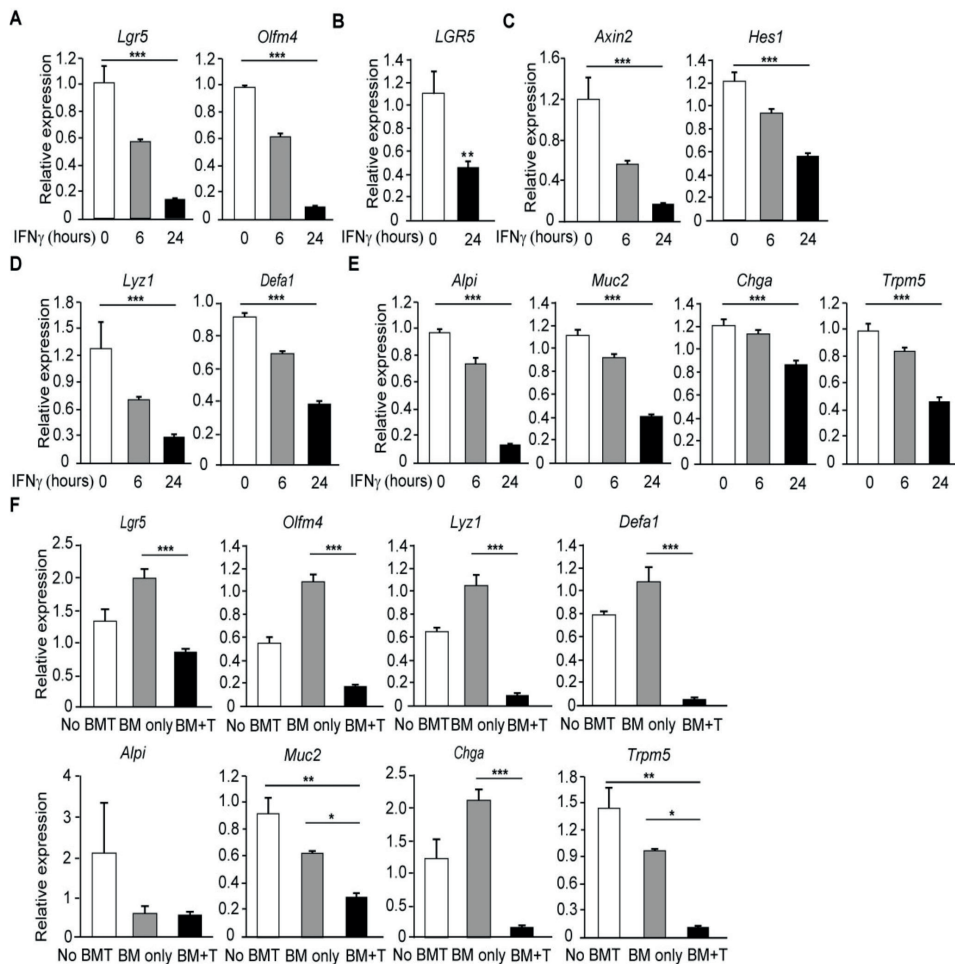


**Fig. S7. Epithelial lineage markers *ex vivo* and *in vivo*.** (A to E) qPCR analysis of mouse or human SI organoids cultured with recombinant mouse or human IFN $\gamma$  (1 ng/ml) for 6 or 24 hours; n = 6 wells/group. Shown are mouse (A) or human (B) ISC genes, and mouse Wnt/ $\beta$ -catenin or Notch target genes (C), Paneth cell-related genes (D), and marker genes for differentiated cell lineages (E). (F) B6-into-BDF1 BMT: gene expression shown from SI crypts isolated 10 days after BMT; n = 3 (No BMT), n = 6 (TCD BM only), or n = 10 (BM + T) mice per group. \*P < 0.05, \*\*P < 0.01, \*\*\*P < 0.001. Data analyzed by Mann-Whitney for experiments with two groups or by Kruskal-Wallis for experiments with more than two groups. Data are representative of two independent experiments (A, C to E), combined from 3 different donors (B), or combined from two experiments (F).

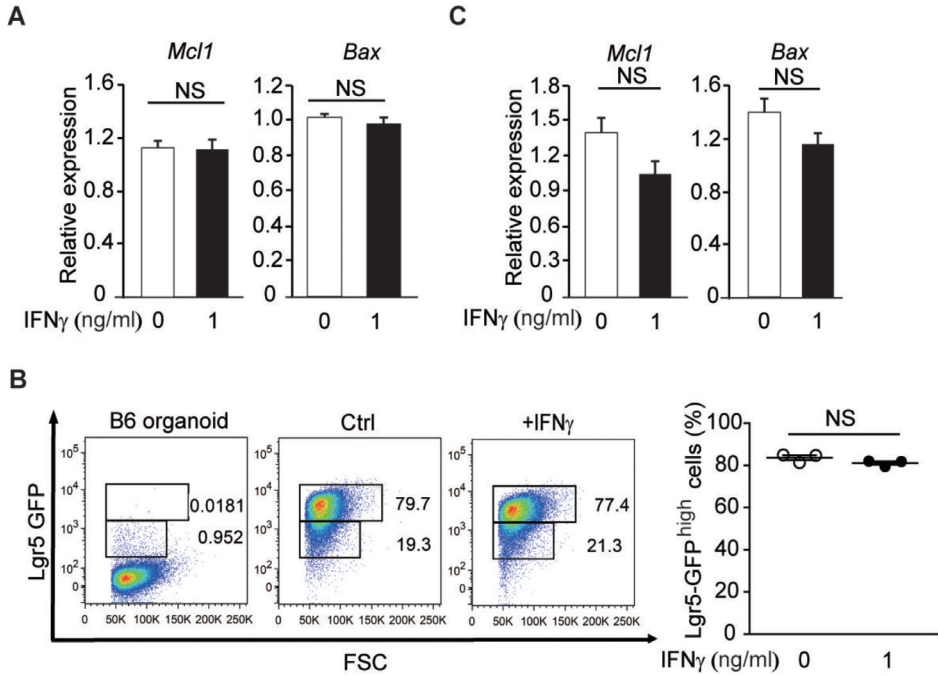


**Fig. S8. Supplemental analyses of IFN $\gamma$ -induced apoptosis in intestinal epithelium.** (A) qPCR analysis of mouse SI organoids cultured with rmIFN $\gamma$  for 6 hours; n = 6 wells/group; Mann–Whitney U analysis. (B) FACS analysis of Lgr5-GFP<sup>high</sup> ISCs: negative control WT B6 SI organoids (left FACS plot) and SI ISC colonies cultured +/- rmIFN $\gamma$  for 24 hours (right and middle FACS plots); n = 3 wells/group; t-test analysis. (C) qPCR analysis of mouse SI ISC colonies cultured with rmIFN $\gamma$  for 24 hours; n = 6 wells/group; Mann–Whitney U analysis. Graphs indicate mean and s.e.m.; \*P < 0.05, \*\*P < 0.01. Data are representative of two independent experiments.

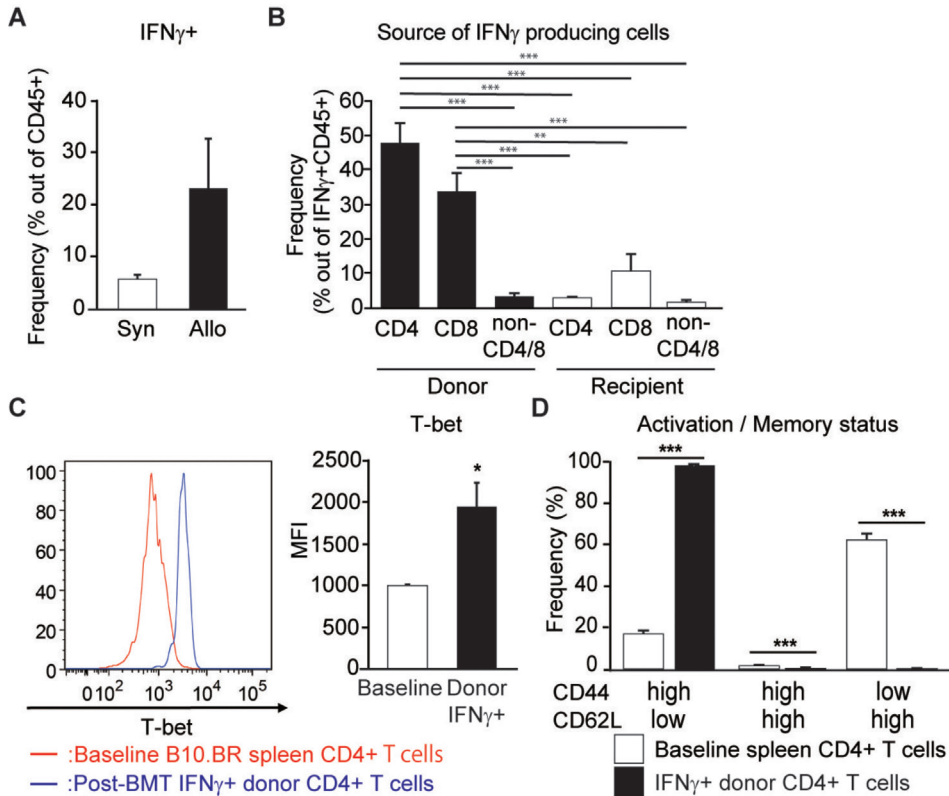


**Fig. S9. Phenotyping of IFN $\gamma$ <sup>+</sup> cells in recipient intestinal mucosa after BMT.** SI crypt region LPLs were isolated after mechanical disruption of the villi, and LPLs were then incubated in the presence of golgi inhibition without any stimulatory molecules to allow for natural cytokine accumulation prior to intracellular cytokine staining and flow cytometry. **(A)** Frequency of IFN $\gamma$ <sup>+</sup> cells among all CD45<sup>+</sup> cells after syngeneic (B6 $\times$ B6) or MHC-mismatched allogeneic (B10.Br $\times$ B6) BMT. **(B)** CD4, CD8, and donor/host phenotyping of CD45+IFN $\gamma$ <sup>+</sup> cells after B10.Br $\times$ B6 allogeneic BMT. **(C)** T-bet staining (MFI) in IFN $\gamma$ <sup>+</sup> donor B10.Br CD4 T cells after allogeneic BMT vs. splenic B10.Br CD4 T cells typically used in BMT experiments. **(D)** Activation/memory phenotype of normal splenic B10.Br CD4 T cells vs. donor B10.Br T cells after allogeneic BMT. n=2 mice/group (A), n=4 mice/group (B), n=3-4 mice/group (C and D). Graphs indicate mean and s.e.m.; comparisons performed with t-tests; \*P < 0.05, \*\*P < 0.01, \*\*\*P < 0.001. Data are representative of two independent experiments.

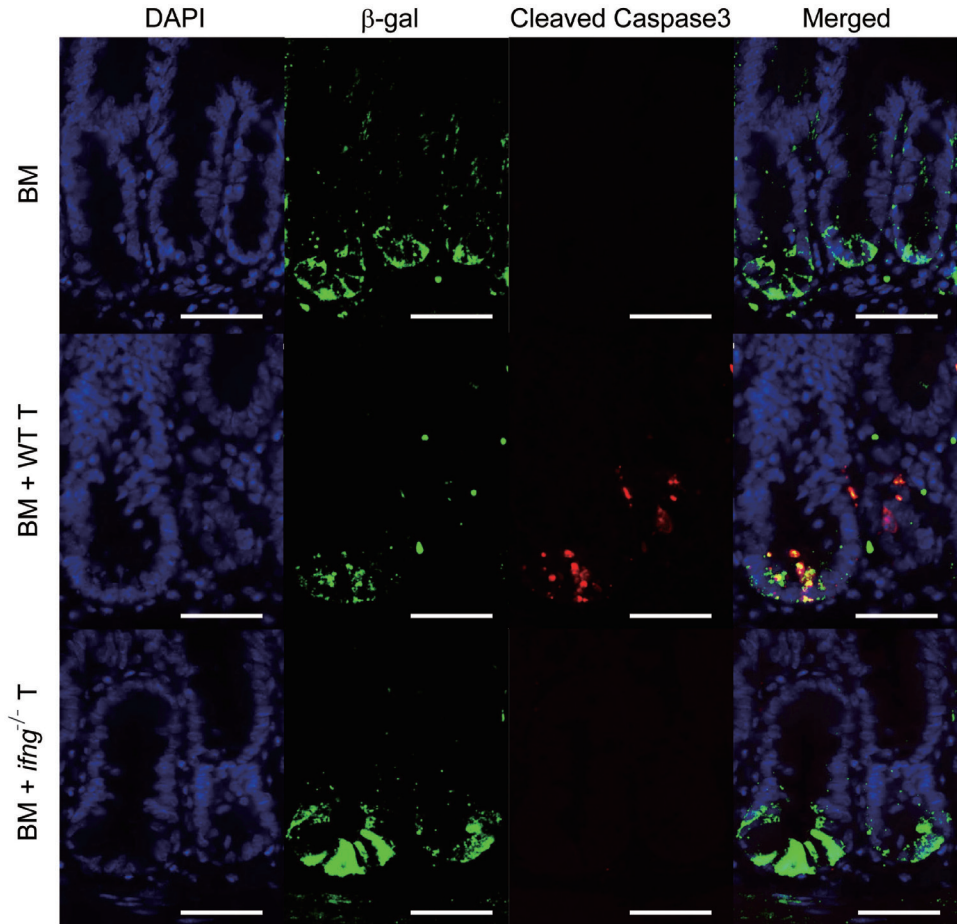


**Fig. S10. IFN $\gamma$  induces ISC apoptosis *in vivo*.** B6-into-BDF1 BMT with wild type or *ifng*<sup>-/-</sup> T cells. Shown are representative single-color images of DAPI staining (blue) and immunofluorescent staining of  $\beta$ -gal (green) and cleaved caspase-3 (red) from Lgr5-LacZ recipient mice 10 days after BMT, as shown in the merged images in Figure 6L and included here to the right. Scale bars = 50 $\mu$ m. Data are representative of two independent experiments.



5





# 6

## Corticosteroids impair epithelial regeneration in immune-mediated intestinal damage

Viktor Arnhold, Suze A. Jansen, Winston Y. Chang, Govindarajan Thangavelu,  
Marco Calafiore, Paola Vinci, Ya-Yuan Fu, Takahiro Ito, Shuichiro Takashima,  
Anastasiya Egorova, Jason Kuttiyara, Marliek van Hoesel, Chen Liu,  
Bruce R. Blazar, Caroline A. Lindemans, Alan M. Hanash

Under revision

## Abstract

Corticosteroids (CS) represent first-line treatment for gastrointestinal graft-versus-host disease (GI GVHD), and CS failure is associated with severe morbidity and mortality. While the immune system is the intended CS target, the glucocorticoid receptor is widely expressed, and direct CS effects on intestinal epithelium following immune-mediated damage are poorly understood. In healthy mice, we found that *in vivo* administration of clinically relevant CS doses reduced epithelial proliferation in the intestines without inducing overt pathology. Similar findings were observed *ex vivo* using murine and human intestinal organoid cultures. However, CS exposure exacerbated organoid toxicity mediated by T cells and Interferon- $\gamma$ . Furthermore, *in vivo* CS treatment after murine allogeneic bone marrow transplantation (allo-BMT) impaired epithelial regeneration and increased crypt loss. Conversely, Interleukin-22 (IL-22) administration overcame CS-mediated attenuation of regeneration, augmenting *ex vivo* organoid growth and promoting *in vivo* crypt recovery following radiation injury and allo-BMT despite CS treatment. These findings indicate that CS can suppress epithelial proliferation in the intestines and exacerbate GI damage if they fail to control the damage-inducing immune response. However, deleterious CS side effects can be counterbalanced by promotion of epithelial regeneration, providing rationale for combining immunosuppression with tissue-supporting therapeutics to optimize management of GVHD and immune-mediated GI damage.

## Introduction

The epithelial lining of the gastrointestinal (GI) tract undergoes turnover every 5-7 days<sup>1</sup>. This renewal is driven by the cycling of Leucine-rich repeat-containing G-protein coupled receptor 5<sup>+</sup> (Lgr5<sup>+</sup>) intestinal stem cells (ISCs) that reside in the intestinal crypt base<sup>2</sup>. Cycling ISCs produce highly-proliferative progenitors that move up the crypt as they divide and subsequently differentiate into mature enterocytes of the surface epithelium. The highly-proliferative cells in transition between ISCs and differentiated cells encompass the transit-amplifying (TA) progenitor compartment. Despite the importance of precursor proliferation for epithelial maintenance and recovery after immune-mediated GI injury, there is limited understanding of the mechanisms underlying regeneration in this setting or how they are impacted by immunosuppressive treatments.

Damage to the GI tract is a frequent occurrence after allogeneic hematopoietic/bone marrow transplantation (allo-BMT). The transplant conditioning regimen, consisting of chemotherapeutic agents and ionizing irradiation, can cause severe intestinal injury<sup>3,4</sup>. Furthermore, injury to intestinal crypt epithelium is a common histopathological finding of graft-versus-host disease (GVHD) in BMT recipients<sup>5,6</sup>. Lower GI GVHD, which is associated with high morbidity and mortality, often manifests in ileal as well as colonic mucosa<sup>7,8</sup>. GVHD, occurring in 30-70% of patients undergoing BMT, is an immune-mediated complication arising from a donor T cell-mediated response against recipient tissues<sup>9</sup>. The systemic administration of synthetic corticosteroids (CS) is the first-line therapy for GVHD patients, with a response rate ranging from 50-70%<sup>10</sup>. However, the optimal CS dosing for an individual patient is not always clear, and high-dose CS can be associated with substantial side effects<sup>11-13</sup>. Additionally, CS treatment courses involve prolonged tapers, leading to systemic CS use over several weeks. Even when CS treatment fails, administration often continues alongside other second-line agents. It is thus clinically necessary to examine the direct effects of CS treatment on the intestinal epithelium and to improve our understanding of steroid refractory GVHD (SR-GVHD) pathophysiology.

Therapeutic effects of CS in inflammatory settings have primarily been ascribed to their pleiotropic suppression of immune function<sup>14</sup>. However, the GI epithelium is known to express the glucocorticoid receptor (GR)<sup>15-19</sup>, and little is known about the direct effects of systemic CS treatment on the intestinal mucosa during GVHD-related tissue injury and regeneration. We thus sought to examine the tissue-specific impact of synthetic CS in GVHD-related tissue damage in the intestines. A combination of phenotypic and functional characterizations of intestinal epithelium were utilized to examine CS administration in the settings of conditioning-related and immune-mediated injury *in vivo* as well as in *ex vivo* intestinal organoid cultures and organoid injury models. We report here that CS treatment suppresses epithelial proliferation with complex context-dependent implications,



potentially resulting in exacerbated intestinal epithelial damage in certain settings if the CS treatment does not also suppress the pathologic response that is initiating the damage. In addition, we found that administration of exogenous Interleukin (IL)-22 could counteract this CS-mediated toxicity, restoring epithelial regeneration and promoting intestinal recovery.

## Results

### **Corticosteroid administration reduces epithelial proliferation in vivo**

In murine GVHD models, CS efficacy appears to be timing-dependent, with a greater likelihood of effectiveness when initiated earlier<sup>20,21</sup>. We performed a major histocompatibility complex (MHC)- mismatched GVHD model and tested early CS treatment from day 1 to 28 post-BMT at different concentrations (1, 3, and 6 mg/kg prednisolone). We found that CS treatment significantly improved survival in a dose-dependent manner, with high-dose CS (6 mg/kg prednisolone) increasing median survival to 46 days, compared to 8 days in the vehicle-treated control group (Figure 1A). Lower doses of CS had less impact on median survival (Figure 1A). CS also reduced the clinical signs of GVHD in a dose-dependent manner, although low-dose CS (1mg/kg prednisolone) failed to improve clinical GVHD scores (Figure 1A). Notably, weight loss in association with injury of the GI epithelium is a common finding in GVHD (8), and GVHD-related weight loss was unchanged by CS in any group with the doses administered here (Figure 1A). Given this discrepancy, we sought to scrutinize the effects of CS treatment on the intestinal epithelium.

It has been shown that GR is expressed across many tissues including the GI tract<sup>14-16</sup>. To examine GR gene *Nr3c1* expression in distinct small intestine (SI) epithelial cell populations, we analyzed a single-cell RNA sequencing (scRNA-seq) dataset (GSE92332) of SI epithelial cells from naïve wild-type (WT) C57BL/6 (B6) mice<sup>22</sup>. Unsupervised graph clustering partitioned the cells into eight groups, which we visualized using uniform manifold approximation and projection (UMAP) and annotated using the expression of known marker genes (Figure 1B). Each cluster was associated with a distinct cell type or state: stem cells, transit amplifying (TA) progenitor cells, more differentiated enterocyte precursors, enterocytes, goblet, Paneth, enteroendocrine, or tuft cells (Figure 1B). We found that *Nr3c1* was predominantly expressed in stem and TA cells as well as cells of the enterocyte lineage (Figure 1B). Indeed, immunohistochemical (IHC) staining for GR in WT mouse SI sections indicated GR staining in epithelial cells along the crypt/villus axis (Figure 1C).

Having confirmed the presence of GR within SI epithelial cells, we next investigated the impact of systemic CS administration on epithelial cells in healthy WT mice during homeostasis. Intraperitoneal administration of methylprednisolone (MP) did not change SI crypt or Lgr5<sup>+</sup> ISC frequency (Figure 1D). However, we observed a significant reduction in

SI crypt height, including the total height and the TA compartment specifically, leading to an increase in the villus/crypt ratio in MP-treated animals (Figure 1E and F). The reduction in the height of the TA compartment suggested reduced proliferation of SI epithelial cells. Indeed, IHC staining for Ki67 revealed a decreased frequency of proliferating cells upon MP treatment (Figure 1G). MP administration also induced expression of the key cell cycle checkpoint molecule *Cdkn1a* in SI tissue (Figure 1H). Taken together, these results suggested that systemic administration of CS doses used here did not exhibit signs of toxicity in healthy mice, but it did reduce epithelial proliferation within the GI mucosa.

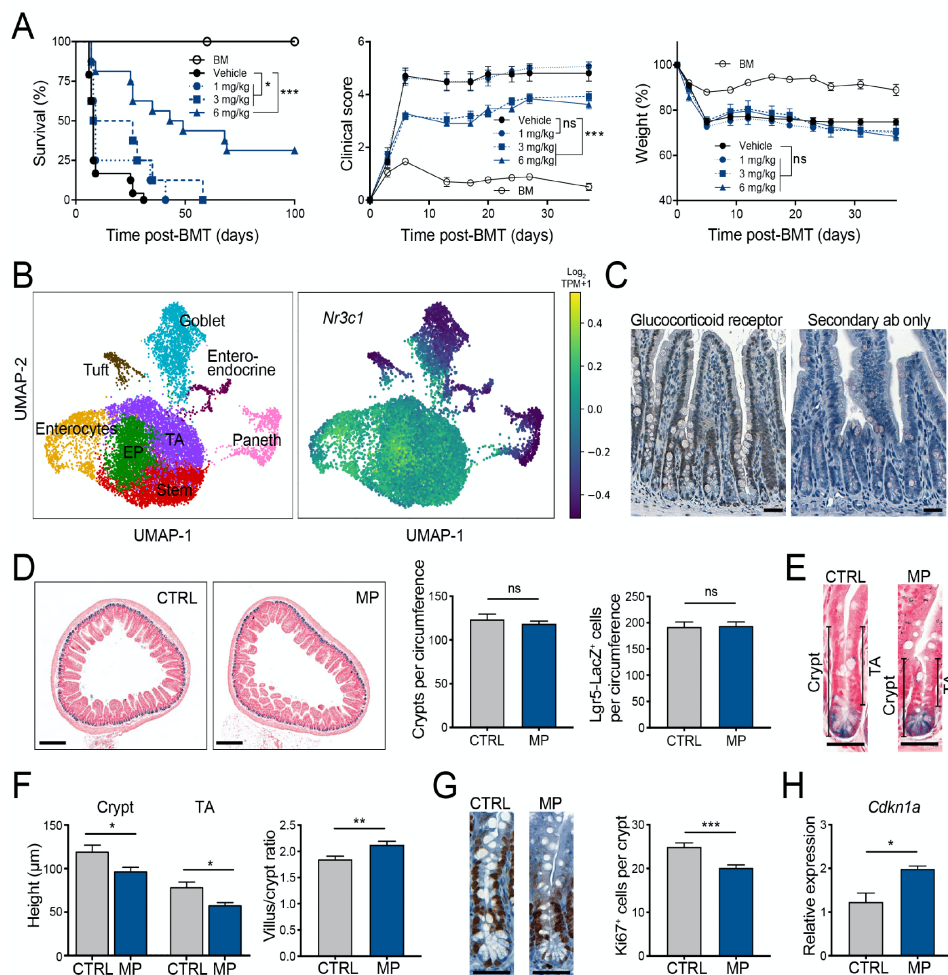


**Figure 1. Corticosteroid treatment reduces epithelial proliferation *in vivo*.** (A) Percentage survival, clinical score of GVHD and relative weight of a B6-into-BALB/c BMT, +/- prednisolone (1, 3, or 6 mg/kg i.p. daily from day 1 to 28 after BMT); n=13 (BM only), n=24 (BM + T cells -- vehicle), n=8 (BM + T cells -- 1 mg/kg), n=8 (BM + T cells -- 3 mg/kg), and n=16 (BM + T -- 6 mg/kg) mice per group. Data combined from two independent experiments. (B) UMAP visualization of 12,457 SI epithelial cells from

naïve WT B6 mice. Left, unsupervised clustering, based on the expression of known marker genes. Right, expression of *Nr3c1*. EP, enterocyte precursor; TA, transit amplifying; TPM, transcripts per million. (C) Immunohistochemistry staining of GR in SI sections from naïve WT mice; scale bars, 50  $\mu$ m. (D-H) WT B6 mice treated with methylprednisolone (MP, 2 mg/kg i.p. daily for 7 days) or vehicle (CTRL); one of two experiments. (D) Representative images, SI crypt and ISC frequency; n= 8-9 independent sections per group; scale bars, 250  $\mu$ m. (E) Representative SI crypt images. (F) SI crypt height, TA height, and villus/crypt ratio; n= 8-9 independent sections per group; scale bars, 50  $\mu$ m. (G) Ki67 IHC images and Ki67<sup>+</sup> cell frequency; n= 62-69 crypts from 3 mice per group; scale bars, 50  $\mu$ m. (H) qPCR of *Cdkn1a* in SI tissue; n=3 mice per group. Data are mean and s.e.m.; comparisons performed with log-rank analysis (A) or t-tests (D-H); NS, not significant; \*p<0.05, \*\*p<0.01, \*\*\*p<0.001.

### Corticosteroids reduce epithelial proliferation in mouse and human intestinal organoids

Interpreting effects of CS that are administered systemically can be complicated by the numerous potential CS targets *in vivo*, including epithelial, stromal, and hematopoietic cells. To address this limitation, we utilized *ex vivo* SI organoid cultures to explore direct effects of CS on murine and human epithelium. Assessing a variety of clinically relevant CS agents, we found that addition of MP, dexamethasone, or budesonide to standard EGF/Noggin/R-spondin-1 (ENR) culture conditions all resulted in decreased murine organoid size without affecting organoid numbers (Figure 2A). CS culture also attenuated organoid crypt bud formation (Figure 2B). Furthermore, *in vivo* administration of MP prior to crypt isolation from mice resulted in a significant reduction of organoid size without additional MP treatment *ex vivo* (Figure 2C). We also identified that *Nr3c1*<sup>-/-</sup> organoids were significantly resistant to growth inhibition by MP, further indicating a direct GR-mediated effect of CS on intestinal epithelium leading to reduced growth (Figure 2D).

We next examined the effects of CS on human intestinal tissue. First, we explored *NR3C1* expression in human SI epithelial cell populations by analyzing a previously published scRNA-seq dataset (GSE119969, GSM3389578) of EpCAM<sup>+</sup> live single cells from human SI tissue<sup>23</sup>. Unsupervised graph clustering partitioned the cells into 10 groups, which we visualized using UMAP and labelled by the expression of known marker genes (Figure 2E). Consistent with the scRNAseq analysis of murine SI tissue (Figure 1B), we detected *NR3C1* expression in stem and TA cells as well as enterocyte lineage cells (Figure 2E). Furthermore, MP treatment significantly decreased the size of human intestinal organoids generated from primary duodenal tissue without affecting organoid numbers (Figure 2F). Overall, our *ex vivo* studies with mouse and human SI organoids indicated that CS directly suppressed intestinal epithelial growth in a GR-dependent manner.

Flow-cytometry-based intracellular Ki67-DAPI analysis of cell cycle revealed an MP-dependent down-regulation of cell cycling, as evidenced by an expansion of G1 phase in organoid cells after 5 days in culture (Figure 3A). *Lgr5* is a well-established marker for ISCs, and ISCs represent a constitutively active and highly proliferative stem cell population<sup>24</sup>. Using organoids from *Lgr5*-GFP<sup>+</sup> mice, we observed a pronounced suppression of ISC

proliferation upon organoid exposure to CS (Figure 3B). Consistent with this suppression of ISC proliferation, MP treatment significantly reduced the frequency Lgr5-GFP<sup>+</sup> cells within SI organoids (Figure 3C). To further evaluate the direct effects of corticosteroids on ISCs, we generated ISC colonies by sorting Lgr5-GFP<sup>+</sup> cells and culturing them in the presence of glycogen synthase kinase3 $\beta$  (GSK3 $\beta$ ) and histone deacetylase (HDAC) inhibitors to promote strong Wnt and Notch signaling, which results in cultures primarily composed of ISCs. Exposure of these ISC colonies to MP for 4 days increased expression of the cell cycle checkpoint molecule *Cdkn1a* and reduced expression of cyclins *Ccna2* and *Ccnb1* in ISC colonies (Figure 3D). Additionally, use of the CellTrace Violet cell proliferation assay indicated that human SI organoids cultured with MP retained significantly higher dye fluorescence than untreated human organoids, indicative of reduced proliferation following treatment with CS (Figure 3E and F). Together with the *in vivo* findings from mice treated with CS (Figure 1), these data suggested that MP and other CS suppress proliferation within the intestinal epithelium, including proliferation of Lgr5<sup>+</sup> ISCs and progenitors.

### Effects of corticosteroid treatment after irradiation are timing-dependent

Following radiation injury, surviving crypts become highly proliferative to mediate recovery of the intestinal mucosa, which can be observed by day 3 following total body irradiation (TBI)<sup>25,26</sup>. Since CS directly suppressed proliferation of epithelial crypt cells, we next investigated CS-mediated effects on radiation-induced intestinal injury and regeneration. MP treatment of mice starting 24 hours following TBI mitigated epithelial injury four days later, as evidenced by increased preservation of ileal crypt numbers (Figure 4A and B). In this context, there was no difference in crypt height with or without MP treatment (Figure 4B). In contrast, delaying initiation of MP by two days had the opposite effect. Four days of MP treatment starting day 3 post-TBI (Figure 4C), during the proliferative phase of the epithelial response to radiation injury, resulted in increased pathology as demonstrated by a reduction in ileal crypt numbers compared to controls (Figure 4D). Ileal crypt height and Ki67<sup>+</sup> cells were also significantly reduced, suggesting that epithelial proliferation was attenuated in MP-treated animals (Figure 4D and E). Consistent with this, we observed reduced expression of the cyclins *Ccna2* and *Ccnb1* in SI tissue of MP-treated animals (Figure 4F). These *in vivo* studies indicated that while early initiation of MP treatment could mitigate the severity of intestinal radiation injury, MP-induced suppression of epithelial proliferation during the regenerative phase of the response to radiation injury could exacerbate the severity of crypt damage.



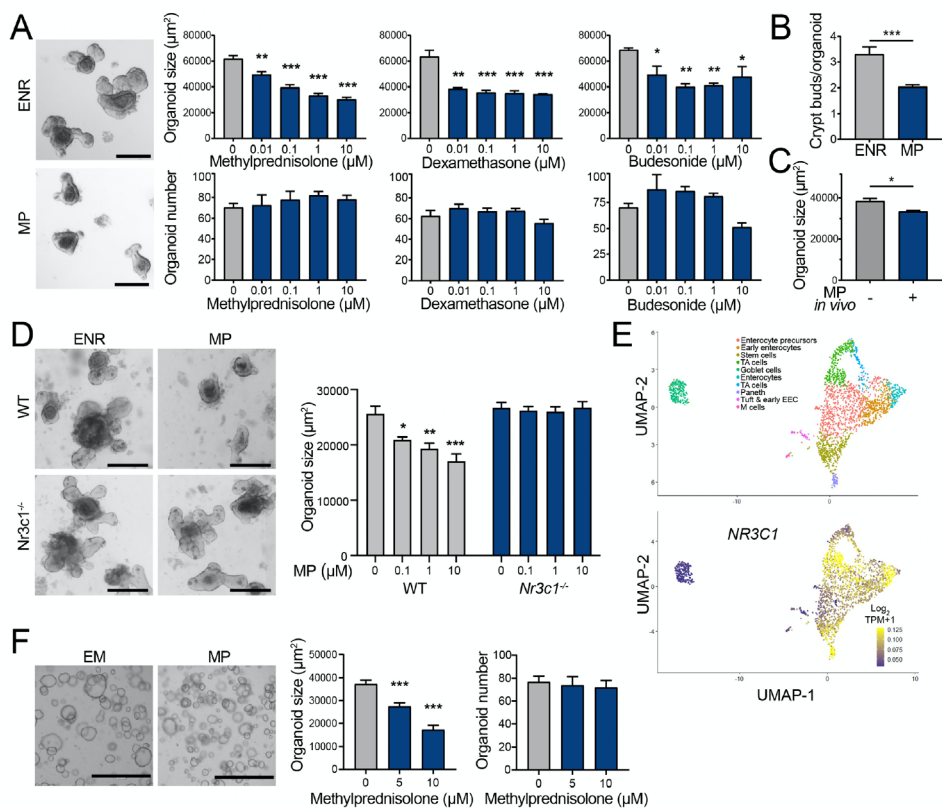


**Figure 2. Corticosteroids limit the growth of murine and human intestinal organoids.** (A) Representative images, size and frequency of murine SI organoids cultured in ENR +/- MP, dexamethasone, or budesonide for 7 days; n=4 wells per group; scale bars, 200 μm. (B) Frequency of crypt bud formation in SI organoids cultured +/- MP for 5 days; n=8 wells per group. (C) Size of SI organoids derived from harvested crypts of WT mice treated i.p with MP or vehicle *in vivo*; organoids cultured in ENR for 6 days; n=6 wells per group. (D) Size of WT or *Nr3c1*<sup>-/-</sup> SI organoids cultured +/- MP for 4 days; n=4 wells per group; scale bars, 200 μm. (E) UMAP visualization of 2,342 cells from human ileum intestinal epithelial crypts. Top, unsupervised clustering, based on the expression of known marker genes. Bottom, expression of *NR3C1*. TA, transit amplifying; EEC, enteroendocrine cells; TPM, transcripts per million. (F) Representative images, size and frequency per field of human SI organoids cultured +/- MP; n = 18 fields of view (in 9 wells) from 4 different donors per group; scale bars, 1000 μm. Data are mean and s.e.m.; comparisons performed with t-tests (two groups) or one-way analysis of variance (ANOVA) (multiple groups); \*p<0.05, \*\*p<0.01, \*\*\*p<0.001. Data are representative of at least two independent experiments or combined from two independent experiments (F).



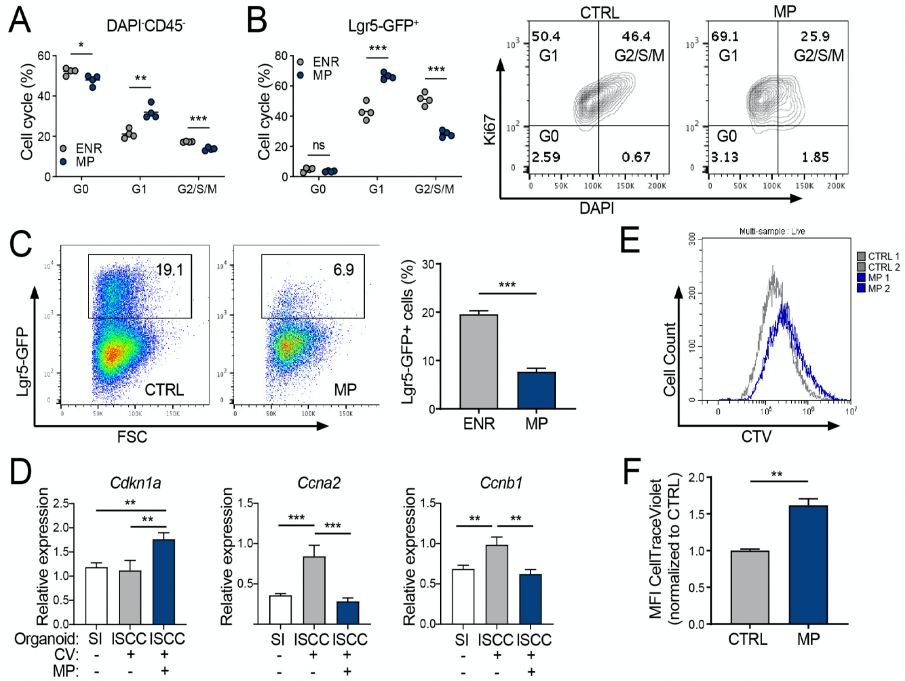


**Figure 3. Corticosteroid exposure reduces proliferation in murine and human organoids.** (A) Quantifications of intracellular Ki67-DAPI cell cycle analysis in live organoid cells cultured +/- MP (10  $\mu$ M) for 5 days (n=4 wells per group). (B) Flow cytometry plots and quantifications of intracellular Ki67-DAPI cell cycle analysis in Lgr5-GFP<sup>+</sup> cells from SI organoids cultured +/- MP (10  $\mu$ M) for 5 days (n=4 wells per group). (C) Flow cytometry plots and quantifications of Lgr5-GFP<sup>+</sup> cell fractions from murine SI organoids cultured +/- MP (10  $\mu$ M) for 5 days (n=3 wells per group). (D) qPCR of *Cdkn1a*, *Ccna2*, and *Ccnb1* in organoids derived from SI crypts cultured in ENR or in ISC colonies (ISCC) cultured in ENR supplemented with histone deacetylase and GSK3 $\beta$  inhibition (CV) +/- MP (10  $\mu$ M) for 4 days (n=3 wells per group). (E-F) Flow cytometry plots and quantifications of CellTrace Violet (CTV) dilution in human SI organoids cultured +/- MP (10  $\mu$ M) for 5 days (n=3 donors per group). Data are mean and s.e.m.; comparisons performed with t-tests (two groups) or one-way ANOVA (multiple groups); NS, not significant; \*p<0.05, \*\*p<0.01, \*\*\*p<0.001. Data are representative of at least two independent experiments.



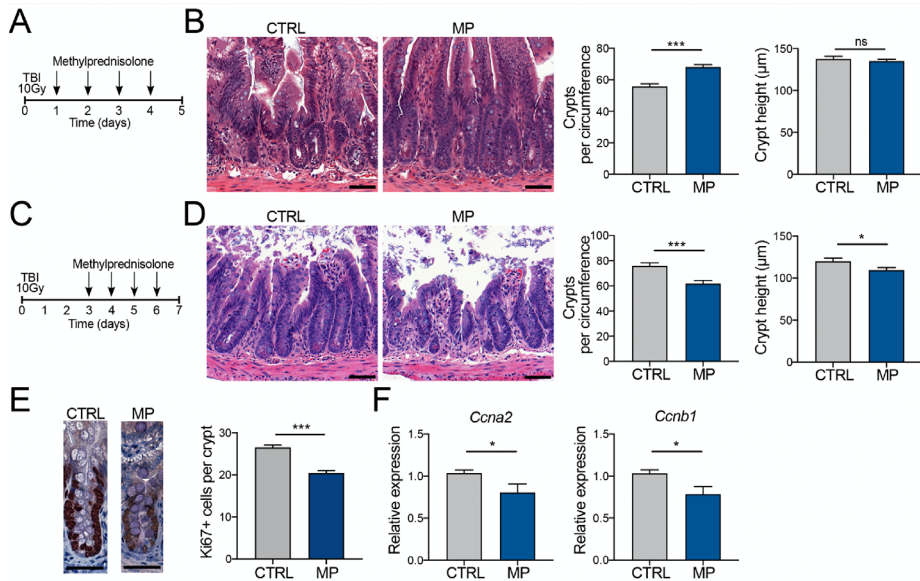


**Figure 4. Epithelial effects of corticosteroid treatment after irradiation are timing-dependent.** (A-B) WT B6 mice were treated with MP (2 mg/kg) or vehicle i.p. daily starting 24 hours after TBI. (B) Representative images, SI crypt frequency and height, 5 days after TBI (n=21-25 sections per group); scale bars, 50  $\mu$ m. (C-F) WT B6 animals were treated with MP (2 mg/kg) or vehicle i.p. daily starting 72 hours after TBI. (D) Representative images, SI crypt frequency and height (n= 15-21 sections per group), 7 days after TBI. (E) Representative images and Ki67<sup>+</sup> cell frequency, 7 days after TBI (n= 20-21 sections per group); scale bars, 50  $\mu$ m. (F) qPCR of *Ccna2* and *Ccnb1* in enriched SI crypts, 7 days after TBI (n=8 animals per group). Data are mean and s.e.m.; comparisons performed with t tests (two groups) or one-way ANOVA (multiple groups); NS, not significant; \*p<0.05, \*\*\*p<0.001. Data are combined from at least two independent experiments.

### Corticosteroids impair the epithelial response to immune-mediated GI damage

We next investigated CS-induced effects on epithelial regeneration during immune mediated GI damage resulting from GVHD (Figure 5A). CS may be less effective at controlling the alloreactive immune response when initiation is delayed<sup>20,21</sup>, allowing for evaluation of immune-mediated tissue damage in the presence of steroids. Recipients of B6-into-BALB/c MHC- mismatched allo-BMT were thus treated with MP daily for seven days starting day 7 after transplant, once GVHD had already been established, as evidenced by mean weight loss of over 20% in recipients of allogeneic BM and T cells at the time of CS initiation (data not shown). Recipient tissues were analyzed on day 14. In this CD4-driven model<sup>27</sup>, vehicle-treated mice demonstrated T cells with an activated effector phenotype in the spleen as well as lymphocytic tissue infiltration within the intestines (Figure 5B-D). In addition, vehicle-treated GVHD mice demonstrated ileal crypt loss as well as increased height and Ki67<sup>+</sup> cell frequency in residual crypts compared to BM only controls (Figure 5E-G), indicating the presence of damage-induced epithelial regeneration. Reflecting steroid-refractory disease in this delayed

treatment model, CS administration failed to reduce T cell activation or lymphocytic infiltration (Figure 5B-D). However, MP treatment appeared to attenuate regeneration and worsen intestinal pathology, as evidenced by exacerbated crypt loss in association with reduced crypt height and Ki67<sup>+</sup> cell frequency (Figure 5E-G).

To better understand these *in vivo* findings, we next investigated CS effects on epithelial cells in *ex vivo* organoid models of immune-mediated damage. By co-culturing intestinal organoids with activated T cells, immune-mediated epithelial injury can be modeled *ex vivo*, and both allogeneic and syngeneic T cells are effective at including this injury<sup>28</sup>. To distinguish between the potential impacts of CS on T cells vs. the epithelium, and to model a steroid-refractory T cell response, we performed co-culture experiments using GR-deficient T cells from *Nr3c1<sup>fl/fl</sup>;CD4-Cre* mice. Addition of MP to standard ENR organoid cultures once again had no impact on organoid viability, while co-culture with *Nr3c1<sup>-/-</sup>* (GR-deficient) T cells in standard ENR culture conditions resulted in substantial organoid loss (Figure 5H). Addition of MP to co-cultures with GR-deficient T cells resulted in more severe organoid reduction than co-cultures with GR-deficient T cells in the absence of MP (Figure 5H), indicating that MP could act directly on the epithelium to increase toxicity. Additionally, we co-cultured WT T cells with SI crypts from mice that were treated *in vivo* with MP or with vehicle. Pre-treatment with MP *in vivo* prior to crypt harvest and organoid culture resulted in increased sensitivity to T-cell-mediated killing *ex vivo* (Figure 5I). T-cell-derived IFN $\gamma$  is a major mediator of crypt injury in GVHD and in organoid models<sup>28</sup>. Therefore, we exposed intestinal organoids to MP and IFN $\gamma$  concurrently and found that exposure to MP augmented IFN $\gamma$ -mediated organoid loss (Figure 5J). Furthermore, co-culture of MP and IFN $\gamma$  reduced the formation capacity of human SI organoids compared to IFN $\gamma$  alone (Figure 5K). Modelling of GVHD immunopathology *in vivo* and *ex vivo* thus indicated that CS exposure could exacerbate immune-mediated GI damage induced by T cells and their effector cytokines.

### **IL-22 treatment reverses corticosteroid-induced inhibition of epithelial proliferation.**

CS are currently a necessary standard of care for clinical treatment of GI GVHD (10). IL-22 has been shown to promote epithelial recovery in experimental GVHD models<sup>29-30</sup>, and has recently been investigated in a clinical trial for treatment of GI GVHD along with systemic CS (NCT02406651). Given the intestinal suppression identified above, we investigated if IL-22 treatment could promote epithelial regeneration and recovery in the presence of CS. First, we co-cultured murine SI organoids together with MP and recombinant mouse (rm)IL-22. The combined treatment did not affect organoid formation or survival, but addition of IL-22 to MP-treated organoids promoted their growth despite the suppression induced by MP (Figure 6A). Consistently, exposure to rmlL-22 reversed MP-mediated effects on cell cycle regulators, such as the induction of *Cdkn1a* expression and inhibition of *Ccna2* expression (Figure 6B). Furthermore, addition of recombinant human (rh)IL-22 to human SI organoids



cultured with MP also promoted human organoid growth despite the suppression induced by MP on its own (Figure 6C).

We next evaluated the potential of F-652, a clinical grade rhIL-22-dimer and Fc-fusion protein, to overcome MP-mediated suppression of epithelial proliferation *in vivo*. During homeostasis in healthy WT mice, F-652 and MP treatments had no effect on SI crypt frequency, suggesting the treatments were not toxic alone or in combination (Figure 6D). Moreover, treatment with F-652 reversed the MP-mediated reduction of SI crypt height (Figure 6D). We next tested the combination of F-652 and MP treatments in models of intestinal injury. Daily MP treatment for four days starting three days after TBI once again worsened radiation-associated crypt loss and reduced regeneration-associated crypt height and Ki67<sup>+</sup> cell frequency (Figure 6E). However, combined administration with F-652 increased SI crypt recovery on day 7 and increased Ki67<sup>+</sup> cell frequency as well (Figure 6E), indicating enhanced regenerative capacity of intestinal crypts despite the presence of systemic CS treatment. Finally, F-652 administration also reversed the CS-associated crypt loss and reduction of crypt height and Ki67<sup>+</sup> cell frequency observed in mice with GVHD, indicating reduced epithelial injury and enhanced regeneration (Figure 6F).

**Figure 5. Corticosteroid-induced impairment of epithelial regeneration is associated with increased severity of immune-mediated intestinal injury [Figure at next page].** (A-G) B6-into-BALB/c transplant; recipients treated with MP (2 mg/kg) or vehicle i.p. daily starting on day 7 after BMT. (B) CD44<sup>+</sup>CD62L<sup>-</sup> cell frequency out of live CD45<sup>+</sup>CD3<sup>+</sup>CD4<sup>+</sup>CD8<sup>-</sup> splenocytes, 14 days after BMT (n= 3-5 animals per group). (C) Representative images of SI tissue, 14 days after BMT. (D) Semiquantitative SI lymphocytic infiltrate histopathology score, 14 days after BMT (n= 8-9 animals per group). (E and F) SI crypt frequency and height, 14 days after BMT (n= 20-26 independent sections per group); scale bars, 50  $\mu$ m. (G) Representative images and Ki67<sup>+</sup> cell frequency, 14 days after BMT (n= 42-84 crypts per group); scale bars, 50  $\mu$ m. (H) Representative images and B6 organoid frequency after culture +/- anti-CD3/CD28-activated *Nr3c1*<sup>-/-</sup> B6 T cells +/- MP (10  $\mu$ M) for 4 days (n=6 wells per group); scale bars, 500  $\mu$ m. (I) B6 organoid frequency after *in vivo* MP (or vehicle) treatment prior to crypt isolation and subsequent culture with anti-CD3/CD28-activated WT B6 T cells; day 6 of culture (n = 12 wells per group). (J) Representative images and organoid frequency after culture +/- MP (10  $\mu$ M) and IFN $\gamma$  (0-1 ng/ml; 0.05 ng/ml in images) for 6 days (n=6 wells per group); scale bars, 500  $\mu$ m. (K) Representative images and human organoid frequency after culture +/- MP (10  $\mu$ M) and rhIFN $\gamma$  (2 ng/ml) for 7 days (n=12 fields of view in 6 wells from 2 donors per group); scale bars, 1000  $\mu$ m. Data are mean and s.e.m.; comparisons performed with t-tests (two groups) or one-way ANOVA (multiple groups); NS, not significant; \*p<0.05, \*\*p<0.01, \*\*\*p<0.001. Data are representative of at least two independent experiments (B, H, I) or combined from two experiments.

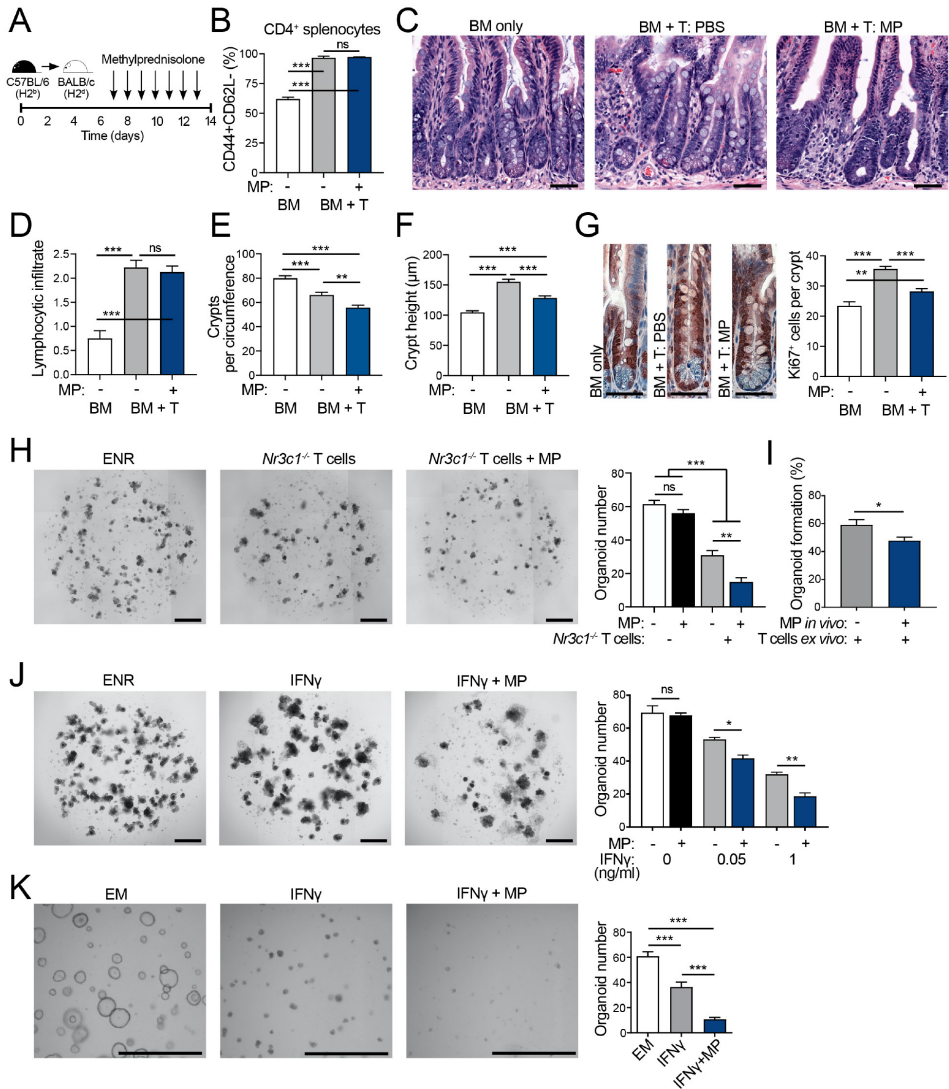
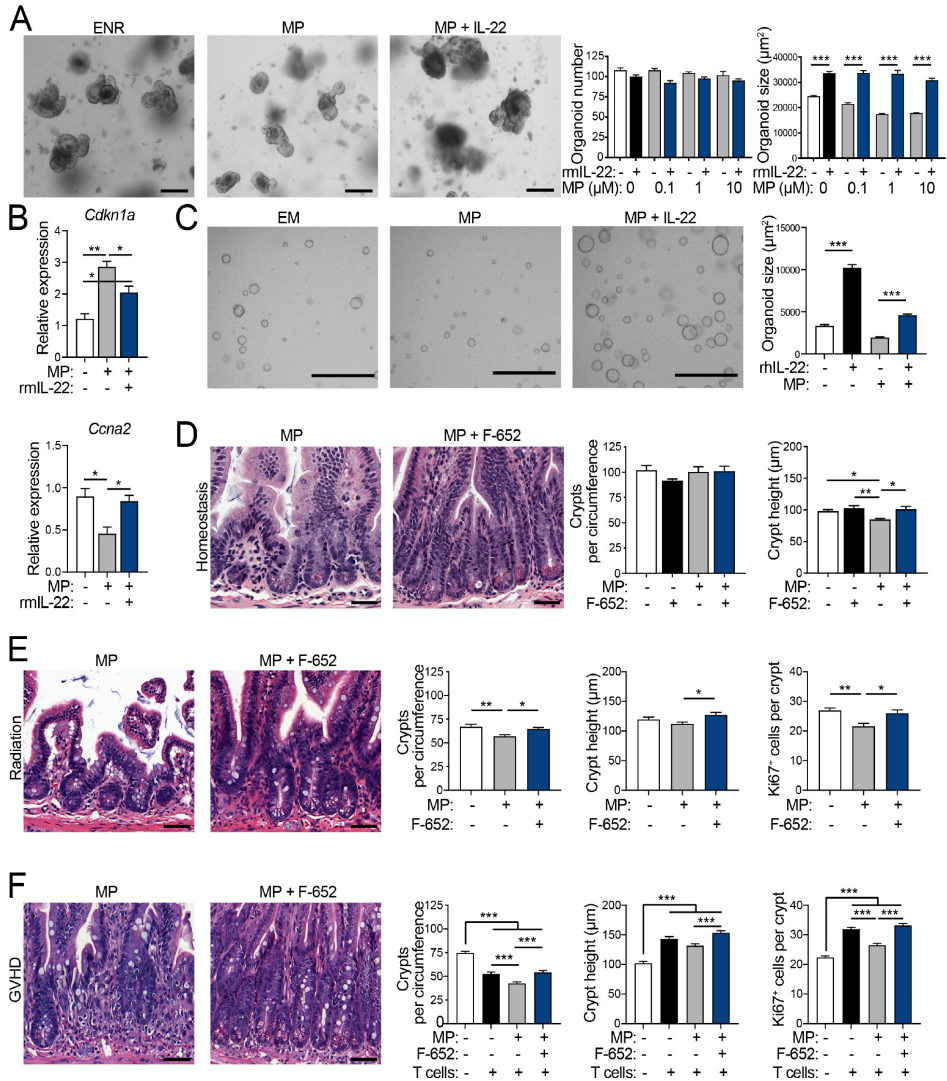


Figure 5. Corticosteroid-induced impairment of epithelial regeneration is associated with increased severity of immune-mediated intestinal injury [Legend at previous page].



**Figure 6. IL-22 administration overcomes *ex vivo* and *in vivo* corticosteroid-mediated inhibition of epithelial regeneration.** (A) Representative images, frequency and size of organoids cultured +/- MP and rmlL-22 0.5 ng/ml for 5 days (n=4 wells per group); scale bars, 200  $\mu\text{m}$ . (B) qPCR of *Cdkn1a* and *Ccna2* in organoids cultured +/- MP (1  $\mu\text{M}$ ) and rmlL-22 (1 ng/ml) for 3 days (n=3 wells per group). (C) Representative images and size of human organoids cultured +/- MP (10  $\mu\text{M}$ ) and rIL-22 (10 ng/ml) for 6 days (n=6 wells from 2 human organoid donors per group); scale bars, 1000  $\mu\text{m}$ . (D) B6 mice treated +/- MP (2 mg/kg i.p. daily) +/- F-652 (100  $\mu\text{g}/\text{kg}$  s.c. every other day). Representative images, SI crypt frequency and height on day 7 (n= 8-12 independent sections per group); scale bars, 50  $\mu\text{m}$ . (E) WT B6 mice were treated +/- MP (2 mg/kg i.p. daily) +/- F-652 (100  $\mu\text{g}/\text{kg}$  s.c. every other day) starting 72 hours after TBI. Representative images, SI crypt frequency and height (n= 20-23 independent sections per group), and Ki67<sup>+</sup> cell frequency (n= 41-53 crypts per group) on day 7; scale bars, 50  $\mu\text{m}$ . (F) B6-into-BALB/c transplant; recipients treated +/- MP (2 mg/kg i.p. daily) +/- F-652 (100  $\mu\text{g}/\text{kg}$  s.c. every other day) starting on day 7 after BMT. SI crypt frequency and height (n= 25-31 independent sections per group), and Ki67<sup>+</sup> cell frequency (n= 103-163 crypts per group) on day 14; scale bars, 50  $\mu\text{m}$ . Data are mean and s.e.m.; comparisons performed with t-tests (two groups) or one-way ANOVA (multiple groups); \*p<0.05,

\*\*p<0.01, \*\*\*p<0.001. Data are representative of at least two independent experiments or combined from two experiments (E, F).

## Discussion

Although synthetic CS have long been used as a principal treatment for immune-mediated GI disorders, there is little understanding of the direct impacts CS may have on the targeted tissue, in particular under non-homeostatic conditions. By re-analyzing murine and human scRNAseq datasets (GSE92332, GSE119969) and performing IHC staining, we confirmed that SI epithelial cells express *Nr3c1* (*NR3C1*) and GR and also identified that this epithelial expression is predominantly detected within stem cells, progenitors, and the enterocyte lineage. We further observed that CS administration can cause suppression of epithelial proliferation *in vivo*. Considering that GR is expressed by numerous cell types in various tissues and that secretion of endogenous CS is part of a physiologic stress response<sup>14</sup>, it is challenging to comprehensively and accurately elucidate the specific effects of exogenously administered CS on intestinal epithelial cells. To overcome this limitation, we utilized an *ex vivo* organoid system enabling us to exclusively study effects on the intestinal epithelium. We found that CS can directly inhibit proliferation of SI epithelial cells in a GR-dependent fashion. Flow cytometry and gene expression analyses revealed CS-mediated cell cycle inhibition in SI organoids, including reduction of proliferation within the ISC compartment. The GR is a broadly active transcriptional regulator, and proliferation-promoting cell cycle genes contain negative GC response elements that enable CS-induced direct repression via GR binding<sup>31</sup>. Our study provides evidence that CS directly inhibit proliferation of crypt epithelial cells, and that this reduced proliferation impaired regeneration *in vivo*.

Using a radiation injury model and administering systemic CS at different time points, we sought to scrutinize the effects of CS treatment on epithelial injury and regeneration. Notably, we uncovered opposing results depending on the timing of treatment initiation. While early treatment mitigated radiation-induced SI epithelial injury, delaying treatment to a timepoint with severe injury (day 3 post-TBI) led to impaired epithelial regeneration by suppressing crypt proliferation. Although the mechanism of action for CS-mediated mitigation of radiation injury remains unclear, this observation is consistent with a study demonstrating that administration of a glucocorticoid-acting androgen, nandrolone, 24 hours after lethal TBI alleviated GI injury and extended survival<sup>32</sup>.

Balancing immune and tissue tolerance has recently been proposed as a more comprehensive model for understanding GVHD pathophysiology and developing treatment strategies that include overcoming tissue-compromising effects and promoting



tissue recovery<sup>40</sup>. To address this need, we tested a strategy to increase “tissue tolerance” without forgoing the beneficial immunosuppressive effects of CS treatment. IL-22 has emerged as a key regulator of intestinal epithelium after damage and has shown potential to effectively protect GI mucosa from radiation injury, genotoxic stress, and T cell-mediated damage and to promote epithelial regeneration as well<sup>29,30,41,42</sup>. By combining IL-22 and CS treatment, we identified that IL-22 treatment could overcome the tissue-compromising effects of CS exposure and could support intestinal crypt regeneration despite the presence of exogenously administered CS in both radiation and T cell-mediated injury models. Our study provides support for a comprehensive treatment strategy combining standard immunosuppression with tissue-supportive strategies to enhance recovery of damaged mucosa. Host-derived IL-22-producing lymphocytes are depleted in GVHD models, providing rationale for administration of IL-22<sup>29,43,44</sup>. Notably, CS have been shown to suppress IL-22 production in peripheral blood mononuclear cells<sup>45</sup>, further supporting the rationale for administering IL-22 in this setting.

In summary, we report that CS treatment suppressed SI epithelial proliferation in a GR- dependent manner. Within the epithelium, GR expression predominantly localized to the stem cells, progenitors, and mature non-secretory enterocytes. Organoid cultures demonstrated direct targeting of intestinal epithelium by CS, which led to impaired regeneration and worsened T cell- mediated injury. These findings indicate that CS treatment can exacerbate GI damage if the treatment fails to control the pathologic immune response. However, deleterious side effects of CS can be counterbalanced by promotion of epithelial regeneration, providing rationale for combining immunosuppression with tissue-supporting therapeutics to optimize intestinal recovery in GVHD. IL-22 promoted epithelial regeneration both *ex vivo* and *in vivo* despite the presence of CS, and thus may provide a complementary treatment option reducing the negative effects of CS without forgoing the beneficial anti-inflammatory immunosuppressive effects they can provide.

## Materials and methods

**Mice.** B6 (H-2<sup>b</sup>), BALB/c (H-2<sup>d</sup>), and B6.Cg-Nr3c1<sup>tm1.1Jda/J</sup> (*Nr3c1<sup>fl/fl</sup>*) mice were purchased from Jackson Laboratories. Lgr5-LacZ B6, B6 Lgr5-GFP-IRES-CreERT2 (Lgr5–GFP) and Olfm4-GFP-IRES-CreERT2 (Olfm4-CreERT2) mice were provided by Hans Clevers. Nr3c1<sup>fl/fl</sup>×Olfm4-CreERT2 (*Nr3c1<sup>ΔIEC</sup>*) mice were created by crossing Nr3c1<sup>fl/fl</sup> mice with Olfm4-CreERT2 mice. Nr3c1<sup>fl/fl</sup>×Cd4-Cre mice were created by crossing Nr3c1<sup>fl/fl</sup> mice with Cd4-Cre mice (B6.Cg-Tg(Cd4-cre)1Cwi/BfluJ, Jackson Laboratories). All animal experiments were performed in accordance with the institutional protocol guideline of the Memorial Sloan Kettering Cancer Center (MSKCC) Institutional Animal Care and Use Committee. Mice were housed in micro-



isolator cages, five per cage, in MSKCC pathogen-free facilities, and received standard chow and autoclaved sterile drinking water. The investigations assessing clinical outcome parameters were performed by blinded technicians.

**Crypt isolation and cell dissociation.** Isolation of intestinal crypts and the dissociation of cells for flow cytometry analysis were performed as previously described<sup>30</sup>. In brief, after asphyxiating the mice with CO<sub>2</sub>, the SI was harvested, opened longitudinally, and washed with PBS. To dissociate the crypts, SI was incubated with shaking at 4°C in EDTA (10 mM) for 20 min. To further isolate single cells, SI crypts were incubated in 1x TrypLE Express (Gibco).

**Organoid and ISC colony culture.** For mouse organoids, depending on the experiments, 50–100 crypts per well were suspended in growth-factor-reduced Matrigel (Corning) mixed with DMEM/F12 medium (Gibco). After Matrigel polymerization, complete ENR medium containing advanced DMEM/F12 (Sigma), 2 mM Glutamax (Invitrogen), 10 mM HEPES (Sigma), 100 U/ml penicillin, 100 µg/ml streptomycin (Sigma), N2 supplement (Invitrogen), 50 ng/ml mouse EGF (Peprotech), 100 ng/ml mouse Noggin (Peprotech) and 5-10% human R-spondin-1-conditioned medium (CM) from R-spondin-1-transfected HEK 293T cells was added to cultures. Media was replaced every 2–3 days. Along with medium changes, treatment wells received different concentrations of MP, dexamethasone, or budesonide (Tocris Bioscience) as well as rmIFN $\gamma$  (R&D systems) or rmlL-22 (R&D Systems).

For experiments with *Nr3c1*<sup>-/-</sup> organoids, *Nr3c1*<sup>ΔIEC</sup> mice (and littermate controls) were given an intraperitoneal injection of tamoxifen (2 mg per mouse, Sigma, dissolved in sunflower oil) for 5 consecutive days prior to crypt isolation to achieve deletion of GR from SI epithelium. ISC colonies were cultured from sort-purified single *Lgr5*-GFP<sup>high</sup> cells<sup>46</sup>. Approximately 3,000 ISCs were plated in 10 µl Matrigel and cultured in ENR-CV media with CHIR99021 (C, 3 µM Stemgent) and valproic acid (V, 1.5 mM, Sigma), containing Rho-kinase/ROCK inhibitor Y-27632 (10 µM) and Jagged1 (1 µM) for the first 48h. Under these culture conditions ISCs divide symmetrically without differentiating, growing into homogeneous stem cell colonies. Along with medium changes, treatment wells received different concentrations of MP (Tocris Bioscience).

As described previously<sup>28</sup>, for co-culture of intestinal organoids with T cells, CD5 cells were isolated from splenocytes using magnetic MicroBeads with the MACS system (Miltenyi Biotec) according to the manufacturer's instructions. T cell purity was determined by flow cytometry, and was routinely greater than 90%. T cells were cultured at a concentration of 1x10<sup>5</sup> T cells per well with 5 µg/ml plate-bound anti-CD3 monoclonal antibodies (mAbs) and 2 µg/ml anti-CD28 mAbs. After 3-5 days of culture, harvested T cells and freshly isolated SI crypts were cultured in Matrigel with a 500:1 T cell: crypt ratio.



Healthy human duodenal organoids were cultured from banked frozen organoids (> passage 7) that had been previously generated from biopsies obtained during duodenoscopy of healthy human controls. All healthy controls had been investigated for celiac disease, but ultimately found to be free of pathologic findings. They had previously provided written informed consent to participate in this study according to a protocol reviewed and approved by the review board of the UMC Utrecht, the Netherlands (METC 10-402/K; TCBio 19-489). Organoids were passaged via single cell dissociation using 1x TrypLE Express (Gibco) and resuspended in medium without growth factors (GF-), comprised of Advanced DMEM/F12 (Gibco), 100 U/ml penicillin-streptomycin (Gibco), 10 mM HEPES (Gibco) and Glutamax (Gibco), and 50-66% Matrigel (Corning). After plating and Matrigel polymerization, human SI organoid expansion medium (hSI EM) was added consisting of GF-, Wnt CM (50% final concentration), R-spondin CM (20% final concentration), Noggin CM (10% final concentration), 50 ng/ml murine EGF (Peprotech), 10 mM nicotinamide (Sigma), 1.25 mM N-acetyl (Sigma), B27 (Gibco), 500 nM TGF- $\beta$  inhibitor A83-01 (Tocris), 10  $\mu$ M P38 inhibitor SB202190 (Sigma), and 100  $\mu$ g/ml Primocin (optional) (Invitrogen). Medium was refreshed every 2-3 days. Along with medium changes, treatment wells received different concentrations of MP (Pfizer) or rhIFN $\gamma$ (R&D systems). RhIL-22 (Genscript) was added daily.

**Imaging of organoids and colonies.** Random representative non-overlapping images of organoids and colonies were acquired from each well using a Zeiss Axio Observer Z1 inverted microscope or LSM880 (Carl Zeiss) using 20x/0.8NA objective. For human SI organoids, images were acquired using an EVOS FL Cell Imaging System (Thermo Fisher Scientific). For size evaluation, the images were analyzed using ImageJ software.

**Total body irradiation.** Animals were exposed to a single dose of 10 Gy using a GammaCell 40 irradiator to induce epithelial injury.

**BMT.** BMT procedures were performed as previously described<sup>47</sup>. A major histocompatibility antigen-mismatched BMT model (B6 into BALB/c, H-2<sup>b</sup> into H-2<sup>d</sup>) was used. Female mice were typically used as recipients for transplantation at an age of 8-10 weeks. Recipient mice received 850 cGy in 2 doses split at 3-4 h intervals to reduce gastrointestinal toxicity. To obtain bone marrow cells from euthanized donor mice, the femurs and tibias were collected aseptically, and the bone marrow canals washed out with sterile media. Bone marrow cells were depleted of T cells by incubation with anti-Thy 1.2 and low-TOX-M rabbit complement (Cedarlane Laboratories). The TCD bone marrow was analyzed for purity by quantification of the remaining T cell contamination using flow cytometry. T cell contamination was usually about 0.2% of all leukocytes after a single round of complement depletion. Donor T cells were prepared as above. Recipients typically received  $5 \times 10^6$  TCD bone marrow cells with or without  $0.5 \times 10^6$  T cells per mouse via tail injection.

For survival experiments, BALB/c mice were lethally irradiated at 700 cGy on day -1 followed by transplantation (i.v) with  $1 \times 10^7$  non-T-cell-depleted BM with/without  $2 \times 10^6$  purified T cells from C57BL/6 donors on day 0. Donor T cells were purified from splenocytes using biotin-labeled anti-CD19 (1D3), CD45R (RA3–6B2), CD11b (M1/70), CD11c (N418), CD49b (DX5), NK1.1 (PK136), TCR  $\gamma\delta$  (GL3) and TER-119 (TER-119), followed by streptavidin RapidSpheres depletion with EasySep magnet (StemCell Technologies). Purity of T cells > 98%. Survival was monitored daily, and weights and clinical scores were recorded twice per week.

***In vivo* treatment.** Prednisolone (Merck) was administered by i.p. injection at a daily dose of 1, 3, or 6 mg/kg starting from day 1 to day 28 after BMT. MP (Tocris Bioscience) was administered by i.p. injection at a daily dose of 2 mg/kg at indicated time points. F-652 (Generon Corporation) was administered by s.c. injection at a daily dose of 100  $\mu$ g/kg at indicated time points. The control groups received vehicle alone.

**GVHD histopathology analysis.** Mice were sacrificed for histopathological analysis at indicated time points after TBI with or without BMT using CO<sub>2</sub> asphyxiation. The SI were formalin-preserved, paraffin embedded, sectioned, and stained with hematoxylin and eosin. GVHD histopathology assessment of the sections for evidence of GVHD was performed by a blinded pathologist. A semiquantitative score consisting of 19 different parameters associated with GVHD was calculated, with a maximum score of 3 for an individual parameter<sup>48</sup>.

**LacZ staining.** For evaluation of stem cell numbers, SI were collected from Lgr5-LacZ recipient mice or non-transplanted controls.  $\beta$ -galactosidase (LacZ) staining was performed as previously described<sup>2</sup>. Washed 2.5-cm-sized SI fragments were incubated with an ice-cold fixative, consisting of 1% formaldehyde, 0.02% Igepal and 0.2% glutaraldehyde. After removing the fixative, organs were stained for the presence of LacZ according to manufacturer's protocol (LacZ Staining Kit, Invivogen). The organs were then formalin-preserved, paraffin-embedded, sectioned, and counterstained with Nuclear Fast Red (Vector Labs).

**Immunohistochemical staining.** Formalin-fixed tissue sections were deparaffinized with SafeClear II (Fisher Scientific), heat-induced antigen retrieval was performed with sodium citrate buffer and sections were blocked for 60 min with 1.5% blocking serum (Vector Laboratories). Slides were incubated with anti-Ki67 (Abcam, 1:800) and anti-Olfm4 (Cell Signaling, 1:200) antibodies in 1.5% normal serum overnight, followed by a 60-min incubation with biotinylated goat anti-rabbit IgG (Vector Laboratories). The detection was performed with an AMEC Red detection kit (Vector Laboratories) according to the manufacturer's instructions. Slides were counterstained with hematoxylin (Vector Laboratories), and coverslips were added with VectaMount (Vector Laboratories).



For some experiments, IHC detection of Ki67 was performed at the Molecular Cytology Core Facility of MSKCC using a Discovery XT processor (Ventana Medical Systems). Formalin-fixed tissue sections were deparaffinized with EZPrep buffer (Ventana Medical Systems), antigen retrieval was performed with CC1 buffer (Ventana Medical Systems) and sections were blocked for 30 min with Background Buster solution (Innovex). Slides were incubated with anti-Ki67 (Abcam, 1 µg/ml), isotype (4 µg/ml) for 6 h, followed by a 60-min incubation with biotinylated goat anti-rabbit IgG (Vector Laboratories) at 1:200 dilution. The detection was performed with a DAB detection kit (Ventana Medical Systems) according to the manufacturer's instructions. Slides were counterstained with hematoxylin (Ventana Medical Systems), and coverslips were added with Permount (Fisher Scientific).

**Flow cytometry.** For flow cytometry of mouse small intestine organoid cells, organoids were dissociated using TrypLE Express (37°C). After vigorously pipetting through a p200 pipette causing mechanical disruption, the crypt suspension was washed with 10 ml of DMEM/F12 medium containing 10% FBS and 2 kU/ml DNase1 and passaged through a 40 µm cell strainer. For intracellular Ki67 and DAPI staining, cells were stained with surface markers, fixed, and permeabilized using the Fixation/Permeabilization kit (eBioscience) according to the manufacturer's instructions. All staining with organoid cells was performed in DMEM/F12 medium with 2% FBS. Lymphoid organs from GVHD mice were processed into single-cell suspensions, and surface staining was performed with the corresponding cocktail of antibodies. For flow cytometry of splenocytes, spleens were collected from euthanized mice and processed into single cell suspension. After thorough washing, cells were stained with the appropriate mixture of antibodies. Fluorochrome-labelled antibodies were purchased from BD Pharmingen (CD4, CD8, CD45), eBioscience (CD44), and Invitrogen (CD62L). Fixable Live/Dead Cell Stain Kits (Invitrogen) were used for viability staining. Flow cytometry analyses were performed with an LSRII or LSRFortessa X-50 cytometer using FACSDiva (BD Biosciences), and the data were analyzed with FlowJo software (Treestar).

**CellTrace Violet cell proliferation assay.** For evaluation of the effect of MP treatment on proliferation in human duodenal organoids, organoids were dissociated into single cells and stained with CellTraceViolet (CTV) (Invitrogen, 5 µM in PBSO) before plating. After 5 days of culture, organoids were harvested, processed into single cells, stained with live/dead marker Zombie NIR (Biolegend), and analyzed by flow cytometry for CTV MFI in live cells on a CytoFLEX Flow Cytometer (Beckman Coulter) with CytExpert Software.

**RT-qPCR.** For qPCR, RNA was isolated from organoids after *ex vivo* culture or crypts isolated from BMT recipients. Extracted RNA was also stored at -80°C. Reverse transcriptase PCR (RT-PCR) was performed with a HighCapacity RNA-to-cDNA Kit (Applied Biosystems). Specific primers were obtained from Applied Biosystems: *Gapdh*: Mm99999915\_g1; *Cdkn1a*: Mm00432448\_m1. Other primers were obtained from PrimerBank: *Gapdh* (ID 6679937a1),

*Cdkn1a* (ID 6671726a1), *Ccna2* (ID 6753308a1), *Ccnb1* (ID 28195398a1). cDNAs were amplified with TaqMan or SYBR master mix (Applied Biosystems) using the QuantStudio 7 Flex System (Applied Biosystems). Relative amounts of mRNA were calculated by the comparative  $\Delta\text{Ct}$  method with *Gapdh* as housekeeping gene.

**Computational analysis of single cell RNA sequencing.** To explore expression of *Nr3c1* in epithelial cells of SI in homeostasis we analyzed a scRNA-seq data set (GSE92332) based on SI epithelial cells from WT B6 mice<sup>22</sup>. All *in silico* analyses downstream of gene quantification were done using Scanpy<sup>49,50</sup>. Prior to filtering, the data set consisted of 13,353 cells and 27,998 genes. For quality control, cells with less than 700 genes, less than 1,500 or greater than 40,000 unique molecular identifier (UMI) counts per cell, higher fraction of mitochondrial genes than 0.2 were removed. Genes detected in less than 20 cells were excluded. After filtering, a total of 12,457 cells and 12,818 genes were processed for downstream analysis. The filtered data matrix was normalized to median library size and log transformed prior to analysis. Using ComBat, batch correction was performed to adjust for batch effects from the 6 samples that were loaded<sup>51</sup>. After log normalization, 4,000 highly variable genes were identified and extracted. The normalized expression levels then underwent linear regression to remove effects of total reads per cell and cell cycle genes, followed by a z-transformation. Dimension reduction was performed using principal component analysis (PCA) and then uniform manifold approximation and projection (UMAP) on the top 50 principal components (PCs) and 30 nearest neighbors for visualization on two dimensions<sup>52</sup>. For de-noising and imputation, we used the MAGIC algorithm<sup>53</sup>. Clusters of cells within the data were calculated using the Louvain algorithm within Scanpy with a resolution of 0.5<sup>54</sup>. Detected clusters were mapped to cell types or intermediate states using markers for intestinal epithelial cell subtypes<sup>22</sup>.

To explore the expression of *NR3C1* in human SI epithelial cells under homeostatic conditions, we re-analyzed a scRNA-seq dataset (GSE119969, GSM3389578 Human\_SI\_tissue) of human ileum intestinal epithelial crypts<sup>23</sup>, largely as previously described<sup>23</sup> using the R package Seurat<sup>55-58</sup>. In brief, cells with <2,5% or >15% UMI reads mapped to mitochondrial genes and less than 200 expressed genes were removed. Genes expressed in less than three cells were excluded. A total of 2,342 cells and 17,562 genes were processed for downstream analysis. The expression matrix was log-normalized by the NormalizeData function. Using the ScaleData function, total UMI counts per cell and proportions of mitochondrial reads were corrected by negative binomial regression. Variably expressed genes were identified with the FindVariableFeatures function, with scaled dispersion >0.5 and log-normalized average expression between 0.125 and 3 and used to perform linear dimensionality reduction with RunPCA. Subsequently, cellclusters were identified with the FindNeighbors and FindClusters functions, using the top 25 PCs with the following parameters: k.param = 20, prune.SNN = 1/15 and resolution 0.6. For visualization in tow



dimensions, UMAP plots were generated using the RunUMAP function using the top 25 PCs. With the FindAllMarkers function differentially expressed genes (Wilcoxon Rank Sum test) in each cluster were identified with at least a 0.25 log fold increase. Markers for intestinal epithelial cell types were used to assign cell identity to the clusters<sup>23</sup>. The cluster of immune cells, also described in the original manuscript, was excluded using the Subset function in the Seurat package, after which all previous steps of analysis were repeated from the identification of variably expressed genes until cluster identification, using the same parameters on the remaining 2,262 cells. Finally, the MAGIC function in the Rmagic package was used for de-noising and imputation, after which (marker) genes were projected on the UMAP plots<sup>53</sup>.

**Quantification and Statistical Analyses.** To detect an effect size of >50% difference in means, with an assumed coefficient of variation of 30%, common in biological systems, we attempted to have at least five samples per group, particularly for *in vivo* studies. All experiments were repeated at least once, unless otherwise stated. No mice were excluded from experiments. Occasional individual mice that died post-transplant before analysis could not be included for tissue evaluation.

Graphs indicate the mean and standard error of the mean (s.e.m.) for the various groups. Statistics are based on 'n' biological replicates. All statistical tests performed were two-sided. For the comparisons of two groups, a t-test or non-parametric test was performed. Adjustments for multiple comparisons were made. In most cases, non-parametric testing was performed if normal distribution could not be assumed. RT-qPCR reactions and ordinal outcome variables were tested non-parametrically. All analyses of statistical significance were calculated and displayed compared with the reference control group unless otherwise stated.

Statistical analyses of organoid numbers were based on individual wells. To account for intra-individual and intra-experimental variation as well, all *ex vivo* experiments were performed at least twice with several wells per condition, unless otherwise stated, and sample material coming from at least two different mice or two different human donors. Statistical analyses of cell numbers (stem cells, Ki67<sup>+</sup> cells), crypt numbers, or measurements (crypt, villus) *in vivo* were performed on several independent sections from multiple mice. Statistical analyses and display graphs were generated using Graphpad Prism. A p-value < .05 was considered statistically significant.

### **Author contributions**

V.A. designed, performed, and analyzed *in vivo* and *ex vivo* experiments and drafted the manuscript. S.A.J. designed, performed and analyzed human *ex vivo* experiments. W.Y.C. performed and analyzed *in vivo* and *ex vivo* experiments. G.T. designed, performed and analyzed survival experiments. M.C. and S.T. provided input, designed and performed

experiments, and helped with various assays. P.V., Y.F., and T.I. performed and analyzed *in vivo* experiments. A.E. and J.K. performed and monitored bone marrow transplants and maintained the mouse colonies. C.L. analyzed intestinal histopathology. B.R.B., C.A.L., and A.M.H. supervised the research.

### **Acknowledgements**

We thank H. Clevers for sharing mice and Sean M. Devlin for assisting with statistical analyses, and we gratefully acknowledge the technical assistance of the MSKCC Research Animal Resource Center and Molecular Cytology Core Facility.

### **Funding**

This research was supported by NIH award numbers R01-HL125571, R01-HL146338, and R01-HL145631 (A.M.H.); R01 HL56067, R01 HL155114, R01 HL11870 and R37 AI34495 (B.R.B.); P30-CA008748 (MSKCC Core Grant). Support was also received from the Susan and Peter Solomon Divisional Genomics Program, the Ludwig Center for Cancer Immunotherapy, the Parker Institute for Cancer Immunotherapy, and the Anna Fuller Fund (A.M.H.). V.A. was supported by the German Research Foundation (DFG). S.T. was supported by a scholarship from the Mochida Memorial Foundation for Medical and Pharmaceutical Research and an ASBMT (now ASTCT) New Investigator Award. Y.F. was also supported by an ASBMT/ASTCT New Investigator Award and an Amy Strelzer Manasevit Research Fellowship, and P.V. was supported by an ASBMT/ASTCT New Investigator Award and the American Italian Cancer Foundation. C.A.L. was supported by the WKZ Fund of the UMC Utrecht, and S.A.J. was supported by an Alexandre Suerman Stipend of the UMC Utrecht.

### **Conflict of interest**

Evive Biotech (formerly Generon LLC) provided F-652 for use in experimental models presented here and provided funding for a separate clinical trial using F-652 in patients with GI GVHD. C.A.L. and A.M.H. hold intellectual property related to Interleukin-22 and GVHD. B.R.B. receives remuneration as an advisor to Magenta Therapeutics and BlueRock Therapeutics, has research funding from BlueRock Therapeutics, Rheos Medicines, Equilibre Biopharmaceuticals, and Carisma Therapeutics, Inc., and is a co-founder of Tmunity Therapeutics.



## References

1. Peled JU, Hanash AM, and Jenq RR. Role of the intestinal mucosa in acute gastrointestinal GVHD. *Blood*. 2016;128(20):2395-402.
2. Barker N, van Es JH, Kuipers J, Kujala P, van den Born M, Cozijnsen M, et al. Identification of stem cells in small intestine and colon by marker gene Lgr5. *Nature*. 2007;449(7165):1003-7.
3. Hill GR, Crawford JM, Cooke KR, Brinson YS, Pan L, and Ferrara JL. Total body irradiation and acute graft-versus-host disease: the role of gastrointestinal damage and inflammatory cytokines. *Blood*. 1997;90(8):3204-13.
4. van der Velden WJ, Herbers AH, Feuth T, Schaap NP, Donnelly JP, and Blijlevens NM. Intestinal damage determines the inflammatory response and early complications in patients receiving conditioning for a stem cell transplantation. *PLoS One*. 2010;5(12):e15156.
5. Melson J, Jakate S, Fung H, Arai S, and Keshavarzian A. Crypt loss is a marker of clinical severity of acute gastrointestinal graft-versus-host disease. *Am J Hematol*. 2007;82(10):881-6.
6. Washington K, and Jagasia M. Pathology of graft-versus-host disease in the gastrointestinal tract. *Hum Pathol*. 2009;40(7):909-17.
7. Kreisel W, Dahlberg M, Bertz H, Harder J, Potthoff K, Deibert P, et al. Endoscopic diagnosis of acute intestinal GVHD following allogeneic hematopoietic SCT: a retrospective analysis in 175 patients. *Bone Marrow Transplant*. 2012;47(3):430-8.
8. Naymagon S, Naymagon L, Wong SY, Ko HM, Renteria A, Levine J, et al. Acute graft-versus-host disease of the gut: considerations for the gastroenterologist. *Nat Rev Gastroenterol Hepatol*. 2017;14(12):711-26.
9. Zeiser R, and Blazar BR. Acute Graft-versus-Host Disease - Biologic Process, Prevention, and Therapy. *N Engl J Med*. 2017;377(22):2167-79.
10. Martin PJ, Rizzo JD, Wingard JR, Ballen K, Curtin PT, Cutler C, et al. First- and second-line systemic treatment of acute graft-versus-host disease: recommendations of the American Society of Blood and Marrow Transplantation. *Biol Blood Marrow Transplant*. 2012;18(8):1150-63.
11. Hill L, Alousi A, Kebriaei P, Mehta R, Rezvani K, and Shpall E. New and emerging therapies for acute and chronic graft versus host disease. *Ther Adv Hematol*. 2018;9(1):21-46.
12. Mielcarek M, Storer BE, Boeckh M, Carpenter PA, McDonald GB, Deeg HJ, et al. Initial therapy of acute graft-versus-host disease with low-dose prednisone does not compromise patient outcomes. *Blood*. 2009;113(13):2888-94.
13. Van Lint MT, Uderzo C, Locasciulli A, Majolino I, Scime R, Locatelli F, et al. Early treatment of acute graft-versus-host disease with high- or low-dose 6-methylprednisolone: a multicenter randomized trial from the Italian Group for Bone Marrow Transplantation. *Blood*. 1998;92(7):2288-93.
14. Rhen T, and Cidlowski JA. Antiinflammatory action of glucocorticoids—new mechanisms for old drugs. *N Engl J Med*. 2005;353(16):1711-23.
15. Aranda CJ, Arredondo-Amador M, Ocon B, Lavin JL, Aransay AM, Martinez-Augustin O, et al. Intestinal epithelial deletion of the glucocorticoid receptor NR3C1 alters expression of inflammatory mediators and barrier function. *FASEB J*. 2019;33(12):14067-82.
16. Muzzi C, Watanabe N, Twomey E, Meers GK, Reichardt HM, Bohnenberger H, et al. The Glucocorticoid Receptor in Intestinal Epithelial Cells Alleviates Colitis and Associated Colorectal Cancer in Mice. *Cell Mol Gastroenterol Hepatol*. 2021;11(5):1505-18.
17. Gama P, Goldfeder EM, de Moraes JC, and Alvares EP. Cell proliferation and death in the gastric epithelium of developing rats after glucocorticoid treatments. *Anat Rec*. 2000;260(3):213-21.
18. Gunin AG, and Nikolaev DV. Effect of acute and chronic glucocorticoid treatments on epithelial cell proliferation in the esophagus and small intestine of rats. *J Gastroenterol*. 1999;34(6):661-7.
19. Jung S, Fehr S, Harder-d'Heureuse J, Wiedenmann B, and Dignass AU. Corticosteroids impair intestinal epithelial wound repair mechanisms in vitro. *Scand J Gastroenterol*. 2001;36(9):963-70.
20. Song Q, Wang X, Wu X, Kang TH, Qin H, Zhao D, et al. IL-22-dependent dysbiosis and mononuclear phagocyte depletion contribute to steroid-resistant gut graft-versus-host disease in mice. *Nat Commun*. 2021;12(1):805.
21. Toubai T, Rossi C, Tawara I, Liu C, Zajac C, Oravec-Wilson K, et al. Murine Models of Steroid Refractory Graft-versus-Host Disease. *Sci Rep*. 2018;8(1):12475.
22. Haber AL, Biton M, Rogel N, Herbst RH, Shekhar K, Smillie C, et al. A single-cell survey of the small intestinal epithelium. *Nature*. 2017;551(7680):333-9.
23. Fujii M, Matano M, Toshimitsu K, Takano A, Mikami Y, Nishikori S, et al. Human Intestinal Organoids Maintain Self-Renewal Capacity and Cellular Diversity in Niche-Inspired Culture Condition. *Cell Stem Cell*. 2018;23(6):787-93 e6.
24. Sato T, Vries RG, Snippert HJ, van de Wetering M, Barker N, Stange DE, et al. Single Lgr5 stem cells build crypt-villus structures in vitro without a mesenchymal niche. *Nature*. 2009;459(7244):262-5.
25. Hua G, Thin TH, Feldman R, Haimovitz-Friedman A, Clevers H, Fuks Z, et al. Crypt base columnar stem cells in small intestines of mice are radioresistant. *Gastroenterology*. 2012;143(5):1266-76.
26. Martin ML, Adileh M, Hsu KS, Hua G, Lee SG, Li C, et al. Organoids Reveal That Inherent Radiosensitivity of Small and Large Intestinal Stem Cells Determines Organ Sensitivity. *Cancer Res*. 2020;80(5):1219-27.



27. Reddy P, Negrin R, and Hill GR. Mouse models of bone marrow transplantation. *Biol Blood Marrow Transplant.* 2008;14(1 Suppl 1):129-35.
28. Takashima S, Martin ML, Jansen SA, Fu Y, Bos J, Chandra D, et al. T cell-derived interferon-gamma programs stem cell death in immune-mediated intestinal damage. *Sci Immunol.* 2019;4(42).
29. Hanash AM, Dudakov JA, Hua G, O'Connor MH, Young LF, Singer NV, et al. Interleukin-22 protects intestinal stem cells from immune-mediated tissue damage and regulates sensitivity to graft versus host disease. *Immunity.* 2012;37(2):339-50.
30. Lindemans CA, Calafiore M, Mertelsmann AM, O'Connor MH, Dudakov JA, Jenq RR, et al. Interleukin-22 promotes intestinal-stem-cell-mediated epithelial regeneration. *Nature.* 2015;528(7583):560-4.
31. Surjit M, Ganti KP, Mukherji A, Ye T, Hua G, Metzger D, et al. Widespread negative response elements mediate direct repression by agonist-liganded glucocorticoid receptor. *Cell.* 2011;145(2):224-41.
32. Ishihara H, Tanaka I, Yakumaru H, Tanaka M, Satoh A, Ishiwata A, et al. Acceleration of regeneration of mucosa in small intestine damaged by ionizing radiation using anabolic steroids. *Radiat Res.* 2011;175(3):367-74.
33. Malard F, Huang XJ, and Sim JPY. Treatment and unmet needs in steroid-refractory acute graft-versus-host disease. *Leukemia.* 2020;34(5):1229-40.
34. Zeiser R, von Bubnoff N, Butler J, Mohty M, Niederwieser D, Or R, et al. Ruxolitinib for Glucocorticoid-Refractory Acute Graft-versus-Host Disease. *N Engl J Med.* 2020;382(19):1800-10.
35. Nishiwaki S, Nakayama T, Murata M, Nishida T, Terakura S, Saito S, et al. Dexamethasone palmitate ameliorates macrophages-rich graft-versus-host disease by inhibiting macrophage functions. *PLoS One.* 2014;9(5):e96252.
36. Theiss-Suennemann J, Jorss K, Messmann JJ, Reichardt SD, Montes-Cobos E, Luhder F, et al. Glucocorticoids attenuate acute graft-versus-host disease by suppressing the cytotoxic capacity of CD8(+) T cells. *J Pathol.* 2015;235(4):646-55.
37. Toubai T, and Magenau J. Immunopathology and biology-based treatment of steroid-refractory graft-versus-host disease. *Blood.* 2020;136(4):429-40.
38. Holtan SG, Shabaneh A, Betts BC, Rashidi A, MacMillan ML, Ustun C, et al. Stress responses, M2 macrophages, and a distinct microbial signature in fatal intestinal acute graft-versus-host disease. *JCI Insight.* 2019;5.
39. Takahashi S, Hashimoto D, Hayase E, Ogasawara R, Ohigashi H, Ara T, et al. Ruxolitinib protects skin stem cells and maintains skin homeostasis in murine graft-versus-host disease. *Blood.* 2018;131(18):2074-85.
40. Wu SR, and Reddy P. Tissue tolerance: a distinct concept to control acute GVHD severity. *Blood.* 2017;129(13):1747-52.
41. Gronke K, Hernandez PP, Zimmermann J, Klose CSN, Kofoed-Branzk M, Guendel F, et al. Interleukin-22 protects intestinal stem cells against genotoxic stress. *Nature.* 2019;566(7743):249-53.
42. Stefanich EG, Rae J, Sukumaran S, Lutman J, Lekkerkerker A, Ouyang W, et al. Pre-clinical and translational pharmacology of a human interleukin-22 IgG fusion protein for potential treatment of infectious or inflammatory diseases. *Biochem Pharmacol.* 2018;152:224-35.
43. Bruce DW, Stefanski HE, Vincent BG, Dant TA, Reisdorf S, Bommiasamy H, et al. Type 2 innate lymphoid cells treat and prevent acute gastrointestinal graft-versus-host disease. *J Clin Invest.* 2017;127(5):1813-25.
44. Dudakov JA, Mertelsmann AM, O'Connor MH, Jenq RR, Velardi E, Young LF, et al. Loss of thymic innate lymphoid cells leads to impaired thymopoiesis in experimental graft-versus-host disease. *Blood.* 2017;130(7):933-42.
45. Ziesche E, Scheiermann P, Bachmann M, Sadik CD, Hofstetter C, Zwissler B, et al. Dexamethasone suppresses interleukin-22 associated with bacterial infection in vitro and in vivo. *Clin Exp Immunol.* 2009;157(3):370-6.
46. Yin X, Farin HF, van Es JH, Clevers H, Langer R, and Karp JM. Niche-independent high-purity cultures of Lgr5+ intestinal stem cells and their progeny. *Nat Methods.* 2014;11(1):106-12.
47. Alpdogan O, Muriqlan SJ, Eng JM, Willis LM, Greenberg AS, Kappel BJ, et al. IL-7 enhances peripheral T cell reconstitution after allogeneic hematopoietic stem cell transplantation. *J Clin Invest.* 2003;112(7):1095-107.
48. Cooke KR, Kobzik L, Martin TR, Brewer J, Delmonte J, Jr., Crawford JM, et al. An experimental model of idiopathic pneumonia syndrome after bone marrow transplantation: I. The roles of minor H antigens and endotoxin. *Blood.* 1996;88(8):3230-9.
49. Luecken MD, and Theis FJ. Current best practices in single-cell RNA-seq analysis: a tutorial. *Mol Syst Biol.* 2019;15(6):e8746.
50. Wolf FA, Angerer P, and Theis FJ. SCANPY: large-scale single-cell gene expression data analysis. *Genome Biol.* 2018;19(1):15.
51. Johnson WE, Li C, and Rabinovic A. Adjusting batch effects in microarray expression data using empirical Bayes methods. *Biostatistics.* 2007;8(1):118-27.
52. Becht E, McInnes L, Healy J, Dutertre CA, Kwok IWH, Ng LG, et al. Dimensionality reduction for visualizing single-cell data using UMAP. *Nat Biotechnol.* 2018.
53. van Dijk D, Sharma R, Nainys J, Yin K, Kathail P, Carr AJ, et al. Recovering Gene Interactions from Single-Cell Data Using Data Diffusion. *Cell.* 2018;174(3):716-29 e27.
54. Blondel VD, Guillaume J-L, Lambiotte R, and Lefebvre E. Fast unfolding of communities in large networks. *Journal of Statistical Mechanics: Theory and Experiment.* 2008;2008(10):P10008.
55. Butler A, Hoffman P, Smibert P, Papalexi E, and Satija R. Integrating single-cell transcriptomic data across different conditions, technologies, and species. *Nat Biotechnol.* 2018;36(5):411-20.



56. Hao YH, Hao S, Andersen-Nissen E, Mauck WM, Zheng SW, Butler A, et al. Integrated analysis of multimodal single-cell data. *Cell*. 2021;184(13):3573-+.
57. Satija R, Farrell JA, Gennert D, Schier AF, and Regev A. Spatial reconstruction of single-cell gene expression data. *Nat Biotechnol*. 2015;33(5):495-502.
58. Stuart T, Butler A, Hoffman P, Hafemeister C, Papalexi E, Mauck WM, 3rd, et al. Comprehensive Integration of Single-Cell Data. *Cell*. 2019;177(7):1888-902 e21.





# 7

## Challenges and opportunities targeting mechanisms of epithelial injury and recovery in acute intestinal Graft-versus-Host disease

Suze A. Jansen, Edward E. S. Nieuwenhuis, Alan M. Hanash, Caroline A. Lindemans

Mucosal Immunol. 2022 Apr;15(4):605-619.  
doi: 10.1038/s41385-022-00527-6. Epub 2022 Jun 2. PMID: 35654837.

## Abstract

Despite advances in immunosuppressive prophylaxis and overall supportive care, gastrointestinal (GI) graft-versus-host disease (GVHD) remains a major, lethal side effect after allogeneic hematopoietic stem cell transplantation (allo-HSCT). It has become increasingly clear that the intestinal epithelium, in addition to being a target of transplant-related toxicity and GVHD, plays an important role in the onset of GVHD. Over the last two decades, increased understanding of the epithelial constituents and their microenvironment has led to the development of novel prophylactic and therapeutic interventions, with the potential to protect the intestinal epithelium from GVHD-associated damage and promote its recovery following insult. In this review, we will discuss intestinal epithelial injury and the role of the intestinal epithelium in GVHD pathogenesis. In addition, we will highlight possible approaches to protect the GI tract from damage posttransplant and to stimulate epithelial regeneration, in order to promote intestinal recovery. Combined treatment modalities integrating immunomodulation, epithelial protection, and induction of regeneration may hold the key to unlocking mucosal recovery and optimizing therapy for acute intestinal GVHD.

## Introduction

Damage to the gastrointestinal (GI) tract is a common occurrence following allogeneic hematopoietic stem cell transplantation (allo-HSCT)<sup>1,2</sup>. Several factors are thought to contribute to this damage, including pretransplant conditioning, posttransplant activation of alloreactive T cells, and both tissue-targeted and immunomodulatory effects of the intestinal microbiota (Figs. 1, 2). Before transplantation of a donor allograft, the recipient receives chemotherapy±irradiation conditioning to kill residual malignant cells, weaken the recipient's immune system, and create space for donor hematopoietic engraftment. However, the required pretransplant conditioning can also cause significant damage to cycling cells in the epithelial gut lining, resulting in mucositis and disruption of the mucosal barrier. Impaired barrier function leads to exposure of the basolateral intestinal epithelial cell (IEC) membranes and lamina propria leukocytes to luminal contents. Activation of the immune system in this context may cause the development of acute Graft-versus-Host Disease (aGVHD). In aGVHD, transplanted donor T cells recognize antigens in the recipient and launch an inflammatory attack against the recipients' tissues such as the skin, intestines, and liver<sup>1,3,4</sup>. Despite prophylactic immunosuppression and careful HLA-matching, ~30–50% of allo-HSCT patients develop GVHD symptoms, half of which include significant GI tract involvement manifesting in nausea, anorexia, and diarrhea. In addition, poor barrier function contributes to potentially life-threatening bloodstream infections in these immunocompromised patients. The immunosuppression and high dose corticosteroids necessary for treatment of GI-GVHD provide additional potential complications, even when GVHD can be successfully treated. As such, GI-GVHD remains an important cause of transplant-related morbidity and mortality<sup>1,2</sup>.

Current GI-GVHD treatment focuses mainly on suppressing posttransplant aberrant immune responses with corticosteroids<sup>3,5</sup>, but this approach is often ineffective. Up to 50% of patients develop steroid-refractory (SR)-GVHD and require additional treatment<sup>6</sup>. The Jak1/2-inhibitor Ruxolitinib (Rux) is currently the only FDA-approved treatment for SR-GVHD<sup>7</sup>. Other second and third-line therapies lack consistent demonstrated benefit, and are mostly based on providing additional immunosuppression. This causes most GVHD therapeutic approaches to be accompanied by an increased risk of infection and a potentially reduced graft-versus-leukemia (GVL) effect.

An evolving understanding of intestinal homeostasis and its related epithelial constituents has led to new treatment opportunities that aim to protect the intestines peri-transplant, without impairing the recovery of physiologic immune function posttransplant. It has also become increasingly clear that the intestinal epithelium is not only a direct target of GVHD-associated damage, but in addition may take part in the development and propagation of the disease, and possibly in its resolution as well<sup>8</sup>. In this review we focus specifically on the



role of the intestinal epithelium and epithelial injury in GVHD initiation, and how it can be protected from transplant-associated insult. Furthermore, strategies to promote epithelial restoration by improving regeneration and augmenting posttransplant epithelial recovery are discussed, both through regulating epithelial-intrinsic constituents as well as factors supplied by the microenvironment.

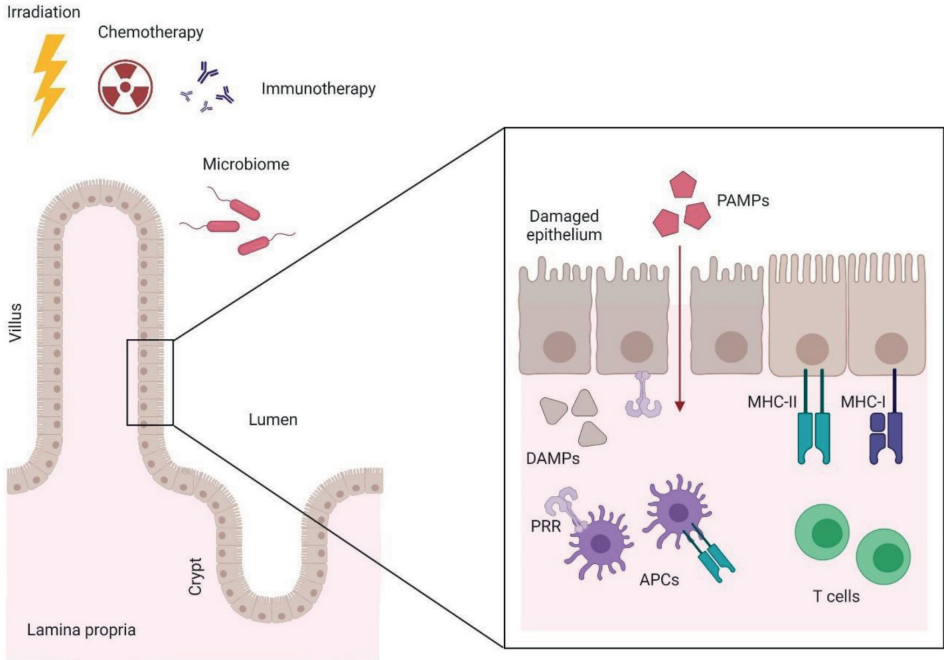


**Figure 1. The pivotal role of the intestinal epithelium and epithelial damage in GVHD onset.**

Irradiation, chemotherapy and/or immunotherapy used in the conditioning regimen before HSCT damages the intestinal epithelial cells and disrupts barrier protecting the recipient from luminal pathogens. Translocating PAMPs and released DAMPs bind to their corresponding PRRs and activate the innate immune system, including APCs. Antigen presentation by APCs, including the intestinal epithelium, lead to the propagation and activation of alloreactive T cells, which cause further damage through cytokine- and cell-cell mediated toxicity in the then developed GVHD. Created with BioRender.com.



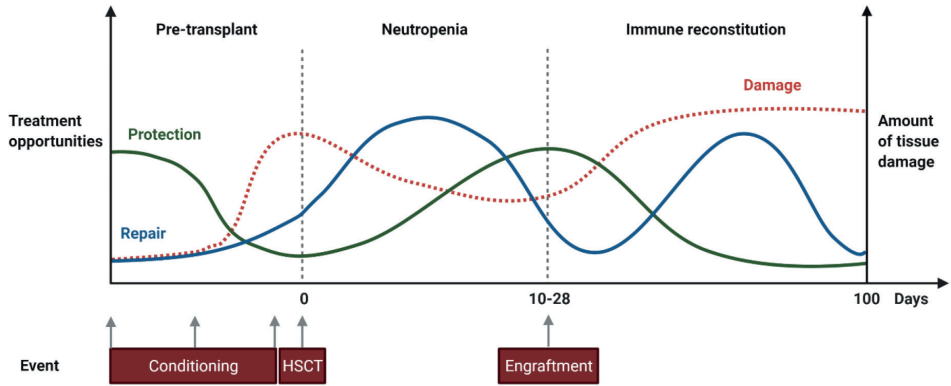


**Figure 2. Opportunities for intestinal protection and repair over the course of HSCT.**

Damage to the intestinal epithelium over the course of HSCT occurs in different phases. As such, opportunities for protection against the insult and repair of the injury occur in parallel, rather than after the fact. The timing of these different approaches will be crucial, since certain treatment opportunities may have pleiotropic effects on other cell types at different time points during the post-transplant period. Created with BioRender.com.

## Preventing intestinal epithelial damage

### Minimizing conditioning-induced injury

The intestinal epithelial barrier forms the first line of defense between the lumen and the underlying immune system in the gut<sup>9</sup>. As such it protects the recipient from harmful gut contents, including pathogens. The barrier is formed by the plasma membranes of a single layer of IECs that are tightly connected with tight junctions (TJ). The IEC lining is covered with a protective, extracellular layer of mucus produced by epithelial Goblet cells, which inhibits direct contact between the IEC and gut luminal particles and bacteria. The mucosal immune cells are present within the epithelial compartment, as well as in the lamina propria below, and in designated lymphoid regions called Peyer's patches. In addition to providing a physical barrier, the epithelial cell layer is essential for the absorption and transport of nutrients and water. Both integrity and functionality of the epithelial barrier are crucial elements in the course of transplant, as loss is associated with systemic infections, severe GI symptoms like anorexia/diarrhea and poor outcome in general<sup>2</sup>.

Pretransplant conditioning is recognized as an early insult to this barrier integrity<sup>10</sup>. In both preclinical models and human studies overall aGVHD severity is associated with the intensity of the pretransplant conditioning regimen<sup>11,12</sup>. In mice, high intensity regimens were associated with reduced mucus layer thickness and the presence of bacterial RNA in the colon lamina propria<sup>13</sup>. Indeed, total body irradiation (TBI) and chemotherapy treatment led to significant leakage



of orally administered FITC-labeled dextran into the bloodstream, indicating consequential compromise of the epithelial barrier<sup>14</sup>. In a study by Nalle et al. preconditioning-induced damage to the epithelium was even required to induce aGVHD in a MHC-matched minor-histocompatibility-antigen (miHA)-mismatched transplantation<sup>10,15</sup>. In humans, compromised epithelial integrity, as measured by 51Cr-EDTA absorption, has been documented in association with myeloablative regimens even 14 days after stem cell infusion<sup>16,17</sup>. Conditioning toxicity is also associated with the release of pro-inflammatory cytokines in the GI tract, which can contribute to GVHD development<sup>11,18,19</sup>. In particular, TBI appears to be associated with both a higher aGVHD incidence<sup>20</sup> and treatment-related mortality<sup>21</sup>.

The implementation of reduced intensity conditioning (RIC) regimens has decreased conditioning-associated tissue toxicity and enabled older and more fragile patients to undergo allo-HSCT. Regimens typically include an alkylating agent like busulfan (Bu), melphalan or cyclophosphamide (Cy) and a purine analog such as fludarabine (Flu), with or without low-dose TBI. Clinical GI toxicity of RIC transplants is reported to be moderate<sup>22,23</sup>, and the associated intestinal epithelial damage<sup>16,17</sup> and mucositis<sup>24</sup> have been found to be less severe. The occurrence of aGVHD after RIC is reduced as well<sup>25</sup>. Additionally, more favorable combinations of agents have been applied to this approach. For example, in reducing the number of combined alkylators, Bu/Flu has a more favorable toxicity profile than Bu/Cy in patients across HSCT indications, while still providing a myeloablative regimen<sup>26,27,28</sup>.

More recent developments in conditioning regimen tolerability have focused on tailored dosing based on chemotherapy plasma levels of the individual patient to reduce exposure and consequent epithelial damage. This concept is known as reduced toxicity conditioning (RTC). The superiority of pharmacokinetic (PK)-directed dosing for intravenous Bu in adults has been established for over a decade with both enhanced safety<sup>29</sup> and efficacy<sup>30</sup>. Similar results were found in children<sup>31,32</sup>. Additionally, Flu exposure, as calculated by a PK-model, was recently retrospectively demonstrated to be a strong predictor of HSCT survival in adults<sup>33</sup>. In conclusion, PK-directed dosing of favorable chemotherapeutic combinations will hopefully further reduce conditioning-related toxicity and development of acute GVHD in the near future.

### **Preventing deleterious responses to PAMPS and DAMPS**

Upon intestinal barrier breach, translocating pathogen-associated molecular patterns (PAMPs) and tissue-released damage-associated molecular patterns (DAMPs) are recognized by pattern recognition receptors (PRRs), which activate the innate immune system. Concurrently, the development of alloreactive responses can be initiated<sup>34,35,36</sup>. As such, many DAMPs, PAMPs and corresponding PRRs have been implicated in the development of GVHD, and multiple approaches have been taken to dampen the response at this level (Table 1). Firstly, scavenging or breaking down the PAMPs and DAMPs would ascertain they do not reach

the target immune cell. Examples are treatment with anti-LPS<sup>37</sup>, HSP90-inhibitor 17AAG<sup>38</sup>, locked nucleic acid anti-miRNA-29a<sup>39</sup>, uricase for uric acid<sup>40</sup>, apyrase for ATP<sup>41</sup>, NecroX-7 for HMGB1 blockade<sup>42</sup> and alpha-1-antitrypsin (AAT) targeting heparin sulfate<sup>43</sup>, all of which have been shown to reduce GVHD in mouse models and AAT in addition SR-GVHD in humans<sup>44</sup>. Secondly, binding of DAMPs to target immune cells can be blocked, e.g., by P2X7R antagonists, blocking ATP binding<sup>41,45</sup>, or anti-TIM-1 monoclonal antibodies, inhibiting binding to phosphatidylserine on apoptotic cell debris<sup>46</sup>. Thirdly, responsiveness of immune cells to DAMPS could be modulated. MicroRNA-155 deficiency in host DCs protected against GVHD through reduced purinergic receptor and inflammasome-associated gene expression, and concurrent reduced IL-1 $\beta$  release<sup>47</sup>. Inhibiting microRNA-155 with antagomir could be a promising new approach. Contrarily, Siglecs play a crucial role in mitigating specifically DAMP-induced immune responses<sup>48,49</sup>. Following conditioning-mediated tissue damage, the interaction of Siglec-G on host APCs with the glycoprotein CD24 on T cells was essential for GVHD protection in both a MHC-matched and mismatched mouse model<sup>50</sup>. Enhancing the Siglec-CD24 interaction with a CD24-Fc fusion protein mitigated GVHD in experimental GVHD<sup>50,51</sup>. The results of a phase II trial testing the safety of CD24-Fc for the prevention of aGVHD following myeloablative allo-HSCT are expected shortly.

**Table 1. All DAMPS/PAMPS implicated in GI-GVHD and targeted therapy options**

Receptor	DAMP/PAMP	Signaling pathway	Effect on GVHD	Therapeutic options	Ref
TLR3	dsRNA	TRIF	=	-	215
TLR2/4	HMGB1	MyD88	-	NecroX-7	42
TLR4	LPS	MyD88/TRIF	-	Anti-LPS	37
TLR4	Heparan sulphate	MyD88	-	AAT	43,44
TLR4	S100 proteins	MyD88	-	-	216
TLR4/CD14	HSP90	MyD88	-	17-AAG	38
TLR5	Flagellin	MyD88	+	Flagellin treatment	217
TLR7/8	ssRNA MiR29a	MyD88	-	locked nucleic acid anti-miRNA-29a	39,218
TLR9	Bacterial DNA	MyD88	-	-	54,184
cGAS	Bacterial DNA	STING	+	DNA treatment	184
RIG-I	dsRNA	MAVS	+	3pRNA treatment	184
Caspase-11	LPS	Pyroptosis/ NLRP3	-	-	56
?	Uric acid	NLRP3	-	Uricase	40
P2X7	ATP	NLRP3	-	Apyrase P2X7R antagonists	41,45
NOD2	Eg MDP	NLRC	+	-	190
?	?	NLRP6	-	-	52
TIM	Phosphatidylserine	?	-	Anti-TIM	46
ST2	IL-33	MyD88	-	ST2-Fc treatment	219

+ alleviating, = no effect, - worsening.



Additionally, targeting innate signaling pathways downstream of PRRs might be a future therapeutic approach<sup>52,53,54,55,56</sup>. Interestingly, host TLR deficiency was found to be protective against GVHD in murine studies<sup>53,54</sup>, but inhibition of TLR and inflammasome pathway signaling (via MyD88 and TRIF) only in host hematopoietic cells did not reduce GVHD<sup>55</sup>. This suggests a GVHD-promoting role of non-hematopoietic tissue signaling. More importantly, deficiency of TLR9<sup>54</sup> and NLRP6 inflammasome<sup>52</sup> was protective only when it was restricted to the non-hematopoietic compartment, indicating that TLR signaling at the tissue level, which includes the intestinal epithelial compartment, may be a future target for GVHD reduction. Despite the numerous possibilities of molecules and pathways to block, only very few damage-modulating agents have led to successful clinical trial results. Probably, the concurrent involvement of many different damage molecules as well as redundant downstream signaling pathways, make achieving significant clinical improvements by targeting just one molecule unlikely. Alternatively, involved molecules and signaling pathways may have concurrent roles in the resolution of GVHD, and targeting them would abrogate this, giving no net improvement.

### **Preventing cell death within the epithelial compartment**

Under homeostatic conditions, the intestinal epithelium is continuously regenerated by stem and progenitor cells that are present within the crypt region (Fig. 3). While a point of longstanding debate, work from the last 15 years has identified Lgr5-expressing crypt base columnar (CBC) cells as intestinal stem cells (ISCs) capable of giving rise to all other cell types of mouse and human intestinal epithelium *in vivo* and *ex vivo*<sup>57,58,59</sup>. Olfm4 is another marker identifying ISCs<sup>60</sup> in humans and in mouse small intestine. ISCs are maintained by both secreted and membrane-bound molecules of surrounding cells, together constituting the ISC niche<sup>61</sup>. These niche cells include Paneth cells (PCs), which lie interspersed between CBC ISCs at the bottom of the crypt and promote stemness through the release of Wnt3 and EGF, which bind to their respective receptors Frizzled–LRP5–LRP6 complex and ERBB1 on CBCs<sup>62,63</sup>. PCs also express Notch ligands DLL1 and DLL4 on the cell-surface that directly interact with ISC Notch receptors such as NOTCH1 to maintain stemness and inhibit differentiation into secretory-cell lineages<sup>62</sup>. Crypt-adjacent stromal cells also promote ISC maintenance through the secretion of Wnts<sup>64</sup> and R-spondins (Rspo)<sup>65,66</sup>. Rspo-binding of LGR5 on the ISC potentiates Wnt signaling by phosphorylation and stabilization of  $\beta$ -catenin in the cytoplasm, thus promoting subsequent translocation to the nucleus<sup>67</sup>. To protect ISCs from mesenchymal-derived epithelium-maturing BMP2 and BMP4 signals<sup>68,69</sup>, myofibroblasts and smooth muscle cells around the crypt bottom secrete BMP-inhibitor proteins such as Gremlin 1 and Gremlin 2 that sequester BMPs before they can bind the BMP receptors<sup>70,71</sup>. As epithelial precursors continue to proliferate and move up the crypt, they give rise to the highly proliferative transit amplifying (TA) cell compartment. Finally, differentiation into the destined cell type of for instance the absorptive or secretory lineage occurs under the influence of both environmental and intrinsically programmed factor dynamics<sup>63</sup>.

When aGVHD of the gut develops, the histopathology characteristically demonstrates epithelial apoptosis within intestinal crypts<sup>72,73</sup>. In addition to crypt loss, the number of CBC ISCs per crypt is reduced in experimental GVHD<sup>74,75,76,77</sup>. Severe colonic crypt loss at the time of GVHD has been associated with delayed recovery, persistence of symptoms, and the development of SR-GVHD<sup>78</sup>, suggesting an impaired capacity to recover beyond the initial insult. In addition, PCs are reduced in GVHD<sup>76,77,79,80,81,82,83</sup>, which may hamper their ability to provide the indispensable niche factors Wnt3, EGF and membrane-bound Notch ligands for the maintenance of ISC integrity. Besides their role as regulators of ISC proliferation, PCs play an important physiologic role in the production of antimicrobial (AMP) and the release of immunomodulatory proteins (e.g., IgA, IL-1 $\beta$ ), both key components of host defense in the gut<sup>84</sup>. A-defensins are a major class of AMPs produced by PCs, and their production is markedly reduced in experimental GVHD<sup>80,81</sup>, as well as in GVHD patients<sup>83</sup>. Loss of PC  $\alpha$ -defensins has been associated with decreased bacterial diversity and domination of bacterial species such as Proteobacteria at the phylum level, Enterobacteriales at the order level, and Escherichia and Bacteroides at the genus level, some of which pathogenic<sup>80,81</sup>. Interestingly, increased plasma levels of the AMP REG3 $\alpha$  act as a biomarker of GI-GVHD, predictive of response to therapy, non-relapse mortality and survival<sup>85</sup>. Murine transplant recipients deficient in Reg3 $\gamma$ , the claimed mouse ortholog of REG3 $\alpha$ , developed more severe GI-GVHD with increased crypt apoptosis<sup>86</sup>. As such, PC deficiency may contribute to GVHD pathology due to the impairment of ISC niche functions as well as through a reduction in bacterial containment.

Up until recently it was uncertain whether crypt loss in GVHD was directly caused by the effector mechanisms of allo-T cells. Using 3D microscopy, donor T cells were shown to primarily invade the intestinal crypt region early after allo-BMT<sup>77,87</sup>. The potential of allo-T cells to damage the intestinal crypt compartment was studied using so-called intestinal organoid cultures; self-organizing, 3D mini-guts, that form from isolated crypts or purified ISCs when cultured in the presence of defined ISC niche growth factors EGF, Rspo-1 and BMP-inhibitor Noggin<sup>58</sup>. Intestinal organoids contain multiple epithelial cell types, including Lgr5+ ISCs, and ex vivo culture models with allogeneic T cells recapitulated in vivo ISC damage<sup>77</sup>. Interferon (IFN)- $\gamma$  secreted by allo-T cells directly caused ISC apoptosis through signaling via the IFN $\gamma$  receptor (IFN $\gamma$ R) expressed by ISCs<sup>77</sup>. Interestingly, blocking IFN $\gamma$ R signaling with the JAK1/2-specific inhibitor Ruxolitinib early after allo-BMT protected ISCs from IFN $\gamma$ -induced damage<sup>77</sup>. Ruxolitinib has recently been approved by the FDA for treatment of SR-GVHD<sup>7</sup>. The rationale for its use in GVHD is based on the suppression of allo-T cell activation, proliferation, cytokine production, and promoting a more favorable regulatory T cell to conventional T cell ratio. The findings of this study indicate that earlier posttransplant use might have a beneficial, target-tissue-protective effect in patients developing GI-GVHD<sup>88</sup>.



Finally, other protective mechanisms downstream of T cell-induced cytotoxicity have recently been described, that could protect epithelial cells in preclinical models. For example, inhibition of HSP90 by 17AAG after allo-HSCT protected the ISC niche<sup>38</sup>. HSP90 is released during tissue damage and induces the intracellular response to ER stress, which PCs are particularly sensitive to<sup>89</sup>. Administration of 17AAG was found to decrease the ER stress actor expression and increase the level of spliced XBP1 important for the regulation of the unfolded-protein response, and preserved both PCs and ISCs in two MHC-mismatched models<sup>38</sup>. A second example concerns serine protease inhibitor 6 (Spi6), the only known endogenous inhibitor of the cytolytic serine protease Granzyme B (GzmB) which protects immune cells from GzmB-mediated damage. In a GVHD model, host Spi6 expression in the non-hematopoietic compartment played a prominent role in GVHD protection, independently of donor-derived GzmB, and Spi6 was upregulated in the intestinal epithelium upon irradiation and subsequent GVHD induction<sup>90</sup>. A third example is found in the inhibitors of apoptosis proteins (IAPs), which are classically involved in the inhibition of cell death proteases such as caspase 3. IAP inhibition was found to exacerbate GVHD, but not when IAP1/XIAP deficiency was limited to the immune system. This suggests intact tissue IAPs are relevant to tissue protection in GVHD<sup>91</sup>. Patients with XIAP deficiency undergoing allo-HSCT after myeloablative conditioning appear to have a poor overall outcome and extra protection against GVHD may be crucial for successful transplantation of these recipients<sup>92</sup>. A fourth example suggests manipulating epithelial integrity regulators to protect the epithelium in GVHD<sup>93</sup>. The expression of MLCK210, an established factor in epithelial tight junction regulation, was found to be increased in the intestinal epithelium of GVHD patients and mice<sup>93</sup>. MLCK210 deficiency in the host led to decreased barrier dysfunction, lower clinical GVHD sores and increased survival in multiple mouse GVHD models. Target-tissue allo-T cell numbers were lower in MLCK210-deficient hosts, and the GzmB-expressing CD8 T cell fraction in mesenteric lymph nodes (MLNs) was reduced<sup>93</sup>. Multiple mechanisms can attribute to this however, including activation, proliferation and homing of the allo-T cells, as well as epithelial–T cell interaction specific factors. Lastly, a recent study describes the disruption of oxidative phosphorylation in IECs exposed to allo-T cells, caused by a reduction in succinate dehydrogenase A (SDHA), a component of mitochondrial complex II<sup>94</sup>. In colonic biopsies from confirmed GI-GVHD patients the amount of SDHA was reduced in comparison to patients suspected of GI-GVHD that could not be histopathological confirmed. Genetically increasing SDHA levels in an experimental GVHD model reduced clinical and histopathological intestinal GVHD severity. Further study of all four approaches is required to establish usefulness in the clinical setting.

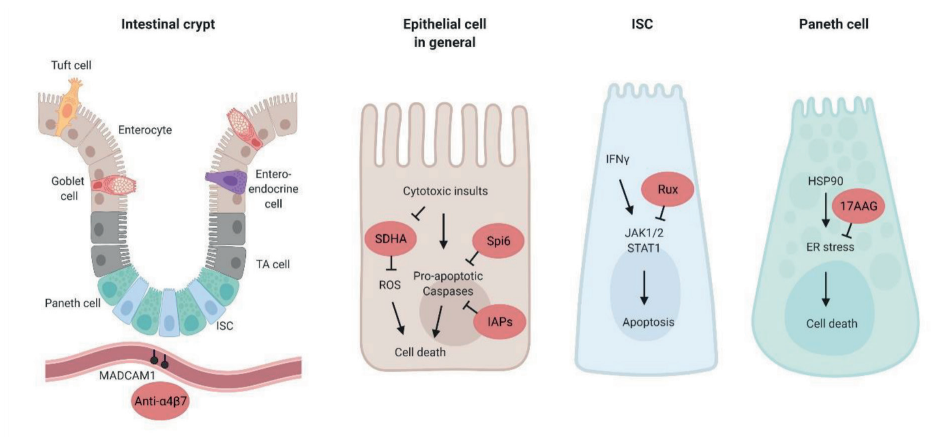


**Figure 3. The intestinal crypt as target, and mechanisms of protection.**

The intestinal epithelium is maintained by intestinal stem cells (ISCs) which reside at the base of intestinal crypts, interspersed between their supportive Paneth cells (PCs) in the small intestine. Along the crypt-villus axis the ISCs differentiate into transit amplifying (TA) cells and their destined lineage, including absorptive (eg enterocyte), secretory (eg PC, Goblet cell, Tuft cells) and enteroendocrine cells. In the vasculature near the intestinal crypt the addressin MAdCAM-1 is expressed, which binds  $\alpha 4\beta 7$ -integrin expressed on gut-directed immune cells. Several approaches to protect at the level of the intestinal epithelial cell in general or in addition at the ISC and PC level specifically are indicated in red.  $\alpha 4\beta 7$  blockade inhibits the influx of T cells into the lower crypt regions of the small intestine; the serine protease inhibitor Spi6 present in the epithelium protects against GVHD-induced damage, possibly through inhibition of caspase 3/7; intestinal epithelial Inhibitor of Apoptosis Proteins (IAPs) inhibits the function of pro-apoptotic caspases; the SDHA enzyme is reduced in IECs after allo T cell insult, increasing reactive oxygen species (ROS) levels; Ruxolitinib (Rux) inhibits JAK1/2-STAT1 signaling, relieving IFN $\gamma$  induced epithelial apoptosis; and 17AAG was reported to suppress ER stress and thereby cell death in a.o. Paneth cells. Created with BioRender.com.

### Preventing T cell trafficking to the gut

Given the epithelial damage caused by allo-T cells, blocking their entry into the intestines provides a promising strategy for tissue protection without increasing global immunosuppression and associated risks of relapse or infection elsewhere. Expression of  $\alpha 4\beta 7$  integrin is an important contributor to T cell homing to the GI tract, and plays a major role in the homing of allo-T cells to the GI tract as well<sup>95,96</sup>. Blocking  $\alpha 4\beta 7$  binding to its constitutively expressed receptor MAdCAM-1 on intestinal endothelium with anti-MAdCAM-1 antibody after GVHD induction<sup>96</sup>, or using  $\alpha 4\beta 7$ -deficient donor T cells<sup>95</sup>, selectively reduced CD8 T cell infiltration in the gut<sup>96</sup> and led to less GI-GVHD<sup>95</sup>. Interestingly, it was recently discovered that MAdCAM-1 expression in the small intestine vasculature localizes predominantly to vessels located in the lower crypt region, offering a possible explanation for the observed pattern of allo-T cells invading the crypt region early posttransplant. As such, inhibition of the  $\alpha 4\beta 7$ -integrin/MAdCAM-1 axis reduced T cell infiltrate into the crypt base region of the mucosa and protected the ISC compartment from GVHD<sup>87</sup>. In a clinical setting, patients with GI-GVHD had a significantly higher percentage of  $\alpha 4\beta 7$ -expressing memory T cell subsets



than patients with skin-only GVHD or patients with no evidence of GVHD<sup>97</sup>. Retrospective studies indicated potential efficacy of vedolizumab, an anti- $\alpha 4\beta 7$  antibody, for reduction of GI-GVHD severity<sup>98,99</sup>. Results of a prospective, dose-finding trial of vedolizumab starting 1 day prior to transplant are promising; the treatment was well tolerated, and the incidence of subsequent GI-GVHD development was low<sup>100</sup>. Blocking the  $\alpha 4\beta 7$  integrin pathway with monoclonal antibodies is therefore a promising strategy for protecting the crypt compartment following allo-HSCT. Antibodies that block only the  $\beta 7$  subunit may hold promise as well. These, in addition to antagonizing the  $\alpha 4\beta 7$ -MAdCAM-1 mediated T cell influx, also target the  $\alpha E\beta 7$ -E-cadherin interaction, believed to be important for T cell retention in the intraepithelial compartment<sup>101</sup>. A phase II clinical trial of the recombinant human anti- $\beta 7$  etrolizumab for inflammatory bowel disease had promising results<sup>102</sup>. Future study will have to show if it can be useful in the treatment of GVHD as well.

In addition to protecting the intestinal epithelium from the effector phase of aGVHD, prophylactic inhibition of T cell entry to the gut may also protect against epithelium-dependent contributions to GVHD development. It was recently reported that intestinal epithelial antigen presentation can propagate alloreactive T cell responses. This is contrary to the notion that host and donor professional antigen presenting cells (APCs) are the principle APC populations contributing to the activation of alloreactive donor T cells<sup>103</sup>. Despite the dominant role of hematopoietic APCs in propagating MHC-I-restricted/CD8 T cell-dependent GVHD<sup>104</sup>, radio-resistant non-hematopoietic APCs could contribute to the initiation of MHC-I-dependent GVHD as well<sup>105</sup>. Furthermore, profound deletion of professional host APCs did not decrease CD4-dependent GVHD in both a MHC-matched miHA-mismatched and a MHC-II-mismatched mouse model<sup>106</sup>. The action of recipient non-hematopoietic, non-professional APCs was sufficient to induce lethal GVHD<sup>107</sup>. MHC-II expression on IECs specifically could thus initiate lethal GVHD immune responses, even in the presence of other types of APCs<sup>108</sup>. As such, approaches to reduce intestinal epithelial MHC-II expression, for instance through the initiation of a high fat diet in mice<sup>109</sup>, may reduce the development of experimental GVHD. Nonetheless, preventing donor T cells from reaching the intestinal epithelium with agents such as vedolizumab may be the most promising approach for reducing intestinal epithelial antigen presentation at the present time.

### **Preventing acute GVHD to prevent chronic GVHD**

In some cases acute GVHD can progress or contribute to the development of chronic GVHD (cGVHD)<sup>110,111</sup>, and aGVHD is a well-defined risk factor for cGVHD<sup>12</sup>. While certain aspects of acute GVHD pathophysiology may be shared with cGVHD, such as the involvement of Th17/Tc17<sup>112,113</sup>, there is a paucity in research data studying the links between intestinal epithelial injury and the development of consequent cGVHD of the gut. Most recent insight in the pathobiology include an allogeneic 'auto-immune'-like course of events, with defective thymic deletion of self-reactive T cells and aberrant B cell activation and production of



antibodies<sup>114</sup>. Therefore, new targets of therapy include T and B cell-signaling pathways that are operational during cGVHD<sup>115</sup>. As aberrant tissue repair mechanisms, an inflammatory local milieu and continuous antigen exposure are also contributors in the development of cGVHD<sup>116</sup>, approaches discussed above to prevent intestinal epithelial injury and the development of acute GVHD are in essence applicable in the prevention of cGVHD as well.

## Stimulating epithelial cell restoration

GVHD treatments have traditionally emphasized immunosuppression, and advances have focused on novel ways to accomplish this. In order to make continued meaningful progress, it is necessary to approach GVHD from additional perspectives. A promising and complimentary approach may be to focus on stimulating epithelial repair. Several processes are involved in the maintenance and recovery of the epithelium, including proliferation and differentiation of intestinal cells, as well as cell migration. Major pathways involved in these processes are multifactorial, and some examples are listed in Table 2. While it has been postulated that GVHD is mainly a disease of the inability to regenerate<sup>8</sup>, evidence exists that regeneration does take place, but may not be enough to overcome the continuous insult. This is for instance illustrated by the fact that intestinal epithelial crypts that survive allo-T cell insult in fact proliferate more than crypts of matched controls<sup>77</sup>. In addition, enterocytes of patients suffering from refractory GI-GVHD showed significant telomere shortening, which is associated with compensatory proliferation<sup>117</sup>. Below we will discuss regenerative approaches that hold promise to support the epithelium in the context of GVHD, either by stimulating epithelial constituents to promote recovery of the lining itself or by influencing the mucosal microenvironment (Fig. 4).

### **Restoration from within the epithelial compartment**

Despite growing insights into ISC maintenance under homeostatic conditions, the principles underlying epithelial regeneration for maintenance of barrier function after tissue damage remain incompletely understood. Although radiation injury can cause a significant loss of ISCs, the Lgr5+ CBC cell pool is relatively resistant to radiation injury, reportedly due to their ability to repair DNA damage<sup>118</sup>. Crypt repopulation originated from surviving CBC cells<sup>118</sup>, which are essential, as Lgr5 genetic deletion and subsequent irradiation severely hinders the regenerative response<sup>119</sup>. There appears to be considerable plasticity in intestinal progenitor cells in response to damage. Upon CBC ablation, progenitors were able to dedifferentiate and regain stemness, thereby replenishing the ISC pool and subsequently the mature enterocytes at the epithelial surface<sup>120</sup>. Both secretory<sup>121,122</sup> and enterocyte<sup>123</sup> progenitors are capable of this reversion, and even fully differentiated enterocytes can contribute to crypt repopulation under specific circumstances of extreme damage<sup>124</sup>. In both instances, the expression of Lgr5 reappeared at the base of the crypt<sup>121,123</sup>, preceded by the re-expression



of the ISC-restricted transcription factor *Ascl2*<sup>125</sup>. Even a subset of Paneth cells acquired multipotency upon irradiation through Notch activation<sup>126</sup>. The reprogramming of adult differentiated cells appears to have a developmental link<sup>122</sup>, as fetal mouse IECs can give rise to the adult ISC pool irrespective of their location or *Lgr5* status<sup>127</sup>. Additionally, during infectious insult fetal-type gene expression programs play a role in epithelial recovery, as the murine ISC niche can revert to a fetal-like state upon parasitic helminth infection<sup>128</sup>. The importance of these complex crypt stem cell and progenitor dynamics in regeneration during GVHD-induced damage is currently unknown. The prolonged damage to the GI tract present in GVHD likely includes substantial insult to the cells with regenerative potential that are responsible for overall epithelial reconstitution.

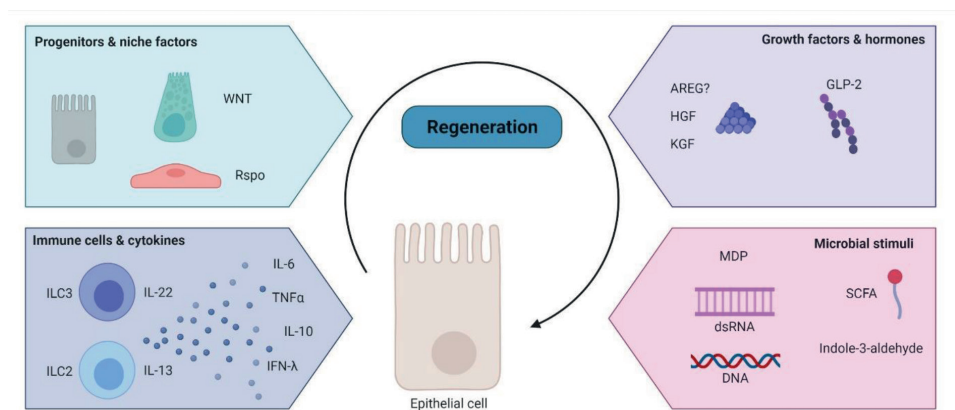


**Figure 4. Regenerative treatment options in GI-GVHD.**

Restoration of the epithelial barrier during the course of GVHD occurs at several levels. The epithelium reconstitutes from within, deriving from progenitors under the influence of supportive niche factors. It can also be supported in its regeneration from its immediate surroundings, for instance through the action of immune cells or particular excreted cytokines, growth factors and hormones. Finally microbial components can contribute to intestinal epithelial healing. Created with BioRender.com.

Tables

**Table 2. Major pathways involved in intestinal epithelial regeneration and repair**

Signaling pathway	(S)timulation/ (I)nhibition	Effect	Example of eliciting factor and/or mechanism	Ref
mTORC1/SIRT1	S	ISC expansion	Caloric restriction	220
PI3K/AKT	S	IEC proliferation, G1 cell cycle progression	Binding of EGF, TGF-α	221
WNT/Rspondin/β-catenin	S	ISC proliferation, suppressed IEC differentiation	Arachidonic acid presence	67,222
STAT5/NFκB	STAT5 S	ISC proliferation, crypt regeneration	Cytokine receptor activation	223
	NFκB I	Mucosal wound healing	Decreased MLCK phosphorylation and TJ permeability	224

**Table 2.** *Continued.*

Signaling pathway	(S)timulation/ (I)nhibition	Effect	Example of eliciting factor and/or mechanism	Ref
<b>Hippo/YAP-TAZ</b>	Hippo I, YAP S	Intestinal regeneration in DSS colitis Low Wnt signaling, wound-healing response Excessive PC differentiation, crypt regeneration Increased organoid growth	Binding of stroma-derived Immunoglobulin superfamily containing leucine-rich repeat protein (ISLR)  Binding of bile acids to TGR5	225,226  227
	Hippo S, YAP I	Maintenance Wnt signaling, canonical stem cell function	-	228
<b>SMAD</b>	S	Increased barrier function through TJ protein upregulation	Binding of TGF- $\beta$	229
<b>BMP/SMAD</b>	I	ISC maintenance, expansion	Relief of direct, HDAC1-mediated transcriptional repression of stem cell signature genes	230
<b>ERK/MAPK</b>	S	ISC expansion, crypt formation, IEC proliferation	Binding of HGF to MET	175
		Increased barrier function through TJ-protein upregulation	Binding of TGF- $\beta$	229
		Enhanced IEC migration	Binding of Flagellin	231
<b>STAT3</b>	S	Intestinal mucosa regeneration, organoid formation	Downstream FAK activation and integrin signaling	148
		ISC expansion, crypt formation, organoid proliferation	Binding of IL-22 to IL-22R	76
<b>Myd88/NF<math>\kappa</math><math>\beta</math></b>	S/I	Regulation of intestinal epithelial integrity and inflammatory responses	NF $\kappa$ $\beta$ inhibition leads to severe chronic inflammation and epithelial apoptosis	232
			Epithelial MyD88 required for survival in multiple colitis models	233
<b>c-Jun/AP-1</b>	S	Promotion of epithelial restitution after wounding through cell migration	Upregulation of PLC $\gamma$ 1-induced Ca <sup>2+</sup> signalling	234
<b>JNK2</b>	S	Epithelial barrier maintenance, enhanced Goblet cell and EEC differentiation and mucus production	Protection from DSS colitis, reduced barrier dysfunction and enterocyte apoptosis, increased Atoh1 expression	235

### Restoration through replenishment of ISC niche factors

Several niche factors secreted by cells in the microenvironment of the crypt compartment could contribute to restoration of crypt damage in allo-HSCT. Wnt signaling is essential for ISC maintenance, with cytoplasmic  $\beta$ -catenin translocating to the nucleus, interacting with transcription factors of the TCF/LEF family, and subsequently activating expression of target proteins involved in proliferation, such as Myc<sup>67</sup>. Wnt is required for crypt regeneration after damage<sup>129,130</sup> and during inflammation, as seen in a DSS colitis model<sup>131</sup>. Short term Wnt agonism has been proposed as a therapeutic countermeasure against irradiation-induced



gastrointestinal damage in mice<sup>132</sup>. GSK3 $\beta$  is an essential kinase of the Wnt/ $\beta$ -catenin pathway involved in the control of the cytoplasmic levels of  $\beta$ -catenin and its inhibition increases  $\beta$ -catenin availability and downstream Myc expression<sup>133</sup>. In an observational pilot study the known GSK3 $\beta$ -inhibitor lithium was used to salvage SR-GVHD, with promising results<sup>134</sup>.

Another approach to potentiate the Wnt pathway in the experimental transplant setting is through R-spondin-dependent modulation of Lgr5 signaling. It has recently been proposed that the most abundant R-spondin in the intestines, Rspo-3, is predominantly produced by lymphatic endothelial cells (LECS) in the lamina propria. LECS were found to be reduced in number and their Rspo-3 production impaired in experimental GVHD<sup>135</sup>. Exogenous administration of Rspo-3 promoted stem cell recovery and epithelial regeneration in the colon in a murine DSS-induced colitis model<sup>124</sup>. Another source of R-spondins are the recently described MAP3K2-regulated intestinal stromal cells at the bottom of colon crypts, which release Rspo-1 to maintain Lgr5+ ISCs during DSS colitis<sup>66</sup>. A prophylactic strategy of enhancing Wnt signaling with administration of Rspo-1 reduced murine colon pathology resulting from radiation<sup>136</sup> and chemotherapy injury<sup>136,137</sup>. Furthermore, in a MHC-mismatched allogeneic BMT model, pretransplant treatment with Rspo-1 was associated with increased Olfm4+ ISCs and reduced GVHD mortality<sup>75</sup>. In addition, Rspo1 administration stimulated differentiation of ISCs towards PCs, increasing their numbers, with a positive impact on the secretion of luminal  $\alpha$ -defensins and microbiome diversity<sup>81</sup>. Rspo administration might therefore be a promising approach, but future clinical studies are necessary to investigate efficacy and safety.

Also other stem cell niche factors are important for crypt regeneration and intestinal epithelial integrity after damaging or inflammatory insults. For instance, mice with impaired EGF-receptor signaling in the gut were more susceptible to inflammation in DSS colitis, due to impaired IEC regeneration and consequent barrier compromise<sup>138</sup>. In a phase I study, patients receiving urinary-derived human chorionic gonadotropin (uhCG) that could supplement EGF as supportive care in aGVHD had a promising biochemical response correlating with day 28 clinical response<sup>139</sup>. Also Notch ligands like Jag1 and DLL3 have been implicated in intestinal epithelial reconstitution and proliferation during inflammation, downstream of YAP pathway activation<sup>140</sup>, but have thus far not been studied in the context of GVHD.

### **Restoration through the regulation of immune cells & cytokines**

In addition to epithelial and stromal contributions to the ISC niche, there is a growing appreciation that the local immune system can regulate the ISC compartment and its regeneration<sup>141</sup>. The IL-10-type cytokine IL-22<sup>142</sup> is produced by a variety of immune cells and is involved in antimicrobial immunity and in both induction and resolution of inflammation

in the intestine<sup>143,144,145</sup>. In addition, IL-22 has been implicated in the maintenance of the intestinal barrier and epithelial repair, due to its influence on mucus production<sup>145</sup> and IEC proliferation<sup>76,146</sup>. IL-22 derived from group 3 ILCs (ILC3s) was shown to be protective in the GI tracts of transplant recipients in experimental GVHD<sup>74</sup>. However, the pathophysiological process of gut GVHD leads to loss of intestinal ILC3s and their protective IL-22 production<sup>74</sup>. Furthermore, patients with low numbers of ILCs in circulation prior to transplant had an increased risk of developing GVHD<sup>147</sup>. Interestingly, *in vivo* treatment of transplanted mice with the recombinant human IL-22 dimer/Fc fusion molecule F-652 (Generon Corp., Shanghai) reduced GVHD-related clinical scoring and mortality in a MHC-matched GVHD model<sup>76</sup>. IL-22 activated STAT3 phosphorylation in small intestine ISCs and organoids, promoting ISC survival and expansion as well as overall epithelial regeneration and recovery<sup>76</sup>. Findings of the role of the IL-22-STAT3 axis in crypt regeneration have been validated by the fact that STAT3 was required for damage-induced crypt regeneration after radiation injury<sup>148</sup>. In addition, IL-22 was required for an effective DNA damage response in protecting ISCs from genotoxic stress<sup>149</sup>. The influence of IL-22 on crypt regeneration under homeostatic conditions *in vivo* has not yet been studied. A Phase II trial for treatment of newly diagnosed GI-GVHD with a combination of corticosteroids and a recombinant human IL-22 dimer has recently been performed to investigate the safety potential of this novel tissue-regenerative approach to GVHD treatment (NCT02406651).

While therapy with IL-22 appears promising, additional immune-mediated pathways of regeneration may hold translational potential as well. IL-22-independent effects of ILC3s on epithelial regeneration involving the Hippo-YAP1 pathway have been described after methotrexate-induced GI damage<sup>150</sup>. The authors proposed a dichotomy between stem cell maintenance, which could be ILC3/IL-22/STAT3 dependent, and crypt proliferation, which they found to occur in a ILC3-dependent but IL-22 independent manner<sup>150</sup>. As such, the application of an ILC3-based cell therapy, instead of only administering IL-22, may have additional benefits for GVHD patients.

Also another type of innate lymphocyte cells, ILC2s residing in MLNs and Peyer's patches, are known to support the intestinal barrier function, by inducing Goblet cell expansion through IL-13 secretion in response to Tuft-cell-derived IL-25<sup>151</sup>. Goblet cells are important for barrier function by secreting mucus that shields the intestinal epithelium from gut contents and microbes, and were found to be reduced in GVHD in mice and patients<sup>13</sup>. As mentioned earlier, ILCs are lost in GVHD, but pretransplant administration of IL-25 led to protective Goblet cell induction, decreased bacterial translocation, and ameliorated GVHD, increasing survival in a haploidentical and MHC-mismatched model<sup>13</sup>. In addition, ILC2-derived IL-13 may have a direct regenerative effect through binding the IL-13R expressed on ISCs. IL-13 increased ISC self-renewal and  $\beta$ -catenin signaling<sup>152</sup>.



Recently, it was reported that type III IFNs (IFN- $\lambda$ ), known for their role in epithelial viral defense, have an epithelial protective effect in experimental GVHD<sup>153</sup>. In vivo treatment of naïve mice with recombinant IFN- $\lambda$  in the form of PEGylated (PEG-)IL-29, which has been tested in phase I-III clinical trials as an adjunctive treatment for hepatitis C virus, increased ISC numbers and led to more efficient ISC-derived organoid growth ex vivo. In experimental GVHD, prophylactic PEG-IL-29 administration prolonged survival, reduced GVHD severity and increased epithelial proliferation<sup>153</sup>.

Some other, classic pro-inflammatory cytokines have been shown to also play a role in maintaining epithelial integrity. Many of these cytokines may be inhibited by immunosuppressive GVHD therapies. For instance, TNF $\alpha$  has long been implicated in GI-GVHD pathogenesis<sup>154</sup>, but also has epithelial-supportive effects in vitro. Low-dose TNF $\alpha$  increased the number of human fetal intestinal organoids, while higher doses impaired organoid formation<sup>155</sup>. Mechanistically, TNF treatment directly promoted Wnt/B-catenin signaling<sup>156</sup> and increased the expression of several stem cell markers in murine intestinal<sup>156</sup> and human fetal intestinal organoids<sup>155</sup>, including Acl2. This epithelial-supportive mechanism provides insights as to why TNF $\alpha$ -blockade has had inconsistent results in the treatment of GI-GVHD<sup>157</sup>. A similar paradox can be found with the pro-inflammatory cytokine IL-6. IL-6 inhibition through blockade of IL6R-signaling with tocilizumab has had some promising results in both experimental and clinical GVHD, and has been associated with induction of allo-T cell suppressive Tregs<sup>158,159</sup>. However, IL-6 administration in healthy mice has been associated with STAT3-induced epithelial regenerative effects such as increased intestinal villus height, elongated enterocyte lifespan and a concurrent decrease in pro-apoptotic caspase activity<sup>160</sup>. Accordingly, in a GI damage model of mechanical wound injury, IL-6 inhibition resulted in impaired healing due to decreased proliferation<sup>161</sup>. As such, care should be taken with IL-6-blocking therapeutic approaches in GI-GVHD.

An additional example of cytokine-mediated restoration can be found in the regulatory cytokine IL-10. IL-10- and IL10R deficiency are known to cause severe intestinal disease in both mice and humans<sup>162</sup>, and disruption of the IL-10 signaling pathway resulted in exacerbation of experimental GVHD<sup>163</sup>. Nonetheless, treatment of IL-10 or co-culture with peripherally induced Tregs led to the expansion of ISC numbers in murine organoids, and increased clonogenicity after passage<sup>164</sup>. In addition, human recombinant IL-10 was shown to promote intestinal epithelial proliferation by activation of CREB signaling<sup>165</sup>. Despite the fact that treatment of GVHD by exogenous IL-10 does not seem to be clinically feasible due to its pleiotropic and divergent effects<sup>163</sup>, there may be a crypt-protective effect if epithelial-targeted administration would be possible.

**Table 3. Ongoing trials aimed at protecting or regenerating the intestinal epithelium in GI-GVHD treatment or prevention (per February 1<sup>st</sup>, 2022)**

Trial agent	(Proposed) mechanism of action	Phase	Trial number
Reducing DAMPs or response to DAMPS			
Alpha-1 Antitrypsin (AAT)	Serine protease inhibitor degrading heparan sulfate	III	NCT04167514
		II/III	NCT03805789
Blocking allo-reactive T cell influx to the gut			
Vedolizumab	$\alpha 4\beta 7$ -integrin inhibitor	III	NCT03657160
Natalizumab	Selective $\alpha 4$ subunit adhesion molecule inhibitor	II	NCT02133924
Blocking cytokine-mediated killing			
Ruxolitinib	JAK1/2 inhibitor	II	NCT04384692
		II	NCT04061876
		II	NCT03701698
		I/II	NCT03491215
		IV	NCT02386800
		I	NCT05121142
Baricitinib	JAK1/2 inhibitor	I	NCT04131738
Pacritinib	JAK2 inhibitor	I/II	NCT02891603
Itacitinib	JAK1 inhibitor	I	NCT04070781
		II	NCT03846479
		I	NCT03755414
Tocilizumab	IL-6 inhibitor	II	NCT04395222
		I	NCT04070781
		II	NCT03434730
		II	NCT04688021
Jaktinib	JAK1/2/3 inhibitor	II	NCT04971551
TQ05105	JAK2 inhibitor	I/II	NCT04941404
Regeneration of the epithelium			
Pregnyl	human Chorionic Gonadotrophin (hCG)/EGF	I/II	NCT02525029
		I/II	NCT05123040
IL-22Fc	IL-22R binding	Ib	NCT04539470
Lactobacillus Plantarum	Producers of indole-3-aldehyde	III	NCT03057054
Galacto-oligosaccharide	Prebiotic sustaining butyrate-producing bacteria	I/II	NCT04373057

### Restoration through use of growth factors and hormones

In addition to previously discussed niche factors, stromal cells surrounding the epithelial crypts are important sources of EGF-like growth factors for the intestinal epithelium. Keratinocyte growth factor (KGF) is one of the most well-studied for its protective role during conditioning-induced damage and oral mucositis<sup>166</sup>. While initially described as a growth factor for skin epithelium, KGF can enhance intestinal epithelial proliferation<sup>167</sup>, and crypt cell survival after irradiation<sup>168</sup>. In experimental GVHD, KGF administration started prior to and continued after the transplant reduced GVHD mortality and severity in the GI tract<sup>169,170</sup>. However, administration of palifermin, a recombinant human KGF, did not reduce GVHD incidence or improve overall survival in allo-transplant patients in two randomized controlled trials<sup>171,172</sup>, although it did reduce mucositis incidence and severity in a subgroup of patients<sup>171</sup>. Another EGF-like growth factor in preclinical development is the potent liver mitogen Hepatocyte Growth Factor (HGF) produced by intestinal fibroblasts



and macrophages<sup>173</sup>. Using a human HGF expression vector injected into muscle at the time of transplant, stable expression of hHGF in HSCT recipient mice reduced GVHD histopathology and crypt apoptosis<sup>174</sup>. Interestingly, HGF was found to be a possible substitute for EGF in intestinal organoid cultures. Mice lacking the receptor for HGF in their epithelium had reduced numbers of proliferating crypts and ISCs after irradiation<sup>175</sup>. Perhaps the protective effect of HGF in experimental GVHD is a result of directly targeting the intestinal epithelium. Lastly, it has been postulated that amphiregulin (AREG), a weak EGF-receptor agonist produced by a multitude of immune, stromal and epithelial cells, may have intestinal epithelial regenerative effects in the GVHD setting. It has been implicated as a possible plasma biomarker for risk stratification and steroid response in aGVHD<sup>176</sup>. Genetic disruption of Areg significantly impaired intestinal regeneration after radiation injury in full knockout mice<sup>177</sup>. Nonetheless, the beneficial effects of AREG on experimental GVHD incidence and mortality observed thus far do not directly implicate epithelial regeneration as the main mechanism and could still be ascribed to allo-immune suppression, such as through Treg function enhancement<sup>178,179,180</sup>. Taken together, the intestinal regenerative effect of growth factor substituents may be promising, but seems to have limited application in the clinic thus far.

In addition to growth factors, enteroendocrine hormones may have intestinal epithelial protective effects<sup>181</sup> in the context of GI-GVHD. Glucagon-like peptide (GLP)-2 is produced by intestinal L-cells, which are a subset of enteroendocrine cells. L-cells are reduced in mice and patients that develop GVHD<sup>182</sup>. In vivo, GLP-2 agonism acutely increased the proportion of Lgr5+ ISCs in S-phase and prolonged treatment increased numbers of Olfm4+ ISCs per crypt<sup>183</sup>. GLP-2 stimulation of intestinal organoids led to increased organoid size<sup>182</sup>. Prophylactic treatment with a GLP-2 agonist injected subcutaneously in a MHC-mismatched mouse model, improved survival, decreased gut GVHD histopathology scores, and restored ISC loss, even when applied as an additive to steroids<sup>182</sup>. Future clinical studies will have to investigate its utility in clinical GVHD patients.

### **Restoration through the supply of protective microbial stimuli**

Despite the pro-inflammatory effects of some innate immune signaling pathways, it was demonstrated that specific innate pattern recognition pathways can exert a protective effect on the intestinal epithelium during GVHD in mice. The RIG-I/MAVS pathway is involved in the sensing of dsRNA during infection, while the cGAS/STING signaling pathway is involved in the recognition of DNA. Perturbation of these innate pathways with genetic STING knockouts, changed the sensitivity to GVHD with contrasting effects on outcomes depending on the donor/recipient disparity and the specifics of the transplant models utilized<sup>184,185</sup>. In a MHC-mismatched model, treatment with 3pRNA or DNA prior to allo-HSCT protected mice from conditioning-induced intestinal damage and GVHD without diminishing the GVL activity of allo-T cells. Mechanistically, activation of the pathways led to the expression of protective



type I IFNs (IFN-I), which were indispensable for the maintenance of gut epithelial barrier integrity, but only when they were induced prior to the TBI insult. Treatment of intestinal organoids with 3pRNA and DNA confirmed the direct epithelial effects with increased IFN-I-dependent proliferation<sup>184</sup>. Intestinal epithelial IFN-I signaling was recently implicated in the regulation of stemness and differentiation into secretory-cell lineages. Mice lacking IEC Interferon regulatory factor 2, which downregulates IFN-signaling, had fewer ISCs, accumulation of immature PCs and impaired regeneration after damage<sup>186</sup>. In clinical studies, treatment with IFN- $\alpha$  before HSCT<sup>187</sup> or after relapse post-HSCT<sup>188</sup> was associated with a higher incidence of overall acute GVHD. Tight regulation of IFN-signaling induction during injury thus appears to be crucial.

Another cytosolic innate immune pathway implicated in the protection against intestinal epithelial injury is NOD2. It binds to the peptidoglycan muramyl dipeptide (MDP), which is produced by most bacteria. In a T cell-induced enteropathy model, NOD2 deficiency outside the intestinal epithelial compartment led to more severe crypt damage, apoptosis and delayed epithelial regeneration<sup>189</sup>. Similarly, in mouse BMT models, host NOD2 expression in the hematopoietic compartment is protective against the development of GVHD<sup>190</sup>. Nevertheless, MDP was shown to directly increase organoid-forming potential of intestinal crypts and to protect ISCs from oxidative-stress-induced cell death<sup>191</sup>. NOD2 also supported intestinal crypt survival and regeneration after irradiation, both in organoid cultures of NOD2 knockout mice and in vivo<sup>192</sup>. Given these findings, a non-hematopoietic protective role of NOD2 signaling in GVHD protection may also be possible. Nonetheless, more study is required to appreciate whether these mechanisms can also be exploited in GVHD patients to promote regeneration.

Over the past decade, several bacterial metabolic products have been associated with gut barrier integrity, including in the context of GVHD. Many studies have focused on short chain fatty acids (SCFAs), such as butyrate and propionate. Butyrate contributes to intestinal health in multiple ways<sup>193,194,195</sup>. It was found to directly increase epithelial regeneration in 3D organoid cultures<sup>196</sup> and improve wound healing through tight junction protein upregulation<sup>196,197</sup>. In the setting of GVHD, intragastric administration of butyrate to allogeneic recipients improved IEC junctional integrity, decreased expression of apoptotic proteins in IECs, and led to decreased GVHD, independent of the induction of Tregs<sup>196</sup>. Clostridia commensals are known butyrate producers, and administration of a microbial cocktail including 17 strains of Clostridiales elevated intraluminal butyrate concentrations, decreased GVHD clinical scores, and increased survival in a mouse GVHD model<sup>196</sup>. This could explain why the presence of Clostridiales<sup>198</sup> and its protection in the microbiome by selective antibiotic use was found to be associated with reduced GVHD-related mortality in clinical studies<sup>199,200</sup>. It also provides a rationale for the use of fecal microbiota transplants for the treatment of GVHD<sup>201,202,203</sup>. Recently, it was demonstrated that signaling through



non-hematopoietic GPR43, a metabolite sensor, is critical for the GVHD treatment effects of SCFAs, independent of baseline microbiota constitution<sup>204</sup>. Given the clear associations of microbial constituents and GVHD outcomes, manipulation of the enteric flora or associated metabolites represent promising approaches for clinical prevention and treatment of GVHD. The tryptophan catabolite indole and its derivatives are other product of commensal bacteria with gut immunomodulatory effects. *Lactobacillus*-derived indole-3-aldehyde, for instance, engages the aryl hydrocarbon receptor (AHR), an environmental sensor and crucial transcription factor for ILC3s in the gut. As such, it can expand ILC3s and their IL-22 production in the intestinal mucosa<sup>205</sup>, as well as influence the immune response via many other immune cell types<sup>206</sup>. AHR ligation however also has a direct epithelial effect, as it was shown to regulate ISC differentiation and thereby maintain barrier integrity<sup>207</sup>. In a GVHD mouse model, administration of indole-3-aldehyde reduced GVHD severity, intestinal epithelial damage, and gut bacterial translocation. The effects were mediated through an IFN-I response observed at the transcriptional level in whole gut samples<sup>208</sup>. In allo-HSCT patients, higher levels of urine 3-indoxyl sulfate, an indole-derived metabolite, correlated with lower treatment-related mortality and higher overall survival<sup>209</sup>. Therefore, indole-3-aldehyde administration represents another potential interventional approach of interest for treatment of GVHD.

## Concluding remarks and future prospects

The intestinal epithelium experiences substantial toxicity during the course of allogeneic transplantation. Given the pivotal role of alloreactive T cells in GVHD pathogenesis, effective immunosuppression is the cornerstone of GVHD treatment strategies. However, in addition to control of the alloreactive immune response, development of target-organ-focused strategies that can protect the epithelium and stimulate its regeneration is important for further progress in improving clinical outcomes for transplant patients. Given advancements in both experimental and clinical research, it is possible that this hope may be realized in the near future.

Most epithelial-targeted factors and pathways discussed here have pleiotropic effects with complex feedback mechanisms in multiple tissues and different cell types. The mere stimulation or inhibition on the systemic level therefore may not result in the intended outcome. New ways to specifically target the intestine, for example through intestine-directed genetically engineered cells<sup>210</sup> or carriers such as nanoparticles<sup>211,212,213</sup>, might make additional GI-targeted approaches more feasible in the future, similar to the wide use of oral budesonide for more targeted administration of corticosteroids to the GI tract. On an even smaller scale, a better understanding of the structural design of factors involved may enable the decoupling of protective functions from pro-inflammatory effects. In a recent study authors were able to design a STAT3-biased IL-22 receptor agonist, which elicited tissue selective STAT3 activation in vivo<sup>214</sup>.

A combinatory approach of factors that hold promise in preliminary trials at different levels of epithelial support could be considered (Table 3). To have an effect, adequate timing of the different strategies will be essential (Fig. 2). Wider use of drug-exposure-targeted pretransplant conditioning to limit the initial damage<sup>29,30,31,33</sup> in combination with early initiation of Jak1/2 inhibition to shield the epithelium from allo-T cell-derived IFN $\gamma$  and protect ISCs<sup>77</sup> may represent a currently attainable approach to improve GVHD prophylaxis. Should GVHD develop, pro-regenerative therapies such as IL-22 could be administered in the front-line setting along with corticosteroids to promote epithelial recovery<sup>76</sup>. Attention must also be paid to maintaining a supportive enteric microbial environment, including preservation of healthy anaerobic commensals such as butyrate producers<sup>199,200</sup>. A comprehensive approach involving these strategies as well as the implementation of additional tissue-targeted modalities currently in development will be necessary to fully incorporate epithelial biology into GVHD treatment strategies and optimize outcomes for HSCT patients.

#### **Author Contributions**

SAJ drafted the manuscript. EEN and AMH provided expert advice and edited the text. CAL supervised the work. All authors read and approved the manuscript.

#### **Conflict of Interest**

CAL and AMH hold IP related to use of IL-22 in GVHD.



## References

1. Ferrara, J. L. M., Levine, J. E., Reddy, P. & Holler, E. Graft-versus-host disease. *Lancet (London, England)* **373**, 1550–1561 (2009).
2. Naymagon, S. *et al.* Acute graft-versus-host disease of the gut: considerations for the gastroenterologist. *Nat. Rev. Gastroenterol. Hepatol.* **14**, 711–726 (2017).
3. Blazar, B. R., Murphy, W. J. & Abedi, M. Advances in graft-versus-host disease biology and therapy. *Nat. Rev. Immunol.* **12**, 443–458 (2012).
4. Zeiser, R. & Blazar, B. R. Acute Graft-versus-Host Disease. *The New England journal of medicine* vol. 378 586 (2018).
5. Penack, O. *et al.* Prophylaxis and management of graft versus host disease after stem-cell transplantation for haematological malignancies: updated consensus recommendations of the European Society for Blood and Marrow Transplantation. *Lancet. Haematol.* **7**, e157–e167 (2020).
6. Deeg, H. J. How I treat refractory acute GVHD. *Blood* **109**, 4119–4126 (2007).
7. Zeiser, R. *et al.* Ruxolitinib for Glucocorticoid-Refractory Acute Graft-versus-Host Disease. *N. Engl. J. Med.* **382**, 1800–1810 (2020).
8. Chakraverty, R. & Teshima, T. Graft-versus-host disease: a disorder of tissue regeneration and repair. *Blood* **138**, 1657–1665 (2021).
9. Odenwald, M. A. & Turner, J. R. The intestinal epithelial barrier: a therapeutic target? *Nat. Rev. Gastroenterol. Hepatol.* **14**, 9–21 (2017).
10. Nalle, S. C. *et al.* Recipient NK cell inactivation and intestinal barrier loss are required for MHC-matched graft-versus-host disease. *Sci. Transl. Med.* **6**, 243ra87 (2014).
11. Hill, G. R. *et al.* Total body irradiation and acute graft-versus-host disease: the role of gastrointestinal damage and inflammatory cytokines. *Blood* **90**, 3204–3213 (1997).
12. Flowers, M. E. D. *et al.* Comparative analysis of risk factors for acute graft-versus-host disease and for chronic graft-versus-host disease according to National Institutes of Health consensus criteria. *Blood* **117**, 3214–3219 (2011).
13. Ara, T. *et al.* Intestinal goblet cells protect against GVHD after allogeneic stem cell transplantation via Lypd8. *Sci. Transl. Med.* **12**, (2020).
14. Fischer, J. C., Wintges, A., Haas, T. & Poeck, H. Assessment of mucosal integrity by quantifying neutrophil granulocyte influx in murine models of acute intestinal injury. *Cell. Immunol.* **316**, 70–76 (2017).
15. Zuo, L., Kuo, W.-T. & Turner, J. R. Tight Junctions as Targets and Effectors of Mucosal Immune Homeostasis. *Cell. Mol. Gastroenterol. Hepatol.* **10**, 327–340 (2020).
16. Johansson, J. E., Brune, M. & Ekman, T. The gut mucosa barrier is preserved during allogeneic, haemopoietic stem cell transplantation with reduced intensity conditioning. *Bone Marrow Transplant.* **28**, 737–742 (2001).
17. Johansson, J.-E. & Ekman, T. Gut toxicity during hemopoietic stem cell transplantation may predict acute graft-versus-host disease severity in patients. *Dig. Dis. Sci.* **52**, 2340–2345 (2007).
18. Hill, G. R. & Ferrara, J. L. The primacy of the gastrointestinal tract as a target organ of acute graft-versus-host disease: rationale for the use of cytokine shields in allogeneic bone marrow transplantation. *Blood* **95**, 2754–2759 (2000).
19. Xun, C. Q., Thompson, J. S., Jennings, C. D., Brown, S. A. & Widmer, M. B. Effect of total body irradiation, busulfan-cyclophosphamide, or cyclophosphamide conditioning on inflammatory cytokine release and development of acute and chronic graft-versus-host disease in H-2-incompatible transplanted SCID mice. *Blood* **83**, 2360–2367 (1994).
20. Nakasone, H. *et al.* Impact of conditioning intensity and TBI on acute GVHD after hematopoietic cell transplantation. *Bone Marrow Transplant.* **50**, 559–565 (2015).
21. Kebriaei, P. *et al.* Intravenous Busulfan Compared with Total Body Irradiation Pretransplant Conditioning for Adults with Acute Lymphoblastic Leukemia. *Biol. Blood Marrow Transplant.* **24**, 726–733 (2018).
22. Slavin, S. *et al.* Nonmyeloablative stem cell transplantation and cell therapy as an alternative to conventional bone marrow transplantation with lethal cytoreduction for the treatment of malignant and nonmalignant hematologic diseases. *Blood* **91**, 756–763 (1998).
23. Blum, W. *et al.* Low-dose (550 cGy), single-exposure total body irradiation and cyclophosphamide: consistent, durable engraftment of related-donor peripheral blood stem cells with low treatment-related mortality and fatal organ toxicity. *Biol. Blood Marrow Transplant.* **8**, 608–618 (2002).
24. Eduardo, F. P. *et al.* Retrospective study of the digestive tract mucositis derived from myeloablative and non-myeloablative/reduced-intensity conditionings with busulfan in hematopoietic cell transplantation patient. *Support. care cancer Off. J. Multinatl. Assoc. Support. Care Cancer* **27**, 839–848 (2019).
25. Abdul Wahid, S. F. *et al.* Comparison of reduced-intensity and myeloablative conditioning regimens for allogeneic hematopoietic stem cell transplantation in patients with acute myeloid leukemia and acute lymphoblastic leukemia: a meta-analysis. *Stem Cells Dev.* **23**, 2535–2552 (2014).
26. Rambaldi, A. *et al.* Busulfan plus cyclophosphamide versus busulfan plus fludarabine as a preparative regimen

- for allogeneic haemopoietic stem-cell transplantation in patients with acute myeloid leukaemia: an open-label, multicentre, randomised, phase 3 trial. *Lancet. Oncol.* **16**, 1525–1536 (2015).
27. Bartelink, I. H. *et al.* Fludarabine and exposure-targeted busulfan compares favorably with busulfan/cyclophosphamide-based regimens in pediatric hematopoietic cell transplantation: maintaining efficacy with less toxicity. *Biol. Blood Marrow Transplant.* **20**, 345–353 (2014).
  28. Harris, A. C. *et al.* Comparison of pediatric allogeneic transplant outcomes using myeloablative busulfan with cyclophosphamide or fludarabine. *Blood Adv.* **2**, 1198–1206 (2018).
  29. Andersson, B. S. *et al.* Busulfan systemic exposure relative to regimen-related toxicity and acute graft-versus-host disease: defining a therapeutic window for i.v. BuCy2 in chronic myelogenous leukemia. *Biol. Blood Marrow Transplant.* **8**, 477–485 (2002).
  30. Kharfan-Dabaja, M. A. *et al.* Higher busulfan dose intensity appears to improve leukemia-free and overall survival in AML allografted in CR2: An analysis from the Acute Leukemia Working Party of the European Group for Blood and Marrow Transplantation. *Leuk. Res.* **39**, 933–937 (2015).
  31. Bartelink, I. H. *et al.* Association of busulfan exposure with survival and toxicity after haemopoietic cell transplantation in children and young adults: a multicentre, retrospective cohort analysis. *Lancet. Haematol.* **3**, e526–e536 (2016).
  32. Bartelink, I. H. *et al.* Association between busulfan exposure and outcome in children receiving intravenous busulfan before hematologic stem cell transplantation. *Biol. blood marrow Transplant. J. Am. Soc. Blood Marrow Transplant.* **15**, 231–241 (2009).
  33. Langenhorst, J. B. *et al.* Fludarabine exposure in the conditioning prior to allogeneic hematopoietic cell transplantation predicts outcomes. *Blood Adv.* **3**, 2179–2187 (2019).
  34. Toubai, T., Mathewson, N. D., Magenau, J. & Reddy, P. Danger Signals and Graft-versus-host Disease: Current Understanding and Future Perspectives. *Front. Immunol.* **7**, 539 (2016).
  35. Ferrara, J. L., Smith, C. M., Sheets, J., Reddy, P. & Serody, J. S. Altered homeostatic regulation of innate and adaptive immunity in lower gastrointestinal tract GVHD pathogenesis. *J. Clin. Invest.* **127**, 2441–2451 (2017).
  36. Penack, O., Holler, E. & van den Brink, M. R. M. Graft-versus-host disease: regulation by microbe-associated molecules and innate immune receptors. *Blood* **115**, 1865–1872 (2010).
  37. Cooke, K. R. *et al.* LPS antagonism reduces graft-versus-host disease and preserves graft-versus-leukemia activity after experimental bone marrow transplantation. *J. Clin. Invest.* **107**, 1581–1589 (2001).
  38. Joly, A.-L. *et al.* The HSP90 inhibitor, 17AAG, protects the intestinal stem cell niche and inhibits graft versus host disease development. *Oncogene* **35**, 2842–2851 (2016).
  39. Zitzer, N. C., Garzon, R. & Ranganathan, P. Toll-Like Receptor Stimulation by MicroRNAs in Acute Graft-vs.-Host Disease. *Front. Immunol.* **9**, 2561 (2018).
  40. Jankovic, D. *et al.* The Nlrp3 inflammasome regulates acute graft-versus-host disease. *J. Exp. Med.* **210**, 1899–1910 (2013).
  41. Wilhelm, K. *et al.* Graft-versus-host disease is enhanced by extracellular ATP activating P2X7R. *Nat. Med.* **16**, 1434–1438 (2010).
  42. Im, K.-I. *et al.* The Free Radical Scavenger NecroX-7 Attenuates Acute Graft-versus-Host Disease via Reciprocal Regulation of Th1/Regulatory T Cells and Inhibition of HMGB1 Release. *J. Immunol.* **194**, 5223–5232 (2015).
  43. Marcondes, A. M. *et al.* Response of Steroid-Refractory Acute GVHD to alpha1-Antitrypsin. *Biol. Blood Marrow Transplant.* **22**, 1596–1601 (2016).
  44. Magenau, J. M. *et al.* alpha1-Antitrypsin infusion for treatment of steroid-resistant acute graft-versus-host disease. *Blood* **131**, 1372–1379 (2018).
  45. Zhong, X. *et al.* The impact of P2X7 receptor antagonist, brilliant blue G on graft-versus-host disease in mice after allogeneic hematopoietic stem cell transplantation. *Cell. Immunol.* **310**, 71–77 (2016).
  46. Iliopoulou, B. P. *et al.* Blockade of TIM-1 on the donor graft ameliorates graft-versus-host disease following hematopoietic cell transplantation. *Blood Adv.* **3**, 3419–3431 (2019).
  47. Chen, S. *et al.* MicroRNA-155-deficient dendritic cells cause less severe GVHD through reduced migration and defective inflammasome activation. *Blood* **126**, 103–112 (2015).
  48. Liu, Y., Chen, G.-Y. & Zheng, P. CD24-Siglec G/10 discriminates danger- from pathogen-associated molecular patterns. *Trends Immunol.* **30**, 557–561 (2009).
  49. Chen, G.-Y., Tang, J., Zheng, P. & Liu, Y. CD24 and Siglec-10 selectively repress tissue damage-induced immune responses. *Science* **323**, 1722–1725 (2009).
  50. Toubai, T. *et al.* Siglec-G-CD24 axis controls the severity of graft-versus-host disease in mice. *Blood* **123**, 3512–3523 (2014).
  51. Toubai, T. *et al.* Siglec-G represses DAMP-mediated effects on T cells. *JCI insight* **2**, (2017).
  52. Toubai, T. *et al.* Host NLRP6 exacerbates graft-versus-host disease independent of gut microbial composition. *Nat. Microbiol.* **4**, 800–812 (2019).
  53. Zhao, Y. *et al.* TLR4 inactivation protects from graft-versus-host disease after allogeneic hematopoietic stem cell transplantation. *Cell. Mol. Immunol.* **10**, 165–175 (2013).
  54. Calcaterra, C. *et al.* Critical role of TLR9 in acute graft-versus-host disease. *J. Immunol.* **181**, 6132–6139 (2008).
  55. Li, H. *et al.* Graft-versus-host disease is independent of innate signaling pathways triggered by pathogens in



- host hematopoietic cells. *J. Immunol.* **186**, 230–241 (2011).
56. Lu, Y. *et al.* Caspase-11 signaling enhances graft-versus-host disease. *Nat. Commun.* **10**, 4044 (2019).
  57. Barker, N. *et al.* Identification of stem cells in small intestine and colon by marker gene Lgr5. *Nature* **449**, 1003–1007 (2007).
  58. Sato, T. *et al.* Single Lgr5 stem cells build crypt-villus structures in vitro without a mesenchymal niche. *Nature* **459**, 262–265 (2009).
  59. Sato, T. *et al.* Long-term expansion of epithelial organoids from human colon, adenoma, adenocarcinoma, and Barrett's epithelium. *Gastroenterology* **141**, 1762–1772 (2011).
  60. Schuijers, J., van der Flier, L. G., van Es, J. & Clevers, H. Robust cre-mediated recombination in small intestinal stem cells utilizing the *olfm4* locus. *Stem cell reports* **3**, 234–241 (2014).
  61. Clevers, H. The intestinal crypt, a prototype stem cell compartment. *Cell* **154**, 274–284 (2013).
  62. Sato, T. *et al.* Paneth cells constitute the niche for Lgr5 stem cells in intestinal crypts. *Nature* **469**, 415–418 (2011).
  63. Gehart, H. & Clevers, H. Tales from the crypt: new insights into intestinal stem cells. *Nat. Rev. Gastroenterol. Hepatol.* **16**, 19–34 (2019).
  64. Kabiri, Z. *et al.* Stroma provides an intestinal stem cell niche in the absence of epithelial Wnts. *Development* **141**, 2206–2215 (2014).
  65. Kang, E., Yousefi, M. & Gruenheid, S. R-Spondins Are Expressed by the Intestinal Stroma and are Differentially Regulated during Citrobacter rodentium- and DSS-Induced Colitis in Mice. *PLoS One* **11**, e0152859 (2016).
  66. Wu, N. *et al.* MAP3K2-regulated intestinal stromal cells define a distinct stem cell niche. *Nature* **592**, 606–610 (2021).
  67. Fevr, T., Robine, S., Louvard, D. & Huelsken, J. Wnt/beta-catenin is essential for intestinal homeostasis and maintenance of intestinal stem cells. *Mol. Cell. Biol.* **27**, 7551–7559 (2007).
  68. Haramis, A.-P. G. *et al.* De novo crypt formation and juvenile polyposis on BMP inhibition in mouse intestine. *Science* **303**, 1684–1686 (2004).
  69. Hardwick, J. C. H. *et al.* Bone morphogenetic protein 2 is expressed by, and acts upon, mature epithelial cells in the colon. *Gastroenterology* **126**, 111–121 (2004).
  70. Martín-Alonso, M. *et al.* Smooth muscle-specific MMP17 (MT4-MMP) regulates the intestinal stem cell niche and regeneration after damage. *Nat. Commun.* **12**, 6741 (2021).
  71. Kosinski, C. *et al.* Gene expression patterns of human colon tops and basal crypts and BMP antagonists as intestinal stem cell niche factors. *Proc. Natl. Acad. Sci. U. S. A.* **104**, 15418–15423 (2007).
  72. Epstein, R. J., McDonald, G. B., Sale, G. E., Shulman, H. M. & Thomas, E. D. The diagnostic accuracy of the rectal biopsy in acute graft-versus-host disease: a prospective study of thirteen patients. *Gastroenterology* **78**, 764–771 (1980).
  73. Bombi, J. A. *et al.* Assessment of histopathologic changes in the colonic biopsy in acute graft-versus-host disease. *Am. J. Clin. Pathol.* **103**, 690–695 (1995).
  74. Hanash, A. M. *et al.* Interleukin-22 protects intestinal stem cells from immune-mediated tissue damage and regulates sensitivity to graft versus host disease. *Immunity* **37**, 339–350 (2012).
  75. Takashima, S. *et al.* The Wnt agonist R-spondin1 regulates systemic graft-versus-host disease by protecting intestinal stem cells. *J. Exp. Med.* **208**, 285–294 (2011).
  76. Lindemans, C. A. *et al.* Interleukin-22 promotes intestinal-stem-cell-mediated epithelial regeneration. *Nature* **528**, 560–564 (2015).
  77. Takashima, S. *et al.* T cell-derived interferon-gamma programs stem cell death in immune-mediated intestinal damage. *Sci. Immunol.* **4**, (2019).
  78. Melson, J., Jakate, S., Fung, H., Arai, S. & Keshavarzian, A. Crypt loss is a marker of clinical severity of acute gastrointestinal graft-versus-host disease. *Am. J. Hematol.* **82**, 881–886 (2007).
  79. Jenq, R. R. *et al.* Regulation of intestinal inflammation by microbiota following allogeneic bone marrow transplantation. *J. Exp. Med.* **209**, 903–911 (2012).
  80. Eriguchi, Y. *et al.* Graft-versus-host disease disrupts intestinal microbial ecology by inhibiting Paneth cell production of alpha-defensins. *Blood* **120**, 223–231 (2012).
  81. Hayase, E. *et al.* R-Spondin1 expands Paneth cells and prevents dysbiosis induced by graft-versus-host disease. *J. Exp. Med.* **214**, 3507–3518 (2017).
  82. Levine, J. E. *et al.* Low Paneth cell numbers at onset of gastrointestinal graft-versus-host disease identify patients at high risk for nonrelapse mortality. *Blood* **122**, 1505–1509 (2013).
  83. Weber, D. *et al.* The association between acute graft-versus-host disease and antimicrobial peptide expression in the gastrointestinal tract after allogeneic stem cell transplantation. *PLoS One* **12**, e0185265 (2017).
  84. Lueschow, S. R. & McElroy, S. J. The Paneth Cell: The Curator and Defender of the Immature Small Intestine. *Front. Immunol.* **11**, 587 (2020).
  85. Ferrara, J. L. M. *et al.* Regenerating islet-derived 3-alpha is a biomarker of gastrointestinal graft-versus-host disease. *Blood* **118**, 6702–6708 (2011).
  86. Zhao, D. *et al.* Survival signal REG3alpha prevents crypt apoptosis to control acute gastrointestinal graft-versus-host disease. *J. Clin. Invest.* **128**, 4970–4979 (2018).
  87. Fu, Y.-Y. *et al.* T Cell Recruitment to the Intestinal Stem Cell Compartment Drives Immune-Mediated Intestinal

- Damage after Allogeneic Transplantation. *Immunity* **51**, 90-103.e3 (2019).
88. Zhang, B. *et al.* Ruxolitinib early administration reduces acute GVHD after alternative donor hematopoietic stem cell transplantation in acute leukemia. *Sci. Rep.* **11**, 8501 (2021).
  89. Kaser, A., Martinez-Naves, E. & Blumberg, R. S. Endoplasmic reticulum stress: implications for inflammatory bowel disease pathogenesis. *Curr. Opin. Gastroenterol.* **26**, 318–326 (2010).
  90. Mohammadpour, H. *et al.* Host-Derived Serine Protease Inhibitor 6 Provides Granzyme B-Independent Protection of Intestinal Epithelial Cells in Murine Graft-versus-Host Disease. *Biol. Blood Marrow Transplant.* **24**, 2397–2408 (2018).
  91. Toubai, T. *et al.* IAPs protect host target tissues from graft-versus-host disease in mice. *Blood Adv.* **1**, 1517–1532 (2017).
  92. Marsh, R. A. *et al.* Allogeneic hematopoietic cell transplantation for XIAP deficiency: an international survey reveals poor outcomes. *Blood* **121**, 877–883 (2013).
  93. Nalle, S. C. *et al.* Graft-versus-host disease propagation depends on increased intestinal epithelial tight junction permeability. *J. Clin. Invest.* **129**, 902–914 (2019).
  94. Fujiwara, H. *et al.* Mitochondrial complex II in intestinal epithelial cells regulates T cell-mediated immunopathology. *Nat. Immunol.* **22**, 1440–1451 (2021).
  95. Petrovic, A. *et al.* LPAM (alpha 4 beta 7 integrin) is an important homing integrin on alloreactive T cells in the development of intestinal graft-versus-host disease. *Blood* **103**, 1542–1547 (2004).
  96. Ueha, S. *et al.* Intervention of MadCAM-1 or fractalkine alleviates graft-versus-host reaction associated intestinal injury while preserving graft-versus-tumor effects. *J. Leukoc. Biol.* **81**, 176–185 (2007).
  97. Chen, Y.-B. *et al.* Up-Regulation of alpha4beta7 integrin on peripheral T cell subsets correlates with the development of acute intestinal graft-versus-host disease following allogeneic stem cell transplantation. *Biol. Blood Marrow Transplant.* **15**, 1066–1076 (2009).
  98. Floisand, Y. *et al.* Safety and Effectiveness of Vedolizumab in Patients with Steroid-Refractory Gastrointestinal Acute Graft-versus-Host Disease: A Retrospective Record Review. *Biol. Blood Marrow Transplant.* **25**, 720–727 (2019).
  99. Coltoff, A., Lancman, G., Kim, S. & Steinberg, A. Vedolizumab for treatment of steroid-refractory lower gastrointestinal acute graft-versus-host disease. *Bone Marrow Transplant.* **53**, 900–904 (2018).
  100. Chen, Y.-B. *et al.* Vedolizumab for prevention of graft-versus-host disease after allogeneic hematopoietic stem cell transplantation. *Blood Adv.* **3**, 4136–4146 (2019).
  101. Cepek, K. L., Parker, C. M., Madara, J. L. & Brenner, M. B. Integrin alpha E beta 7 mediates adhesion of T lymphocytes to epithelial cells. *J. Immunol.* **150**, 3459–3470 (1993).
  102. Vermeire, S. *et al.* Etrolizumab as induction therapy for ulcerative colitis: a randomised, controlled, phase 2 trial. *Lancet (London, England)* **384**, 309–318 (2014).
  103. Koyama, M. & Hill, G. R. The primacy of gastrointestinal tract antigen-presenting cells in lethal graft-versus-host disease. *Blood* **134**, 2139–2148 (2019).
  104. Shlomchik, W. D. *et al.* Prevention of graft versus host disease by inactivation of host antigen-presenting cells. *Science* **285**, 412–415 (1999).
  105. Toubai, T. *et al.* Induction of acute GVHD by sex-mismatched H-Y antigens in the absence of functional radiosensitive host hematopoietic-derived antigen-presenting cells. *Blood* **119**, 3844–3853 (2012).
  106. Li, H. *et al.* Profound depletion of host conventional dendritic cells, plasmacytoid dendritic cells, and B cells does not prevent graft-versus-host disease induction. *J. Immunol.* **188**, 3804–3811 (2012).
  107. Koyama, M. *et al.* Recipient nonhematopoietic antigen-presenting cells are sufficient to induce lethal acute graft-versus-host disease. *Nat. Med.* **18**, 135–142 (2011).
  108. Koyama, M. *et al.* MHC Class II Antigen Presentation by the Intestinal Epithelium Initiates Graft-versus-Host Disease and Is Influenced by the Microbiota. *Immunity* **51**, 885-898.e7 (2019).
  109. Beyaz, S. *et al.* Dietary suppression of MHC class II expression in intestinal epithelial cells enhances intestinal tumorigenesis. *Cell Stem Cell* **28**, 1922-1935.e5 (2021).
  110. Jagasia, M. H. *et al.* National Institutes of Health Consensus Development Project on Criteria for Clinical Trials in Chronic Graft-versus-Host Disease: I. The 2014 Diagnosis and Staging Working Group report. *Biol. blood marrow Transplant. J. Am. Soc. Blood Marrow Transplant.* **21**, 389-401.e1 (2015).
  111. Schoemans, H. M. *et al.* EBMT-NIH-CIBMTR Task Force position statement on standardized terminology & guidance for graft-versus-host disease assessment. *Bone Marrow Transplant.* **53**, 1401–1415 (2018).
  112. Yi, T. *et al.* Reciprocal differentiation and tissue-specific pathogenesis of Th1, Th2, and Th17 cells in graft-versus-host disease. *Blood* **114**, 3101–3112 (2009).
  113. Carlson, M. J. *et al.* In vitro-differentiated TH17 cells mediate lethal acute graft-versus-host disease with severe cutaneous and pulmonary pathologic manifestations. *Blood* **113**, 1365–1374 (2009).
  114. MacDonald, K. P. A., Hill, G. R. & Blazar, B. R. Chronic graft-versus-host disease: biological insights from preclinical and clinical studies. *Blood* **129**, 13–21 (2017).
  115. Cutler, C. S., Koreth, J. & Ritz, J. Mechanistic approaches for the prevention and treatment of chronic GVHD. *Blood* **129**, 22–29 (2017).
  116. Zeiser, R. & Blazar, B. R. Pathophysiology of Chronic Graft-versus-Host Disease and Therapeutic Targets. *N.*



- Engl. J. Med.* **377**, 2565–2579 (2017).
117. Hummel, S. *et al.* Telomere shortening in enterocytes of patients with uncontrolled acute intestinal graft-versus-host disease. *Blood* **126**, 2518–2521 (2015).
  118. Hua, G. *et al.* Crypt base columnar stem cells in small intestines of mice are radioresistant. *Gastroenterology* **143**, 1266–1276 (2012).
  119. Metcalfe, C., Klijavin, N. M., Ybarra, R. & de Sauvage, F. J. Lgr5+ Stem Cells Are Indispensable for Radiation-Induced Intestinal Regeneration. *Cell Stem Cell* **14**, 149–159 (2014).
  120. Buczacki, S. J. A. *et al.* Intestinal label-retaining cells are secretory precursors expressing Lgr5. *Nature* **495**, 65–69 (2013).
  121. van Es, J. H. *et al.* Dll1+ secretory progenitor cells revert to stem cells upon crypt damage. *Nat. Cell Biol.* **14**, 1099–1104 (2012).
  122. Higa, T. *et al.* Spatiotemporal reprogramming of differentiated cells underlies regeneration and neoplasia in the intestinal epithelium. *Nat. Commun.* **13**, 1500 (2022).
  123. Tetteh, P. W. *et al.* Replacement of Lost Lgr5-Positive Stem Cells through Plasticity of Their Enterocyte-Lineage Daughters. *Cell Stem Cell* **18**, 203–213 (2016).
  124. Harnack, C. *et al.* R-spondin 3 promotes stem cell recovery and epithelial regeneration in the colon. *Nat. Commun.* **10**, 4368 (2019).
  125. Murata, K. *et al.* Ascl2-Dependent Cell Dedifferentiation Drives Regeneration of Ablated Intestinal Stem Cells. *Cell Stem Cell* **26**, 377-390.e6 (2020).
  126. Yu, S. *et al.* Paneth Cell Multipotency Induced by Notch Activation following Injury. *Cell Stem Cell* **23**, 46-59.e5 (2018).
  127. Guiu, J. *et al.* Tracing the origin of adult intestinal stem cells. *Nature* **570**, 107–111 (2019).
  128. Nusse, Y. M. *et al.* Parasitic helminths induce fetal-like reversion in the intestinal stem cell niche. *Nature* **559**, 109–113 (2018).
  129. Ashton, G. H. *et al.* Focal adhesion kinase is required for intestinal regeneration and tumorigenesis downstream of Wnt/c-Myc signaling. *Dev. Cell* **19**, 259–269 (2010).
  130. Miyoshi, H., Ajima, R., Luo, C. T., Yamaguchi, T. P. & Stappenbeck, T. S. Wnt5a potentiates TGF-beta signaling to promote colonic crypt regeneration after tissue injury. *Science* **338**, 108–113 (2012).
  131. Liu, S. *et al.* Lgr4 gene deficiency increases susceptibility and severity of dextran sodium sulfate-induced inflammatory bowel disease in mice. *J. Biol. Chem.* **288**, 8794–8803; discussion 8804 (2013).
  132. Romesser, P. B. *et al.* Preclinical murine platform to evaluate therapeutic countermeasures against radiation-induced gastrointestinal syndrome. *Proc. Natl. Acad. Sci. U. S. A.* **116**, 20672–20678 (2019).
  133. Raup-Konsavage, W. M., Cooper, T. K. & Yochum, G. S. A Role for MYC in Lithium-Stimulated Repair of the Colonic Epithelium After DSS-Induced Damage in Mice. *Dig. Dis. Sci.* **61**, 410–422 (2016).
  134. Steinbach, G. *et al.* Pilot study of lithium to restore intestinal barrier function in severe graft-versus-host disease. *PLoS One* **12**, e0183284 (2017).
  135. Ogasawara, R. *et al.* Intestinal Lymphatic Endothelial Cells Produce R-Spondin3. *Sci. Rep.* **8**, 10719 (2018).
  136. Zhao, J. *et al.* R-Spondin1 protects mice from chemotherapy or radiation-induced oral mucositis through the canonical Wnt/beta-catenin pathway. *Proc. Natl. Acad. Sci. U. S. A.* **106**, 2331–2336 (2009).
  137. Kim, K.-A. *et al.* Mitogenic influence of human R-spondin1 on the intestinal epithelium. *Science* **309**, 1256–1259 (2005).
  138. Chalaris, A. *et al.* Critical role of the disintegrin metalloprotease ADAM17 for intestinal inflammation and regeneration in mice. *J. Exp. Med.* **207**, 1617–1624 (2010).
  139. Holtan, S. G. *et al.* Facilitating resolution of life-threatening acute GVHD with human chorionic gonadotropin and epidermal growth factor. *Blood Adv.* **4**, 1284–1295 (2020).
  140. Taniguchi, K. *et al.* A gp130-Src-YAP module links inflammation to epithelial regeneration. *Nature* **519**, 57–62 (2015).
  141. Karin, M. & Clevers, H. Reparative inflammation takes charge of tissue regeneration. *Nature* **529**, 307–315 (2016).
  142. Pestka, S. *et al.* Interleukin-10 and related cytokines and receptors. *Annu. Rev. Immunol.* **22**, 929–979 (2004).
  143. Sonnenberg, G. F. & Artis, D. Innate lymphoid cells in the initiation, regulation and resolution of inflammation. *Nat. Med.* **21**, 698–708 (2015).
  144. Dudakov, J. A., Hanash, A. M. & van den Brink, M. R. M. Interleukin-22: immunobiology and pathology. *Annu. Rev. Immunol.* **33**, 747–785 (2015).
  145. Zheng, Y. *et al.* Interleukin-22 mediates early host defense against attaching and effacing bacterial pathogens. *Nat. Med.* **14**, 282–289 (2008).
  146. Pickert, G. *et al.* STAT3 links IL-22 signaling in intestinal epithelial cells to mucosal wound healing. *J. Exp. Med.* **206**, 1465–1472 (2009).
  147. Munneke, J. M. *et al.* Activated innate lymphoid cells are associated with a reduced susceptibility to graft-versus-host disease. *Blood* **124**, 812–821 (2014).
  148. Oshima, H. *et al.* Stat3 is indispensable for damage-induced crypt regeneration but not for Wnt-driven intestinal tumorigenesis. *FASEB J. Off. Publ. Fed. Am. Soc. Exp. Biol.* **33**, 1873–1886 (2019).



149. Gronke, K. *et al.* Interleukin-22 protects intestinal stem cells against genotoxic stress. *Nature* **566**, 249–253 (2019).
150. Romera-Hernandez, M. *et al.* Yap1-Driven Intestinal Repair Is Controlled by Group 3 Innate Lymphoid Cells. *Cell Rep.* **30**, 37-45.e3 (2020).
151. von Moltke, J., Ji, M., Liang, H.-E. & Locksley, R. M. Tuft-cell-derived IL-25 regulates an intestinal ILC2-epithelial response circuit. *Nature* **529**, 221–225 (2016).
152. Zhu, P. *et al.* IL-13 secreted by ILC2s promotes the self-renewal of intestinal stem cells through circular RNA circPan3. *Nat. Immunol.* **20**, 183–194 (2019).
153. Henden, A. S. *et al.* IFN- $\lambda$  therapy prevents severe gastrointestinal graft-versus-host disease. *Blood* **138**, 722–737 (2021).
154. Levine, J. E. Implications of TNF- $\alpha$  in the pathogenesis and management of GVHD. *Int. J. Hematol.* **93**, 571–577 (2011).
155. Schreurs, R. R. C. E. *et al.* Human Fetal TNF- $\alpha$ -Cytokine-Producing CD4(+) Effector Memory T Cells Promote Intestinal Development and Mediate Inflammation Early in Life. *Immunity* **50**, 462-476.e8 (2019).
156. Bradford, E. M. *et al.* Epithelial TNF Receptor Signaling Promotes Mucosal Repair in Inflammatory Bowel Disease. *J. Immunol.* **199**, 1886–1897 (2017).
157. Couriel, D. R. *et al.* A phase III study of infliximab and corticosteroids for the initial treatment of acute graft-versus-host disease. *Biol. Blood Marrow Transplant.* **15**, 1555–1562 (2009).
158. Drobyski, W. R. *et al.* Tocilizumab for the treatment of steroid refractory graft-versus-host disease. *Biol. Blood Marrow Transplant.* **17**, 1862–1868 (2011).
159. Kennedy, G. A. *et al.* Addition of interleukin-6 inhibition with tocilizumab to standard graft-versus-host disease prophylaxis after allogeneic stem-cell transplantation: a phase 1/2 trial. *Lancet. Oncol.* **15**, 1451–1459 (2014).
160. Jin, X., Zimmers, T. A., Zhang, Z., Pierce, R. H. & Koniaris, L. G. Interleukin-6 is an important in vivo inhibitor of intestinal epithelial cell death in mice. *Gut* **59**, 186–196 (2010).
161. Kuhn, K. A., Manieri, N. A., Liu, T.-C. & Stappenbeck, T. S. IL-6 stimulates intestinal epithelial proliferation and repair after injury. *PLoS One* **9**, e114195 (2014).
162. Shouval, D. S. *et al.* Interleukin 10 receptor signaling: master regulator of intestinal mucosal homeostasis in mice and humans. *Adv. Immunol.* **122**, 177–210 (2014).
163. Zhang, P. & Hill, G. R. Interleukin-10 mediated immune regulation after stem cell transplantation: Mechanisms and implications for therapeutic intervention. *Semin. Immunol.* **44**, 101322 (2019).
164. Biton, M. *et al.* T Helper Cell Cytokines Modulate Intestinal Stem Cell Renewal and Differentiation. *Cell* **175**, 1307-1320.e22 (2018).
165. Quiros, M. *et al.* Macrophage-derived IL-10 mediates mucosal repair by epithelial WISP-1 signaling. *J. Clin. Invest.* **127**, 3510–3520 (2017).
166. Blijlevens, N. & Sonis, S. Palifermin (recombinant keratinocyte growth factor-1): a pleiotropic growth factor with multiple biological activities in preventing chemotherapy- and radiotherapy-induced mucositis. *Ann. Oncol.* **18**, 817–826 (2007).
167. Housley, R. M. *et al.* Keratinocyte growth factor induces proliferation of hepatocytes and epithelial cells throughout the rat gastrointestinal tract. *J. Clin. Invest.* **94**, 1764–1777 (1994).
168. Khan, W. B., Shui, C., Ning, S. & Knox, S. J. Enhancement of murine intestinal stem cell survival after irradiation by keratinocyte growth factor. *Radiat. Res.* **148**, 248–253 (1997).
169. Krivanovski, O. I. *et al.* Keratinocyte growth factor separates graft-versus-leukemia effects from graft-versus-host disease. *Blood* **94**, 825–831 (1999).
170. Clouthier, S. G. *et al.* Repifermin (keratinocyte growth factor-2) reduces the severity of graft-versus-host disease while preserving a graft-versus-leukemia effect. *Biol. Blood Marrow Transplant.* **9**, 592–603 (2003).
171. Blazar, B. R. *et al.* Phase 1/2 randomized, placebo-control trial of palifermin to prevent graft-versus-host disease (GVHD) after allogeneic hematopoietic stem cell transplantation (HSCT). *Blood* **108**, 3216–3222 (2006).
172. Jagasia, M. H. *et al.* Palifermin for the reduction of acute GVHD: a randomized, double-blind, placebo-controlled trial. *Bone Marrow Transplant.* **47**, 1350–1355 (2012).
173. D'Angelo, F. *et al.* Macrophages promote epithelial repair through hepatocyte growth factor secretion. *Clin. Exp. Immunol.* **174**, 60–72 (2013).
174. Kuroiwa, T. *et al.* Hepatocyte growth factor ameliorates acute graft-versus-host disease and promotes hematopoietic function. *J. Clin. Invest.* **107**, 1365–1373 (2001).
175. Joosten, S. P. J. *et al.* MET Signaling Mediates Intestinal Crypt-Villus Development, Regeneration, and Adenoma Formation and Is Promoted by Stem Cell CD44 Isoforms. *Gastroenterology* **153**, 1040-1053.e4 (2017).
176. Holtan, S. G. *et al.* Amphiregulin modifies the Minnesota Acute Graft-versus-Host Disease Risk Score: results from BMT CTN 0302/0802. *Blood Adv.* **2**, 1882–1888 (2018).
177. Shao, J. & Sheng, H. Amphiregulin promotes intestinal epithelial regeneration: roles of intestinal subepithelial myofibroblasts. *Endocrinology* **151**, 3728–3737 (2010).
178. Zaiss, D. M. W. *et al.* Amphiregulin enhances regulatory T cell-suppressive function via the epidermal growth factor receptor. *Immunity* **38**, 275–284 (2013).
179. Bruce, D. W. *et al.* Type 2 innate lymphoid cells treat and prevent acute gastrointestinal graft-versus-host



- disease. *J. Clin. Invest.* **127**, 1813–1825 (2017).
180. Bruce, D. W. *et al.* Third-party type 2 innate lymphoid cells prevent and treat GI tract GVHD. *Blood Adv.* **5**, 4578–4589 (2021).
  181. Rowland, K. J. & Brubaker, P. L. The ‘cryptic’ mechanism of action of glucagon-like peptide-2. *Am. J. Physiol. Gastrointest. Liver Physiol.* **301**, G1-8 (2011).
  182. Norona, J. *et al.* Glucagon like peptide-2 for Intestinal stem cell and Paneth cell repair during graft-versus-host disease in mice and humans. *Blood* (2020) doi:10.1182/blood.2020005957.
  183. Chen, M. E. *et al.* Glucagon-Like Peptide-2 Stimulates S-Phase Entry of Intestinal Lgr5+ Stem Cells. *Cell. Mol. Gastroenterol. Hepatol.* (2022) doi:10.1016/j.jcmgh.2022.02.011.
  184. Fischer, J. C. *et al.* RIG-I/MAVS and STING signaling promote gut integrity during irradiation- and immune-mediated tissue injury. *Sci. Transl. Med.* **9**, (2017).
  185. Bader, C. S. *et al.* STING differentially regulates experimental GVHD mediated by CD8 versus CD4 T cell subsets. *Sci. Transl. Med.* **12**, (2020).
  186. Sato, T. *et al.* Regulated IFN signalling preserves the stemness of intestinal stem cells by restricting differentiation into secretory-cell lineages. *Nat. Cell Biol.* **22**, 919–926 (2020).
  187. Pigneux, A. *et al.* Prior treatment with alpha interferon does not adversely affect the outcome of allogeneic transplantation for chronic myeloid leukaemia. *Br. J. Haematol.* **116**, 193–201 (2002).
  188. Henden, A. S. *et al.* Pegylated interferon-2a invokes graft-versus-leukemia effects in patients relapsing after allogeneic stem cell transplantation. *Blood Adv.* **3**, 3013–3019 (2019).
  189. Zanello, G. *et al.* The Cytosolic Microbial Receptor Nod2 Regulates Small Intestinal Crypt Damage and Epithelial Regeneration following T Cell-Induced Enteropathy. *J. Immunol.* **197**, 345–355 (2016).
  190. Penack, O. *et al.* NOD2 regulates hematopoietic cell function during graft-versus-host disease. *J. Exp. Med.* **206**, 2101–2110 (2009).
  191. Nigro, G., Rossi, R., Commere, P.-H., Jay, P. & Sansonetti, P. J. The cytosolic bacterial peptidoglycan sensor Nod2 affords stem cell protection and links microbes to gut epithelial regeneration. *Cell Host Microbe* **15**, 792–798 (2014).
  192. Lee, C. *et al.* NOD2 Supports Crypt Survival and Epithelial Regeneration after Radiation-Induced Injury. *Int. J. Mol. Sci.* **20**, (2019).
  193. Arpaia, N. *et al.* Metabolites produced by commensal bacteria promote peripheral regulatory T-cell generation. *Nature* **504**, 451–455 (2013).
  194. Willemsen, L. E. M., Koetsier, M. A., van Deventer, S. J. H. & van Tol, E. A. F. Short chain fatty acids stimulate epithelial mucin 2 expression through differential effects on prostaglandin E(1) and E(2) production by intestinal myofibroblasts. *Gut* **52**, 1442–1447 (2003).
  195. Donohoe, D. R. *et al.* The microbiome and butyrate regulate energy metabolism and autophagy in the mammalian colon. *Cell Metab.* **13**, 517–526 (2011).
  196. Mathewson, N. D. *et al.* Gut microbiome-derived metabolites modulate intestinal epithelial cell damage and mitigate graft-versus-host disease. *Nat. Immunol.* **17**, 505–513 (2016).
  197. Ma, X. *et al.* Butyrate promotes the recovering of intestinal wound healing through its positive effect on the tight junctions. *J. Anim. Sci.* **90** Suppl 4, 266–268 (2012).
  198. Romick-Rosendale, L. E. *et al.* Antibiotic Exposure and Reduced Short Chain Fatty Acid Production after Hematopoietic Stem Cell Transplant. *Biol. Blood Marrow Transplant.* **24**, 2418–2424 (2018).
  199. Jenq, R. R. *et al.* Intestinal Blautia Is Associated with Reduced Death from Graft-versus-Host Disease. *Biol. Blood Marrow Transplant.* **21**, 1373–1383 (2015).
  200. Weber, D. *et al.* Rifaximin preserves intestinal microbiota balance in patients undergoing allogeneic stem cell transplantation. *Bone Marrow Transplant.* **51**, 1087–1092 (2016).
  201. van Lier, Y. F. *et al.* Donor fecal microbiota transplantation ameliorates intestinal graft-versus-host disease in allogeneic hematopoietic cell transplant recipients. *Sci. Transl. Med.* **12**, (2020).
  202. Kakahana, K. *et al.* Fecal microbiota transplantation for patients with steroid-resistant acute graft-versus-host disease of the gut. *Blood* **128**, 2083–2088 (2016).
  203. DeFilipp, Z. *et al.* Third-party fecal microbiota transplantation following allo-HCT reconstitutes microbiome diversity. *Blood Adv.* **2**, 745–753 (2018).
  204. Fujiwara, H. *et al.* Microbial metabolite sensor GPR43 controls severity of experimental GVHD. *Nat. Commun.* **9**, 3674 (2018).
  205. Zelante, T. *et al.* Tryptophan catabolites from microbiota engage aryl hydrocarbon receptor and balance mucosal reactivity via interleukin-22. *Immunity* **39**, 372–385 (2013).
  206. Gutiérrez-Vázquez, C. & Quintana, F. J. Regulation of the Immune Response by the Aryl Hydrocarbon Receptor. *Immunity* **48**, 19–33 (2018).
  207. Metidji, A. *et al.* The Environmental Sensor AHR Protects from Inflammatory Damage by Maintaining Intestinal Stem Cell Homeostasis and Barrier Integrity. *Immunity* **49**, 353-362.e5 (2018).
  208. Swimm, A. *et al.* Indoles derived from intestinal microbiota act via type I interferon signaling to limit graft-versus-host disease. *Blood* **132**, 2506–2519 (2018).
  209. Weber, D. *et al.* Low urinary indoxyl sulfate levels early after transplantation reflect a disrupted microbiome and

- are associated with poor outcome. *Blood* **126**, 1723–1728 (2015).
210. Trivett, M. T. *et al.* Preferential Small Intestine Homing and Persistence of CD8 T Cells in Rhesus Macaques Achieved by Molecularly Engineered Expression of CCR9 and Reduced Ex Vivo Manipulation. *J. Virol.* **93**, (2019).
  211. Lee, Y. *et al.* Hyaluronic acid-bilirubin nanomedicine for targeted modulation of dysregulated intestinal barrier, microbiome and immune responses in colitis. *Nat. Mater.* **19**, 118–126 (2020).
  212. Praveschotinunt, P. *et al.* Engineered E. coli Nissle 1917 for the delivery of matrix-tethered therapeutic domains to the gut. *Nat. Commun.* **10**, 5580 (2019).
  213. Gou, S. *et al.* Multi-bioresponsive silk fibroin-based nanoparticles with on-demand cytoplasmic drug release capacity for CD44-targeted alleviation of ulcerative colitis. *Biomaterials* **212**, 39–54 (2019).
  214. Saxton, R. A. *et al.* The tissue protective functions of interleukin-22 can be decoupled from pro-inflammatory actions through structure-based design. *Immunity* **54**, 660-672.e9 (2021).
  215. Toubai, T. *et al.* Host-derived CD8<sup>+</sup> dendritic cells are required for induction of optimal graft-versus-tumor responses after experimental allogeneic bone marrow transplantation. *Blood* **121**, 4231–4241 (2013).
  216. Reinhardt, K. *et al.* Monocyte-induced development of Th17 cells and the release of S100 proteins are involved in the pathogenesis of graft-versus-host disease. *J. Immunol.* **193**, 3355–3365 (2014).
  217. Hossain, M. S. *et al.* Flagellin, a TLR5 agonist, reduces graft-versus-host disease in allogeneic hematopoietic stem cell transplantation recipients while enhancing antiviral immunity. *J. Immunol.* **187**, 5130–5140 (2011).
  218. Taylor, P. A. *et al.* TLR agonists regulate alloresponses and uncover a critical role for donor APCs in allogeneic bone marrow rejection. *Blood* **112**, 3508–3516 (2008).
  219. Reichenbach, D. K. *et al.* The IL-33/ST2 axis augments effector T-cell responses during acute GVHD. *Blood* **125**, 3183–3192 (2015).
  220. Igarashi, M. & Guarente, L. mTORC1 and SIRT1 Cooperate to Foster Expansion of Gut Adult Stem Cells during Calorie Restriction. *Cell* **166**, 436–450 (2016).
  221. Sheng, H., Shao, J., Townsend, C. M. J. & Evers, B. M. Phosphatidylinositol 3-kinase mediates proliferative signals in intestinal epithelial cells. *Gut* **52**, 1472–1478 (2003).
  222. Wang, Q. *et al.* Arachidonic Acid Promotes Intestinal Regeneration by Activating WNT Signaling. *Stem cell reports* **15**, 374–388 (2020).
  223. Gilbert, S. *et al.* Activated STAT5 confers resistance to intestinal injury by increasing intestinal stem cell proliferation and regeneration. *Stem cell reports* **4**, 209–225 (2015).
  224. Gilbert, S. *et al.* Enterocyte STAT5 promotes mucosal wound healing via suppression of myosin light chain kinase-mediated loss of barrier function and inflammation. *EMBO Mol. Med.* **4**, 109–124 (2012).
  225. Xu, J. *et al.* Secreted stromal protein ISLR promotes intestinal regeneration by suppressing epithelial Hippo signaling. *EMBO J.* **39**, e103255 (2020).
  226. Gregorieff, A., Liu, Y., Inanlou, M. R., Khomchuk, Y. & Wrana, J. L. Yap-dependent reprogramming of Lgr5(+) stem cells drives intestinal regeneration and cancer. *Nature* **526**, 715–718 (2015).
  227. Sorrentino, G. *et al.* Bile Acids Signal via TGR5 to Activate Intestinal Stem Cells and Epithelial Regeneration. *Gastroenterology* **159**, 956-968.e8 (2020).
  228. Cheung, P. *et al.* Regenerative Reprogramming of the Intestinal Stem Cell State via Hippo Signaling Suppresses Metastatic Colorectal Cancer. *Cell Stem Cell* **27**, 590-604.e9 (2020).
  229. Howe, K. L., Reardon, C., Wang, A., Nazli, A. & McKay, D. M. Transforming growth factor-beta regulation of epithelial tight junction proteins enhances barrier function and blocks enterohemorrhagic Escherichia coli O157:H7-induced increased permeability. *Am. J. Pathol.* **167**, 1587–1597 (2005).
  230. Qi, Z. *et al.* BMP restricts stemness of intestinal Lgr5(+) stem cells by directly suppressing their signature genes. *Nat. Commun.* **8**, 13824 (2017).
  231. Kondo, Y. *et al.* Stimulation of Cell Migration by Flagellin Through the p38 MAP Kinase Pathway in Cultured Intestinal Epithelial Cells. *J. Cell. Biochem.* **117**, 247–258 (2016).
  232. Nenci, A. *et al.* Epithelial NEMO links innate immunity to chronic intestinal inflammation. *Nature* **446**, 557–561 (2007).
  233. Asquith, M. J., Boulard, O., Powrie, F. & Maloy, K. J. Pathogenic and protective roles of MyD88 in leukocytes and epithelial cells in mouse models of inflammatory bowel disease. *Gastroenterology* **139**, 519–29, 529.e1–2 (2010).
  234. Wang, P.-Y. *et al.* c-Jun enhances intestinal epithelial restitution after wounding by increasing phospholipase C-gamma1 transcription. *Am. J. Physiol. Cell Physiol.* **312**, C367–C375 (2017).
  235. Mandic, A. D. *et al.* c-Jun N-terminal kinase 2 promotes enterocyte survival and goblet cell differentiation in the inflamed intestine. *Mucosal Immunol.* **10**, 1211–1223 (2017).





# 8

General discussion

Acute Graft-versus-Host disease (GVHD) of the gut (GI-) is a severe complication of allogeneic hematopoietic stem cells transplantation (HSCT) and when unresponsive to first-line corticosteroid (CS)-treatment in many cases lethal. As such, it is the most important saboteur of an otherwise lifesaving treatment for hematologic malignancies, immune deficiencies and inborn errors of metabolism. Current treatment targeting the dysregulated immune system falls short, and other options should be explored. In this thesis we explore another side of the coin, investigating how damage to the intestinal epithelium in the course of allo-HSCT and the development and propagation of GVHD could be a target for therapeutic options (Fig. 1). In this chapter, I discuss our main findings, their limitations and implications, and provide a future perspective for research endeavors in the field of allo-HSCT and beyond.

## No response to corticosteroids; then what?

In our retrospective cohort study of **Chapter 2** we describe the clinical course and outcomes of steroid refractory (SR-)GVHD in children in the Netherlands over the past ten years. With a cumulative incidence of almost 50%, a high disease burden and considerable mortality, we illustrate the severity of the condition and identify risk factors for outcome. There is currently no proven effective treatment available for steroid refractory (SR-)GVHD in children due to a lack in prospective studies. The absence of a clearly superior choice of therapy causes divergence in management of the disease and standardization of care<sup>1</sup>. In our study no choice of second-line therapy proved to be superior, despite the multitude of immunosuppressive therapies available. Drawing definitive conclusions in our population is challenging, due to the statistically relatively small and heterogeneous population, in which often many lines of therapy were given concurrently. This underlines the importance of large, multicenter prospective studies. Nonetheless, due to the meticulous reporting of the clinical course in relation to the start of new lines of therapy, we were able to demonstrate the importance of looking beyond just day 28 for a treatment response in this population, reflecting the continued damage to the epithelium<sup>2</sup>. Most of our patients that did recover from SR-GVHD did so after 28 days.

Especially for children it is vital to improve the outcomes of SR-GVHD. Improved knowledge on biology and genetics have broadened the indications of SCT to include benign diseases, such as primary immunodeficiencies and metabolic disorders<sup>3-5</sup>. In those settings the positive graft-versus-leukemia/tumor (GVL) effects that occur in conjunction with the overactive immune system during GVHD are irrelevant due to the lack of underlying malignancy and associated relapse risk. GVHD occurrence is then particularly harmful. Furthermore, limiting treatment-related toxicity like GVHD on the long term becomes increasingly important, since improvements in whole SCT trajectory have significantly increased long-term survival

of children and adolescents<sup>6-8</sup>. Non-relapse mortality is still higher than relapse mortality in children after SCT<sup>7</sup>. Improvement of GVHD outcomes in children will hopefully reduce long term effects, like infections, cataract, pulmonary dysfunction, bone- and joint issues, diabetes, hypothyroidism, cardiac problems, secondary malignancies<sup>9,10</sup>, but also learning disabilities and psychosocial issues<sup>9</sup>.

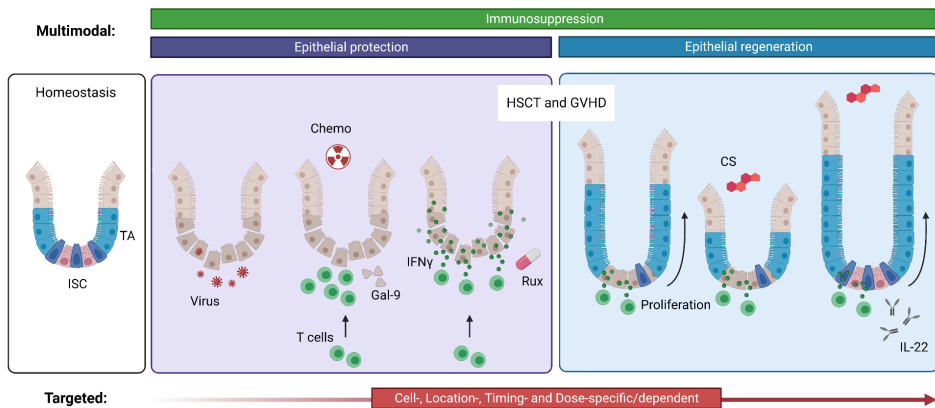


**Figure 1. Multimodal and targeted approach to the treatment of GI-GVHD.** ISC intestinal stem cell, TA transit amplifying cell, IFN $\gamma$  interferon-gamma, Rux ruxolitinib, CS corticosteroids.

## Defining the battlefield in the gut

The cohort of SR-GVHD children of **Chapter 2** illustrates the fact that GVHD of the gut is prevalent, severe, and hard to treat<sup>11</sup>. 84% of the patients suffered from gut GVHD, and 68% from the more severe form (grade III-IV). The combination of malnutrition, dehydration, blood loss, and risk of infection make GVHD patients very vulnerable to death. In almost all children that died in our cohort, gut involvement played a role.

The tolerance of tissues that are targeted in GVHD has been proposed as an important factor in GVHD pathophysiology<sup>12</sup>. In rectal biopsies of GVHD patients that suffered early mortality, the transcriptional signature hinted at a higher degree of DNA damage and stress<sup>13</sup>. Recent early biomarker-based prediction models for both GVHD<sup>14,15</sup> and SR-GVHD<sup>16</sup> outcome include the proclaimed gut-related damage factor REG3a. Another model was superior in the prediction of GVHD outcomes when tissue damage factors ST2 and/or REG3a were included, as compared to using systemic inflammation factors TNFR1 and TIM3 only<sup>17</sup>. In **Chapter 7** we identify all aspects of damaging insults to the gut during the course of HSCT and their possible relation to GVHD, from conditioning injury and danger signals to the actions of alloreactive T cells.



Despite the numerous aspects of epithelial damage as risk factors for the development and severity of GVHD<sup>18</sup>, causality is for most still far out of reach. Nonetheless, the concept of tissue damage already has implications for clinical HSCT management, for instance to increase or slower taper GVHD prophylaxis. Certain conditions with a lot of tissue damage and infection risk, such as common (variable) immunodeficiency, are recognized as indications for which increased GVHD preventive measures should be undertaken. In this thesis, we shed light on the role and mechanism of intestinal epithelial damage in the course of allo-HSCT and in the development and treatment of GVHD using various preclinical models.

### **Chemotherapy conditioning and galectin-9**

Chemotherapy used in the conditioning before HSCT is a well-known risk factor for GVHD. Despite recent developments in the pharmacokinetic modeling of chemotherapy exposure and tailored dosing having reduced toxicity and improved HSCT survival<sup>19–24</sup>, conditioning appears to be a necessary evil to ‘get the cells in’ and to deal a last blow to any remaining leukemic (stem) cells. Thus far, mechanistic propositions of GVHD development after tissue injury have primarily implicated the activation of the innate immune system, which sets the stage for the development of allo-reactive T cell responses. We found that chemo-induced epithelial damage also could exert a direct effect on T behavior in **Chapter 4**. Galectin-9 (gal-9), a galactoside-binding lectin that we identify as an epithelial derived danger signal, influences CD4 and CD8 T cell migration, activation and proliferation. These observations may be of significance for future preventive or even therapeutic approaches.

The role of gal-9 is pleiotropic, ranging from pro-inflammatory to immunosuppressive, even with respect to its direct effects on T cells. High levels of extracellular gal-9 have been shown to induce apoptosis in both CD4<sup>25–27</sup> and CD8 T cells<sup>28,29</sup>, but lower levels may also cause subsequent activation<sup>26,27</sup> and induce pro-inflammatory cytokines such as IFN $\gamma$ <sup>26,27,30</sup> and granzymes/perforin<sup>29</sup>. Conversely, gal-9 can potentiate Treg development and function<sup>31–34</sup>. Gal-9’s capacity to bind to glycosylated parts of the cell, creating lattices, causes highly variable ligand-receptor interactions in a spatiotemporal manner<sup>35,36</sup>. As such, gal-9 has been shown to associate with, and influence downstream processes of multiple receptors<sup>25,33,34,37–39</sup>. Therefore, its netto effect depends on the (combination of) receptors present, glycosylation status of involved cells, as well as gal-9 abundance (high versus low concentration), which highly complicates research endeavors elucidating its effects.

Our findings hint at the pro-inflammatory part of the spectrum, with gal-9 potentiating Th cells and cytotoxic T cells. A similar mechanism was described for the conditioning-induced danger signal IL33, which acted as a costimulatory signal to generate allo Th 1 cells, and inhibit a regulatory phenotype<sup>40</sup>. The pro-inflammatory hypothesis is corroborated by the higher gal-9 plasma levels at time of transplant in HSCT patients that eventually develop



GVHD. A previous clinical study found a similar trend in gal-9 levels (albeit at a much later timepoint) and showed that high gal-9 levels pre-GVHD development were associated with increased GVHD incidence and reduced overall survival<sup>41</sup>. Thus, blocking the gal-9-T cell interaction may be a promising preventive approach. There are several examples in which the blocking of the interaction of damage molecules with the immune system is associated with improved outcome in GVHD (see Table 1 **Chapter 7**). Blocking anti-gal-9 antibodies are currently being developed as checkpoint inhibitors to induce an anti-tumor immune response<sup>39,42–44</sup>, which may facilitate future application in HSCT patients. Nonetheless, considering the application of a checkpoint inhibitor in the treatment of a condition in which an overactive immune system is the hallmark of disease is hard to imagine.

Thus far, results of gal-9 signaling in already established experimental GVHD support a beneficial role of gal-9<sup>41,45,46</sup>, albeit in one study only in the presence of Tregs<sup>46</sup> and not on all envisioned endpoints<sup>45</sup>. We show that gal-9 plasma levels remain high in patients with GVHD beyond the day of transplant. This could 'just' indicate ongoing damage, but may also be part of a (failing) protective feedback loop, for instance facilitating Tregs and suppressing conventional T cells. This notion may be supported by the fact that pre-transplant and pre-conditioning gal-9 levels in patients that did not develop GVHD were actually higher than those who did, perhaps providing a layer of protection pre-insult<sup>41</sup>. Whichever direction it will take, strict regulation of gal-9 targeted therapies must be in place with respect to timing, location, dosage, and cell types involved, which carefully executed future research must elucidate.

Regardless of its (preventive) therapeutic potential, gal-9 could serve as a very early biomarker for the development of GVHD. Current established prediction models predict development of severe GVHD and outcomes based on samples taken on day 7 after transplant<sup>15</sup> or when GVHD has already developed<sup>14,17</sup>. If gal-9 were to be validated as a prognostic biomarker already at the time of transplant, it will give the physician more time to plan and conduct preventive strategies and hopefully reduce the development or severity of GVHD.

Conversely, serious effort is being made to develop methods of conditioning that forgo chemotherapy all together by specifically targeting the hematopoietic compartment, without inducing any bystander tissue damage. The application of CD45-targeted (pan-leukocyte and HSC marker) antibody-drug conjugates (ADCs) proved to be a safe and highly effective non-genotoxic conditioning replacement in mouse HSCT models<sup>47</sup>. Another example is found in ADCs targeting CD117 (c-kit or stem cell factor receptor), which is expressed only by HSC and progenitor cells. Conditioning with CD117-ADCs<sup>48</sup> in combination with antibodies targeting T and NK cells<sup>49,50</sup> resulted in stable HSC reconstitution in MHC-mismatched transplantation in immunocompetent mice. Both 'naked' anti-CD45 and CD117 antibodies



and ADCs are now subject of phase 1 trials, and could be applicable in pediatric HSCT for diseases like severe aplastic anemia, fanconi anemia, sickle cell disease, beta-thalassemia and primary immune disorders<sup>51</sup>. These developments will potentially remove the use of chemotherapy from conditioning regimens, and associated risks with that, but extensive dose finding trials will be necessary before such conclusions can be drawn.

### **Enteric viruses**

A damaging factor influencing clinical decision making not touched upon in our review of **Chapter 7** is the presence of viruses in the gut. While much is known about microbial correlations with GVHD outcomes and allo-HSCT in general, the role of the virome remains to date relatively understudied<sup>52</sup>. Nonetheless, the presence of specific viruses in the gut before<sup>53,54</sup> or within 1 week after<sup>54</sup> transplant has been associated with the occurrence of GI-GVHD. For true virome assessment in the transplant-trajectory unbiased virus detection by NGS technology is required, but this has been limited by the low sensitivity of NSG for this application<sup>55</sup>. Recent strategies for the enrichment of viral nucleic sequences has improved the detection sensitivity<sup>56</sup>. In **Chapter 3** we applied an example of such an approach, named ViroCap, to clinical stool samples of pediatric transplant patients and were able to broadly detect untested viruses and recent variants<sup>57</sup>. This thereby could be a useful approach for studying the role of virus in GVHD etiology and development in future, larger cohorts of patients.

Several hypothesis can be raised as to how viral presence associates with allo-immune activation in the gut. Firstly, viral enteritis could activate the innate immune system through the induction of DAMP-release and fuel alloreactive responses in the way that has already been described. A recent study suggests that in an inflammatory environment viral components can induce MHC-II expression on the intestinal epithelium<sup>58</sup>. Epithelial MHC-II expression has been shown to be indispensable for the induction of lethal GI-GVHD in mice<sup>59</sup>. Thirdly, viral infection may influence the development of immune tolerance to self-antigens. In mice, infection with a specific herpes virus led to the development of auto-immune gastritis, which was associated with a disruption of thymic/central tolerance<sup>60</sup>. After transplant, donor T and B cells exiting the newly engrafted bone marrow undergo selection for tolerance for recipients antigens. Failure may result in acute and chronic GVHD. Knowing more about viral constitution and predisposition for development and severity of GVHD will allow the testing of these hypotheses, and hopefully provide new therapeutic insights.

### **Allo T cells**

#### ***Killing mechanisms***

Despite pre-damaging events in HSCT, the main event in GVHD remains the allo-activation of donor T cells which causes further damage to the already compromised epithelial barrier. It was long unknown how activation of allo-T cells caused damage to the intestinal epithelium.

Direct cytolytic effects of donor T cells through the TNF family member Fas ligand/Fas pathway<sup>61,62</sup> or the release of serine protease granzyme B (GzmB) and pore-forming cytolytic perforin<sup>63</sup> did not or insufficiently explain the mechanism in mice<sup>64</sup>. Nonetheless, gut-infiltrating CD8 T cells in non-human primates with GVHD exemplified a highly cytotoxic profile with high GzmB expression and frequent perforin co-expression<sup>65</sup>. In **Chapter 5**, we demonstrate that the intestinal epithelium is destroyed indirectly, by the allo-activated donor CD4 and CD8 T cell derived cytokine IFN $\gamma$  targeting the intestinal stem cells (ISCs), and thereby hindering epithelial regeneration<sup>66</sup>. In addition to IFN $\gamma$ , plenty other cytokines have been shown to play a role in GI-GVHD development, including TNF $\alpha$ , IL-1 $\alpha/\beta$ , IL-6, IL-21, IL-23, IL-33 and GM-CSF (reviewed in<sup>67</sup>). Their inhibition as – mostly immunosuppressive – therapeutic approach to improve GVHD has been giving contradicting results. As discussed in **Chapter 7**, this is probably due to pleiotropic, temporal effects, which vary between different cell types, and are dependent on the abundancy of cytokines relative to one another. This phenomenon of dichotomy will be discussed in more detail later on in this chapter.

### ***Recruitment to the intestinal epithelium***

In **Chapter 5**, we found that donor T cells preferentially invade the intestinal crypt region after SCT, where the stem cells are residing. Our collaborators found that  $\alpha 4\beta 7$ -integrin expressing donor T cells migrate to the small intestine and interact with endothelial MAdCAM-1, which was especially abundant in the venules surrounding the crypt compartment<sup>68</sup>. As such, the  $\alpha 4\beta 7$ -MAdCAM-1 axis is a promising target for intestinal crypt-protecting therapy in GVHD as discussed in **Chapter 7**.

There are however multiple other ways to prevent T cells from entering the gut during GI-GVHD, which were not discussed in **Chapter 7**. Trapping allo-activated T cells in the lymph nodes (LNs) inhibits their devastating effects on the epithelium. Due to lymphopenic reconstitution, irradiation only sufficed for donor T cells to massively enter the spleen, cutaneous and mesenteric LNs in mice. Subsequent mismatched bone marrow transplantation (BMT) increased the magnitude of infiltration, but did not affect the pattern<sup>69</sup>. In non-human primates the influx pattern of donor CD4 and CD8 T cells into LNs and most organs after HSCT was the same for allogeneic and autologous transplant. However, significantly more T cells infiltrated into the gut in the allogeneic setting<sup>65</sup>. Donor T cell could already be found in the gut as early as 6 hours post-BMT in mice<sup>70</sup>. In spite of T cells simultaneously accessing mouse peripheral LNs and the gut, activation was predominantly seen in the gut<sup>71</sup>. Gut tissue-tropism is already initiated at the anatomical site of the LNs, but with considerable redundancy. Only blocking entry into all sites improved GVHD<sup>72</sup>. Also inhibiting T cell egress from LNs reduced target organ infiltration and diminished GVHD mortality in mice<sup>73</sup>.



Interfering with the migration of T cells from LNs to the gut is another approach. Migration occurs under the influence of attracting chemokines and corresponding receptors<sup>74</sup>, independent from antigen expression<sup>69,75</sup>. For instance, T cell-expressed CCR5 chemokine receptor and its ligands CCL3, 4 and 5 have been implicated in GI-GVHD pathogenesis<sup>65,74,76,77</sup>. Maraviroc, a CCR5 antagonist, may be a potentially effective prophylactic strategy to reduce GI-GVHD in adults<sup>78,79</sup> and children<sup>80,81</sup>, despite conflicting results in animal models<sup>82,83</sup>. One of the reasons for conflicting findings might lie in a shift in balance to prevalence of other chemokine-receptor pairs during inhibition of the one. Patients that developed aGVHD despite maraviroc prophylaxis showed elevation of serum CXCL9 and 10 levels, which suggests the CCR5 blockade is being bypassed by increased CXCR3-mediated lymphocyte migration<sup>84</sup>. CXCR3 signaling has also independently been associated with GVHD<sup>85,86</sup> and its ligands CXCL9, 10 and 11 were found to be upregulated in the gut after conditioning<sup>87</sup> and in GVHD<sup>76</sup>. A third lymphocyte-gut migration pathway involved in experimental GVHD consists of CX3CL1 (or fractalkine) and its receptor CX3CR1<sup>88</sup>. Also in GVHD patients CX3CL1 (both mononuclear cells and epithelial cells stained positive) and its receptor were implicated in GVHD by immunohistochemistry on slides of GVHD patients and blood levels<sup>89</sup>. Lastly, CCR6 expression<sup>90</sup> by and TRPM7 kinase activity<sup>91</sup> in donor T cells were implicated in the development of GI-GVHD through gut-infiltration, and might provide future therapy targets. An important side note in targeting T cell homing in GVHD therapy strategies, is the concurrent, unwanted inhibition of influx of immunosuppressive and gut-protective Tregs<sup>92,93</sup>. Tregs have been shown to be potent suppressors of GVHD<sup>94</sup> and multiple efforts are being made to induce Tregs in the transplant setting either *in vivo*<sup>95,96</sup> or *in vitro* prior to adoptive transfer<sup>97</sup>. In a recent study, homing-receptor expression was exploited to induce gut-directed Tregs *in vitro*. CXCR3-expression allowed the Tregs to migrate towards CXCL10, and induction of  $\alpha 4\beta 7$  and CCR9 expression during expansion enabled the Tregs to infiltrate inflamed intestine *in vivo*<sup>98</sup>. This marks an important trade off, where reducing infiltration of allo-T cells using the chemokine receptor axis hampers possible gut-directed Treg therapies.

### **Toxicity of first-line corticosteroids**

To make matters worse, we discovered in **Chapter 6** that the most effective treatment of GVHD, first-line therapy with immunosuppressive corticosteroids (CS), provides an extra layer of intestinal epithelial damage or failure to recover. Patients are often exposed to CS for long periods of time because of slow tapering to prevent flaring of GVHD. Even in case of SR-GVHD, CS gifts are initially continued alongside a newly started experimental therapy. We show in **Chapter 6** that when alloreactive responses are insufficiently suppressed, CS caused additional toxicity and reduction of epithelial regeneration. This was perhaps to be expected given the well-known atrophic effects of CS on the skin epithelium<sup>99</sup>.

Our findings are in line with those of a recent study using a SR-GVHD mouse model, in which SR-GVHD mice experienced an overall increase in GVHD-specific histopathological

damage to target organs in comparison to steroid-responsive animals, without any significant differences in donor T cell characteristics<sup>100</sup>. Also transcriptomic analysis of biopsies of patients with SR-GVHD as compared to those taken at the time of GVHD diagnosis demonstrate negative regulation of growth and reduced wound healing<sup>13</sup>. No differences in T cell-related expression were found between GVHD diagnosis and SR-GVHD. These observations perhaps provide an explanation as to why it has been so challenging to find an effective treatment for SR-GVHD by focusing solely on the immune system.

However, our findings do not completely resolve the mystery of SR-GVHD. Another recent mouse model suggested that the development of SR-GVHD is associated with a shift in donor T cell subsets. They observed an expansion of interleukin (IL)-22 producing T cells, which caused dysbiosis in a Reg3 $\gamma$  dependent manner<sup>101</sup>. Donor T cell derived IL-22 has previously been shown to enhance GI-GVHD<sup>102,103</sup>. This finding is a stark contrast with the beneficial effect of exogenously administered IL-22 on CS-induced epithelial impairment we found in **Chapter 6**, and the promising results of a recent phase II trial applying recombinant IL-22 in the treatment of GVHD patients<sup>104</sup>. This seeming contradiction will be further discussed later on in this chapter. There are probably multiple facets to the SR-GVHD mechanism, including T cell dependent and independent ones.

## So how to save the tissue?

Tissue resilience, repair and regeneration are essential to overcome the continuous insults to the integrity of the intestinal epithelial barrier in GI-GVHD<sup>12</sup>. In addition to protecting the gut by directly targeting the damaging factors discussed above, we explored several options as to how the intestinal epithelium can be restored in **Chapter 7**.

### **Interferon-gamma: friend or foe?**

Resilience at the level of the intestinal epithelial cell as a GVHD treatment target is exemplified in **Chapter 5**. Due to its pleiotropic roles in the SCT trajectory, targeting IFN $\gamma$  directly to inhibit intestinal epithelial destruction is very challenging<sup>105–109</sup>. As such, merely blocking its function with an antibody like emapalumab does not seem to be an option. Inhibiting the effect of IFN $\gamma$  at the site of the tissue through inhibiting its signaling cascade with JAK inhibition does seem promising<sup>66</sup>, but may have similar issues. Nonetheless, our findings plea for extended use of JAK-inhibitor ruxolitinib (rux), beyond SR-GVHD, either earlier in the course of GVHD<sup>110</sup>, or even as prevention<sup>111,112</sup>. Care should be taken with these approaches however, since ironically we recently found that IFN $\gamma$  also exerts positive effects on epithelial regeneration at a later stage of GVHD<sup>113</sup>. Mice deficient in STAT1, an essential transcription factor for IFN $\gamma$  signaling, initially are protected against IFN $\gamma$ -mediated detrimental effects on the epithelium, but eventually experience reduced epithelial recovery



at a later time point than STAT1 potent littermates. This appears to be caused by a STAT-1-MYC mediated proliferation of ISC. In addition, JAK/STAT signaling may be required for thymic immune recovery<sup>114</sup>. The effect of IFN $\gamma$  and the application of its inhibition is therefore time-dependent.

The effect of IFN $\gamma$  on the intestinal epithelium may also be dose-dependent. When treating intestinal organoids with IFN $\gamma$ , higher concentrations result in organoid loss and epithelial death as shown in **Chapter 5**, while lower concentrations induced increased growth and even increased reconstitution from single cells in organoids<sup>113</sup>. A similar dichotomy is observed with another cytokine important in GVHD pathology, TNF $\alpha$ . Contributions of TNF $\alpha$  to GVHD pathology have resulted in the introduction of TNF $\alpha$  blocking therapies<sup>115–118</sup>. Indeed, TNF $\alpha$  also has a detrimental effect on the intestinal epithelium as indicated by a reduction in fetal intestinal organoid number and impaired ISC proliferation<sup>119</sup>. Nonetheless, low amounts of TNF $\alpha$  were able to induce organoid growth. This provides us with an extra layer of complexity in targeting signaling in the epithelium as a therapeutic approach. The divergent effects do not seem to be relying upon different signaling pathways of the cytokines. At least for IFN $\gamma$  the signaling pathway involved in both destructive and regenerative effects appears to be STAT1, as STAT1-deficient organoids were resistant to IFN $\gamma$ -dependent damage and growth induction. Other mechanisms may be at play resulting in the divergent effects observed, including IFN $\gamma$ -receptor affinity, membrane expression levels, or the stability of and crosstalk between tertiary complexes in the signaling pathway<sup>120</sup>. It will require further careful consideration to understand when exactly the inhibition of IFN $\gamma$  signaling is best to be applied.

### **Local, and cell-specific regeneration**

In addition to opposing effects in timing or dose, the exact anatomical location may be an important factor when targeting the epithelium as well. The microbial metabolite butyrate has positive effects on the gut in GVHD as reviewed in **Chapter 7**. *In vitro*, it specifically increased the growth of small intestinal (SI) organoids (mouse and human) via HDAC inhibition<sup>121</sup>. However, more recently it was described that butyrate actually decreased the growth of organoids derived from mouse colon<sup>122</sup>. Since organoids maintain their location-specific identity *in vitro*<sup>123</sup>, it seems that even the location of the epithelial cells is important for certain regenerative effects. Perhaps divergent biological outcomes of HDAC inhibition/induction in the different parts of the intestine underlies these findings. Inositol derived from *E. Coli* increased the size of colon organoids via induction of HDAC<sup>122</sup>, which is the exact opposite mechanism of the butyrate induced organoid growth in SI.

Another example of a factor supportive of epithelial regeneration with complex dynamics is IL-22, as reviewed in **Chapter 7**. In mice, treatment with IL-22 directly supported ISC survival and proliferation and reduced GI-GVHD pathology and mortality<sup>124</sup>. *In vitro*, IL-22

was recently shown to induce the formation of Paneth cells<sup>125</sup>, which in turn support the ISCs. Incidence of GI-GVHD was higher in children with above median serum IL-22 levels at day 30 after transplant<sup>126</sup>, but no difference was seen in gut biopsy IL-22 expression between patients with and without GVHD<sup>127</sup>. However, IL-22 expression was upregulated in gut biopsies of GVHD patients who survived and low IL-22 expression correlated with increased transplant-related mortality after HSCT<sup>127</sup>. This hints at a protective role for IL-22 also in patients. A Phase II clinical study involving IL-22 IgG2-Fc (F-652) treatment on subjects with grade II-IV lower GI-GVHD has just been conducted in adults, and with reaching the primary endpoint of a treatment response in 70% of patients the results are promising<sup>104</sup>. Tissue regenerative IL-22 is released from innate lymphoid type 3 cells (ILC3s) that perish in experimental and clinical GVHD<sup>128,129</sup>. As briefly mentioned above, ILC3s are not the only cells in the intraepithelial/mucosal compartment excreting it. IL-22 derived from donor T cells was shown to promote both GVHD<sup>102,103</sup> and SR-GVHD<sup>101</sup> in animal models. Recent work studied the contributions of IL-22 from both cell types in the same animal model during *Citrobacter rodentium* infection<sup>130</sup>. They found that IL-22 from both origins induced protective STAT3 phosphorylation in the intestinal epithelium, but prolonged T cell-derived IL-22 was required for controlling the infection. Probably similar spatiotemporal effects of IL-22 are at play in the development of (SR-)GVHD. Thus, anatomical location, cell of origin, and timing appear to be crucial in the workings of IL-22.

Recent data suggests that peri-transplant cell therapy with IL-22 producing ILC3s could be an even more promising approach for the prevention of GVHD. Next to IL-22 production, ILC3s may have additional immunosuppressive<sup>129</sup> and regenerative effects<sup>131</sup>. ILCs are depleted from the blood of patients who undergo conditioning therapy before HSCT<sup>132</sup>. In mice, ILC3s move to the crypt after TBI, and excrete IL-22 there locally<sup>133</sup>. Interestingly, patients with a relatively rapid recovery of ILC numbers after conditioning, before HSCT, experienced less mucositis and acute GVHD after HSCT<sup>132</sup>. Furthermore, presence of ILCs in the HSCT grafts correlated with reduced GVHD<sup>134</sup>. There are now ways of efficiently generating human ILC3s in the lab<sup>135,136</sup>. Nonetheless, ILCs have been shown to be very plastic depending on the condition they are in, easily switching to a pro-inflammatory ILC1 phenotype under inflammatory conditions<sup>137</sup>. Engineering of the cells to stabilize their ILC3 phenotype might be warranted before cell therapy is feasible. In addition, the molecular structure of the IL-22 they excrete can be fine-tuned, rendering only a tissue protective effect through STAT3 signaling<sup>138</sup>.

### **Challenges in a multimodal and targeted approach**

When developing treatments aimed at the resilience or regeneration of the intestinal epithelium, we have to keep in mind that in patients multiple treatments will be given at the same time (Fig. 1). It is important to study how the different approaches affect each other. Since allo-immune activation is the main culprit in GVHD we will never get away from some form



of immunosuppressive therapy. Despite the negative effects of CS on epithelial recovery, it is the most effective therapy we have for GVHD at this time. Luckily, we found in **Chapter 6** that IL-22 could exert regeneration even in the presence of crypt recovery-undermining CS. This is a very relevant finding since in clinical practice patients may still be on CS when IL-22 treatment is considered. The combination of IL-22 with rux, the only registered treatment for SR-GVHD in adults thus far, poses a challenge however. In the future development of IL-22 and/or ILC3s as a treatment for (SR-)GVHD it should be taken into consideration that rux will possibly eliminate IL-22-induced STAT3 effects through the inhibition of upstream JAK1/2. These therapies cannot be applied simultaneously. A possible treatment schedule may include the application of CS with rux early on at GVHD onset, to inhibit alloreactive T cells on the one hand and, in case of rux, protect the epithelium against the cytokine storm on the other hand. Consequently, ruxolitinib can be discontinued to let remaining IFN $\gamma$  support epithelial regeneration, and (ILC3-secreting) IL-22 applied, to boost that same regeneration. Additional research is required to understand which treatment to subscribe exactly when, and based on which clinical parameters or biomarkers these choices should be made. Chemical-pharmaceutical innovations, as well as cell therapeutic technologies, could help to ascertain delivery of just the right compound at just the right time and place. Nanoparticles specifically destined for the gut<sup>139–141</sup> could provide a medium for the delivery of JAK-inhibitors or IL-22. Recent developments in orthogonal IL-IL-Receptor complexes have allowed for the expansion of specific immune cells, facilitating immune tolerance after solid organ transplantation<sup>142</sup>. A similar approach can be imaginable expanding and/or sustaining IL-22 secreting cells, whether these are ILC3s or for instance engineered CAR T cells. In addition, engineering of synthetic CAR T receptor circuits has allowed for their *in vivo* proliferation and secretion of specific interleukins upon encounter of specific peptides, such as tumor antigens<sup>143–149</sup>. Were such cell therapies to be translated to the context of GVHD, one could think of an engineered cell that was to specifically migrate to the intestinal crypt compartment, based on  $\alpha 4\beta 7$ -integrin expression, and there, upon exposure to for instance high levels of IFN $\gamma$  and another damage molecule, for instance gal-9, release IL-22. All these cutting-edge technologies provide exciting new research targets, of which the possibilities seem endless.

## Model systems and translation to The Human

It is challenging to dissect cause from consequence in a multifaceted disease such as GI-GVHD as it develops in the whole complexity of an organism. The nuances in GI-GVHD damage mechanisms and therapeutic targets discussed above have been discovered through the use of existing-, and the development of new disease models, both *in vivo* and in a dish. In the past decades many important lessons about GVHD biology have been learnt through the use of mouse BMT models, and have resulted in many clinical



applications<sup>150</sup>. Also in our studies on mechanisms of donor T cell-induced damage in **Chapter 5** and CS-induced epithelial effects in **Chapter 6**, the use of several mouse BMT models was extremely insightful. Nonetheless, in multiple aspects mice are really not humans, and other methods are necessary to make the step to understand human biology and pathophysiology, hopefully eventually making the use of animal models dispensable.

### Intestinal epithelial organoids

We were the first to demonstrate that mouse epithelial organoids could serve as a proxy for *in vivo* GI-GVHD intestinal crypt function and damage. The application of organoids allowed us to study epithelial specific effects and interactions with T cells which held true *in vivo* in **Chapter 5** and **6**. Despite the fact that not all *in vivo* crypt homeostatic processes are recapitulated in organoids<sup>151</sup>, we were able to use less mice in our investigations. In addition, the use of organoids made it possible to 'leap' from mouse and mouse *in vitro* studies to more clinically relevant human *in vitro* studies<sup>152</sup>.

Despite multiple similarities, quite some differences exist between mouse and human intestinal epithelium<sup>153</sup>, and consequently in therefrom derived organoids<sup>154</sup>. For instance, human crypts have an increased dependency on niche factors and small molecule inhibitors to be sustained in culture, suggesting fundamental differences in self renewal between human and mouse<sup>104,155</sup>. As a consequence, human organoids as used in this thesis contain a limited number of cell types and lack niche-supporting Paneth cells (PC) for example<sup>156</sup>. Furthermore, *in vivo* human epithelium contains unique cell types, such as motilin+ enteroendocrine cells<sup>156</sup>, which are not present in mice, signifying different constrains during crypt development<sup>157</sup>. The limited cell diversity in human organoids presents the biggest limitation in their current applicability to answer clinically relevant questions. A very recent publication describing optimized culture conditions for human SI organoids may overcome this hurdle<sup>125</sup>. Several previous attempts had been made to improve cell diversity in human organoids<sup>156,158,159</sup>, but had not yet led to a new 'golden standard' of culture. In expectance of culture conditions that can give rise to the full spectrum of human intestinal epithelial cells, conditions to specifically differentiate organoids towards certain human cell types have been described<sup>158,160</sup>. The new culture conditions simultaneously induce a great variety of human intestinal epithelial cell types, including a PC, goblet, enteroendocrine and tuft cell phenotype, provoking budding with crypt-villus structures as observed in mouse organoids<sup>122</sup>. Interestingly, the addition of IL-22, the factor previously shown to directly contribute to ISC survival and proliferation, appeared to be pivotal for the induction of PCs. With these developments human organoids have become more similar to *in vivo* intestinal epithelium.

Another shortcoming of both mouse and human intestinal epithelial organoids is the lack of other gut-relevant tissues, such as the submucosal tissue. Certain progress has been made in this respect. Transducing differentiated cells with 4 transcription factors generates



human induced pluripotent stem cells (hiPSC)<sup>161</sup>. Intestinal organoids derived from hiPSC (HIOs) are surrounded by a primitive mesenchyme, which can differentiate into smooth muscle, myofibroblasts, and fibroblasts during a differentiation protocol<sup>162</sup>. However, HIOs have a fetal phenotype and require either transplantation *in vivo* under the kidney capsule of mice<sup>163</sup> or the inclusion of immune components<sup>164</sup> to mature into adult epithelium. This is a long and tardy process. For the purpose of intestinal transplantation efforts are made in combining different gut tissues. In a proof of concept, co-assembling human small intestinal organoids with de-cellularized human intestinal matrices as biological scaffold reliably reconstructed small intestinal mucosal grafts<sup>165</sup>. Finally, since the intestine also contains vasculature and innervation, co-culturing of epithelial organoids with different types of mesenchymal, endothelial and glial cells aims to model cellular interactions within those specific compartments<sup>166</sup>.

### **Translational potential of disease models in a dish**

Many important insights in both intestinal epithelial homeostasis and disease have been gained by the application of organoids<sup>167</sup>. In **Chapter 4, 5** and **6** we make use of co-cultures of human peripheral blood (PB) T cells and intestinal organoids to model parts of the GI-GVHD pathophysiology in a dish. Despite the fact that we were not the first to use this culture combination to answer pathophysiological questions (for instance<sup>93,119</sup>), we were the first to apply it to the field of GI-GVHD. In future studies our models can be used to understand the course of HSCT damage processes in time even better. For instance, it can be used for unravelling the role of specific viruses (**Chapter 3**)<sup>168</sup> and microbiota<sup>169</sup> in the development of alloreactive responses. In addition, new damage-limiting and regeneration-targeted therapies can be tested. For example through the development of a new co-culture system with human ILC3s, as was done recently with ILC1s<sup>170</sup>.

An important point of discussion when modelling GI-GVHD in the lab is the type and origin of the used T cells. Donor IFN $\gamma$ -producing CD4 (Th1) and CD8 (Tc1) T cells are classically identified as the main propagators of GVHD in mice and men<sup>65</sup>, which matched with our identification of IFN $\gamma$  as epithelium damaging factor in **Chapter 5**. The protocols for PB T cell activation we used induced a strong IFN $\gamma$  production response. However, the frequency of certain T cell types implicated in GVHD is low in PB, such as IL-17<sup>171</sup> and IL-22 producing Th17/Tc17, respectively Th22/Tc22, although the latter has thus far only been implicated in mouse studies. Concerning the origin of involved T cells, preclinical studies have supported the role of donor naïve T cells in inducing GVHD as opposed to central memory T cells. But in humans the specific depletion of naïve T cells from the graft reduced only the incidence of chronic GVHD<sup>172</sup>. PB contains both naïve and memory CD4 and CD8 T cells in ratios 1:1 respectively 1:2. A recent elegant study in macaques demonstrates that the phenotype that T cells acquire during GVHD is probably the most important aspect. Donor CD8 T cells developed a tissue resident memory (CD69+CD103+), effector memory (CCR7-CD45RA-)

phenotype with gut-infiltration in GVHD<sup>65</sup>. The transcriptomic profile of these CD8 T cells matched that of T cells in the PB of acute GVHD patients. Therefore PB might not be such a bad place to start for modelling GVHD.

Nonetheless, a patient-based approach will be warranted in future modelling. In mice, the PB T cell clones associated with GVHD were similar to those found in the gut, but very rare compared to clones present pre-transplant<sup>173</sup>. Using PB from patients pre-transplant to model GVHD will therefore include the eventually responsible clones, but also many other clones that will not be involved in case GVHD develops. In addition, GVHD-associated clones were very different between individual mice, even when the same donor repertoire was used. Using the PB of individual GVHD patients when GVHD has developed is required to further shed light on the human setting. Furthermore, contrary to what was known thus far, recent data suggests that also residual patient T cells can contribute to GVHD. Tissue-residing host T cells are relatively resistant to conditioning and HSCT<sup>65,174</sup>, and at least in the skin have been associated with GVHD in humans<sup>174,175</sup>. All these findings underline a need for an individual patient approach when it comes to better recapitulating GI-GVHD in a dish. We are in the process of biobanking both PB T cells as well as those isolated from biopsies of patients with GVHD. Improvements in culture conditions that can sustain intestinal biopsies and its constituents in its entirety 'in situ', including the epithelial, stromal and immune compartment, could be the next step to study all possible cellular interactions in future studies using these materials<sup>176</sup>.

Consequently, our co-culture models can be exploited to work towards further clinical translation. The feasibility of using organoids for this purpose in GVHD is exemplified by the development of IL-22 therapy by our collaborators in New York<sup>104,124</sup>. By generating organoids from patients that still have to undergo the SCT, treatment can be tailored/personalized by testing the most effective treatment with the least side effects on an individual level<sup>177</sup>. Also organoids derived from patients that have already developed GI-GVHD can be used. We have started biobanking organoids derived from different parts of GVHD-damaged small and large intestine of clinical patients. Already it has become apparent that establishing the organoids from the crypts of GVHD damaged tissue is challenging, similar to what we saw in mice in **Chapter 5**. Despite the fact that the epithelium has a clear phenotype of damage in GVHD<sup>13,178,179</sup>, future studies will have to show if the phenotype can be upheld to a relevant level under defined culture conditions.

Finally, the co-culture models can be applied beyond the field of HSCT and GVHD, for instance in studies related to inflammatory bowel disease (IBD) and (hemato-)oncology. In the IBD field the models can be used for elucidating immune-epithelial contributions<sup>177</sup>. In the field of oncology, they can be applied in the development of autologous immunotherapy for solid tumors<sup>180,181</sup> and the optimization of preceding chemo-treatment for potentiating



anti-tumor immune responses<sup>182,183</sup>. Lastly, they can be exploited as tissue-test setting for the construction of (engineered) tumor-specific donor immune cells such as in CAR T cell therapies<sup>184–186</sup>.

### **Untrodden paths of epithelial opportunity**

There are several new paths to embark on concerning the intestinal epithelium as a target in GVHD management. As discussed in **Chapter 7**, the plasticity in the ability of intestinal crypts to regenerate during damage appears to be inexhaustible<sup>187,188</sup>. More and more is now known about transcription factors that are involved in crypt regeneration<sup>189,190</sup>. We need to better understand the role of these concepts in the setting of GI-GVHD to exploit therapeutic possibilities in that respect. As organoids provide a tractable technical platform to understand spatiotemporal regulation of crypt morphogenesis<sup>154</sup> they are eminently the model to use. Another undiscovered field of study is found in epigenetics. There is ample evidence in skin<sup>191,192</sup>, and also some in gut<sup>193</sup>, that initial damage induces epigenetic memory in epithelial (stem) cells that influences immune- or regenerative responses in the epithelium at a later stage. Since the process of HSCT encompasses just that, an initial insult with conditioning and a consequent secondary insult by an alloreactive immune system, targets in epigenetics may be promising for new therapeutic approaches in GVHD.

## Conclusion

In conclusion, the development of SR-GHVD is associated with a high mortality and morbidity due to lack of proven effective therapies. The era of immunosuppressive monotherapy seems to have come to an end. Damage to the intestinal epithelium is in many ways associated with the development and propagation of GI-GVHD, and provides a good target for new, additional therapies. Further application of our developed disease models, but mostly evaluating new tissue targets in prospective clinical trials, is crucial to improve the outcomes of GHVD.

## References

1. Lawitschka A, Lucchini G, Strahm B, et al. Pediatric acute graft-versus-host disease prophylaxis and treatment: surveyed real-life approach reveals dissimilarities compared to published recommendations. *Transpl Int*. 2020;33(7):762-772. doi:10.1111/tri.13601
2. MacMillan ML, DeFor TE, Weisdorf DJ. The best endpoint for acute GVHD treatment trials. *Blood*. 2010;115(26):5412-5417. doi:10.1182/blood-2009-12-258442
3. Chan AY, Leiding JW, Liu X, et al. Hematopoietic Cell Transplantation in Patients With Primary Immune Regulatory Disorders (PIRD): A Primary Immune Deficiency Treatment Consortium (PIDTC) Survey. *Front Immunol*. 2020;11:239. doi:10.3389/fimmu.2020.00239
4. Passweg JR, Baldomero H, Basak GW, et al. The EBMT activity survey report 2017: a focus on allogeneic HCT for nonmalignant indications and on the use of non-HCT cell therapies. *Bone Marrow Transplant*. 2019;54(10):1575-1585. doi:10.1038/s41409-019-0465-9
5. Chiesa R, Wynn RF, Veys P. Haematopoietic stem cell transplantation in inborn errors of metabolism. *Curr Opin Hematol*. 2016;23(6):530-535. doi:10.1097/MOH.0000000000000289
6. Gooley TA, Chien JW, Pergam SA, et al. Reduced mortality after allogeneic hematopoietic-cell transplantation. *N Engl J Med*. 2010;363(22):2091-2101. doi:10.1056/NEJMoa1004383
7. Holmqvist AS, Chen Y, Wu J, et al. Assessment of Late Mortality Risk After Allogeneic Blood or Marrow Transplantation Performed in Childhood. *JAMA Oncol*. 2018;4(12):e182453. doi:10.1001/jamaoncol.2018.2453
8. Brissot E, Rialland F, Cahu X, et al. Improvement of overall survival after allogeneic hematopoietic stem cell transplantation for children and adolescents: a three-decade experience of a single institution. *Bone Marrow Transplant*. 2016;51(2):267-272. doi:10.1038/bmt.2015.250
9. Ferry C, Gemayel G, Rocha V, et al. Long-term outcomes after allogeneic stem cell transplantation for children with hematological malignancies. *Bone Marrow Transplant*. 2007;40(3):219-224. doi:10.1038/sj.bmt.1705710
10. Wilhelmsson M, Vatanen A, Borgström B, et al. Adverse health events and late mortality after pediatric allogeneic hematopoietic SCT—two decades of longitudinal follow-up. *Bone Marrow Transplant*. 2015;50(6):850-857. doi:10.1038/bmt.2015.43
11. Naymagon S, Naymagon L, Wong SY, et al. Acute graft-versus-host disease of the gut: considerations for the gastroenterologist. *Nat Rev Gastroenterol Hepatol*. 2017;14(12):711-726. doi:10.1038/nrgastro.2017.126
12. Wu SR, Reddy P. Tissue tolerance: a distinct concept to control acute GVHD severity. *Blood*. 2017;129(13):1747-1752. doi:10.1182/blood-2016-09-740431
13. Holtan SG, Shabaneh A, Betts BC, et al. Stress responses, M2 macrophages, and a distinct microbial signature in fatal intestinal acute graft-versus-host disease. *JCI Insight*. 2019;5. doi:10.1172/jci.insight.129762
14. Levine JE, Braun TM, Harris AC, et al. A prognostic score for acute graft-versus-host disease based on biomarkers: a multicentre study. *Lancet Haematol*. 2015;2(1):e21-9. doi:10.1016/S2352-3026(14)00035-0
15. Hartwell MJ, Ozbek U, Holler E, et al. An early-biomarker algorithm predicts lethal graft-versus-host disease and survival. *JCI Insight*. 2017;2(3):e89798. doi:10.1172/jci.insight.89798
16. Major-Monfried H, Renteria AS, Pawarode A, et al. MAGIC biomarkers predict long-term outcomes for steroid-resistant acute GVHD. *Blood*. 2018;131(25):2846-2855. doi:10.1182/blood-2018-01-822957
17. Etra AM, Gergoudis SC, Morales G, et al. Assessment of Systemic and Gastrointestinal Tissue Damage Biomarkers for GVHD Risk Stratification. *Blood Adv*. Published online April 2022. doi:10.1182/bloodadvances.2022007296
18. Harris AC, Ferrara JLM, Levine JE. Advances in predicting acute GVHD. *Br J Haematol*. 2013;160(3):288-302. doi:10.1111/bjh.12142
19. Kharfan-Dabaja MA, Labopin M, Bazarbachi A, et al. Higher busulfan dose intensity appears to improve leukemia-free and overall survival in AML allografted in CR2: An analysis from the Acute Leukemia Working Party of the European Group for Blood and Marrow Transplantation. *Leuk Res*. 2015;39(9):933-937. doi:10.1016/j.leukres.2015.04.009
20. Andersson BS, Thall PF, Madden T, et al. Busulfan systemic exposure relative to regimen-related toxicity and acute graft-versus-host disease: defining a therapeutic window for i.v. BuCy2 in chronic myelogenous leukemia. *Biol Blood Marrow Transplant*. 2002;8(9):477-485. doi:10.1053/bbmt.2002.v8.pm12374452
21. Bartelink IH, Lalmohamed A, van Reij EML, et al. Association of busulfan exposure with survival and toxicity after haemopoietic cell transplantation in children and young adults: a multicentre, retrospective cohort analysis. *Lancet Haematol*. 2016;3(11):e526-e536. doi:10.1016/S2352-3026(16)30114-4
22. Bartelink IH, Bredius RGM, Beltser S V, et al. Association between busulfan exposure and outcome in children receiving intravenous busulfan before hematologic stem cell transplantation. *Biol Blood Marrow Transplant*. 2009;15(2):231-241. doi:10.1016/j.bbmt.2008.11.022
23. Bartelink IH, van Reij EML, Gerhardt CE, et al. Fludarabine and exposure-targeted busulfan compares favorably with busulfan/cyclophosphamide-based regimens in pediatric hematopoietic cell transplantation: maintaining efficacy with less toxicity. *Biol Blood Marrow Transplant*. 2014;20(3):345-353. doi:10.1016/j.bbmt.2013.11.027
24. Langenhorst JB, van Kesteren C, van Maarseveen EM, et al. Fludarabine exposure in the conditioning prior to allogeneic hematopoietic cell transplantation predicts outcomes. *Blood Adv*. 2019;3(4):2179-2187. doi:10.1182/



- bloodadvances.2018029421
25. Zhu C, Anderson AC, Schubart A, et al. The Tim-3 ligand galectin-9 negatively regulates T helper type 1 immunity. *Nat Immunol.* 2005;6(12):1245-1252. doi:10.1038/ni1271
  26. Gooden MJM, Wiersma VR, Samplonius DF, et al. Galectin-9 activates and expands human T-helper 1 cells. *PLoS One.* 2013;8(5):e65616. doi:10.1371/journal.pone.0065616
  27. Lhuillier C, Barjon C, Niki T, et al. Impact of Exogenous Galectin-9 on Human T Cells: CONTRIBUTION OF THE T CELL RECEPTOR COMPLEX TO ANTIGEN-INDEPENDENT ACTIVATION BUT NOT TO APOPTOSIS INDUCTION. *J Biol Chem.* 2015;290(27):16797-16811. doi:10.1074/jbc.M115.661272
  28. Wang F, He W, Zhou H, et al. The Tim-3 ligand galectin-9 negatively regulates CD8+ alloreactive T cell and prolongs survival of skin graft. *Cell Immunol.* 2007;250(1-2):68-74. doi:10.1016/j.cellimm.2008.01.006
  29. Nagahara K, Arikawa T, Oomizu S, et al. Galectin-9 increases Tim-3+ dendritic cells and CD8+ T cells and enhances antitumor immunity via galectin-9-Tim-3 interactions. *J Immunol.* 2008;181(11):7660-7669. doi:10.4049/jimmunol.181.11.7660
  30. Su EW, Bi S, Kane LP. Galectin-9 regulates T helper cell function independently of Tim-3. *Glycobiology.* 2011;21(10):1258-1265. doi:10.1093/glycob/cwq214
  31. Oomizu S, Arikawa T, Niki T, et al. Galectin-9 suppresses Th17 cell development in an IL-2-dependent but Tim-3-independent manner. *Clin Immunol.* 2012;143(1):51-58. doi:10.1016/j.clim.2012.01.004
  32. Oomizu S, Arikawa T, Niki T, et al. Cell surface galectin-9 expressing Th cells regulate Th17 and Foxp3+ Treg development by galectin-9 secretion. *PLoS One.* 2012;7(11):e48574. doi:10.1371/journal.pone.0048574
  33. Wu C, Thalhamer T, Franca RF, et al. Galectin-9-CD44 interaction enhances stability and function of adaptive regulatory T cells. *Immunity.* 2014;41(2):270-282. doi:10.1016/j.immuni.2014.06.011
  34. Madreddi S, Eun SY, Mehta AK, et al. Regulatory T Cell-Mediated Suppression of Inflammation Induced by DR3 Signaling Is Dependent on Galectin-9. *J Immunol.* 2017;199(8):2721-2728. doi:10.4049/jimmunol.1700575
  35. Brewer C, Miceli M, Baum L. Clusters, bundles, arrays and lattices: novel mechanisms for lectin-saccharide-mediated cellular interactions. *Curr Opin Struct Biol.* 2002;12(5):616-623. doi:10.1016/S0959-440X(02)00364-0
  36. Rabinovich GA, Toscano MA, Jackson SS, Vasta GR. Functions of cell surface galectin-glycoprotein lattices. *Curr Opin Struct Biol.* 2007;17(5):513-520. doi:10.1016/j.sbi.2007.09.002
  37. Madreddi S, Eun SY, Lee SW, et al. Galectin-9 controls the therapeutic activity of 4-1BB-targeting antibodies. *J Exp Med.* 2014;211(7):1433-1448. doi:10.1084/jem.20132687
  38. Bi S, Hong PW, Lee B, Baum LG. Galectin-9 binding to cell surface protein disulfide isomerase regulates the redox environment to enhance T-cell migration and HIV entry. *Proc Natl Acad Sci U S A.* 2011;108(26):10650-10655. doi:10.1073/pnas.1017954108
  39. Yang R, Sun L, Li CF, et al. Galectin-9 interacts with PD-1 and TIM-3 to regulate T cell death and is a target for cancer immunotherapy. *Nat Commun.* 2021;12(1):832. doi:10.1038/s41467-021-21099-2
  40. Dwyer GK, Mathews LR, Villegas JA, et al. IL-33 acts as a costimulatory signal to generate alloreactive Th1 cells in graft-versus-host disease. *J Clin Invest.* Published online May 2022. doi:10.1172/JCI150927
  41. Yin J, Li L, Wang C, Zhang Y. Increased Galectin-9 expression, a prognostic biomarker of aGVHD, regulates the immune response through the Galectin-9 induced MDSC pathway after allogeneic hematopoietic stem cell transplantation. *Int Immunopharmacol.* 2020;88:106929. doi:10.1016/j.intimp.2020.106929
  42. Yang R, Sun L, Li CF, et al. Development and characterization of anti-galectin-9 antibodies that protect T cells from galectin-9-induced cell death. *J Biol Chem.* 2022;298(4):101821. doi:10.1016/j.jbc.2022.101821
  43. Kandel S, Adhikary P, Li G, Cheng K. The TIM3/Gal9 signaling pathway: An emerging target for cancer immunotherapy. *Cancer Lett.* 2021;510:67-78. doi:10.1016/j.canlet.2021.04.011
  44. Lhuillier C, Barjon C, Baloch V, et al. Characterization of neutralizing antibodies reacting with the 213-224 amino-acid segment of human galectin-9. *PLoS One.* 2018;13(9):e0202512. doi:10.1371/journal.pone.0202512
  45. Sakai K, Kawata E, Ashihara E, et al. Galectin-9 ameliorates acute GVH disease through the induction of T-cell apoptosis. *Eur J Immunol.* 2011;41(1):67-75. doi:10.1002/eji.200939931
  46. Veenstra RG, Taylor PA, Zhou Q, et al. Contrasting acute graft-versus-host disease effects of Tim-3/galectin-9 pathway blockade dependent upon the presence of donor regulatory T cells. *Blood.* 2012;120(3):682-690. doi:10.1182/blood-2011-10-387977
  47. Saha A, Hyzy S, Lamothe T, et al. A CD45-targeted antibody-drug conjugate successfully conditions for allogeneic hematopoietic stem cell transplantation in mice. *Blood.* 2022;139(11):1743-1759. doi:10.1182/blood.2021012366
  48. Czechowicz A, Palchaudhuri R, Scheck A, et al. Selective hematopoietic stem cell ablation using CD117-antibody-drug-conjugates enables safe and effective transplantation with immunity preservation. *Nat Commun.* 2019;10(1):617. doi:10.1038/s41467-018-08201-x
  49. George BM, Kao KS, Kwon HS, et al. Antibody Conditioning Enables MHC-Mismatched Hematopoietic Stem Cell Transplants and Organ Graft Tolerance. *Cell Stem Cell.* 2019;25(2):185-192.e3. doi:10.1016/j.stem.2019.05.018
  50. Li Z, Czechowicz A, Scheck A, Rossi DJ, Murphy PM. Hematopoietic chimerism and donor-specific skin allograft tolerance after non-genotoxic CD117 antibody-drug-conjugate conditioning in MHC-mismatched allotransplantation. *Nat Commun.* 2019;10(1):616. doi:10.1038/s41467-018-08202-w
  51. Li Z, Murphy PM. CD45: a niche marker for allotransplantation. *Blood.* 2022;139(11):1614-1616. doi:10.1182/blood.2021015024

52. Takashima S, Hanash AM. The enteric virome in hematopoietic stem cell transplantation: ready for its close-up. *Nat Med.* 2017;23(9):1012-1013. doi:10.1038/nm.4403
53. van Montfrans J, Schulz L, Versluys B, et al. Viral PCR positivity in stool before allogeneic hematopoietic cell transplantation is strongly associated with acute intestinal graft-versus-host disease. *Biol Blood Marrow Transplant.* 2015;21(4):772-774. doi:10.1016/j.bbmt.2015.01.009
54. Legoff J, Resche-Rigon M, Bouquet J, et al. The eukaryotic gut virome in hematopoietic stem cell transplantation: new clues in enteric graft-versus-host disease. *Nat Med.* 2017;23(9):1080-1085. doi:10.1038/nm.4380
55. Daly GM, Bexfield N, Heaney J, et al. A viral discovery methodology for clinical biopsy samples utilising massively parallel next generation sequencing. *PLoS One.* 2011;6(12):e28879. doi:10.1371/journal.pone.0028879
56. Gaudin M, Desnues C. Hybrid Capture-Based Next Generation Sequencing and Its Application to Human Infectious Diseases. *Front Microbiol.* 2018;9:2924. doi:10.3389/fmicb.2018.02924
57. Jansen SA, Nijhuis W, Leavis HL, Riezebos-Brilman A, Lindemans CA, Schuurman R. Broad Virus Detection and Variant Discovery in Fecal Samples of Hematopoietic Transplant Recipients Using Targeted Sequence Capture Metagenomics. *Front Microbiol.* 2020;11:560179. doi:10.3389/fmicb.2020.560179
58. Gopalakrishnan S, Hansen MD, Skovdahl HK, et al. Tofacitinib Downregulates TNF and Poly(I:C)-Dependent MHC-II Expression in the Colonic Epithelium. *Front Immunol.* 2022;13:882277. doi:10.3389/fimmu.2022.882277
59. Koyama M, Mukhopadhyay P, Schuster IS, et al. MHC Class II Antigen Presentation by the Intestinal Epithelium Initiates Graft-versus-Host Disease and Is Influenced by the Microbiota. *Immunity.* 2019;51(5):885-898.e7. doi:10.1016/j.immuni.2019.08.011
60. Bigley TM, Yang L, Kang L, Saenz JB, Victorino F, Yokoyama WM. Disruption of thymic central tolerance by infection with murine roseolovirus induces autoimmune gastritis. *J Exp Med.* 2022;219(3). doi:10.1084/jem.20211403
61. Stuber E, Buschenfeld A, von Freier A, Arendt T, Folsch UR. Intestinal crypt cell apoptosis in murine acute graft versus host disease is mediated by tumour necrosis factor alpha and not by the FasL-Fas interaction: effect of pentoxifylline on the development of mucosal atrophy. *Gut.* 1999;45(2):229-235. doi:10.1136/gut.45.2.229
62. van Den Brink MR, Moore E, Horndasch KJ, et al. Fas-deficient lpr mice are more susceptible to graft-versus-host disease. *J Immunol.* 2000;164(11):469-480. doi:10.4049/jimmunol.164.1.469
63. Graubert TA, DiPersio JF, Russell JH, Ley TJ. Perforin/granzyme-dependent and independent mechanisms are both important for the development of graft-versus-host disease after murine bone marrow transplantation. *J Clin Invest.* 1997;100(4):904-911. doi:10.1172/JCI119606
64. Du W, Cao X. Cytotoxic Pathways in Allogeneic Hematopoietic Cell Transplantation. *Front Immunol.* 2018;9:2979. doi:10.3389/fimmu.2018.02979
65. Tkachev V, Kaminski J, Potter EL, et al. Spatiotemporal single-cell profiling reveals that invasive and tissue-resident memory donor CD8(+) T cells drive gastrointestinal acute graft-versus-host disease. *Sci Transl Med.* 2021;13(576). doi:10.1126/scitranslmed.abc0227
66. Takashima S, Martin ML, Jansen SA, et al. T cell-derived interferon-gamma programs stem cell death in immune-mediated intestinal damage. *Sci Immunol.* 2019;4(42). doi:10.1126/sciimmunol.aay8556
67. Piper C, Drobyski WR. Inflammatory Cytokine Networks in Gastrointestinal Tract Graft vs. Host Disease. *Front Immunol.* 2019;10:163. doi:10.3389/fimmu.2019.00163
68. Fu YY, Egorova A, Sobieski C, et al. T Cell Recruitment to the Intestinal Stem Cell Compartment Drives Immune-Mediated Intestinal Damage after Allogeneic Transplantation. *Immunity.* 2019;51(1):90-103.e3. doi:10.1016/j.immuni.2019.06.003
69. Vianello F, Cannella L, Coe D, et al. Enhanced and aberrant T cell trafficking following total body irradiation: a gateway to graft-versus-host disease? *Br J Haematol.* 2013;162(6):808-818. doi:10.1111/bjh.12472
70. Koyama M, Kuns RD, Olver SD, et al. Recipient nonhematopoietic antigen-presenting cells are sufficient to induce lethal acute graft-versus-host disease. *Nat Med.* 2011;18(1):135-142. doi:10.1038/nm.2597
71. Na IK, Markley JC, Tsai JJ, et al. Concurrent visualization of trafficking, expansion, and activation of T lymphocytes and T-cell precursors in vivo. *Blood.* 2010;116(11):e18-25. doi:10.1182/blood-2009-12-259432
72. Beilhack A, Schulz S, Baker J, et al. Prevention of acute graft-versus-host disease by blocking T-cell entry to secondary lymphoid organs. *Blood.* 2008;111(5):2919-2928. doi:10.1182/blood-2007-09-112789
73. Kim YM, Sachs T, Asavaroengchai W, Bronson R, Sykes M. Graft-versus-host disease can be separated from graft-versus-lymphoma effects by control of lymphocyte trafficking with FTY720. *J Clin Invest.* 2003;111(5):659-669. doi:10.1172/JCI16950
74. Wysocki CA, Panoskaltis-Mortari A, Blazar BR, Serody JS. Leukocyte migration and graft-versus-host disease. *Blood.* 2005;105(11):4191-4199. doi:10.1182/blood-2004-12-4726
75. Sackstein R. A revision of Billingham's tenets: the central role of lymphocyte migration in acute graft-versus-host disease. *Biol Blood Marrow Transplant.* 2006;12(1 Suppl 1):2-8. doi:10.1016/j.bbmt.2005.09.015
76. Bouazzaoui A, Spacenko E, Mueller G, et al. Chemokine and chemokine receptor expression analysis in target organs of acute graft-versus-host disease. *Genes Immun.* 2009;10(8):687-701. doi:10.1038/gene.2009.49
77. Castor MGM, Rezende B, Resende CB, et al. The CCL3/macrophage inflammatory protein-1alpha-binding protein evasin-1 protects from graft-versus-host disease but does not modify graft-versus-leukemia in mice. *J Immunol.* 2010;184(5):2646-2654. doi:10.4049/jimmunol.0902614



78. Reshef R, Luger SM, Hexner EO, et al. Blockade of lymphocyte chemotaxis in visceral graft-versus-host disease. *N Engl J Med*. 2012;367(2):135-145. doi:10.1056/NEJMoa1201248
79. Reshef R, Ganetsky A, Acosta EP, et al. Extended CCR5 Blockade for Graft-versus-Host Disease Prophylaxis Improves Outcomes of Reduced-Intensity Unrelated Donor Hematopoietic Cell Transplantation: A Phase II Clinical Trial. *Biol Blood Marrow Transplant*. 2019;25(3):515-521. doi:10.1016/j.bbmt.2018.09.034
80. Khandelwal P, Fukuda T, Mizuno K, et al. A Pharmacokinetic and Pharmacodynamic Study of Maraviroc as Acute Graft-versus-Host Disease Prophylaxis in Pediatric Allogeneic Stem Cell Transplant Recipients with Nonmalignant Diagnoses. *Biol Blood Marrow Transplant*. 2016;22(10):1829-1835. doi:10.1016/j.bbmt.2016.08.001
81. Khandelwal P, Fukuda T, Teusink-Cross A, et al. CCR5 inhibitor as novel acute graft versus host disease prophylaxis in children and young adults undergoing allogeneic stem cell transplant: results of the phase II study. *Bone Marrow Transplant*. Published online April 2020. doi:10.1038/s41409-020-0888-3
82. Murai M, Yoneyama H, Ezaki T, et al. Peyer's patch is the essential site in initiating murine acute and lethal graft-versus-host reaction. *Nat Immunol*. 2003;4(2):154-160. doi:10.1038/nri879
83. Wysocki CA, Burkett SB, Panoskaltis-Mortari A, et al. Differential roles for CCR5 expression on donor T cells during graft-versus-host disease based on pretransplant conditioning. *J Immunol*. 2004;173(2):845-854. doi:10.4049/jimmunol.173.2.845
84. Moy RH, Huffman AP, Richman LP, et al. Clinical and immunologic impact of CCR5 blockade in graft-versus-host disease prophylaxis. *Blood*. 2017;129(7):906-916. doi:10.1182/blood-2016-08-735076
85. Duffner U, Lu B, Hildebrandt GC, et al. Role of CXCR3-induced donor T-cell migration in acute GVHD. *Exp Hematol*. 2003;31(10):897-902. doi:10.1016/s0301-472x(03)00198-x
86. He S, Cao Q, Qiu Y, et al. A new approach to the blocking of alloreactive T cell-mediated graft-versus-host disease by in vivo administration of anti-CXCR3 neutralizing antibody. *J Immunol*. 2008;181(11):7581-7592. doi:10.4049/jimmunol.181.11.7581
87. Mapara MY, Leng C, Kim YM, et al. Expression of chemokines in GVHD target organs is influenced by conditioning and genetic factors and amplified by GVHR. *Biol Blood Marrow Transplant*. 2006;12(6):623-634. doi:10.1016/j.bbmt.2006.02.005
88. Ueha S, Murai M, Yoneyama H, et al. Intervention of MAdCAM-1 or fractalkine alleviates graft-versus-host reaction associated intestinal injury while preserving graft-versus-tumor effects. *J Leukoc Biol*. 2007;81(1):176-185. doi:10.1189/jlb.0306231
89. Brissot E, Bossard C, Malard F, et al. Involvement of the CX3CL1(fractalkine)/CX3CR1 pathway in the pathogenesis of acute graft-versus-host disease. *J Leukoc Biol*. 2015;97(2):227-235. doi:10.1189/jlb.5HI0714-325R
90. Varona R, Cadenas V, Gomez L, Martinez-A C, Marquez G. CCR6 regulates CD4+ T-cell-mediated acute graft-versus-host disease responses. *Blood*. 2005;106(1):18-26. doi:10.1182/blood-2004-08-2996
91. Romagnani A, Vettore V, Rezzonico-Jost T, et al. TRPM7 kinase activity is essential for T cell colonization and alloreactivity in the gut. *Nat Commun*. 2017;8(1):1917. doi:10.1038/s41467-017-01960-z
92. Cook L, Stahl M, Han X, et al. Suppressive and Gut-Reparative Functions of Human Type 1 T Regulatory Cells. *Gastroenterology*. 2019;157(6):1584-1598. doi:10.1053/j.gastro.2019.09.002
93. Biton M, Haber AL, Rogel N, et al. T Helper Cell Cytokines Modulate Intestinal Stem Cell Renewal and Differentiation. *Cell*. 2018;175(5):1307-1320.e22. doi:10.1016/j.cell.2018.10.008
94. Edinger M, Hoffmann P, Ermann J, et al. CD4+CD25+ regulatory T cells preserve graft-versus-tumor activity while inhibiting graft-versus-host disease after bone marrow transplantation. *Nat Med*. 2003;9(9):1144-1150. doi:10.1038/nm915
95. Kim BS, Nishikii H, Baker J, et al. Treatment with agonistic DR3 antibody results in expansion of donor Tregs and reduced graft-versus-host disease. *Blood*. 2015;126(4):546-557. doi:10.1182/blood-2015-04-637587
96. Wolf D, Barreras H, Bader CS, et al. Marked in Vivo Donor Regulatory T Cell Expansion via Interleukin-2 and TL1A-Ig Stimulation Ameliorates Graft-versus-Host Disease but Preserves Graft-versus-Leukemia in Recipients after Hematopoietic Stem Cell Transplantation. *Biol Blood Marrow Transplant*. 2017;23(5):757-766. doi:10.1016/j.bbmt.2017.02.013
97. Pozo D, Anderson P, Gonzalez-Rey E. Induction of alloantigen-specific human T regulatory cells by vasoactive intestinal peptide. *J Immunol*. 2009;183(7):4346-4359. doi:10.4049/jimmunol.0900400
98. Hoeppli RE, MacDonald KN, Leclair P, et al. Tailoring the homing capacity of human Tregs for directed migration to sites of Th1-inflammation or intestinal regions. *Am J Transplant*. 2019;19(1):62-76. doi:10.1111/ajt.14936
99. Niculet E, Bobeica C, Tatu AL. Glucocorticoid-Induced Skin Atrophy: The Old and the New. *Clin Cosmet Investig Dermatol*. 2020;13:1041-1050. doi:10.2147/CCID.S224211
100. Toubai T, Rossi C, Tawara I, et al. Murine Models of Steroid Refractory Graft-versus-Host Disease. *Sci Rep*. 2018;8(1):12475. doi:10.1038/s41598-018-30814-x
101. Song Q, Wang X, Wu X, et al. IL-22-dependent dysbiosis and mononuclear phagocyte depletion contribute to steroid-resistant gut graft-versus-host disease in mice. *Nat Commun*. 2021;12(1):805. doi:10.1038/s41467-021-21133-3
102. Lamarthee B, Malard F, Gamonet C, et al. Donor interleukin-22 and host type I interferon signaling pathway participate in intestinal graft-versus-host disease via STAT1 activation and CXCL10. *Mucosal Immunol*. 2016;9(2):309-321. doi:10.1038/mi.2015.61



103. Couturier M, Lamarthée B, Arbez J, et al. IL-22 deficiency in donor T cells attenuates murine acute graft-versus-host disease mortality while sparing the graft-versus-leukemia effect. *Leukemia*. 2013;27(7):1527-1537. doi:10.1038/leu.2013.39
104. Ponce DM, Alousi AM, Nakamura R, et al. A phase 2 study of interleukin-22 and systemic corticosteroids as initial treatment for acute GVHD of the lower GI tract. *Blood*. 2023;141(12):1389-1401. doi:10.1182/blood.2021015111
105. Burman AC, Banovic T, Kuns RD, et al. IFN-gamma differentially controls the development of idiopathic pneumonia syndrome and GVHD of the gastrointestinal tract. *Blood*. 2007;110(3):1064-1072. doi:10.1182/blood-2006-12-063982
106. Ellison CA, Fischer JM, HayGlass KT, Gartner JG. Murine graft-versus-host disease in an F1-hybrid model using IFN-gamma gene knockout donors. *J Immunol*. 1998;161(2):631-640.
107. Wang H, Asavaroengchai W, Yeap BY, et al. Paradoxical effects of IFN-gamma in graft-versus-host disease reflect promotion of lymphohematopoietic graft-versus-host reactions and inhibition of epithelial tissue injury. *Blood*. 2009;113(15):3612-3619. doi:10.1182/blood-2008-07-168419
108. Yang YG, Dey BR, Sergio JJ, Pearson DA, Sykes M. Donor-derived interferon gamma is required for inhibition of acute graft-versus-host disease by interleukin 12. *J Clin Invest*. 1998;102(12):2126-2135. doi:10.1172/JCI4992
109. Yang YG, Qi J, Wang MG, Sykes M. Donor-derived interferon gamma separates graft-versus-leukemia effects and graft-versus-host disease induced by donor CD8 T cells. *Blood*. 2002;99(11):4207-4215. doi:10.1182/blood.v99.11.4207
110. Hou C, Dou L, Jia M, et al. Ruxolitinib Combined with Corticosteroids as First-Line Therapy for Acute Graft-versus-Host Disease in Haploidentical Peripheral Blood Stem Cell Transplantation Recipients. *Transplant Cell Ther*. 2021;27(1):75.e1-75.e10. doi:10.1016/j.bbmt.2020.09.015
111. Zhao Y, Shi J, Luo Y, et al. Calcineurin Inhibitors Replacement by Ruxolitinib as Graft-versus-Host Disease Prophylaxis for Patients after Allogeneic Stem Cell Transplantation. *Biol Blood Marrow Transplant*. 2020;26(5):e128-e133. doi:10.1016/j.bbmt.2020.01.012
112. Kröger N, Shahnaz Syed Abd Kadir S, Zabelina T, et al. Peritransplantation Ruxolitinib Prevents Acute Graft-versus-Host Disease in Patients with Myelofibrosis Undergoing Allogeneic Stem Cell Transplantation. *Biol Blood Marrow Transplant*. 2018;24(10):2152-2156. doi:10.1016/j.bbmt.2018.05.023
113. Takashima S, Sharma R, Egorova A, et al. Immune-Mediated Reprogramming of Intestinal Stem Cells Drives STAT1-Dependent Myc Expression and Epithelial Regeneration in GI-Gvhd. *Blood*. 2021;138, Suppl:86. doi:https://doi.org/10.1182/blood-2021-152647
114. Li L, Shang L, Gao J, et al. Janus kinase inhibitor ruxolitinib blocks thymic regeneration after acute thymus injury. *Biochem Pharmacol*. 2020;171:113712. doi:10.1016/j.bcp.2019.113712
115. Sleight BS, Chan KW, Braun TM, Serrano A, Gilman AL. Infiximab for GVHD therapy in children. *Bone Marrow Transplant*. 2007;40(5):473-480. doi:10.1038/sj.bmt.1705761
116. Jacobsohn DA, Hallick J, Anders V, McMillan S, Morris L, Vogelsang GB. Infiximab for steroid-refractory acute GVHD: a case series. *Am J Hematol*. 2003;74(2):119-124. doi:10.1002/ajh.10392
117. Patriarca F, Sperotto A, Damiani D, et al. Infiximab treatment for steroid-refractory acute graft-versus-host disease. *Haematologica*. 2004;89(11):1352-1359.
118. Couriel D, Saliba R, Hicks K, et al. Tumor necrosis factor-alpha blockade for the treatment of acute GVHD. *Blood*. 2004;104(3):649-654. doi:10.1182/blood-2003-12-4241
119. Schreurs RRCE, Baumdick ME, Sagebiel AF, et al. Human Fetal TNF- $\alpha$ -Cytokine-Producing CD4(+) Effector Memory T Cells Promote Intestinal Development and Mediate Inflammation Early in Life. *Immunity*. 2019;50(2):462-476.e8. doi:10.1016/j.immuni.2018.12.010
120. Moraga I, Spangler J, Mendoza JL, Garcia KC. Multifarious determinants of cytokine receptor signaling specificity. *Adv Immunol*. 2014;121:1-39. doi:10.1016/B978-0-12-800100-4.00001-5
121. Mathewson ND, Jenq R, Mathew A V, et al. Gut microbiome-derived metabolites modulate intestinal epithelial cell damage and mitigate graft-versus-host disease. *Nat Immunol*. 2016;17(5):505-513. doi:10.1038/ni.3400
122. Wu SE, Hashimoto-Hill S, Woo V, et al. Microbiota-derived metabolite promotes HDAC3 activity in the gut. *Nature*. 2020;586(7827):108-112. doi:10.1038/s41586-020-2604-2
123. Middendorp S, Schneeberger K, Wiegerinck CL, et al. Adult stem cells in the small intestine are intrinsically programmed with their location-specific function. *Stem Cells*. 2014;32(5):1083-1091. doi:10.1002/stem.1655
124. Lindemans CA, Calafiore M, Mertelsmann AM, et al. Interleukin-22 promotes intestinal-stem-cell-mediated epithelial regeneration. *Nature*. 2015;528(7583):560-564. doi:10.1038/nature16460
125. He GW, Lin L, DeMartino J, et al. Optimized human intestinal organoid model reveals interleukin-22-dependency of paneth cell formation. *Cell Stem Cell*. 2022;29(9):1333-1345.e6. doi:10.1016/j.stem.2022.08.002
126. Lounder DT, Khandelwal P, Gloude NJ, et al. Interleukin-22 levels are increased in gastrointestinal graft-versus-host disease in children. *Haematologica*. 2018;103(10):e480-e482. doi:10.3324/haematol.2017.174771
127. Ghimire S, Ederer KU, Meedt E, et al. Low Intestinal IL22 Associates With Increased Transplant-Related Mortality After Allogeneic Stem Cell Transplantation. *Front Immunol*. 2022;13:857400. doi:10.3389/fimmu.2022.857400
128. Hanash AM, Dudakov JA, Hua G, et al. Interleukin-22 protects intestinal stem cells from immune-mediated tissue damage and regulates sensitivity to graft versus host disease. *Immunity*. 2012;37(2):339-350. doi:10.1016/j.immuni.2012.05.028



129. Hazenberg MD, Haverkate NJE, van Lier YF, et al. Human ectoenzyme-expressing ILC3: immunosuppressive innate cells that are depleted in graft-versus-host disease. *Blood Adv.* 2019;3(22):3650-3660. doi:10.1182/bloodadvances.2019000176
130. Zindl CL, Witte SJ, Laufer VA, et al. A nonredundant role for T cell-derived interleukin 22 in antibacterial defense of colonic crypts. *Immunity.* 2022;55(3):494-511.e11. doi:10.1016/j.immuni.2022.02.003
131. Romera-Hernandez M, Aparicio-Domingo P, Papazian N, et al. Yap1-Driven Intestinal Repair Is Controlled by Group 3 Innate Lymphoid Cells. *Cell Rep.* 2020;30(1):37-45.e3. doi:10.1016/j.celrep.2019.11.115
132. Munneke JM, Bjorklund AT, Mjosberg JM, et al. Activated innate lymphoid cells are associated with a reduced susceptibility to graft-versus-host disease. *Blood.* 2014;124(5):812-821. doi:10.1182/blood-2013-11-536888
133. Fu YY, Egorova A, Kuttigara J, Hanash AM. IL-22 Producing Innate Lymphocytes Traffic to the Intestinal Stem Cell Compartment after Conditioning-Related Radiation Injury. *Transplantation and Cellular Therapy, Official Publication of the American Society for Transplantation and Cellular Therapy.* 2022;28(3):S33-S34. doi:10.1016/S2666-6367(22)00199-3
134. Kroeze A, van Hoeven V, Verheij MW, et al. Presence of innate lymphoid cells in allogeneic hematopoietic grafts correlates with reduced graft-versus-host disease. *Cytotherapy.* 2022;24(3):302-310. doi:10.1016/j.jcyt.2021.10.011
135. Bennstein SB, Weinhold S, Degistirici Ö, et al. Efficient In Vitro Generation of IL-22-Secreting ILC3 From CD34(+) Hematopoietic Progenitors in a Human Mesenchymal Stem Cell Niche. *Front Immunol.* 2021;12:797432. doi:10.3389/fimmu.2021.797432
136. Hernández DC, Juelke K, Müller NC, et al. An in vitro platform supports generation of human innate lymphoid cells from CD34(+) hematopoietic progenitors that recapitulate ex vivo identity. *Immunity.* 2021;54(10):2417-2432.e5. doi:10.1016/j.immuni.2021.07.019
137. Bal SM, Golebski K, Spits H. Plasticity of innate lymphoid cell subsets. *Nat Rev Immunol.* 2020;20(9):552-565. doi:10.1038/s41577-020-0282-9
138. Saxton RA, Henneberg LT, Calafiore M, et al. The tissue protective functions of interleukin-22 can be decoupled from pro-inflammatory actions through structure-based design. *Immunity.* 2021;54(4):660-672.e9. doi:10.1016/j.immuni.2021.03.008
139. Lee Y, Sugihara K, Gilliland MG 3rd, Jon S, Kamada N, Moon JJ. Hyaluronic acid-bilirubin nanomedicine for targeted modulation of dysregulated intestinal barrier, microbiome and immune responses in colitis. *Nat Mater.* 2020;19(1):118-126. doi:10.1038/s41563-019-0462-9
140. Praveschotinunt P, Duraj-Thatte AM, Gelfat I, Bahl F, Chou DB, Joshi NS. Engineered E. coli Nissle 1917 for the delivery of matrix-tethered therapeutic domains to the gut. *Nat Commun.* 2019;10(1):5580. doi:10.1038/s41467-019-13336-6
141. Gou S, Huang Y, Wan Y, et al. Multi-bioresponsive silk fibroin-based nanoparticles with on-demand cytoplasmic drug release capacity for CD44-targeted alleviation of ulcerative colitis. *Biomaterials.* 2019;212:39-54. doi:10.1016/j.biomaterials.2019.05.012
142. Hirai T, Ramos TL, Lin PY, et al. Selective expansion of regulatory T cells using an orthogonal IL-2/IL-2 receptor system facilitates transplantation tolerance. *J Clin Invest.* 2021;131(8). doi:10.1172/JCI139991
143. Tian Y, Li Y, Shao Y, Zhang Y. Gene modification strategies for next-generation CAR T cells against solid cancers. *J Hematol Oncol.* 2020;13(1):54. doi:10.1186/s13045-020-00890-6
144. Williams JZ, Allen GM, Shah D, et al. Precise T cell recognition programs designed by transcriptionally linking multiple receptors. *Science.* 2020;370(6520):1099-1104. doi:10.1126/science.abc6270
145. Allen GM, Frankel NW, Reddy NR, et al. Synthetic cytokine circuits that drive T cells into immune-excluded tumors. *Science.* 2022;378(6625):eaba1624. doi:10.1126/science.aba1624
146. Choe JH, Watchmaker PB, Simic MS, et al. SynNotch-CAR T cells overcome challenges of specificity, heterogeneity, and persistence in treating glioblastoma. *Sci Transl Med.* 2021;13(591). doi:10.1126/scitranslmed.abe7378
147. Hyrenius-Wittsten A, Su Y, Park M, et al. SynNotch CAR circuits enhance solid tumor recognition and promote persistent antitumor activity in mouse models. *Sci Transl Med.* 2021;13(591). doi:10.1126/scitranslmed.abd8836
148. Zhu I, Liu R, Garcia JM, et al. Modular design of synthetic receptors for programmed gene regulation in cell therapies. *Cell.* 2022;185(8):1431-1443.e16. doi:10.1016/j.cell.2022.03.023
149. Li HS, Israni D V, Gagnon KA, et al. Multidimensional control of therapeutic human cell function with synthetic gene circuits. *Science.* 2022;378(6625):1227-1234. doi:10.1126/science.ade0156
150. Zeiser R, Blazar BR. Preclinical models of acute and chronic graft-versus-host disease: how predictive are they for a successful clinical translation? *Blood.* 2016;127(25):3117-3126. doi:10.1182/blood-2016-02-699082
151. Guiu J, Jensen KB. In Vivo Studies Should Take Priority When Defining Mechanisms of Intestinal Crypt Morphogenesis. *Cell Mol Gastroenterol Hepatol.* 2022;13(1):1-3. doi:10.1016/j.jcmgh.2021.06.028
152. Kim J, Koo BK, Knoblich JA. Human organoids: model systems for human biology and medicine. *Nat Rev Mol Cell Biol.* 2020;21(10):571-584. doi:10.1038/s41580-020-0259-3
153. Li H, Wang X, Wang Y, et al. Cross-species single-cell transcriptomic analysis reveals divergence of cell composition and functions in mammalian ileum epithelium. *Cell Regen.* 2022;11(1):19. doi:10.1186/s13619-022-00118-7

154. Sugimoto S, Sato T. Organoid vs In Vivo Mouse Model: Which is Better Research Tool to Understand the Biologic Mechanisms of Intestinal Epithelium? *Cell Mol Gastroenterol Hepatol*. 2022;13(1):195-197. doi:10.1016/j.jcmgh.2021.06.027
155. Sato T, Stange DE, Ferrante M, et al. Long-term expansion of epithelial organoids from human colon, adenoma, adenocarcinoma, and Barrett's epithelium. *Gastroenterology*. 2011;141(5):1762-1772. doi:10.1053/j.gastro.2011.07.050
156. Fujii M, Matano M, Toshimitsu K, et al. Human Intestinal Organoids Maintain Self-Renewal Capacity and Cellular Diversity in Niche-Inspired Culture Condition. *Cell Stem Cell*. 2018;23(6):787-793.e6. doi:10.1016/j.stem.2018.11.016
157. Sato T, Clevers H. Growing self-organizing mini-guts from a single intestinal stem cell: mechanism and applications. *Science*. 2013;340(6137):1190-1194. doi:10.1126/science.1234852
158. Mead BE, Hattori K, Levy L, et al. Screening for modulators of the cellular composition of gut epithelia via organoid models of intestinal stem cell differentiation. *Nat Biomed Eng*. Published online March 2022. doi:10.1038/s41551-022-00863-9
159. Jardé T, Chan WH, Rossello FJ, et al. Mesenchymal Niche-Derived Neuregulin-1 Drives Intestinal Stem Cell Proliferation and Regeneration of Damaged Epithelium. *Cell Stem Cell*. Published online July 2020. doi:10.1016/j.stem.2020.06.021
160. Ding S, Song Y, Brulois KF, et al. Retinoic Acid and Lymphotoxin Signaling Promote Differentiation of Human Intestinal M Cells. *Gastroenterology*. 2020;159(1):214-226.e1. doi:10.1053/j.gastro.2020.03.053
161. Takahashi K, Tanabe K, Ohnuki M, et al. Induction of pluripotent stem cells from adult human fibroblasts by defined factors. *Cell*. 2007;131(5):861-872. doi:10.1016/j.cell.2007.11.019
162. Spence JR, Mayhew CN, Rankin SA, et al. Directed differentiation of human pluripotent stem cells into intestinal tissue in vitro. *Nature*. 2011;470(7332):105-109. doi:10.1038/nature09691
163. Watson CL, Mahe MM, Múnera J, et al. An in vivo model of human small intestine using pluripotent stem cells. *Nat Med*. 2014;20(11):1310-1314. doi:10.1038/nm.3737
164. Jung KB, Lee H, Son YS, et al. Interleukin-2 induces the in vitro maturation of human pluripotent stem cell-derived intestinal organoids. *Nat Commun*. 2018;9(1):3039. doi:10.1038/s41467-018-05450-8
165. Meran L, Massie I, Campinoti S, et al. Engineering transplantable jejunal mucosal grafts using patient-derived organoids from children with intestinal failure. *Nat Med*. 2020;26(10):1593-1601. doi:10.1038/s41591-020-1024-z
166. Günther C, Winner B, Neurath MF, Stappenbeck TS. Organoids in gastrointestinal diseases: from experimental models to clinical translation. *Gut*. Published online May 2022. doi:10.1136/gutjnl-2021-326560
167. Bar-Ephraim YE, Kretzschmar K, Clevers H. Organoids in immunological research. *Nat Rev Immunol*. 2020;20(5):279-293. doi:10.1038/s41577-019-0248-y
168. Crawford SE, Ramani S, Blutt SE, Estes MK. Organoids to Dissect Gastrointestinal Virus-Host Interactions: What Have We Learned? *Viruses*. 2021;13(6). doi:10.3390/v13060999
169. Puschhof J, Pleguezuelos-Manzano C, Martínez-Silgado A, et al. Intestinal organoid cocultures with microbes. *Nat Protoc*. 2021;16(10):4633-4649. doi:10.1038/s41596-021-00589-z
170. Jowett GM, Norman MDA, Yu TTL, et al. ILC1 drive intestinal epithelial and matrix remodelling. *Nat Mater*. 2021;20(2):250-259. doi:10.1038/s41563-020-0783-8
171. Dander E, Balduzzi A, Zappa G, et al. Interleukin-17-producing T-helper cells as new potential player mediating graft-versus-host disease in patients undergoing allogeneic stem-cell transplantation. *Transplantation*. 2009;88(11):1261-1272. doi:10.1097/TP.0b013e3181bc267e
172. Jiang H, Fu D, Bidgoli A, Paczesny S. T Cell Subsets in Graft Versus Host Disease and Graft Versus Tumor. *Front Immunol*. 2021;12:761448. doi:10.3389/fimmu.2021.761448
173. Wu Y, Fu J, Wang H, Yu XZ. Donor T-Cell Repertoire Profiling in Recipient Lymphoid and Parenchyma Organs Reveals GVHD Pathogenesis at Clonal Levels After Bone Marrow Transplantation in Mice. *Front Immunol*. 2021;12:778996. doi:10.3389/fimmu.2021.778996
174. Divito SJ, Aasebø AT, Matos TR, et al. Peripheral host T cells survive hematopoietic stem cell transplantation and promote graft-versus-host disease. *J Clin Invest*. 2020;130(9):4624-4636. doi:10.1172/JCI129965
175. Strobl J, Pandey RV, Krausgruber T, et al. Long-term skin-resident memory T cells proliferate in situ and are involved in human graft-versus-host disease. *Sci Transl Med*. 2020;12(570). doi:10.1126/scitranslmed.abb7028
176. Neal JT, Li X, Zhu J, et al. Organoid Modeling of the Tumor Immune Microenvironment. *Cell*. 2018;175(7):1972-1988.e16. doi:10.1016/j.cell.2018.11.021
177. Matsuzawa-Ishimoto Y, Hine A, Shono Y, et al. An intestinal organoid-based platform that recreates susceptibility to T-cell-mediated tissue injury. *Blood*. 2020;135(26):2388-2401. doi:10.1182/blood.2019004116
178. Epstein RJ, McDonald GB, Sale GE, Shulman HM, Thomas ED. The diagnostic accuracy of the rectal biopsy in acute graft-versus-host disease: a prospective study of thirteen patients. *Gastroenterology*. 1980;78(4):764-771.
179. Bombi JA, Nadal A, Carreras E, et al. Assessment of histopathologic changes in the colonic biopsy in acute graft-versus-host disease. *Am J Clin Pathol*. 1995;103(6):690-695. doi:10.1093/ajcp/103.6.690
180. Dijkstra KK, Cattaneo CM, Weeber F, et al. Generation of Tumor-Reactive T Cells by Co-culture of Peripheral Blood Lymphocytes and Tumor Organoids. *Cell*. 2018;174(6):1586-1598.e12. doi:10.1016/j.cell.2018.07.009
181. Cattaneo CM, Dijkstra KK, Fanchi LF, et al. Tumor organoid-T-cell coculture systems. *Nat Protoc*. 2020;15(1):15-



39. doi:10.1038/s41596-019-0232-9
182. Vacchelli E, Ma Y, Baracco EE, et al. Chemotherapy-induced antitumor immunity requires formyl peptide receptor 1. *Science*. 2015;350(6263):972-978. doi:10.1126/science.aad0779
183. Roberti MP, Yonekura S, Duong CPM, et al. Chemotherapy-induced ileal crypt apoptosis and the ileal microbiome shape immunosurveillance and prognosis of proximal colon cancer. *Nat Med*. 2020;26(6):919-931. doi:10.1038/s41591-020-0882-8
184. Schnalzger TE, de Groot MH, Zhang C, et al. 3D model for CAR-mediated cytotoxicity using patient-derived colorectal cancer organoids. *EMBO J*. 2019;38(12). doi:10.15252/embj.2018100928
185. Jacob F, Ming GL, Song H. Generation and biobanking of patient-derived glioblastoma organoids and their application in CAR T cell testing. *Nat Protoc*. 2020;15(12):4000-4033. doi:10.1038/s41596-020-0402-9
186. Larson RC, Kann MC, Bailey SR, et al. CAR T cell killing requires the IFN $\gamma$ R pathway in solid but not liquid tumours. *Nature*. Published online April 2022. doi:10.1038/s41586-022-04585-5
187. Higa T, Okita Y, Matsumoto A, et al. Spatiotemporal reprogramming of differentiated cells underlies regeneration and neoplasia in the intestinal epithelium. *Nat Commun*. 2022;13(1):1500. doi:10.1038/s41467-022-29165-z
188. de Sousa E Melo F, de Sauvage FJ. Cellular Plasticity in Intestinal Homeostasis and Disease. *Cell Stem Cell*. 2019;24(1):54-64. doi:10.1016/j.stem.2018.11.019
189. Murata K, Jadhav U, Madha S, et al. Ascl2-Dependent Cell Dedifferentiation Drives Regeneration of Ablated Intestinal Stem Cells. *Cell Stem Cell*. 2020;26(3):377-390.e6. doi:10.1016/j.stem.2019.12.011
190. Lukonin I, Serra D, Challet Meylan L, et al. Phenotypic landscape of intestinal organoid regeneration. *Nature*. 2020;586(7828):275-280. doi:10.1038/s41586-020-2776-9
191. Naik S, Larsen SB, Gomez NC, et al. Inflammatory memory sensitizes skin epithelial stem cells to tissue damage. *Nature*. 2017;550(7677):475-480. doi:10.1038/nature24271
192. Larsen SB, Cowley CJ, Sajjath SM, et al. Establishment, maintenance, and recall of inflammatory memory. *Cell Stem Cell*. 2021;28(10):1758-1774.e8. doi:10.1016/j.stem.2021.07.001
193. Lim AI, McFadden T, Link VM, et al. Prenatal maternal infection promotes tissue-specific immunity and inflammation in offspring. *Science*. 2021;373(6558). doi:10.1126/science.abf3002







## Appendices

## Nederlandse samenvatting

Ieder jaar ondergaan er gemiddeld 75 kinderen in Nederland een allogene stamceltransplantatie (SCT) als laatste redmiddel voor bijvoorbeeld leukemie. Voordat de SCT kan plaatsvinden ondergaat de patiënt bestraling en/of chemotherapie om ruimte te maken voor het transplantaat. Transplantatie vindt vervolgens plaats met de meest compatibele donor op basis van het weefsel HLA-type. Helaas wordt het succes van SCT als behandeling bedreigd door het optreden van acute Graft-versus-Host ziekte (GvHZ). GvHZ ontstaat wanneer donor afweercellen de weefsels van de patiënt als lichaamsvreemd herkennen en grootschalige inflammatie veroorzaken. Met name patiënten met GvHZ van de darm lopen gevaar door het risico op uitdroging en ondervoeding, en een verhoogd risico op infectie.

De behandeling van GvHZ is voornamelijk gericht op het onderdrukken van het overactieve afweersysteem met corticosteroiden (CS). Een balans te vinden tussen het onderdrukken van de afweer tijdens GvHZ enerzijds, en infectiebescherming anderzijds, is daarbij een grote uitdaging. Bovendien reageert ongeveer de helft van de patiënten niet of onvoldoende op CS en ontwikkelt zogenaamde steroïde-refractaire (SR-)GvHZ. Het is cruciaal dat er nieuwe therapieën ontwikkeld worden die zich niet primair richten op het onderdrukken van het immuunsysteem. Darmepitheelschade speelt een grote rol tijdens de ontwikkeling van GvHZ (**Hoofdstuk 7**). Desondanks is er nog veel onbekend over het mechanisme dat hieraan ten grondslag ligt, waardoor potentiële behandelingsmogelijkheden op dit vlak nog niet kunnen worden benut.

In dit promotieonderzoek brachten we ten eerste in kaart hoe het de kinderen verging die SR-GvHZ ontwikkelden na SCT in Nederland, en wat de risicofactoren waren voor slechtere uitkomsten (**Hoofdstuk 2**). Verder hebben we op verschillende momenten in het SCT traject bestudeerd wat de rol is van darmepitheelschade bij het ontstaan van en in stand houden van GvHZ. Hiervoor zijn verschillende GvHZ muismodellen gebruikt en kweekmodellen ontwikkeld met organoids, 'mini-darmpjes', om specifieke aspecten van GvHZ na te kunnen bootsen.

We ontdekten dat het cytokine interferon-gamma (IFN $\gamma$ ) dat wordt uitgescheiden door donor T cellen ervoor zorgt dat darmepitheelstamcellen ten onder gaan (**Hoofdstuk 5**). De stamcellen konden beschermd worden door de cel signalering van IFN $\gamma$  in het epitheel te remmen met het medicijn ruxolitinib. Momenteel wordt ruxolitinib alleen aan volwassenen met SR-GvHZ voorgeschreven, maar eerdere of zelfs preventieve behandeling zou veelbelovend kunnen zijn.

Vervolgens bestudeerden we wat het effect is van behandeling met CS op het darmepitheelherstel in GvHZ (**Hoofdstuk 6**). CS belemmerde het herstel aanzienlijk, maar



behandeling met epitheelstamcel-stimulerend interleukine (IL)-22 kon dit overwinnen. Dit is een belangrijke bevinding, omdat in klinische trials met volwassenen IL-22 tegelijkertijd met CS wordt gegeven.

Ook brachten we het directe effect van epitheelschade door chemotherapie op donor T cel responsen voorafgaand aan SCT in kaart (**Hoofdstuk 4**). Epitheelschade door chemo bleek T cellen aan te trekken en bij te dragen aan hun activatie. Het door epitheel uitgescheiden eiwit galectin (gal)-9 speelde bij beide processen een rol, en bleek ook verhoogd te zijn in het serum van kinderen die uiteindelijk GvHZ ontwikkelden na SCT. Afhankelijk van de precieze rol van gal-9 in het ziekteproces, zou het een aangrijpingspunt voor preventie of behandeling van GvHZ kunnen zijn.

Ten slotte pasten we een methode toe om efficiënt virussen aan te kunnen tonen in de ontlasting van kinderen die worden verdacht van GvHZ van de darm (**Hoofdstuk 3**). Er zijn aanwijzingen dat de aanwezigheid van bepaalde virussen predisponeren voor het ontwikkelen van GvHZ, maar het onderzoek daarnaar is beperkt. Een van de uitdagingen is het efficiënt kunnen identificeren van de virussen. Door de verrijking van virale nucleïnezuuren (RNA/DNA) met ViroCap voorafgaand aan *next-generation sequencing* konden we niet eerder gevonden virussen aantonen, inclusief een nieuwe variant. Door dit in de toekomst toe te passen op een groter cohort kunnen associaties tussen virussen en uitkomsten in kaart gebracht worden.

Concluderend is het optreden van SR-GvHZ bij kinderen geassocieerd met een hoge mortaliteit en morbiditeit door het ontbreken van een bewezen effectieve behandeling. De era van immunosuppressieve monotherapie lijkt daarmee voorbij. Schade aan het darmepitheel is op veel verschillende manieren geassocieerd met de ontwikkeling en instandhouding van GvHZ van de darm, en is daarmee een goed aangrijpingspunt voor nieuwe, aanvullende therapieën. Verdere toepassing van de door ons ontwikkelde ziektemodellen, maar voornamelijk toetsing van de daaruit behaalde resultaten in prospectieve klinische trials, is cruciaal voor de verbetering van de uitkomsten voor patiënten met GvHZ.



## Dankwoord

Lieve **Caroline**, ruim 12 jaar onderweg nu. Zonder jou was dit promotietraject er nooit gekomen. Wat een geluk dat er over IPSC al zoveel geschreven was dat Paul mij voor een literatuurstudie naar jou doorverwees, en dat hij dat nogmaals deed toen ik op zoek was naar een wetenschapsstage in het buitenland. Ik heb altijd het idee gehad dat we het samen deden. Ontzettend benaderbaar (al moest ik in het begin wel wennen aan de 'ok' appjes), altijd meedenkend en een ster in praktische oplossingen. Niet altijd makkelijk met het drukke schema met klinische taken en een jong gezin ernaast. Onze gedeelde passie voor NYC, met leuke tripjes naar TCT congressen in Orlando en Salt Lake City, lekkere wijn en lekker eten. Steeds meer een vriendin. Enorm bedankt, en ik hoop dat we in de toekomst nog veel mogen samenwerken!

Lieve **Edward**, eerst docent tijdens het blok kindergeneeskunde, later lid 2 van het tweekop-pig duo dat tijdens mijn ASAS op vrijdagmiddag naast me kwam zitten in de assistentenkamer op afdeling Eekhoorn om te vragen 'hoe het ging'. Tijdens mijn PhD inhoudelijk meer op afstand, maar altijd de deur wijd open om te horen hoe het was. Waardevolle persoonlijke begeleiding tijdens mijn PhD en in de keuzes richting mijn toekomst. Heel bijzonder om tijdens mijn stage in NYC op Oudejaarsdag met jou en je gezin oesters te eten op Grand Central. Heel erg bedankt!

Dear **Paul**, you offered the first stepping stone for my scientific career. Through the Honours programme committee, and eventually as supervisor. I learnt how to pipet in your lab (waarvoor dank, **Evelien!**) and I always felt taken very seriously. Funny how our ways crossed again when you became co-supervisor of the chemo-project when Ale joined. I admire your ability to see story opportunities in almost all lab data. Very dependable, thank you!

Lieve **Marliek**, heel even mijn eigen analist! En wat voor één. Ontzettend fijn en gezellig om met jou te hebben samengewerkt. Slim, enthousiast, kalm en stabiel en gewoon ook heel goed. Echt een gemis toen we je moesten laten gaan. Gelukkig als vriendin altijd betrokken gebleven en vandaag met extra ondersteuning als paranimf.

Lieve **Maaïke**, we werkten aan andere projecten, maar we kweekten of qPCR-erden altijd samen (jij won wel altijd qua hoeveelheden). Heerlijk slap ouwehoeren, roddelen en lachen in het organoid lab, en daarbuiten. Je bent de meest optimistische en oprechte persoon die ik ken, een hele fijne vriendin!

Lieve **Irena**, harde werker, je startte vaak veel vroeger dan wij, en werkte soms nog tot langer door. Maar altijd tijd door een praatje op het lab en een drankje of een feestje daarbuiten. Jij vraagt echt door, op een open manier, waardoor ik altijd verder kwam na een gesprek met jou. Ben benieuwd hoe je het in NYC gaat hebben!

Lieve **Gautam**, in bijna alles mijn tegenpool, behalve de passie voor ons vak en onderzoek.

Altijd een ongezouten mening, onconventionele oplossingen, en heerlijke schijt aan alles en iedereen. Zo vaak oneens met elkaar, maar zo veel lol. Goud waard!

Lieve Borrelclub, lieve **Marliek, Maaïke, Irena** en **Gautam**, samen hebben we elkaar door de PhD tijd gesleept, met veel bijkletsen, lachen, en lekker afgeven op supervisors en collega's onder het genot van meestal een drankje of twee. In coronatijd vaak online of op locatie buiten op afstand. En nog steeds zien we elkaar regelmatig. Onmisbaar!

Lieve **Sabine** Middendorp, bedankt voor het er zijn toen ik begon op het lab. Het was heel fijn om een aanspreekpunt te hebben. En natuurlijk bedankt voor de Stem study organoids, die zijn voor alle hoofdstukken gebruikt!

Dear **Michal**, our RNA specialist and the one with smart and creative ideas of how to make or finish a story. Thanks for continuing helping with some of the interpreting of the RNA seq data and logistics around submitting for depositories!

Lieve **Sabine** Fuchs, hartelijk dank voor het kritische meedenken afgelopen jaren. En het organiseren van gezellige borrels aan de singel met/zonder bootje varen!

Lieve (oud) ped-gastro-ers, **Imre, Indi, Ibrahim, Marit, Vivian, Zahra, Ema, Sawsan, Bich, Gaby, Matthijs, Martijn**, bedankt voor alle gezelligheid en hulp! Jorik, bedankt voor je praktische kweektips in het begin, **Anke**, bedankt voor de goede organisatie en alle mooie en duidelijke protocollen. En **Claartje**, bedankt voor je vriendschap en de goede gesprekken bij een kopje Genmab koffie.

Lieve **Anna Vera**, eigenlijk ook een oud ped-gastro-er, maar dat zou ik inmiddels bijna vergeten. Een hele fijne vriendin, met gedeelde ambities en interesses op bijna alle vlakken. Altijd zoveel herkenning bij jou!

Dear **Shuichiro, Viktor, Paola**, and of course, **Alan**, thank you for the amazing collaboration that started with my internship in the lab in NYC in 2016. It has been truly inspiring, and formed the basis of this whole thesis. I learned so much from you guys! I very much look forward to continue working with you, or for those that have moved on, to work with each other again in the future!

Dear **Ale**, great to have joined forces on the chemo project. Together we got so much further than I would have gotten alone. Good luck with finishing your thesis, and I'm curious what the future will bring for you!

Dear **Enric**, thanks for all the brainstorm sessions and great ideas, even if our ways of working did not always match. Always a lot of fun working with you!

Lieve **Cindy** en **Cornelieke**, heel hartelijk dank voor alle praktische tips en ondersteuning afgelopen jaren!

Lieve **Bahar**, zo fijn dat jij aan de slag kon op het MSC project, waar Magdalena en ik al een aantal studenten op hadden begeleid. Uiteindelijk daarmee een mooi project geworden met



leuke resultaten, die we hopelijk op korte termijn met het publiek kunnen delen. Dear **Magdalena**, thank you for the collaboration!

Lieve Nierkens clan, **Annelisa**, **Maud** en natuurlijk **Stefan**, hartelijk dank voor de input en het meedenken! **Coco**, bedankt voor ideeën voor de T cel FACs panels jaren geleden en de mooie Olink data plotjes. **Ester** and **Vania**, thanks for the collaboration and help with the WT1 co-culture experiment, they didn't make the thesis, but were very cool to do and worked well!

Lieve **Anne** en **Emmeline**, wat een fijne samenwerking aan het SR-GVHD project! Het is er helaas nog steeds niet van gekomen om samen een hapje te gaan eten, moeten we snel een keer doen!

Beste **Rob Schuurman** en **Wouter Nijhuis**, hartelijk dank voor de leuke samenwerking op het ViroCap project!

Beste **Jeffrey Beekman** en **Manon Maurice**, hartelijk dank voor de begeleiding in mijn begeleidingscommissie! En, samen met Femke van Wijk, Helen Leavis en Mette Hazenberg, hartelijk dank voor het beoordelen van mijn proefschrift.

Lieve (ex)Beekmannen, in het bijzonder **Sylvia**, **Eyleen**, **Hetty**, **Juliet** en **Lisa**, heel erg bedankt voor de gezelligheid en gekkigheid in ons gedeelde lab, en **Sylvia**, voor je kweektips en troubleshooting bij problemen.

Dear students: **Leire**, **Aina**, **Madeleine**, **Dorian** and **Lotte**. Thanks for your enthusiasm and help!

Lieve Suermannen, met name **Mimount**, **Wouter** en **Tobias**, wat een inspirerende groep mensen. Wat heb ik veel van jullie geleerd door onze workshops en gesprekken samen. Enorm waardevol om elkaar nog steeds te ontmoeten. Ik hoop dat dat nog vele jaren mag voortduren! Lieve **Lisan**, bedankt voor je empathie en jouw gave om altijd het onderliggende probleem bloot te leggen, heel bevrijdend!

Lieve **collega's** uit het ZGV in Ede, een warm bad om in terecht te komen na mijn onderzoek. Wat vond ik het spannend en uitdagend in het begin, en wat hebben jullie mij daar goed doorheen gesleept. Ontzettend bedankt!

Lieve medewerkers van **30ml** op de **Nachtegaalstraat**, altijd staat er een heerlijk warm bakkie (troost) met prachtige melkkunst klaar. Een goed gesprek, schaterlach, of een arm om mijn schouder. Mijn tweede woonkamer. Bedankt!

Lieve lieve vriendinnen van Awesome (wat een vreselijke naam is het toch): **Iris, Joey, Sanne, Maud, Clara, Bianca** en **Carlijn**. Wat een ongelofelijke fijne en warme groep vriendinnen zijn jullie. Zo verschillend, maar zo met elkaar begaan. Van koffiewandelingetjes in Rhijnauwen, tot festivals en jaarlijkse weekendjes weg; van wereldreizen met elkaar tot elkaar opzoeken op de meest exotische (werk)locaties. Zo ontzettend blij dat jullie er zijn! Ook dank aan de aanhang die er met de jaren bij is geweest en gekomen: **Daniel, Tijn, Tom, Jamie, Harry, Berry** en **Lester**. Hele fijne mensen!

Lieve 133, lieve **Eric, Katrien, Rogier, Robbert, Patrick, Cecile** en **Erna**. We zien elkaar niet heel erg vaak, maar als we elkaar zien voelt het als thuiskomen. Wat hebben wij elkaar goed leren kennen in dat ene jaar. Ik ben het meest grenzeloos met jullie, omdat ik me altijd me-gaveilig voel. Bedankt!

Lieve RAAKies, en in het bijzonder **Willemijn, Marleen, Linde**. Bedankt voor jullie bijzondere vriendschap, de goede gesprekken en de mooie tripjes de afgelopen jaren!

Lieve (oud)huisgenootjes van de Kerkstraat, **Lotte, Denise, Sanne, Jade, Judith** en **Nynke**. Bedankt voor alle steun de afgelopen jaren! Altijd klaar met een theetje, voor een praatje of met de nodige repen Tony's. Heel bijzonder, en ik mis jullie soms nog steeds. Al is het maar jullie gerommel op de achtergrond.

Lieve **Roos**, oud-huisgenootje van de ASW, we go way back. Veel meegemaakt samen de afgelopen jaren, en zeker niet alleen maar in positieve zin. Sprankelend ben je! En altijd in voor iets nieuws of cools of gek. Ontzettend leuk!

Lieve, lieve **familie**, van de warme en de koude kant, teveel namen om op te sommen! Jullie weten wie jullie zijn. Hartelijk dank voor jullie interesse en steun!

Lieve **papa, mama** en **Stijn**, mijn fijne, sterke en veilige basis. Jullie staan altijd achter mij, en dat voelt geweldig. Ik voel me bijzonder en gewaardeerd door jullie, en jullie hebben mij enorm gesteund tijdens dit traject. Daarnaast zijn jullie ook nog eens ontzettend gezellig; de grootste lol hebben we met elkaar, of we nou samen (uit)eten of op vakantie zijn. Ik hou van jullie!



## Curriculum vitae

Suze Anne Jansen was born on the 8<sup>th</sup> of December 1990 in Rotterdam, The Netherlands to parents Peter and Anneliek Jansen, and as older sister to Stijn Jansen. After graduating from bilingual high school in Rotterdam she chose to attend medical school at the UMC Utrecht (UMCU) because of a fascination with the human body.

During her Bachelor studies Suze participated in an honors program that allowed her to gain research experience in a wet lab – the Paul Coffey lab – which lay the foundation for future research endeavors. In her Master she had the opportunity to do an internship at the Alan Hanash lab at Memorial Sloan Kettering Cancer Center in New York City, the USA. In addition she went to Malawi for an elective internship tropical medicine. During her studies Suze was an active member of the student rowing club Triton as a rower and coach, and fulfilled a full time position on the board supported by a Utrecht University (UU) grant for one year.

After obtaining her medical degree, Suze was awarded an Alexandre Suerman stipend by the UMCU, which allowed her work full-time on her PhD research under supervision of Dr. Caroline A. Lindemans and Prof. Dr. Edward. E.S. Nieuwenhuis at the Regenerative Medicine Center Utrecht (UMCU) and the Princess Máxima Center of Pediatric Oncology. In addition it provided her with a personal development program focusing on 'soft skills' such as collaboration, leadership and communication skills. Her research focused on mechanisms of intestinal epithelial injury in graft-versus-host disease (GVHD) of the gut after allogeneic stem cell transplantation and its contribution to the development of GVHD itself. She collaborated closely with the Hanash lab, as well as with the Coffey group, Lorenowicz group, pediatric transplanters from the LUMC and the UMCU virology department. During her time as PhD candidate she advocated for fellow PhD's at the UU Graduate School of Life Sciences of the Utrecht University and Promovendi Network Utrecht (PROUT).

Next to her passion for work, Suze likes to get physical with cross training, cycling, skiing and hiking. She enjoys practicing contemporary dance and visiting performances of professional dancers. She likes to cook, but loves to eat food even more.

After having finished her thesis, Suze will continue to work as a medical doctor in Pediatrics in the Gelderse Vallei hospital in Ede.

## List of publications

Calafiore M, Fu Y, Vinci P, Arnhold V, Chang W, **Jansen SA**, Egorova A, Takashima S, Kuttiyara J, Ito T, Serody J, Nakae S, Turnquist HR, van Es J, Clevers H, Lindemans CA, Blazar BR\*, Hanash AM\*. A tissue-intrinsic IL-33/EGF circuit promotes epithelial regeneration after intestinal injury. *Nat Commun.* 2023 Sep 5;14(1):5411. doi: 10.1038/s41467-023-40993-5. PMID: 37669929.

**Jansen SA**, Cutilli A, de Koning C, van Hoesel M, Sierra LS, Nierkens S, Mokry M, Nieuwenhuis EES, Hanash AM, Mocholi E, Coffey PJ, Lindemans CA. Chemotherapy-induced intestinal injury promotes Galectin-9-driven modulation of T cell function. *bioRxiv [Preprint]*. 2023 Apr 30:2023.04.30.538862. doi: 10.1101/2023.04.30.538862. PMID: 37163028.

Verbeek AB\*, **Jansen SA**, von Asmuth EGJ, Lankester AC, Bresters D, Bierings M, Mohseny AB, Lindemans CA, Buddingh EP. Clinical Features, Treatment, and Outcome of Pediatric Steroid Refractory Acute Graft-Versus-Host Disease: A Multicenter Study. *Transplant Cell Ther.* 2022 Sep;28(9):600.e1-600.e9. doi: 10.1016/j.jtct.2022.06.008. Epub 2022 Jun 16. PMID: 35717003.

**Jansen SA**, Nieuwenhuis EES, Hanash AM, Lindemans CA. Challenges and opportunities targeting mechanisms of epithelial injury and recovery in acute intestinal graft-versus-host disease. *Mucosal Immunol.* 2022 Apr;15(4):605-619. doi: 10.1038/s41385-022-00527-6. Epub 2022 Jun 2. PMID: 35654837.

Jung JM, Ching W, Baumdick ME, Hofmann-Sieber H, Bosse JB, Koyro T, Möller KJ, Wegner L, Niehrs A, Russu K, Ohms M, Zhang W, Ehrhardt A, Duisters K, Spierings E, Hölzemer A, Körner C, **Jansen SA**, Peine S, Königs I, Lütgehetmann M, Perez D, Reinshagen K, Lindemans CA, Altfeld M, Belderbos M, Dobner T, Bunders MJ. KIR3DS1 directs NK cell-mediated protection against human adenovirus infections. *Sci Immunol.* 2021 Sep 17;6(63):eabe2942, doi: 10.1126/sciimmunol.abe2942. Epub 2021 Sep 17. PMID: 34533978.

**Jansen SA**, Nijhuis W, Leavis HL, Riezebos-Brilman A, Lindemans CA<sup>§</sup>, Schuurman R<sup>§</sup>. Broad Virus Detection and Variant Discovery in Fecal Samples of Hematopoietic Transplant Recipients Using Targeted Sequence Capture Metagenomics. *Front Microbiol.* 2020 Nov 17;11:560179. doi: 10.3389/fmicb.2020.560179. PMID: 33281758.



Takashima S<sup>\*</sup>, Martin ML<sup>\*</sup>, **Jansen SA<sup>\*</sup>**, Fu Y, Bos J, Chandra D, O'Connor MH, Mertelsmann AM, Vinci P, Kuttiyara J, Devlin SM, Middendorp S, Calafiore M, Egorova A, Kleppe M, Lo Y, Shroyer NF, Cheng EH, Levine RL, Liu C, Kolesnick R, Lindemans CA<sup>§</sup>, Hanash AM<sup>§</sup>. T cell-derived interferon- $\gamma$  programs stem cell death in immune-mediated intestinal damage. *Sci Immunol.* 2019 Dec 6;4(42):eaay8556. doi: 10.1126/sciimmunol.aay8556. PMID: 31811055.

**Jansen SA<sup>\*</sup>**, Kleerekooper I<sup>\*</sup>, Hofman ZL<sup>\*</sup>, Kappen IF<sup>\*</sup>, Stary-Weinzinger A, van der Heyden MA. Grayanotoxin poisoning: 'mad honey disease' and beyond. *Cardiovasc Toxicol.* 2012 Sep;12(3):208-15. doi: 10.1007/s12012-012-9162-2. PMID: 22528814.

<sup>§</sup>contributed equally







Artist  
Anneloes Gerdien  
[anneloesgerdien.nl](http://anneloesgerdien.nl)



